UNIVERSITÄT ZU LÜBECK

From the Institute for Systemic Inflammation Research

of the University of Lübeck

Director: Prof. Dr. med. Jörg Köhl

Role of Interleukin-10 in the Natural Course of Epidermolysis Bullosa Acquisita

Dissertation

for Fulfillment of

Requirements

for the Doctoral Degree

of the University of Lübeck

from the Department of Natural Sciences

Submitted by

Ann-Katrin Clauder

From Malsch, Germany

Lübeck, June 2019

First referee: Prof. Dr. rer. nat. Rudolf Manz

Second referee: Prof. Dr. rer. nat. Hauke Busch

Date of oral examination: 23rd of September 2019

Approved for printing: Lübeck, 30th of September 2019

The important thing in science

is not so much to obtain new facts

as to discover new ways of thinking about them.

William Lawrence Bragg *(1890-1971)*

Statement of authenticity

I hereby declare that I have written the present thesis independently, without assistance from external parties and without use of other resources than those indicated in the text. Any concepts or quotations applicable to these sources are clearly attributed to them. This dissertation has not been submitted in the same or similar version, not even in part, to any other authority for grading.

Lübeck, June 2019 _____

Ann-Katrin Clauder

Acknowledgment

Foremost, I would like to express my sincere gratitude to my supervisor Prof. Dr. Rudolf Manz for the opportunity to work on this fascinating immunological research topic and for the continuous support, motivation and guidance throughout the whole time of my thesis. His immense knowledge enlivened our discussions and strongly enhanced my understanding of immunology.

Furthermore, I would like to thank my mentors PD Dr. Kathrin Kalies and Dr. Katja Bieber for their helpful suggestions and discussions during the past years. In addition, I thank Dr. Katja Bieber for providing mice and reagents which were essential for the experimental work.

My sincerely thanks go to all the recent and former members of AG Manz who always supported me during experiments. Due to their expert knowledge and their practical expertise I was able to learn and to improve many immunological methods. Especially, I would like to thank Kathleen Kurwahn for her practical support, her assistance during all experiments and her unrestricted help when problems were encountered. Thanks to Timo Lindemann, Christina Rau and Dr. Larissa Almeida for the inspiring discussions and the many funny situations inside and outside the office, which lightened up everyday life. I also thank the many former members of the group for the support and help during the last years, especially Britta Frehse, Katharina Hofmann, Sara Comdühr, Dr. Melanie Abram, Dr. Christopher Link, Dr. Asmaa El Beidaq, Julian Kottlau, Anna Gramalla and Fabienne Irrgang. In addition, I thank Jenny Tillmann, Dr. Bálint Kovács and PD Dr. Christian Karsten for providing their knowledge about neutrophils and their help for the analysis of their functions.

Moreover, I would like to thank the clinical research unit (CRU303) and the research training group (GRK1727) for the financial support, without this research would not have been possible. In particular, I thank the GRK1727 for the opportunity to learn and deepen my knowledge in autoimmunity and to discuss my results with PhD students working in the same field.

Last but not the least, I would like to thank my boyfriend Eike Christian Koopmann and my parents sincerely for their support, encouragement and faith in me during my life in general and especially during the last three years of my PhD thesis.

Table of Contents

1. Abstract

Although the phenotype and origin of interleukin (IL)-10-producing B cells and plasma cells is still controversial, their potential to restrict various autoimmune disorders has clearly been demonstrated during recent years. Previous work from our group could show that intense but non-physiological B-cell receptor crosslinking induces IL-10-expressing plasma cells, which have the capacity to limit inflammation of an autoimmune blistering skin disease, probably via direct inhibition of neutrophil migration. However, no information was available on the suppressive capacity of IL-10 and in particular IL-10-producing plasma cells under pathophysiological conditions. Therefore, this thesis aimed to investigate the characteristics of IL-10-producing plasma cells and the potential of IL-10 to suppress the natural course of the autoimmune skin disease epidermolysis bullosa acquisita (EBA) by using different established experimental mouse models. Immunization of susceptible IL-10 reporter mice with the autoantigen revealed that plasma cells are the dominant source of induced IL-10 production and that both autoreactive and non-self-reactive plasma cells produce this cytokine. The kinetics of appearance and the localization of these cells indicate that IL-10-producing plasma cells can be derived either directly via an (auto)antigen-driven pathway in lymph nodes or secondarily via a systemic, inflammation-driven route, which suggests the existence of distinct IL-10-producing plasma cell subsets. IL-10 was able to down-modulate EBA skin inflammation and blistering in the natural course of the disease despite the presence of autoantibodies, as shown by IL-10 receptor blockade in autoantigen-immunized susceptible mice. IL-10 directly or indirectly inhibited effector cell functions such as the release of reactive oxygen species by innate effector cells, a hallmark of EBA pathogenesis. Furthermore, comparison of the immune reaction to the autoantigen in susceptible and congenic, non-susceptible mice with different major histocompatibility complex-haplotypes revealed that in addition to IL-10, the quantity and pathogenic potential of autoantibodies and autoreactive lymphocytes, but not a tight immunological tolerance or the expansion of a protective lymphocyte subset, are important factors associated with EBA susceptibility. In conclusion, these data indicate that IL-10 controls skin inflammation under pathophysiological conditions in the immunization-induced EBA mouse model and that plasma cells represent a dominant source of this cytokine. Moreover, the inhibition of oxidative burst by innate effector cells appears to be an important mechanism by which IL-10 can curtail EBA skin inflammation. Further characterization and functional analysis of IL-10-producing plasma cells would provide new insights into the therapeutic potential of these cells to treat human autoimmune diseases.

2. Zusammenfassung

Trotzdem der Phänotyp und die Herkunft von Interleukin (IL)-10-produzierenden B-Zellen und Plasmazellen noch kontrovers diskutiert wird, konnte ihr immunsuppressives Potential in etlichen Autoimmunerkrankungen klar demonstriert werden. Vordaten zeigen, dass durch artifizielle B-Zell-Rezeptor Quervernetzung IL-10-produzierende Plasmazellen expandiert werden, die die Entzündungsreaktion einer Autoimmundermatose, vermutlich über die direkte Inhibition von Neutrophilen, supprimiert. Im Gegensatz dazu gibt es bisher keine Studien, die die inhibitorische Wirkung von IL-10 und IL-10-exprimierenden Plasmazellen unter pathophysiologischen Bedingungen analysiert haben. Das Ziel dieser Arbeit war es daher, IL-10-produzierende Plasmazellen näher zu charakterisieren und das immunsuppressive Potential von IL-10 im natürlichen Verlauf der Autoimmundermatose Epidermolysis bullosa acquisita (EBA) mithilfe von etablierten Mausmodellen zu untersuchen. Die aktive Immunisierung von suszeptiblen IL-10-Reportermäusen mit dem Autoantigen zeigte, dass Plasmazellen die dominante induzierte IL-10-Quelle darstellen und dass sowohl autoreaktive als auch nicht-autoreaktive Plasmazellen dieses Zytokin produzieren. Die Bildungskinetik und die Lokalisation dieser Zellen weist darauf hin, dass IL-10$^+$ Plasmazellen entweder über einen direkten, (Auto)antigen-abhängigen Weg im Lymphknoten entstehen oder über einen sekundären, entzündungsvermittelten Weg. IL-10 war in der Lage, die Entzündung und Blasenbildung im natürlichen Verlauf der EBA trotz der Anwesenheit von Autoantikörpern zu reduzieren. Dies konnte mit Hilfe von IL-10-Rezeptor-blockierenden Antikörpern in suszeptiblen Mäusen gezeigt werden. Dabei inhibierte IL-10 direkt oder indirekt die Funktionen von Effektorzellen, wie die Freisetzung von reaktiven Sauerstoffspezies, was einen entscheidenden Prozess in der EBA Pathogenese darstellt. Des Weiteren zeigte der Vergleich der Immunreaktion von suszeptiblen mit kongenen, nicht-suszeptiblen Mäusen, die sich in ihrem Haupthistokompatibilitätskomplex-Haplotyp unterscheiden, dass zusätzlich zu IL-10 auch die Menge und Pathogenität von Autoantikörpern und autoreaktiven Lymphozyten, nicht jedoch eine strikte immunologische Toleranz oder die Expansion von protektiven Lymphozyten-Populationen, mit der EBA Suszeptibilität assoziiert sind. Zusammenfassend legen die Daten nahe, dass IL-10 die Hautentzündung unter den pathophysiologischen Bedingungen im Immunisierungsinduzierten EBA Modell reguliert und dass Plasmazellen eine dominante Quelle dieses Zytokins darstellen. Die Inhibition des oxidativen Bursts von Effektorzellen scheint ein wichtiger Mechanismus zu sein, durch den IL-10 die Hautentzündung abschwächen kann. Die weitere Charakterisierung und funktionelle Analyse von IL-10$^+$ Plasmazellen würde dazu beitragen, neue Therapien zur Behandlung von humanen Autoimmunerkrankungen zu entwickeln.

3. Introduction

3.1 Immunity and autoimmunity

The immune system comprises two main branches of immunity: the innate and the adaptive immune system. In order to achieve an appropriate overall immune response, both arms need to interact tightly in a controlled manner. Dysregulation of one of the components or disbalance between effector and regulatory immune reactions can lead to detrimental conditions such as immunodeficiency or autoimmune diseases. Autoimmunity develops when one or more of the multiple mechanisms controlling self-reactivity are defective or circumvented, leading to breakdown of tolerance [1] (chapter 3.1.2).

Lymphoid tissues are essential for maturation and maintenance of immune cells

Within the human body, the immune system is compartmentalized and located at various places and organs. Apart from skin and mucous membranes, representing the first mechanical protection barrier against microorganisms, distinct organs as well as the blood and lymph vessel system contribute. On the one hand, primary/central lymphoid organs, such as bone marrow and thymus, control the formation and maturation of immune cells from progenitor cells [2]. Moreover, these organs are essential for the elimination and control of self-reactive lymphocytes, thus, preventing autoimmune diseases [3]. On the other hand, secondary/peripheral lymphoid organs, such as lymph nodes, spleen and mucosal-associated lymphoid tissue, maintain mature immune cells and are crucial for the initiation of the adaptive immune response [2] (chapter 3.1.1). Lymph nodes, which are found in close proximity to the place of infection, mediate the acute local inflammation, whereas the spleen plays an important role in the systemic regulation of the immune response, e.g. by accumulation of immunosuppressive cells [4,5].

The innate immune system is the first line of defense against microorganisms

The evolutionary old innate immune system represents the first line of defense using germline-encoded receptors to recognize the conserved molecular pattern of common microorganisms [6]. In particular, the structurally fixed pathogen-associated molecular pattern (PAMP) can be easily detected by pattern recognition receptors (PRRs), including the large family of toll-like receptors (TLRs) [2]. PRR-PAMP binding immediately results in the activation of a protective humoral and cellular response. However, these receptors do not undergo rearrangement to improve their affinity, thus, there is only a limited number of these germline-encoded proteins and no formation of memory [6]. Apart from PRRs,

key players of the innate immune reaction include the complement system and phagocytic cells, such as macrophages, neutrophils or dendritic cells (DCs). The innate immune system provides several mechanisms to respond to pathogenic challenges, e.g. the release of cytokines and chemokines to promote inflammation and attraction of other immune cells from the blood stream, proteolytic enzymes to directly kill invading pathogens or respiratory burst to support phagocytosis [6]. These factors and cells are not only essential for detection and elimination of foreign pathogens but also contribute to tissue homeostasis, e.g. via clearance of apoptotic cells and cell debris [7].

Due to the lack of memory formation, the innate immune system is not able to properly handle recurrent infections and some pathogens can even evade this first line of defense [2]. Accordingly, a second, more specialized and flexible defense mechanism has evolved: the adaptive immune system. Cells involved in the adaptive immune response are able to recognize an almost infinite diversity of antigens and to generate a memory, enabling them to handle a broad variety of pathogens.

3.1.1 The adaptive immune system

Major histocompatibility complexes present proteins antigen

In contrast to the broad innate immune response, realized within hours after pathogenic challenge, the specific adaptive immune response needs several days to establish but is long-lasting due to memory formation [2]. DCs and other antigen-presenting cells (APCs) are essential crosslinkers between innate and adaptive immunity. APCs are able to present both self and foreign peptides (antigens) on their surface by major histocompatibility complex (MHC) II and these proteolytically processed antigens can be detected by cluster of differentiation (CD)4^+ T helper (Th) cells [6]. DCs, monocytes, macrophages and B cells constitutively express MHCII [8]. By contrast, "endogenous" antigen-presentation via MHCI allows the immune system to identify microbe-infected host cells and initiate clearance by $CD8^+$ cytotoxic T cells [8]. Of note, susceptibility to over 40 diseases has been linked to distinct human leucocyte antigen (HLA) alleles, a highly polymorphic gene complex encoding for MHC molecules in humans [9]. In the mouse, these genes are known as H2 genes.

Non-protein antigens are recognized by specialized T-cell subsets

Antigen presentation to $CD8^+$ and $CD4^+$ T cells, both expressing αβ T-cell receptors (TCRs), is restricted to protein antigens. However, there are also other subclasses of T cells such as natural killer T (NKT) cells or γδ T cells which are able to recognize lipid or

glycolipid antigens, e.g. presented via the MHC-like molecule CD1 [8]. Both T-lymphocyte subsets are a part of the adaptive immune response, however, displaying rapid innate-like responses and pleiotropic effector functions such as the release of a broad range of cytokines [10,11].

T helper cells are activated by antigen-presenting cells

When DCs have encountered and engulfed a pathogen, they present peptide antigens on MHCII and migrate via lymphatic vessels to the T-cell zone in lymph nodes to initiate the adaptive immune response by the activation of $CD4^+$ T helper cells specific for the presented antigen [6]. Interaction of the TCR with the MHCII-antigen complex is not sufficient to completely activate naïve $CD4^+$ T cells since additional receptors such as CD3, CD28 and CD80/86 are required to form an immunological synapse [8]. This leads to production of interleukin (IL)-2 by the T cell and further stimulation results in clonal expansion and differentiation into either Th1, Th2 or other phenotypes depending on the produced cytokine at the site of activation [8]. The Th1/Th2 hypothesis suggests that Th1 cells produce mainly IL-2 and interferon (IFN)-γ, driving cellular immunity, whereas Th2 cells express IL-4, IL-5 and IL-13, supporting humoral immunity [12]. However, the Th2-Th2 paradigm is an over-simplified perspective since additional pathways of T-cell activation and cytokine-producing T-cell subsets, such as Th17, regulatory T cells and T follicular helper cells, have been described [13,14].

Activated B lymphocytes proliferate and form germinal centers

After stimulation through APCs, $CD4^+$ T cells are now able to migrate from the T-cell zone to the border of the B-cell zone and provide help for further activation of B lymphocytes specific for the same antigen. In particular, a specialized T-cell subset called follicular T helper (Tfh) cell helps the B cell to generate high affinity antibodies and is crucial to establish and maintain germinal centers (GC) [14,15]. In order to receive T-cell help, B cells must be already pre-activated by antigen-binding to its B-cell receptors (BCR), leading to internalization and presentation of antigen-peptides via MHCII on the surface. Thereby, an immunological synapse is formed between the activated B cell and its cognate T lymphocyte containing different receptor and adhesion complexes as well as secreted effector cytokines [16]. In addition to the MHCII-TCR complex, the interaction between CD40 on B cells and its ligand (CD40L, CD154) on T cells and the release of cytokines (e.g. IL-4, IL-5, IL-6) are crucial for B-cell proliferation, differentiation and isotype switching [8,16]. The Tfh cytokine IL-21 is not only important for the development of Tfh cells from naïve $CD4^+$ T cells, but it is also essential for the survival and proliferation of

B cells in the GC as well as plasma cell formation [17]. Furthermore, different co-receptors such as CD19 or CD22 can regulate the B-cell activation threshold or inhibit B-cell receptor singling, respectively [6]. The T cell-dependent stimulation of activated B cells gives rise to secondary follicles containing GC. By contrast, T cell-independent B-cell responses can be achieved by crosslinking and clustering of the BCR with polymeric antigens, e.g. lipopolysaccharide (LPS), without further co-stimulatory signals from T cells [8]. This type of activation is common in distinct B-cell subpopulations such as marginal zone B cells, thereby allowing a rapid response to pathogens independent of GC formation [18].

Antibody-secreting plasma cells develop from activated B cells

Most of the activated B cells proliferate and migrate to the follicles to form GC. However, some of these cells differentiate into (short-lived) plasmablasts in the primary focus, thus, mediating a rapid extrafollicular response by producing low-affinity antibodies, e.g. of the immunoglobulin (Ig) M subclass [19]. Antibodies are the secreted form of the BCR and are composed of a constant and a variable region as well as two light and two heavy chains, and the isotype of the constant region of the heavy chain mediates its effector function [20]. In contrast to the early extrafollicular plasmablast response, a more effective immune response is achieved later by the GC reaction including somatic hypermutation and class switching of antibodies [21]. In particular, activated B cells undergo several rounds of mutation in the variable region of the antibody, thereby increasing its affinity to the antigen, as well as deoxyribonucleic acid (DNA) rearrangements in the constant region, which determine the isotype and the effector function of the antibody [22]. Switching of the antibody subclass is mediated by distinct cytokines, e.g. IL-4 has been shown to induce switching to IgG1 and transforming growth factor (TGF)-β to IgG2b and IgA [23]. Initially, IgM and IgD are the dominant subclasses expressed by activated B cells, but IgG later becomes more abundant [20]. Antibodies have neutralizing and opsonizing functions and can induce cell death by antibody-dependent cellular cytotoxicity (ADCC) and by complement-mediated lysis [24]. In addition, IgG antibodies can be differentially glycosylated on their fragment crystallizable region (Fc) portion, thus exhibiting different inflammatory capacities by binding to Fcγ receptors (FcγRs) [25,26].

Plasma cells and memory B cells mediate long-term protection

The GC reaction leads to the formation of both plasma cells/plasmablasts and memory B cells, which have the ability to produce high-affinity antibodies [21]. Plasmablasts are considered a precursor stage of plasma cells with a high proliferative capacity and surface expression of immunoglobulins and MHCII in contrast to mature plasma cells [18]. Plasma

cells are able to migrate to the bone marrow or spleen and a portion of them can survive for extended periods in niches supported by stromal or other immune cells, thereby mediating long-term protection [19]. In addition, memory B cells can rapidly differentiate into plasmablasts and induce a secondary GC after antigen rechallenge, leading to a strong antibody response to pathogens [27]. It has been suggested that the majority of (long-lived) plasma cells in the bone marrow is derived from memory B cells activated during a secondary antigen encounter [19].

3.1.2 Break of tolerance in autoimmunity

Genetic and environmental factors mediate autoimmune susceptibility

Almost 100 different autoimmune diseases have been identified, however, they are considered rare and they affect only between three and five percent of the population [28]. Autoimmune diseases can be distinguished by their effector mechanism (autoantibodies, immunocomplexes and/or cytotoxic T cells) and the targeted organ or tissue. In particular, autoimmune diseases such as multiple sclerosis (MS), type 1 diabetes or pemphigoid diseases are organ-specific, whereas systemic lupus erythematosus (SLE) or Sjögren's syndrome are considered systemic autoimmune disorders [29]. It is generally accepted that a combination of different factors, such as genetic predisposition, environmental factors, defective immunological regulation and/or gender predisposition, strongly increases the risk of developing an autoimmune disease [3]. Especially MHC alleles, encoding for molecules involved in antigen presentation to T cells, have been shown to confer disease susceptibility or protection by influencing central and peripheral tolerance mechanisms [30,31]. However, the majority of autoimmune disorders is characterized by multiple genetic factors, e.g. mutations in non-HLA loci or epigenetic aberrations [28]. Moreover, different environmental factors such as heavy tissue damage, infections and the microbiome contribute to the development of autoimmune diseases [3].

In 1957, the "clonal selection theory" of MACFARLANE BURNET provided the first evidence that autoimmune diseases arise from "forbidden clones" which have not been deleted during lymphocyte development [29]. The immune system attempts to provide as much protection as possible by detecting a wide variety of (foreign) antigens but, on the other hand, it has to limit the repertoire to reduce the risk of autoimmune diseases by the detection of self-antigens through autoreactive lymphocytes. This balance between establishing immunological competence and preventing autoimmune diseases is achieved by selection mechanisms and checkpoints during lymphocyte maturation and activation.

Central tolerance mechanisms delete autoreactive lymphocytes

Central tolerance is achieved in the bone marrow for B lymphocytes and in the thymus for T lymphocytes. One important tolerance mechanism is the clonal deletion of autoreactive lymphocytes by apoptosis. T cells are negatively selected in the thymus when they detect too strongly self-antigens presented by MHC molecules, mainly on bone marrow-derived APCs [32]. Accordingly, MHC class II polymorphisms are crucial for shaping the T-cell receptor repertoire through different interaction strengths with the TCR during thymic development [30]. Similarly, B cells which experience a strong BCR-crosslinking during B-cell maturation in the bone marrow either go through a process called receptor editing, thereby eliminating the unwanted self-binding via light chain rearrangements, or they undergo apoptotic cell death if the editing was not successful [33].

Peripheral tolerance restricts activation of autoreactive lymphocytes

Central tolerance is an incomplete mechanism and some autoreactive lymphocytes are able to evade this first checkpoint. Therefore, additional peripheral tolerance mechanisms exist to prevent the activation of self-reactive T and B lymphocytes. Apart from apoptotic cell death, induction of anergy and immunological ignorance are two important mechanisms for the establishment of peripheral tolerance. Anergy is regarded as "unresponsiveness" to the autoantigen, induced by a weak and chronic crosslinking of the BCR, or TCR activation, in the absence of sufficient costimulatory signals [34,35]. Normally, anergic B cells do not receive T-cell help, are excluded from the GC reaction and thus die far more rapidly than other B-cell subsets. Approximately 5 to 7 % of peripheral B cells are in an anergic state and are characterized by a reduced antibody secretion and hyporesponsiveness to BCR-crosslinking [1,34,36]. However, anergic B cells are not actively deleted and thus can serve as a source of autoreactive B cells in the periphery [1]. Loss of anergy strongly contributes to the development of SLE or type I diabetes, among other autoimmune diseases [34].

Immunological ignorance is induced by low affinity and non-crosslinking molecules during B-cell development and by low levels of MHC-presented self-antigens in T cells [37,38]. An important reason why ignorant autoreactive lymphocytes do not respond to their cognate autoantigen is antigen segregation. Under normal conditions, the autoantigen is sequestered due to intracellular expression or existence at immunoprivileged sites [1]. However, anergic or ignorant lymphocytes can still be activated under certain circumstances, e.g. with sufficient (co-)stimulation, during inflammation or after heavy tissue damage, making the self-antigen accessible and increasing its availability in the periphery [1,34,37].

Regulatory T cells can suppress autoreactive lymphocytes in the periphery

Another important mechanism of self-tolerance in the periphery is the inhibition of autoreactive lymphocytes by regulatory T cells (Tregs). Tregs are a heterogeneous subset of $CD4^+$ T helper cells developing either from thymus (natural Tregs) or in the periphery (induced Tregs) [39]. It is suggested that natural Tregs express TCRs with higher affinity for self-antigens during thymic development and are even rescued from clonal deletion, thus, being more self-reactive than conventional T cells [1,40]. Treg activation and proliferation is dependent on recognition of its cognate antigen, hence its suppressive capacity is antigen-dependent. However, it is still under debate whether autoreactivity is increased among Tregs or whether it is rather an exception compared to conventional T helper cells [41]. Nevertheless, they are able to recognize self-antigens implicated in autoimmune diseases, which allows them to suppress autoimmunity as a peripheral tolerance mechanism [41,42]. Natural Tregs are able to inhibit the immune response of activated autoreactive T cells via IL-10 and TGF-β, among other mechanisms, thereby preventing their development into effector cells or their effector functions [39,42]. A defective regulation by Tregs, such as reduction or absence of Tregs or dysregulation of their functions, has been found in many human autoimmune disorders and under experimental conditions [43,44].

3.1.3 The anti-inflammatory cytokine interleukin-10

In 1989, FIORENTINO and colleagues first described IL-10 as cytokine synthesis inhibitory factor (CSIF) due to its ability to suppress the activation and effector functions of murine Th1 cells [45]. However, subsequent studies revealed that IL-10 is a pleiotropic cytokine produced by a broad range of immune cells, which acts on various cell types throughout the body.

Different leukocytes are able to produce IL-10 after stimulation

IL-10 is secreted by innate and adaptive immune cell types, including DCs, monocytes/macrophages, neutrophils, different B- and T-lymphocyte subsets as well as non-immune cells such as keratinocytes [46,47]. Under steady state conditions, only a low frequency of cells produces IL-10 but the expression can be induced by different stimuli dependent on the target cell. Pathogen-derived products (e.g. LPS) are able to induce IL-10 expression by different myeloid cells, and high doses of APC-presented antigens and IL-12 favor the development of IL-10-producing T helper cells [48,49]. In addition, TFG-β can induce the production of IL-10 in Tregs [48]. Furthermore, B cells have been shown to

represent an important source of IL-10 (chapter 3.1.4), stimulated by various mechanisms including TLRs (e.g. via LPS or CpG-oligonucleotides) and CD40 ligation as well as BCR signaling [50]. Similarly, different pro- and anti-inflammatory cytokines, such as IL-21, IL-6, IL-1β or IL-35, can induce IL-10-producing B cells in humans and mice [51].

IL-10 suppresses the expression of proinflammatory target genes

It has been shown that human and murine IL-10 are 73 % identical with well conserved sequences [52] and act as homodimers on cells expressing the heterotetrametric IL-10 receptor (IL-10R) complex comprised of two IL-10R1 and two IL-10R2 subunits with distinct functions [53-55]. IL-10R1 bears the high affinity ligand-binding domain and is constitutively expressed on most hematopoietic cells but can also be up- or down-modulated after cell activation. By contrast, IL-10R2 is expressed on many cell types at a basal level. Ligation of the receptor complex leads to the activation of Janus kinase 1 (JAK1), tyrosine kinase 2 (TYK2) and subsequent tyrosine phosphorylation and activation of down-stream transcription factors, such as signal transducer and activator of transcription (STAT)1/3/5 [56,57] or suppressor of cytokine signaling 3 (SOCS3) [58]. These factors translocate to the nucleus and suppress proinflammatory cytokine expression, MHCII-dependent antigen presentation or activation of macrophages, among other functions [59].

IL-10 regulates differentiation, function and survival of hematopoietic cells

Different cell types secrete IL-10 and respond to IL-10 but due to its short half-life of several hours *in vivo*, IL-10 often acts locally, e.g. at the site of inflammation [47,60]. Since the IL-10R is expressed on many hematopoietic and some non-hematopoietic cells (keratinocytes, endothelial cells) and is able to suppress proinflammatory functions, IL-10 represents a crucial factor for limiting the magnitude of inflammatory responses and to restore tissue homeostasis. In particular, IL-10 modulates the expression of cytokines/chemokines and cell surface molecules involved in the response to pathogens but also in autoimmune inflammation [46,47]. IL-10 can directly act on monocytes/macrophages inhibiting the release of proinflammatory cytokines and chemokines important for the attraction of other myeloid cells to the site of inflammation [46]. In addition, phagocytosis and nitric oxide production by macrophages and respiratory burst by neutrophils is inhibited by IL-10 [61,62]. Furthermore, IL-10 not only directly suppresses the proinflammatory cytokine production by T cells but also indirectly inhibits activation and proliferation of these cells by down-regulation of MHCII and other costimulatory receptors on antigen-presenting DCs and macrophages [46,63]. Since T cells

are also able to produce IL-10, in turn suppressing MHCII-dependent T-cell activation, this represents a negative feedback loop that prevents immunopathology [48]. Interestingly, anergy of T cells and differentiation of regulatory $CD4^+$ T cells can be induced by IL-10, thereby contributing to peripheral tolerance [64,65]. In contrast to T cells, IL-10 positively affects B cells survival, differentiation, antibody production and class switching to IgG1, IgG3 and IgA [46,66,67]. Despite the fact that IL-10 is generally considered an immunosuppressive cytokine, its stimulatory role for B-cell survival and functions has been linked to autoimmune diseases such as SLE [68,69]. Furthermore, IL-10 also impairs pathogen clearance and host defense after an infection, e.g. by inhibition of neutrophils or Th1 responses [70-72].

IL-10 is an important regulator of autoimmune diseases

Since IL-10 exerts various immunoregulatory functions, mainly anti-inflammatory activities, its role in autoimmune diseases has been studied extensively during the last decade. Data gained from experimental autoimmune diseases models suggest that IL-10 has a protective role that is primarily mediated by its ability to suppress proinflammatory cytokine expression and antigen-specific T-cell activation and to support differentiation of regulatory $CD4^+$ T cells [73]. A deficiency of IL-10 exacerbated inflammation and autoimmune pathology in models of rheumatoid arthritis (RA), MS, SLE and pemphigus [74-77] and induced chronic enterocolitis [78]. Moreover, mice transgenic for IL-10 have been shown to be protected from experimental MS due to the regulation of pathogenic T-cell responses [75]. Administration of recombinant IL-10 down-modulates SLE, RA and pemphigus vulgaris, among other diseases [76,77,79]. By contrast, polymorphisms in the IL-10 locus and elevated IL-10 serum levels have been implicated in different autoimmune diseases such as SLE, systemic sclerosis and bullous pemphigoid [80].

3.1.4 IL-10-producing B cells and plasma cells

The production of the anti-inflammatory cytokine IL-10 can be attributed to many cells of the immune system, and IL-10-competent T-cell subsets (e.g. Tregs and type 1 regulatory T cells) have been shown to establish immune tolerance and regulate autoimmunity. However, research over the last decade revealed that especially IL-10 expression by B lineage cells is crucial for the suppression of autoimmune and allergic inflammation [81].

IL-10-producing B cells modulate human and murine autoimmune diseases

B cells have the ability to modulate autoimmune diseases via various mechanisms. Beyond their classical role as producers of pathogenic autoantibodies promoting the disease, they express different cytokines that have the ability to orchestrate autoimmune inflammation directly or indirectly through innate and adaptive immune cells such as T lymphocytes, DCs and monocytes [82]. In particular, B cell-derived IL-6 has been shown to promote T cell-mediated autoimmune diseases such as experimental autoimmune encephalomyelitis (EAE) [83], whereas IL-35-producing B cells counteract the disease [84]. However, inhibitory functions of B lineage cells are mainly achieved by IL-10 through suppression of APC-mediated autoreactive T-cell activation, proinflammatory cytokine expression and induction and maintenance of Tregs [85,86] (figure 1). In 1996, it was already suggested that B cells exhibit an immunomodulatory role under acute autoimmune inflammation [87]. However, the first report that IL-10 from B cells exerts a suppressive function was in 2002 by FILLATREAU and colleagues, which demonstrated that B cell-specific IL-10 deficient mice do not recover from EAE [88]. Meanwhile, the protective role of IL-10$^+$ B cells has been linked to various experimental autoimmune diseases such as collagen-induced arthritis [89], SLE [90] and inflammatory bowel disease [91]. Moreover, plasma cells and plasmablasts were described to be the major producer of IL-10 in murine spleen [84] or lymph nodes [92] and are able to limit ongoing EAE.

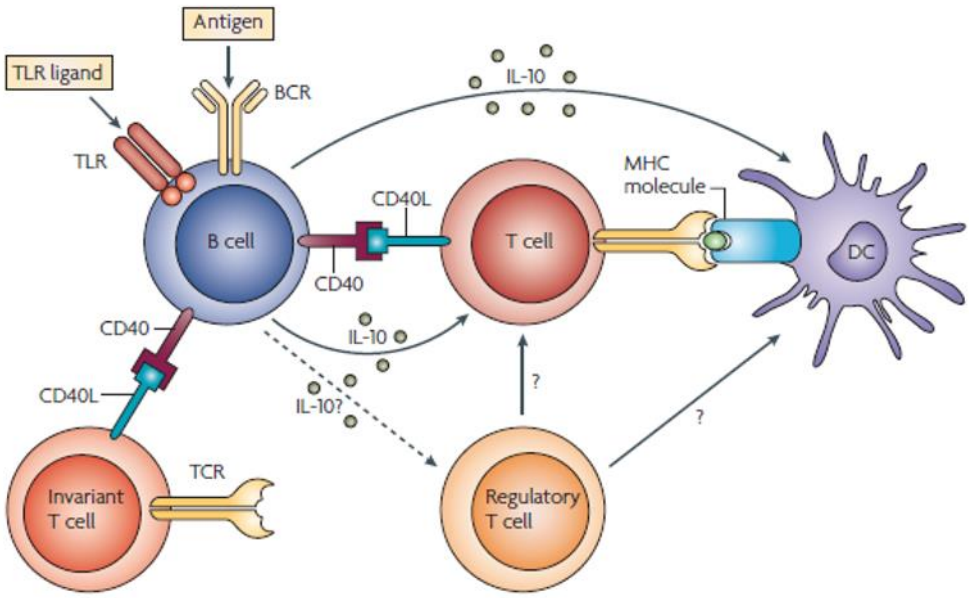

Figure 1: Induction and function of IL-10-producing B cells. B cells can be stimulated to produce interleukin (IL)-10 via ligation of the B-cell receptor (BCR), toll-like receptor (TLR) or CD40. In turn, IL-10 has direct and indirect effects on innate immune cells such as dendritic cells (DCs) and adaptive immune cells such as CD4$^+$ effector T cells and regulatory T cells. Figure adapted from FILLATREAU *et al.* [50] with modifications. *MHC, major histocompatibility complex; CD40L, cluster of differentiation 40 ligand.*

In 2004, DUDDY and colleagues identified IL-10-producing B cells in humans and later described their regulatory capacity in MS patients [93,94]. Later, IWATA and colleagues showed that the frequency of human peripheral IL-10-producing B cells was strongly upregulated in autoimmune diseases such as SLE, RA and autoimmune bullous diseases [95]. However, different studies during recent years revealed no clear correlation between human IL-10-producing B cells and autoimmune disease activity [81,96]. By contrast, the suppressive capacity of these cells was often impaired as they were unable to inhibit pathogenic T-cell responses *in vitro*, e.g. in Bullous pemphigoid [81,97].

The phenotype and origin of "regulatory B cells" is controversial

In line with the IL-10-dependent suppressive functions of regulatory T cells, IL-10-expressing B lineage cells have been termed as "regulatory B cells" (Breg) or "B10" cells. However, unlike Tregs, no transcription factor or surface marker is unique to "regulatory B cells" and thus far, they are only functionally defined by their provision of anti-inflammatory cytokines, such as IL-10 and IL-35, after *in vitro* restimulation and, in turn, their suppressive capacity [51]. Therefore, the origin and phenotype of IL-10-producing B lineage cells is still controversial [98,99]. In experimental mouse models, several phenotypically distinct B-cell subsets have been described to produce IL-10 with the ability to limit autoimmune diseases, including $CD5^+$ $CD1d^{hi}$ "B10" cells, $CD5^+$ B cells, transitional type 2-marginal zone precursors (T2-MZP), marginal zone B cells and $CD138^{hi}$ plasma cells/plasmablasts [98]. Likewise, IL-10-dependent regulatory functions in humans have also been attributed to various stages of B-cell development, such as immature/transitional B cells, naïve B cells, $CD38^{hi}$ plasmablasts and $CD27^+$ memory B cells [51,100]. Additional surface markers have been found to be associated with IL-10 expression in human and murine B cells, e.g. T-cell Ig and mucin domain-containing protein 1 (TIM-1) [101], lymphocyte-activation gene 3 (LAG-3) [71] and tumor necrosis factor receptor 2 (TNFR2) [102]. Therefore, it is still under debate whether any B cell can acquire regulatory properties under certain environmental stimuli or whether these cells arise from specific "Breg"-progenitors through BCR and/or toll-like receptor (TLR) stimulation, thereby indicating a unique lineage [98,99].

Plasma cells and plasmablasts represent an important source of IL-10

Although the phenotype of "regulatory B cells" has not yet been clearly defined, several studies indicate the potential of IL-10-expressing plasma cells/plasmablasts to limit autoimmune diseases, e.g. via inhibition of DC or neutrophil functions [70,84,92]. Autocrine IL-10 has the potential to promote differentiation into IgG- and IgM-secreting

plasmablasts [103] and "B10" cells have been shown to differentiate into antibody-secreting cells with a plasma cell phenotype *in vitro* and *in vivo* [104], indicating that IL-10-competence in B cells is transient through distinct environmental stimuli. Moreover, bone marrow IgM^+ plasma cells acquire competence for IL-10 upon antigenic challenge [105]. Recently, the "regulatory plasmablast" hypothesis from MAURI and BLAIR suggested that different developmental pathways can lead to IL-10-secreting plasma cells/plasmablasts with regulatory functions [106]. On the one hand, immature B cells or other "Breg"-progenitors can mature into "regulatory plasmablasts". Furthermore, "natural regulatory plasma cells", characterized by the surface expression of LAG-3 and IgM, rapidly produce immunosuppressive IL-10 upon TLR ligation [71]. This developmental pathway is supported by the observation that several murine and human "regulatory B cell" subsets are characterized by IgM expression, which could be precursors of rapidly induced IgM^+ "regulatory plasmablasts" [106]. On the other hand, mature B cells in the lymph nodes might develop into regulatory plasmablasts, giving rise to somatically hypermutated and/or class-switched $IL\text{-}10^+$ plasma cells. Recently, strong but non-physiological BCR-crosslinking was shown to induce splenic IL-10-producing $CD138^{hi}$ plasma cells, which limit an autoimmune bullous skin disease via inhibition of neutrophil functions and promotion of $IL\text{-}10^+$ regulatory T cells [70]. Together, these studies suggest that plasma cells/plasmablasts represent a considerable source of IL-10 with the capacity to modulate autoimmune diseases.

3.2 Autoimmune bullous skin diseases

The skin not only represents a protective mechanical barrier but also mediates immune responses against pathogenic microorganisms or other hazardous environmental stimuli [107]. Particularly, resident or attracted immune cells mediate host defense and retain tissue homeostasis. Dysregulation of this fine-tuned immunoregulatory network in the skin can occur in the context of (chronic) inflammatory skin diseases or during autoimmune inflammation. Autoimmune blistering skin diseases (AIBD) are a heterogeneous group of diseases caused by autoantibodies that target adhesion molecules and structural components in skin and mucous membranes [108]. AIBD represent important organ-specific, autoantibody-mediated diseases with distinct, well-known and locally restricted antigens and therefore serve as a paradigm for other autoimmune disorders [109].

Autoantibodies target components of the skin-anchoring complex in AIBD

The human skin is composed of three main layers: epidermis, basement membrane and dermis with the underlying adipose tissue, which harbors various immune cell types such as macrophages, Langerhans cells or T lymphocytes [107] (figure 2A). The basement membrane is connected to the dermis via hemidesmosomal structures containing integrins, laminins and collagens in the *lamina lucida*, *lamina densa* and *sublamina densa* [110] (figure 2B). By contrast, epidermal keratinocytes are connected via desmosomes composed of different desmogleins [108].

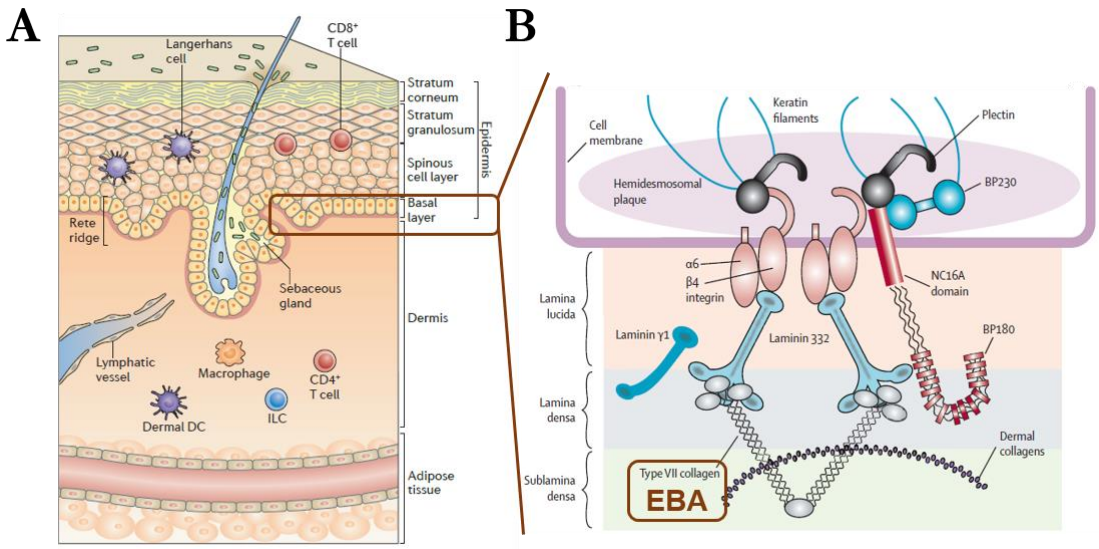

Figure 2: Schematic overview of the skin layers and the hemidesmosomal anchoring complex at the dermal-epidermal junction. (A) Human skin is composed of a thick epidermis layer, basement membrane (basal layer and connected anchoring fibrils), dermis and underlying adipose tissue. The different skin layers are characterized by distinct immune cell types mediating host defense and retaining tissue homeostasis. **(B)** Hemidesmosomal anchoring structures connect epidermis and dermis at the dermal-epidermal junction (DEJ). In pemphigoid diseases, autoantibodies target different molecules at the DEJ, depending on the type of disease, e.g. integrins, laminins or collagens. Epidermolysis bullosa acquisita (EBA) is characterized by autoantibodies against collagen type VII located between *lamina densa* and *sublamina densa*. Figures adapted from PASPARAKIS *et al.* [107] and SCHMIDT and ZILLIKENS [110] with slight modifications. *DC, dendritic cell; ILC, innate lymphoid cell; BP, bullous pemphigoid; NC16A, non-collagenous domain 16A.*

The binding of autoantibodies to the skin initiates an inflammatory cascade, leading to loss of adhesion and blister formation [110]. Depending on the target protein and its corresponding location in the skin layers, AIBD are divided into pemphigus and pemphigoid diseases [111]. Pemphigus diseases are characterized by an intraepidermal loss of adhesion through autoantibodies binding desmosomal structures. However, autoantibodies against hemidesmosomal proteins result in subepidermal split formation, which is a hallmark of pemphigoid diseases (PD) [108,111]. The heterogeneous group of PD contains various diseases with autoantibodies that target different adhesional and

structural molecules at the dermal-epidermal junction (DEJ), e.g. bullous pemphigoid (BP), mucous membrane pemphigoid (MMP) and epidermolysis bullosa acquisita (EBA) [112]. BP and MMP are characterized by autoantibodies that target different adhesion molecules, e.g. BP180, BP230, laminin 332 or α6β4 integrin, whereas EBA is induced only by type VII collagen (COL7)-specific autoantibodies [110] (figure 2B). Of note, COL7 is located at the DEJ but it is not a component of the hemidesmosome and therefore an exception within the group of PD [113].

3.2.1 Epidermolysis bullosa acquisita (EBA)

EBA is a rare autoimmune bullous skin disease

The name epidermolysis bullosa acquisita can be translated as "acquired bullous loosening of the skin" [114]. EBA is a chronic mucocutaneous autoimmune blistering skin disease and belongs to the heterogeneous group of PD [115]. It can affect all age groups, from children to the elderly, with an average onset at the age of 50 years and the most recent reports showed no clear gender predisposition [113,116]. In contrast to the more frequent BP, EBA is considered a rare disease with an estimated prevalence of 2.8 cases per million and an incidence of 0.2 to 0.5 new cases per million inhibitions per year in Germany [116,117]. However, EBA is a prototypical autoimmune disease due to the distinct and locally restricted autoantigen (collagen type VII) in skin and mucous membranes [115]. In addition, experimental EBA mouse models are well established and are able to mimic most features of the disease (chapter 3.2.4). Therefore, EBA serves as a paradigm for other organ-specific, autoantibody-driven autoimmune diseases [118].

EBA is characterized by subepidermal blisters and erosions

The clinical manifestations in EBA patients are very heterogeneous and the disease can be classified into two major subgroups: the non-inflammatory mechanobullous phenotype and the inflammatory phenotype, with the latter accounting for approximately 75% of the cases [115]. The inflammatory subtype mimics other AIBD such as BP or MMP and the most common inflammatory subset is often called BP-like EBA, which was first described by GAMMON and colleagues in 1982 [119,120]. BP-like EBA patients suffer from widespread vesiculobullous eruptions on trunk and extremities, usually accompanied by pruritus, tense bullae and erosions on skin and, less frequently, on mucous membranes [121,122]. The subepidermal blistering and the formation of lesions, erosions and crusts in these patients is mimicked by experimental BP-like EBA models, which have greatly contributed to the understanding of EBA pathogenesis.

3.2.2 Pathophysiology of EBA

Collagen type VII is the autoantigen in EBA

EBA is an antibody-mediated organ-specific autoimmune diseases and due to thorough research during the last decade, it is well-characterized in terms of clinical, histological and immunopathological features [118]. In 1981, deposits of IgG below the lamina densa were observed in EBA skin samples and in 1984, WOODLEY and colleagues identified the 290 kDa COL7 in the basement membrane as the autoantigen for EBA [123,124]. Later, epitope mapping of human and murine COL7 revealed that the 145 kDa non-collagenous domain 1 (NC1) is the immunogenic part where most of the autoantibodies bind [125,126] (figure 3). The anchoring fibrils connect epidermis and dermis (figure 2B) and consist of anti-parallel dimers of COL7 that adhere with the NC1 domain to the lamina densa, whereas COL7 itself is a homotrimer that forms triple-helical structures [127,128]. Subepidermal blister formation develops via a direct loss of anchoring fibril adhesion in the mechanobullous subtype or via an indirect pathway in the inflammatory subtype [127,129].

Autoreactive lymphocytes are activated in the afferent phase of the disease

Most of our knowledge about the EBA pathophysiology is derived from mouse models due to limited human data. The pathogenic scenario suggested for inflammatory EBA (figure 3) is initiated by the break of tolerance to COL7 and the activation of autoreactive T and B lymphocytes, a hallmark of the afferent/initial phase of the disease [130,131]. It has been shown that EBA disease susceptibility depends on environmental factors and genetic predisposition [119]. In particular, susceptibility is strongly associated with the MHC alleles in humans, e.g. the HLA-DR [132,133] and the H2s haplotype in mice [134]. T cells with an autoreactive TCR become activated by APCs presenting fragments of COL7 on MHCII and provide further help for autoreactive B cells. Circulating autoreactive T cells have been found in humans and mice [131,135] and, at least in mice, the disease induction was $CD4^+$ T cell-dependent [136,137]. Interestingly, different APCs (e.g. B cells and DCs) are able to support an autoreactive T-cell response [137] and a Th1-like cytokine profile has been linked to the disease in experimental EBA models [138].

Autoantibodies bind to the dermal-epidermal junction

Autoreactive B cells become activated and develop into autoantibody-secreting plasma cells in peripheral lymph nodes [135], which produce mainly immunoglobulins of the IgG subclass (IgG1, IgG3, IgG4), however, pathogenic IgA has also been found in EBA patients [115,139,140]. In mice, the deposition of IgG2a and IgG2b autoantibodies was

associated with disease susceptibility [134,141]. Direct immunofluorescence microscopy revealed a rapid binding of COL7-specific autoantibodies at the murine DEJ within 24 hours [142]. Although autoantibodies are a prerequisite to induce skin inflammation, they are not sufficient to induce the disease, since PD-specific antibodies have been found in healthy individuals [143]. After binding of anti-COL7 antibodies at the NC1 domain of COL7 at the DEJ [125], the complement system is activated via the Fc domain of complement-fixing antibodies, such as IgG1/IgG3 in humans [140] and IgG2a/IgG2b in mice [138,141]. These processes are regarded as the first steps of the effector phase [119]. Important complement factors in EBA are C3, which linearly deposits at the DEJ via Fc-mediated fixation, and C5a, which is a potent chemoattractant for neutrophils [144-146]. In particular, the alternative pathway of the complement system has been shown to be required for blister induction, and C5- as well as C5aR-deficient mice are protected from the disease in mouse models of EBA [147-149].

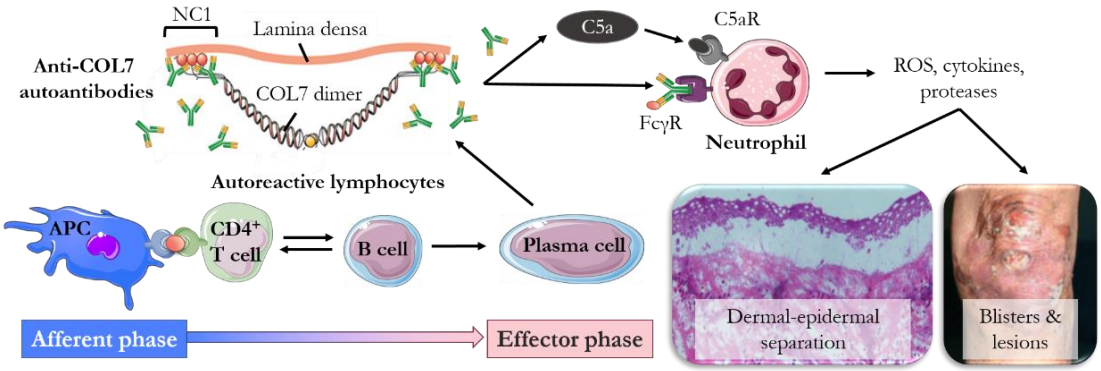

Figure 3: Pathogenic scenario for inflammatory EBA. Due to a break of tolerance, **a**utoreactive lymphocytes become activated in the afferent phase and plasma cells produce autoantibodies targeting the non-collagenous domain 1 (NC1) of collagen type VII (COL7) at the dermal-epidermal junction. In the effector phase, neutrophils are recruited to the skin, which in turn are activated via C5a receptors (C5aR) and/or immune complex-binding Fcγ receptors (FcγRs). Neutrophils release reactive oxygen species (ROS), proinflammatory cytokines and proteases, leading to cleavage of the anchoring complex, dermal-epidermal separation, inflammation and finally blister formation. Principle scheme adapted and combined from KIM and KIM [127] and KOGA *et al.* [119] with modifications. Histological picture from LUDWIG [115] and clinical picture from KIM and KIM [127]. *APC, antigen presenting cell; C5a, complement factor 5a.*

Neutrophils are recruited to the skin and mediate tissue injury

Histological analysis of human blister infiltrates revealed that lymphocytes and granulocytes, primarily neutrophils, are recruited to the site of inflammation [150,151]. Moreover, EBA mouse models demonstrated that neutrophils are the major innate effector cells responsible for blister formation [152]. It is suggested that neutrophils are attracted to the site of inflammation, e.g. via C5a or proinflammatory cytokines, which is dependent on distinct adhesion molecules [127,130]. C5a/C5aR binding can induce upregulation of

activating Fcγ receptors (FcγRs) and down-regulation of the inhibitory FcγRIIb on neutrophils [153]. In an FcγR-dependent manner, neutrophils bind the Fc-part of anti-COL7 antibodies, resulting in immune complex-mediated neutrophil activation [112]. Interestingly, T-cell cytokines such as IFNγ and IL-17 are able to modulate the Fc glycosylation pattern of autoantibodies [154]. A pro- or anti-inflammatory pattern has been reported to affect the disease outcome of experimental EBA, e.g. via their modulation of FcγR expression or C5aR signaling inhibition [155,156]. Once the neutrophil is activated by the tissue-bound immune complexes, a signaling cascade via Src kinases [157] is activated, which leads to the release of reactive oxygen species (ROS), matrix metalloproteinases (MMPs) and further proinflammatory cytokines [158,159]. Subsequently, matrix components are proteolyzed and inflammation is further promoted, finally leading to loss of adhesion between dermis and epidermis, infiltration of additional inflammatory cells and subepidermal blister formation [119,127]. Interestingly, monocytes/macrophages are present in lesional skin from diseased mice and are, e.g. via their ROS production, involved in blister formation [160], but their role in the EBA pathogenesis is not clear yet.

T and B lymphocytes modulate the EBA effector phase

Apart from innate effecter cells such as neutrophils and monocytes, several T-cell subsets have been suggested to modulate the effector phase of EBA. T cell-deficient mouse strains were almost completely protected from EBA induction [136,161]. In contrast to $CD4^+$ and $CD8^+$ T cells, γδ T cells and NKT cells support cutaneous inflammation, e.g. via neutrophil recruitment, whereas regulatory T cells have the capacity to suppress inflammation and blistering in the effector phase of EBA or BP [161-163]. Furthermore, Th17 cells are promotors of EBA development [164]. Although B lymphocytes represent a prominent cell type in blister fluids, the contribution of B cells/plasma cells in the EBA effector phase has not yet been investigated in detail. However, induced IL-10^+ plasma cells have been reported to exhibit profound anti-inflammatory activities in EBA, at least during experimental plasmacytosis [70].

3.2.3 Treatment options

EBA is diagnosed by circulating and tissue bound autoantibodies

Clinical manifestations of EBA are heterogeneous and often not easy to distinguish from other AIBD such as BP [165]. Since an appropriate diagnosis of EBA is essential for the disease outcome and survival, the international bullous disease group defined a diagnosis

criteria catalogue for EBA in 2018 [121]. In particular, confirmation of linear IgG, IgA and/or C3 deposition at the DEJ by direct immunofluorescence of perilesional skin and detection of circulating COL7-specific autoantibodies were determined. In addition, EBA is characterized by dermal- but not epidermal-binding of autoantibodies from patients in salt-split human skin evaluated via indirect immunofluorescence [146].

Treatment of EBA relies on corticosteroids and immunosuppressive agents

EBA is a rare autoimmune disease, thus randomized therapy trials are lacking and EBA therapy remains a challenge [119]. The conventional treatment with systemic corticosteroids (e.g. prednisolone) and immunosuppressive agents (e.g. methotrexate or azathioprine) is the first choice and the treatment regimen is entirely dependent on the expertise of specialized clinicians [115]. However, the conventional treatment often does not result in clinical improvement and can harbor adverse side-effects due to systemic immunosuppression [115]. Apart from anti-inflammatory corticosteroids, high-dose intravenous immunoglobulin (IVIG) [166], Dapsone [167,168] and rituximab (anti-CD20 antibodies) [169,170] and combinations of them have been used to treat EBA more successfully, at least in individual treatment-resistant cases [115].

Mouse models are crucial for the development of new treatment approaches

The molecular mechanisms driving the pathogenesis of PD are only poorly understood. Experimental EBA mouse model have been studied in detail in recent years, allowing further insights into the pathogenesis and novel treatment options for the rare human EBA and related diseases. Mouse models revealed new treatment options for EBA and other AIBD, e.g. by specifically targeting the autoantibody generation (afferent phase) or by inhibition of the autoantibody-induced tissue damage (effector phase) [171]. In particular, blockade of heat-shock protein 90 (HSP90) prevented the onset and improved the established disease in mice [172] and is currently investigated in clinical trials [171]. Although various proinflammatory cytokines such as tumor necrosis factor (TNF) and granulocyte-macrophage colony-stimulating factor (GM-CSF) have been suggested as therapeutically inhibitable targets for interference with murine EBA [160,173], the induction or application of anti-inflammatory cytokines such as IL-10 as a treatment option have not been studied thus far.

3.2.4 Experimental mouse models for EBA

During the last decade, animal models for autoimmune bullous diseases have been extensively studied, providing further insights into the pathogenesis of EBA and related blistering diseases. Moreover, novel treatment strategies have been developed and evaluated with these mouse models, which is a prerequisite for the establishment of individual patient-based therapies with minimal side-effects [171]. Experimental EBA models serve as a paradigm for other pathogenically related autoantibody-driven autoimmune diseases, since the autoantigen and the pathogenic scenario for EBA have been investigated in detail (chapter 3.2.2) [118]. EBA mouse models can be divided into two *in vivo* systems: the autoantibody-transfer models and the autoantigen-immunization models. EBA can be either induced by the transfer of autoantibodies targeting immunodominant epitopes of murine COL7 (mCOL7) in skin and mucous membranes or established by immunization with the autoantigen, which is a fragment of the NC1 domain of mCOL7 (figure 4A) [174].

Induction of EBA by transfer of autoantibodies

The autoantibody-transfer-induced EBA model in adult mice was first described by SITARU and colleagues in 2005 [149]. EBA was induced by repeated transfer of purified polyclonal rabbit IgG antibodies that were generated in rabbits by immunization with different fragments of the NC1 domain of mCOL7. Subepidermal blisters developed after two to four days in a dose-dependent manner, resembling the clinical signs in humans. Moreover, linear deposits of anti-mCOL7 IgG and C3 at the DEJ, circulating autoantibodies and neutrophil infiltration were found in diseased mice. Extensive widespread lesions and inflamed skin were seen after four to seven days after the first injection of autoantibodies. In contrast to the immunization-induced model, various inbred mouse strains, e.g. C57Bl/6 or BALB/c mice, were shown to be susceptible to passively induced EBA [149].

During recent years, various improvements and modifications of this model have been established [130]. In particular, the transfer of human COL7 and serum from EBA patients can induce skin inflammation and lesions in mice [175,176]. Moreover, transfer of affinity-purified specific rabbit anti-mCOL7 IgG targeting a distinct subdomain of NC1 induces clinical signs of EBA in mice in a dose-dependent manner [177]. Using affinity-purified specific anti-mCOL7 IgG, much lower amounts of the antibody are needed to induce the disease [161,177] compared to total rabbit IgG from mCOL7-immunized rabbits [149]. However, the usage of polyclonal rabbit IgG induces a xenogeneic response and therefore contributes to inflammation in this model, especially later in the disease [178].

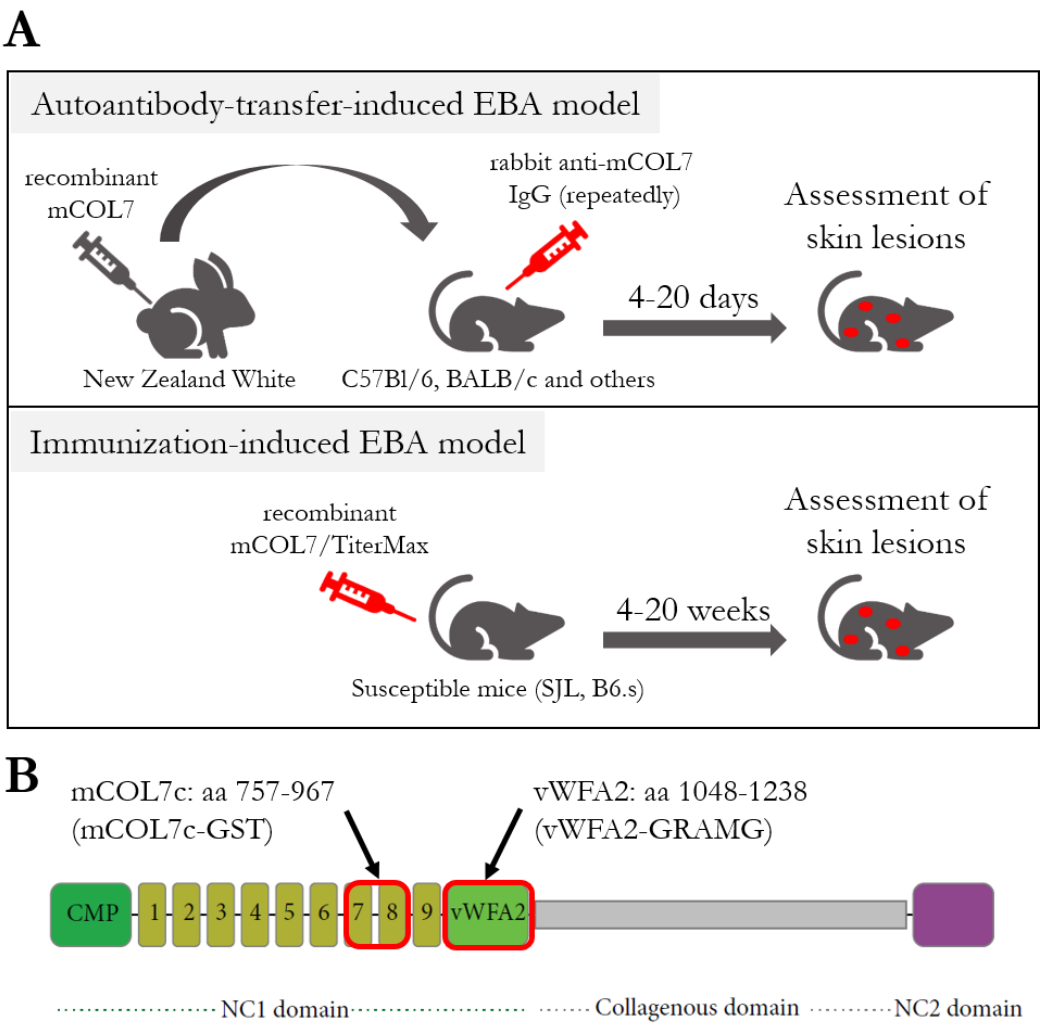

Figure 4: General principle of the autoantibody-transfer-induced and immunization-induced EBA model and schematic structure of murine collagen type VII. (A) Experimental setup for the autoantibody-transfer-induced EBA model (upper panel) and the immunization-induced EBA model (lower panel). New Zealand White rabbits are immunized with a recombinant fragment of murine collagen type VII (mCOL7) and total or specific rabbit anti-mCOL7 IgG is repeatedly injected into C57Bl/6 or other mouse strains to induce EBA skin lesions and blistering from day four. By contrast, susceptible mice such as SJL or B6.s are immunized with an emulsion of recombinant mCOL7 in TiterMax and EBA skin disease manifests from four weeks. **(B)** mCOL7 consists of a collagenous domain flanked by two non-collagenous (NC) domains. Recombinant fragments used for induction of EBA in the immunization-induced model are mCOL7c and von Willebrand factor A–like domain 2 (vWFA2), which are located at different places within the NC1 domain. mCOL7c covers the amino acids (aa) 757-967 and vWFA2 the amino acids 1048-1238. Part **(A)** adapted from BIEBER *et al.* [174] with modifications according to SITARU [118]. Part **(B)** adapted from LUDWIG [115] with modifications according to IWATA *et al.* [137]. *CMP, cartilage matrix protein; GRAMG; additional N-terminal amino acid sequence of vWFA2 for recombinant expression; GST, glutathione S-transferase.*

Induction of EBA by immunization with the autoantigen

The immunization-induced EBA model was established in 2006 by SITARU and colleagues by using a recombinant fragment of mCOL7 [141]. A protein spanning the amino acids 757 to 967 within the NC1 domain of mCOL7 was linked to a glutathione S-transferase (GST)-tag for purification ("mCOL7c-GST") and then used for subcutaneous

immunization of mice (figure 4B). To boost the immune response, the polymeric adjuvant TiterMax was used and the immunization was repeated three times [141]. Autoantibodies were already detected after one week and mice developed clinical symptoms three to four weeks after immunization, which were preserved for at least 24 weeks. In line with the pathogenic scenario suggested for EBA (chapter 3.2.2), the deposition of complement-fixing IgG2 autoantibodies was associated with disease susceptibility [134,141]. The genetic background of the mouse strain, in particular the MHC haplotype, has a strong influence on the disease susceptibility. Mice carrying the H2s haplotype (e.g. SJL mice) develop signs of blistering and inflammation whereas mice with H2b haplotype (e.g. C57Bl/6 mice) are protected from the disease despite the presence of autoantibodies [134,141].

Although immunization with mCOL7c-GST closely resembles the human clinical phenotype and other pathological features, the GST-tag used for affinity purification induces an additional, mCOL7c-indepenent immune response by generation of GST-specific plasma cells [135]. To circumvent this additive, artificial immune response, IWATA and colleagues developed a new immunization protocol with another recombinant fragment of mCOL7 spanning the amino acids 1048 to 1238 with five additional N-terminal amino acids (GRAMG) for recombinant expression [137] (figure 4B). One subdomain of the NC1 region shows a high homology to the von Willebrand factor, thus, it was termed von Willebrand factor A-like domain 2 (vWFA2) [179]. Epitope mapping of COL7 revealed that EBA patient's sera recognize various immunodominant regions in the NC1 domain [125], and antibodies to different epitopes of this region induce blister formation in mice [126,180], both including the vWFA2 domain.

In line with previous findings, susceptibility to immunization with vWFA2 is strongly dependent on the genetic background of the mouse strain [137]. Susceptible B6.s (B6.SJL-H2^{s} C3^{c}/1CyJ) and SJL mice with an H2s haplotype show serum and tissue-bound autoantibodies as well as C3 deposition at the DEJ. By contrast, non-susceptible C57Bl/6 mice with an H2b haplotype develop circulating and tissue-bound autoantibodies but lack C3 deposits and clinical symptoms. vWFA2-immunized susceptible mice rapidly produce autoantibodies which reach a plateau after three to four weeks whereas the first signs of the disease do not manifest earlier than four weeks after immunization [137]. Susceptible B6.s mice show, independently of the gender, a heavily increasing disease score from week four until the end of the observation period [137].

In contrast to the autoantibody-transfer-induced model mimicking the effector phase, the immunization-induced model reflects the whole pathogenesis of EBA and thus more closely resembles the human disease. For instance, the induction of autoreactive plasma cells and $CD4^+$ T cells in lymph nodes as well as circulating and tissue-bound autoantibodies have been reported in this model [135,137]. Therefore, it is more suitable to investigate preventive and therapeutic treatment approaches as well as long-term interventions [174]. However, the artificial immunization with an antigen-adjuvant mixture must be considered since it does not reflect the cause of the disease in EBA patients [118].

3.3 Aim of the study

Previous work from our group showed that the induction of IL-10-producing plasma cells through injection of a B-cell receptor crosslinking reagent limits EBA skin inflammation, presumably via the inhibition of neutrophils as the major innate effector cells driving the pathogenesis. However, neither the role of IL-10 nor of IL-10-expressing plasma cells in the natural course of the disease have been studied thus far. Therefore, this thesis aims to investigate whether and how naturally occurring IL-10 and in particular IL-10-producing plasma cells have the potential to restrict EBA skin inflammation and blistering in two established mouse models of this disease: the immunization-induced and the autoantibody-transfer-induced model. In addition, this thesis aims to characterize the nature and origin of IL-10-producing plasma cells in the context of the pathophysiological immune response in EBA and their relationship to "regulatory plasma cells", which have been described as potent immunosuppressive cells.

4. Material

4.1 Mice

C57Bl/6J mice were purchased from Charles River Laboratory (Sulzfeld, Germany). All other mouse strains were bred and kept under specific pathogen-free (SPF) conditions in individual ventilated cages (IVC) in the animal facility of the University of Lübeck/Gemeinsame Tierhaltung. IL-10 reporter mice (Vert-x, B6.(Cg)-Il10$^{tm1.1Karp}$; on C57Bl/6J background with H2b haplotype and with H2s haplotype on B6.SJL-H2^{s} C3^{c}/1CyJ background) and B-cell IL-10 knock-out mice (Cd19$^{tm1(cre)Cgn}$ x Il10$^{tm1.1Roer}$) were bred by AG Manz. Susceptible mice with H2s haplotype (B6.s, B6.SJL-H2^{s} C3^{c}/1CyJ) and congenic C57Bl/6J (B6) mice, used for the experiments shown in figure 37-figure 41, were kindly provided by the Department of Dermatology by Dr. Katja Bieber/AG Ludwig. Animals were fed acidified drinking water and standard chow *ad libitum* and held on a 12 h light-dark cycle. Mice used for the experiments were between two and seven months old and only male mice were used. However, the experiments presented in figure 37-figure 44 were performed with mixed genders. All experiments were approved by the Ministerium für Energiewende, Landwirtschaft, Umwelt und ländliche Räume of the state Schleswig-Holstein with the permission number V242-43397/2016 (84-7/16) and were performed by certified personnel under sterile conditions in a laminar flow cabinet.

4.2 Enzymes and primer sequences for genotyping

All transgenic or congenic mice were genotyped using polymerase chain reaction (PCR) prior to experiments. All PCR protocols and cycling conditions are listed in chapter 5.1. The enzymes used for PCR are listed in table 1. All primers were purchased from biomers.net (Ulm, Germany) and sequences are listed in table 2.

Table 1: Enzymes used in PCR for genotyping of transgenic and congenic mice

Enzyme	Company	Product No.
DreamTaq DNA polymerase (5 U/µl) with 10 x PCR buffer	Thermo Fisher Scientific	EP0703
HotStarTaq Plus DNA polymerase (5 U/µl) with 10 x PCR buffer	Qiagen GmbH	203603
Kapa2G Fast HotStart Genotyping Mix (1 U/µl)	Kapa Biosystems/ Thermo Fisher Scientific	KK5621

Table 2: Primer sequences for genotyping

Gene	Mouse line	Primer sequence 5'-3'	Amplicon
Il10-eGFP	B6.s IL-10 reporter	Common primer AGTAGGGGAACCCTCTGAGC	370 bp (wildtype) or 250 bp (transgene)
		Wildtype forward CCTCTGATACCTCAGTTCCCATT	
		Transgene reverse GTGGGCTCTATGGCTTCTGA	
Cd19cre	B-cell IL-10 KO	Wildtype forward CCT CTC CCT GTC TCC TTC CT Wildtype reverse TGG TCT GAG ACA TTG ACA ATC A	477 bp (wildtype)
		Transgene forward AAA TGC TTC TGT CCG TTT GC Transgene reverse ATG TTT AGC TGG CCC AAA TG	163 bp (transgene)
Il10flox	B-cell IL-10 KO	Forward CCA GCA TAG AGA GCT TGC ATT ACA	480 bp (wildtype) or 514 bp (transgene)
		Reverse GAG TCG GTT AGC AGT ATG TTG TCC AG	
MhcII (D17Mit22)	B6.s IL-10 reporter	Forward coupled to Cy5 Cy5-GGTAAGCATTAGATAGAGAG	160 bp (wildtype) or 158 bp (congenic)
		Reverse TTATGATCTCCACACACGTG	

4.3 Reagents for EBA induction in mice

Experimental EBA was either induced by subcutaneous (s.c.) injection of the antigen/adjuvant-emulsion (immunization-induced model) or by intraperitoneal (i.p.) injection of the autoantibody (autoantibody-transfer-induced model). All regents are listed in table 3. vWFA2 and autoantibodies were stored at -20°C and TiterMax at 4°C and were diluted with phosphate-buffered saline (PBS) to the final concentration prior to use.

Table 3: Reagents used for induction of experimental EBA

Reagent	Stock concentration	End concentration	Source
vWFA2 (antigen)	1.8 or 2 mg/ml in PBS	2 mg/ml in PBS and 1 mg/ml in TiterMax	Provided by the Department of Dermatology, University of Lübeck (Dr. K. Bieber)
TiterMax Adjuvant	-	-	HISS Diagnostics/CytRx Corporation #R-10
Total rabbit anti-mCOL7c IgG	2.5 mg/ml in PBS	2.5 mg/ml	Provided by the Department of Dermatology, University of Lübeck (S. Tofern)
Specific rabbit anti-mCOL7c IgG	0.7 mg/ml in PBS	0.7 mg/ml	Provided by the Department of Dermatology, University of Lübeck (Dr. K. Bieber)

4.4 Antibodies for injection in mice

Antibodies used for i.p. injection into mice were stored at -80°C and diluted under sterile conditions with PBS to the final concentration prior to use (table 4).

Table 4: Antibody used for IL-10 receptor blockade and control antibody

Antibody	Clone	Stock concentration	End concentration	Source
Anti-IL-10R antibody	1B1.3	2.3 mg/ml	2 mg/ml	In-house production
IgG from rat serum	polyclonal	2.5 mg/ml	2 mg/ml	Sigma Aldrich #I4131

4.5 Antibodies for flow cytometry

In table 5, all antibodies used for flow cytometry are listed. Commercially available rat IgG1, IgG2a and IgG2b (purchased from Biolegend or eBiosciences) with the same fluorochrome as the staining antibody were used as isotype controls. As an exception, anti-IL-17A IgG (allophycocyanin, APC) was used as an isotype control for anti-TACI IgG, anti-IL-10 IgG (APC/Cy7) for anti-CD19 IgG and anti-Ly6G IgG, and anti-CD5 IgG (phycoerythrin (PE)/Cy7) for anti-NK1.1 IgG. For all isotype controls, the same amount (ng) was used as for the staining antibody. All antibodies were stored in the dark at 4°C and titrated for the best dilution prior to experiments. The final concentration was between 0.25 and 1 μg/ml.

Table 5: Primary antibodies for flow cytometry and their specification

Primary Antibody	Con-jugation	Clone	Host species and isotype	Source
Anti-CD11b	Pacific blue	M1/70	Rat IgG2b	Biolegend #101223
Anti-CD138	PE	281-2	Rat IgG2a	Biolegend #142504
Anti-CD154 (CD40L)	APC PE	MR1	Arm. hamster IgG	Biolegend #106509 Biolegend #106506
Anti-CD16 (FcγRIII)	Uncoupled	polyclonal	Goat IgG	Thermo-Fisher #PA5-47230
Anti-CD16.2 (FcγRIV)	APC	9E9	Arm. hamster IgG	Biolegend #149506
Anti-CD16/ CD32	Uncoupled	2.4G2	Rat IgG2b	BD Biosciences #553142
Anti-CD161b/c (NK1.1)	PE/Cy7	PK136	Mouse IgG2a	Biolegend #108713
Anti-CD185 (CXCR5)	BV650	L138D7	Rat IgG2b	Biolegend #145517
Anti-CD19	APC/Cy7 PE/Cy7	6D5	Rat IgG2a	Biolegend #115529 Biolegend #115519
Anti-CD192 (CCR2)	PE/Cy7	Sa203G11	Rat IgG2b	Biolegend #150611
Anti-CD223 (LAG-3)	PE/Cy7	C9B7W	Rat IgG1	Biolegend #125225
Anti-CD267 (TACI)	APC	8F10-3	Rat IgG2a	eBioscience #17-5942-82
Anti-CD279 (PD-1)	PE/Cy7	29F.1A12	Rat IgG2a	Biolegend #135215
Anti-CD3	APC/Cy7 FITC	17A2	Rat IgG2b	Biolegend #100221 Biolegend #100203
Anti-CD32b (FcγRIIb)	FITC	K9.361	unknown	Provided by AG Köhl
Anti-CD4	APC A405 eF450	GK1-5 GK1.5 RM4-5	Rat IgG2b Rat IgG2b Rat IgG2a	Biolegend #100412 In-house prod. eBioscience #48-0042-82
Anti-CD45R (B220)	A405 A647	RA3.B2	Rat IgG2a	In-house prod.
Anti-CD5	PE/Cy7	L17F12	Mouse IgG2a	Biolegend #364007
Anti-Foxp3	PE	FJK-16s	Rat IgG2a	eBioscience #12-5773-82
Anti-IFNγ	APC BV711	XMG1.2	Rat IgG1	Biolegend #505810 Biolegend #505835

Anti-IgM	PE/Cy7	eB121-15F9	Rat IgG2a	eBioscience #25-5890-82
Anti-IL-10	FITC APC APC/Cy7	Jes5-16E3	Rat IgG2b	Biolegend #505006 Biolegend #505010 Biolegend #505035
Anti-IL-17A	BV650 APC	TC11-18H10.1 ebio17B7	Rat IgG1 Rat IgG2a	Biolegend #506929 eBioscience #17-7177-81
Anti-IL-21	PE	mhalx21	Rat IgG2a	eBioscience #12-7213-82
Anti-Ly6G	APC/Cy7	1A8	Rat IgG2a	Biolegend #127623
Anti-γδ TCR	PE	UC7-13D5	Arm. Hamster IgG	Biolegend #107507

For the uncoupled anti-CD16 (FcγRIII) antibody, a secondary PE-labeled donkey anti-goat IgG was used (table 6). A control omitting the primary anti-CD16 antibody and a fluorescence minus one (FMO) control sparing both antibodies were used.

Table 6: Secondary antibodies for flow cytometry and their specification

Secondary antibody	Conjugate	Source
Donkey anti-goat IgG ($F(ab)_2$)	PE	Santa Cruz Biotechnology #Sc-3857

4.6 Antibodies for enzyme-linked immunosorbent assay (ELISA)

For detection of vWFA2-specific serum autoantibodies, secondary antibodies listed in table 7 were used for an ELISA. All antibodies were stored at 4°C and diluted to 1 µg/ml with PBS/0.5 % bovine serum albumin (BSA) prior to use.

Table 7: Secondary antibodies used for ELISA and their specificity

Antibody	Conjugation	Source
Goat anti-mouse IgG	Biotin	Southern Biotech #1030-08
Goat anti-mouse IgG1	Biotin	Southern Biotech #1070-08
Goat anti-mouse IgG2b	Biotin	Southern Biotech #1090-08
Goat anti-mouse IgG2c	Biotin	Southern Biotech #1079-08
Goat anti-mouse IgM	Biotin	Southern Biotech #1021-08

4.7 Stimuli and inhibitors

Stimuli and inhibitors are listed in table 8. Phorbol 12-myristate 13-acetate (PMA) and ionomycin were solved in dimethyl sulfoxide (DMSO), LPS was solved in RPMI1640 medium and all reagents were stored at -20°C. Recombinant murine (rm)IL-10 was solved in sterile PCR water, rmC5a was kindly provided by AG Köhl and both reagents were stored at -80°C. Brefeldin A was stored at 4°C and directly added to cell culture medium.

Table 8: Stimuli and inhibitors used for modulation of cells *in vitro*

Reagent	Stock concentration	Final concentration	Source
Brefeldin A	3 mg/ml	3 µg/ml	eBioscience #00-4506-51
Ionomycin Calcium Salt	1 mg/ml	1 µg/ml	Merck Millipore #407952
Lipopolysaccharide (LPS) from *E.coli* serotype 055:B5	1 mg/ml	10 µg/ml	Sigma Aldrich #L4524
Phorbol 12-myristate 13-acetate (PMA)	1 mg/ml 0.5 mg/ml	3.33 ng/ml 5 µg/ml	Sigma Aldrich #79346 Provided by AG Köhl
rmC5a	12.5 mM	12.5 nM	Hycult Biotech #HC1101 Provided by AG Köhl
rmIL-10	100 µg/ml	1-100 ng/ml	Immunotools #12340102

4.8 Commercial kits and buffers

Table 9: Commercially available kits and buffers and their specifications

Kit	Source	Application
ALP reagent kit	Roche #12173107	ELISA
Dulbecco's phosphate-buffered saline (DPBS) (1 x)	Gibco/Thermo Fisher Scientific #14190	For cell preparation, cell culture and assays
Fixation buffer (1 x) and Permeabilization Wash (10 x)	Biolegend #420801 Biolegend #421002	Intracellular cytokine staining
Fluorochrome coupling kit Alexa Fluor 405	Invitrogen #A30000	Coupling of vWFA2 for flow cytometry
FOXP3 Fix/Perm Buffer Set	Biolegend #421403	Foxp3 staining
Hemacolor Rapid staining of blood smear	Merck Millipore #1116610001	Neutrophil migration assay
Pierce BCA Protein Assay kit	Thermo Fisher Scientific #23225	Protein determination (for MPO assay)
Red blood cell lysis buffer (10 x)	Biolegend #420301	Bone marrow and blood cell preparation

4.9 Buffers and solutions

Unless otherwise specified, buffers were prepared with double-distilled water (ddH_2O).

Table 10: Buffers, solutions and their ingredients

Buffer/Solution	Ingredients	Source
Agarose gel	1x TAE buffer 1.5 % or 1.2 % Agarose 0.0016 % GelRed Stain	In-house production Life Technologies #16500-500 Biotrend #41003-1
Anesthetics (1 x)	5 mg/ml Ketanest S 1.5 mg/ml Rompun	Pfizer #847028001G Bayer Healthcare # 1320422
Bicarbonate buffer (1 M)	0.2 M $NaHCO_3$ 0.2 M Na_2CO_3 pH 9.6	Th. Geyer #6885.2 VWR International #1.063.920.500
Cell culture medium	RPMI1640+Glutamax 10% FCS 1% Penicillin/Streptomycin 0.2 % β-2-mercaptoethanol	Gibco/Thermo Fisher #61870-044 Gibco/Thermo Fisher #10270-106 Gibco/Thermo Fisher #15140-122 Th. Geyer # M3148
DNase I	100 mg/ml DNase I 0.15 M NaOH	Roche Diagnostics #10104159001 Th. Geyer #50000302
Extraction buffer	0.1 M Tris HCl 0.154 M NaCl	Merck Millipore #648317 Merck Millipore #567440
Medium for ROS release assay	RPMI1640 w/o phenol red 1% FCS	Gibco/Thermo Fisher #11835-063 Gibco/Thermo Fisher #10270-106
PBS buffer (10 x)	80 g/l NaCl 2 g/l KCl 18 g/l Na_2HPO_4 x 2 H_2O 2.4 g/l KH_2PO_4 pH 7.4	Merck Millipore #567440 Merck Millipore #529552 Sigma Aldrich #30435 Merck Millipore #104877
PBS/0.5 % BSA (PBS/BSA)	0.5 % BSA 1x PBS	Sigma Aldrich #A9418 In-house production
Potassium phosphate buffer	0.2 M KH_2PO_4 0.2 M K_2HPO_4 pH 6.0	Merck Millipore #104877 Merck Millipore #137010
TAE buffer (50 x)	100 mM Tris HCl, pH 8.5 200 mM NaCl 5 mM EDTA, pH 8 0.2 % w/v SDS	Merck Millipore #648317 Merck Millipore #567440 Sigma Aldrich #ES134 Bio-Rad Laboratories #161-0301
TE buffer (1 x)	10 mM Tris HCl 1 mM EDTA, pH 8	Merck Millipore #648317 Sigma Aldrich #ES134
TLS buffer (1 x)	2 M Tris base 50 mM EDTA, pH 8 10 M Acetic acid	Sigma Aldrich #93362 Sigma Aldrich #ES134 Th. Geyer #3738.4
Washing buffer	1x PBS 0.05 % Tween20	In-house production Sigma Aldrich #P7949

4.10 Other reagents and chemicals

Table 11: Reagents and chemicals not listed in other tables thus far

Reagent	Source	Application
1-Step Turbo TMB-ELISA Substrate Solution	Thermo Fisher Scientific #34022	MPO assay
DMSO	Sigma Aldrich #276855	Pre-dilution of PMA/Ionomycin
DNA Gel Loading Dye (6 x)	Fermentas #R0611	Gel electrophoresis
DNA Size Standard Kit 400	Beckman Coulter #608098	Genotyping of B6.s mice
dNTP set (100 mM)	Fermentas #R0182	PCR
Ethanol absolute (100 %)	Th. Geyer #2246	DNA Isolation
Eye cream	Bepanthen	For mice
Fixable Viability Dye eF780	eBioscience #65-0865-14	Live/Dead stain
GeneRuler DNA Ladder Mix (0.1 µg/ml)	Thermo Scientific #SM0333	Gel electrophoresis
HTAB (5 %)	Sigma Aldrich #814119	MPO assay
Luminol (97 %)	Sigma Aldrich #123072	ROS release assay
Mineral Oil	Beckman Coulter #B1010	Genotyping of B6.s mice
Myeloperoxidase from human leukocytes (25 U)	Alexis biochemicals #Alx-200-600A-4025	MPO assay
Propan-2-ol	Th. Geyer #I9516	DNA Isolation
Proteinase K from *Tritrachium Album*	Sigma Aldrich #P6556	Tissue digestion for genotyping
Sample loading solution (SLS)	Beckman Coulter #608082	Genotyping of B6.s mice
Separation Buffer	Beckman Coulter #608012	
Separation Gel	Beckman Coulter #391438	
Sodium Azide BioUltra 99.5%	Th. Geyer #71289	Protein storage after coupling to A405
Spitacid	Ecolab Healthcare #303840	Disinfection
Streptavidin-ALP conjugate (1 000 U)	Sigma Aldrich #11089161001	ELISA
Sulfuric acid (100 %)	Sigma Aldrich #1.12223	MPO assay
Trypan blue solution 0.4 %	Life Technologies #15250-061	Cell counting
VectaMount permanent mounting medium	Vector Laboratories #H-5000	Neutrophil migration assay
Zombie Yellow Fixable Viability Dye	Biolegend #423103	Live/Dead stain

4.11 Laboratory equipment and material

Laboratory materials of daily use such as pipettes, pipette tips, reaction tubes and cell culture material (plates, serological pipettes) were purchased from Sarstedt, Eppendorf and Th. Geyer. Further equipment and materials are listed in table 12 and table 13.

Table 12: Laboratory equipment and provider

Equipment	Source
Beckman Coulter Ceq 8800 Genetic Analysis System	Beckman Coulter
CASY TT cell Counting System	OLS Omni Life Science
Centrifuge 5810 R	Eppendorf
Centrifuge Microfuge 22R	Beckman Coulter
CO_2 Incubator Autoflow Direct Heat (NU5510/E)	NuAire
Compact M gel chamber	Biometra Biosciences
Image Quant 350 (UV transilluminator)	GE Healthcare
Julabo SW-20C shaking water bath	Julabo
Labocult Incubator for ELISA plates	Servoprax
Laminar Flow Cabinet (LabGard Class II Biological Safety Cabinet NU-437)	NuAire/IBS Integra Biosciences
Light Microscope DMi1	Leica Microsystems
LSRII Flow cytometer	BD Biosciences
Nanodrop ND-1000 Spectrometer	PeqLab Biotechnology
Omega FLUOstar ELISA reader	BMG Labtech
pH meter	Mettler Toledo
Pipetus	Hirschmann Instruments
Polymax 1040 plate shaker	Heidolph Instruments
PowerPac HC or Basic (electric devise for gel electrophoresis)	Bio-Rad Laboratories
Thermal Cycler C1000	Bio-Rad Laboratories
ThermoMixer 5436	Eppendorf
Vacusafe aspiration device	Integra Biosciences
Vortex Genie 2	Scientific Instruments
Will Wetzlar Wilovert Inverted Microscope	Hund Wetzlar

Table 13: Other small material used for experiments

Material	Source
96-well microplate flat bottom (for genotyping of B6.s mice, buffer plate)	Beckman Coulter #609844
96-well microplate flat bottom high binding Corning 9018 (for ELISA)	Th. Geyer #7608496
96-well microplate non-binding (for MPO assay)	Greiner Bio-One #655901
96-well microplate white conical (for genotyping of B6.s mice, sample plate)	AB SCIEX Germany #609801
96-well microplate white flat bottom LUMITRAC Corning 3922 (for ROS release assay)	Greiner Bio-One #655074
Boyden Chamber 48-well micro for chemotaxis	Neuro Probe #AP48
Cannulas for syringes (18G or 26G)	BD Medical Technology #303129 and #303800
Cell strainer (70 µm)	Th. Geyer #7671784
ELISA plate sealer	R&D Systems #DY992
Fluorescent Dye Removal Columns	Thermo Fisher Scientific #22858
Kombi-Stopfen Luer-Lock	Fresenius Kabi #8501512
MiniCollect Tube 0.8 ml Serum Separator	Greiner Bio-One #450472
MiniCollect Tube 1 ml K3EDTA	Greiner Bio-One #450474
Neubauer Chamber improved	Marienfeld-Superior #0640011
PCR microcentrifuge tube (8-strips)	Nerbe Plus #04-032-0100
Perfektum Syringe Adapter Luer-to-Luer	Sigma Aldrich #Z116319-2EA
Polycarbonate Membrane for Boyden Chamber (3 µm)	Neuro Probe #PFB3
Separation Capillary Array	Beckman coulter #608087
Syringe for injections (1 ml)	Braun #9166017V
Syringes (1 ml Luer-Lok, 5 ml, 10 ml)	BD Medical Technology #309628, #309050 and #309110

4.12 Software

Table 14: Software used for data acquirement and evaluation

Software name	Version	Developer	Application
CEQ 8800 genetic analysis system	9.0.25	Beckman Coulter, Inc.	Genetic analysis and sequencing
BD FACSDiva	8.0.1	BD Biosciences	Flow cytometry
Flow Jo	X 10.0.7r2	FlowJo LLC	Flow cytometry data evaluation
FLUOstar Omega	2.10	BMG Labtech	ELISA
GraphPad PRISM	5.03	Graphpad Software, Inc	Graphics and statistics
IQuant Capture 350	1.02	GE Healthcare	DNA detection with UV light
MARS Data Analysis Software	2.30R2	BMG Labtech	ELISA data evaluation
Microsoft Office	365 ProPlus	Microsoft Corporation	Data and protocol management
Nanodrop ND-1000	V3.8.1	Thermo Scientific	DNA and protein concentration

5. Methods

5.1 Genotyping of mice

Prior to all experiments, transgenic and congenic mice were genotyped to select the mice with the desired modifications. B-cell IL-10 knock-out mice (*Cd19cre* and *Il10flox* genes) and B6.s IL-10 reporter mice (*Il10-eGFP* gene) were genotyped using PCR and gel electrophoresis. By contrast, susceptible B6.s mice were genotyped using PCR followed by a capillary electrophoreses to estimate the size of the amplified DNA fragment. For genotyping, all biopsies were digested with 1.5 µl proteinase K in 300 µl tail lysis solution (TLS) at 55°C and 600 rpm overnight. After digestion, 100 µl TLS buffer was added and the sample was centrifuged for three min at 14,000 x g. The supernatant was added to 300 µl propan-2-ol in a new tube for DNA precipitation. After centrifugation for three min at 14,000 x g, the supernatant was carefully removed and 300 µl 70 % ethanol was added for washing. After the final centrifugation step for three min at 14,000 x g, the supernatant was again carefully removed, and the remaining ethanol was able to evaporate for ten min at 37°C. The DNA precipitate was solved in 50 µl Tris-ethylene diamine tetra-acetic acid (EDTA) buffer (TE buffer) and incubated at 65°C for 55 min at 600 rpm to inactivate proteinase K. DNA concentration was measured with NanoDrop (absorbance at 260 nm) and then diluted in TE buffer to a concentration between 30-50 ng/µl and stored at -20°C. All PCR reactions were performed in special PCR reaction tubes to avoid external DNA contamination. All primer pairs were tested in advance in a gradient PCR to determine the optimal annealing temperature.

5.1.1 Susceptible B6.s mice

B6.s mice (B6.SJL-H2^{s} C3^{c}/1CyJ) are a congenic strain carrying the H2s haplotype from the susceptible SJL/J strain on a C57Bl/6J background [181]. Susceptible B6.s and non-susceptible C57Bl/6J mice only differ on their *H2* and *C3* loci. To detect the susceptible H2s haplotype, a PCR reaction with a cyanine 5 (Cy5)-5'-labeled forward primer and an unlabeled reverse primer was performed and fragments were detected using capillary electrophoreses. The amplified fragments of B6.s and C57Bl/6J mice only differ in a two-nucleotide-length. With capillary electrophoreses using the Backman Coulter CEQ8800 system it is possible to distinguish fragments of 158 base pairs (bp) (B6.s) and 160 bp (C57Bl/6J). The PCR reaction was performed with the reagents and volumes listed in table 15 and the cycling conditions depicted in table 16.

Table 15: PCR reaction for genotyping of B6.s mice

Reagent	Volume for 1 reaction [µl]
DNA sample	2
Primer mix (2 µM each)	1
dNTPs (2.5 mM each)	0.8
10x DreamTaq buffer	1
DreamTaq Polymerase	0.05
PCR water	5.15

Table 16: PCR cycling protocol for genotyping of B6.s mice

Step	Temperature [°C]	Time [min]
1. Heat-up	95	3
2. Denaturation	95	0.5
3. Annealing	44	0.5
4. Extension	72	1
Repeat step 2-4 37 x		
5. Last extension	72	10
6. Hold	4	∞

After amplification, all fragments carry a fluorescent tag (Cy5) and can be separated by capillary electrophoreses according to their size (time, x-axis) and their quantity (peak height, y-axis). A master mix containing 22.6 µl sample loading solution (SLS) and 0.4 µl DNA size standard kit 400 per sample was prepared and added together with 3 µl of the amplified PCR product into a special 96-well plate (table 13). One droplet of mineral oil was added to the surface to avoid evaporation of the liquids during measurement. In parallel, a 96-well plate with separation buffer was prepared with the same layout as the sample plate. The sample plate was measured with a capillary array in Beckman Coulter CEQ8800. Susceptible B6.s mice showed only one fluorescence peak at 158 bp, C57Bl/6J mice had an intense peak at 160 bp and a minor peak at 158 bp, and heterozygous mice were characterized by an intense peak at 158 bp and a minor peak at 160 bp.

5.1.2 IL-10 reporter mice

IL-10 reporter mice (Vert-x) express enhanced green fluorescent protein (eGFP) under the control of the *Il10* promotor, which make these mice useful for the analysis of IL-10 expression in different cell types, especially B and T lymphocytes and myeloid cells. IL-10 reporter mice are transcriptional reporters with the *eGFP* gene downstream of exon five of the *Il10* gene on chromosome 1 [181]. IL-10 reporter mice such as Vert-x are able to show that cells have been actively transcribing the *Il10* gene [182]. Nevertheless, it has been shown that eGFP expression correlates well with IL-10 protein expression [70,183].

IL-10 reporter mice were genotyped with a PCR reaction containing the reagents listed in table 17 and with the cycling conditions listed in table 18. The PCR products and a size standard were loaded onto a 1.5 % agarose gel containing 0.0016 % GelRed Nucleic Acid Stain to visualize the distinct bands with ultraviolet (UV) light. The gel ran for 65 min at a constant voltage of 110 V and bands were detected with an UV transilluminator. The *Il10-eGFP* transgene shows a signal at 250 bp and the *Il10* wildtype gene at 350 bp.

Table 17: PCR reaction for genotyping of IL-10 reporter mice

Reagent	Volume for 1 reaction [µl]
DNA sample	0.5
Primer mix (20 µM each)	0.6
Kapa2G mix with dye	6
PCR water	4.9

Table 18: PCR cycling protocol for genotyping of IL-10 reporter mice

Step	Temperature [°C]	Time [min]
1. Heat-up	94	3
2. Denaturation	94	0.5
3. Annealing	62	0.5
4. Extension	72	0.5
Repeat step 2-4 37 x		
5. Last extension	72	2
6. Hold	4	∞

5.1.3 B-cell IL-10 knock-out mice

B-cell IL-10 KO (knock-out) mice (CD19cre^{+} IL-10$^{flox/flox}$) are a useful tool to study the role of B lineage-derived IL-10 in autoimmune diseases. The Cre recombinase is expressed under the control of the *Cd19* promotor and simultaneously destroys the *Cd19* gene [181]. Therefore, experimental mice must be heterozygous avoiding CD19- and, in turn, B cell-deficiency. CD19cre mice were crossed with IL-10-floxed mice to achieve B-cell IL-10 conditional knock-out mice. Cre recombinase is expressed in B lineage cells and recognizes the *loxP* sites placed around the *Il10* gene and leads to deletion of the DNA sequence and thereby inactivation of the gene.

B-cell IL-10 KO mice and littermate controls were genotyped with two different PCRs. Table 19 shows the PCR reactions for the *Cd19* wildtype gene and *Cd19cre* transgene and table 20 the reaction for the *Il10* wildtype or *Il10flox* gene. Cycling conditions are listed in table 21 for both PCRs.

Table 19: PCR reactions for genotyping of CD19cre mice

Reagent	Volume for 1 reaction [µl]
DNA sample	1
dNTPs (10 mM each)	0.4
Primer mix (10 µM each) **either wildtype or transgene**	0.2
10 x HotStar buffer	2
HotStarTaq Plus DNA polymerase	0.25
PCR water	16.15

Table 20: PCR reaction for genotyping of IL-10flox mice

Reagent	Volume for 1 reaction [µl]
DNA sample	0.5
Primer mix (10 µM each)	0.6
Kapa2G mix with dye	7.5
PCR water	6.6

Table 21: PCR cycling protocol for genotyping of CD19cre and IL-10flox mice

	CD19cre PCR		IL-10flox PCR	
Step	**Temp. [°C]**	**Time [min]**	**Temp. [°C]**	**Time [min]**
1. Heat-up	95	5	95	3
2. Denaturation	94	1	95	0.25
3. Annealing	59	1	60	0.75
4. Extension	72	1	72	0.5
	Repeat step 2-4 30 x		Repeat step 2-4 35 x	
5. Last extension	72	10	72	2
6. Hold	4	∞	4	∞

The PCR products and a size standard were loaded onto a 1.5 % agarose gel (CD19cre) or 1.2 % agarose gel (IL-10flox) containing 0.0016 % GelRed Nucleic Acid Stain. The gels ran for 60 min (CD19cre) or 110 min (IL-10flox) at a constant voltage of 110 V. The *Cd19cre* transgene shows a signal at 163 bp and the *Cd19* wildtype gene at 477 bp. In case of IL-10, the wildtype gene displays a band at 480 bp and the *Il10flox* transgene at 514 bp.

5.2 Immunization-induced EBA mouse model

The immunization-induced EBA model (or "active" model) is used to reflect the complete EBA disease development from the break of tolerance until the effector phase. In the autoimmune disease EBA, COL7 in skin and mucous membranes is the target of autoantibodies. An immunodominant part of the COL7 molecule is vWFA2 [125], which has been used for immunization and induction of EBA in mice for several years [137,174]. The genetic background of the mouse strain appears to strongly influence EBA disease development [118]. Susceptible mouse strains carrying the H2s haplotype, e.g. B6.s or SJL mice, develop signs of blistering after four weeks. By contrast, EBA-resistant strains with H2b haplotype, e.g. C57Bl/6 mice, produce autoantibodies but do not develop the skin disease [134,137]. Approximately 91% of B6.s mice [137] but only 82 % of SJL mice [141] show signs of EBA skin inflammation. Therefore, the more stable B6.s mouse model was used in this thesis for immunization with the EBA autoantigen.

5.2.1 Production of the autoantigen

Recombinant murine vWFA2 (amino acids 1048-1238 with five additional amino acids [GRAMG] at the N-terminus) was produced in a prokaryotic expression system (*E.coli*) and affinity-purified with its N-terminal intein affinity tag as described by published protocols [137,184]. The protein was kindly provided by the Department of Dermatology, University of Lübeck (Dr. Katja Bieber/AG Ludwig). vWFA2 was stored at -20°C until usage.

5.2.2 Preparation of the emulsion of antigen and adjuvant

For immunization, a 1:2 emulsion of vWFA2 in TiterMax with a final concentration of 1 mg/ml vWFA2 was prepared as previously described [160]. The polymer TiterMax is a non-toxic adjuvant used to induce a long-lasting immune response to diverse antigens by forming a stable water-in-oil emulsion entrapping the antigen [185,186]. TiterMax consists of a block copolymer, squalene and a stabilizer [186].

The antigen vWFA2 was thawed rapidly at room temperature and the adjuvant TiterMax was mixed to a homogeneous solution by shaking. The desired amount of vWFA2 protein solution (2 mg/ml) or PBS was used as a control and thereafter the same amount of TiterMax was sucked into a 5 ml syringe through an 18 G cannula to produce a 1:2 mixture. The syringe was sealed with a cap and the solution was mixed thoroughly for at least 20 min full speed at room temperature (RT) to reach a white emulsion with a consistency of a solid polymer. To check the stability of the emulsion, one droplet was placed onto the surface of water to determine whether the droplet was not diverging anymore. The emulsion was then carefully transferred into a 1 ml syringe via a syringe adapter, sealed with a cap and directly stored on ice until usage.

5.2.3 Immunization of mice with the antigen

Mice were anesthetized by i.p. injection of 10 µl/g body weight of 1 x anesthetics (containing 5 mg/ml Ketanest S and 1.5 mg/ml Rompun) and immunized s.c. in both hind footpads with each 60 µl of the vWFA2/TiterMax emulsion as previously described [160]. The final vWFA2 concentration in the mixture was 1 mg/ml vWFA2 and, in total, 120 µg protein was injected into each mouse. Mice were supplied with eye cream and placed under red light for recovery from anesthesia. The immunization was conducted once on day zero. As a control, mice were treated with a 1:2 emulsion of PBS in TiterMax and injected as described above. In addition, the initial weight was measured to control the health condition of the mouse over the duration of the experiment.

5.3 Autoantibody-transfer-induced EBA mouse model

The transfer of autoantibodies targeting mCOL7 directly and systemically induces EBA skin inflammation after several days ("passive model") [149]. This model only reflects the effector phase of the disease. In contrast to the immunization-induced model, various inbred mouse strains, e.g. C57Bl/6 mice, are susceptible to autoantibody-transfer-induced EBA [149,174]. Autoantibodies bind to the murine DEJ, induce dermal-epidermal separation and blister formation, and the dose of IgG administered correlates with the extent of EBA skin disease [149].

5.3.1 Production of the autoantibody

Autoantibodies were produced in New Zealand White rabbits immunized with recombinant mCOL7c as described in the initial protocol by SITARU *et al.* [149]. The IgG fraction from rabbit serum was purified with a protein G affinity chromatography to receive total rabbit anti-mCOL7c IgG. Specific rabbit anti-mCOL7c IgG was produced by mCOL7c-affinity chromatography as described in published protocols [161]. The total and the specific anti-mCOL7c IgG were kindly provided by the Department of Dermatology (Dr. Katja Bieber/AG Ludwig and Sabrina Tofern/AG Schmidt). The antibodies were stored at -20°C and kept on ice after thawing.

5.3.2 Treatment of mice with autoantibodies

The autoantibodies were injected i.p. into mice on day zero, two and four. For the IL-10R blockade experiment, the total anti-mCOL7c IgG was used in a final concentration of 2.5 mg/ml, and 100 µl was injected at each time point to obtain a total of 750 µg per mouse. For the IL-10 kinetics and B-cell IL-10-deficiency experiment, specific anti-mCOL7c IgG was used in a final concentration of 0.7 mg/ml, and 150 µl was injected at each time point to achieve a total of 300 µg per mouse as described in published protocols [161]. In addition, the initial weight was measured to monitor the health condition of the mouse.

5.4 Scoring of EBA skin inflammation

In the immunization-induced model, the first signs of skin inflammation can be detected four to five weeks after immunization and EBA skin disease further progresses in B6.s mice [137]. In the autoantibody-transfer-induced model, the first signs can be observed after two to four days with a full-blown disease visible after five to six days [118,149]. In the experiments presented here, mice already started to recover after nine to twelve days.

In order to quantify the skin disease, the percentage of the affected body surface area was assessed. Therefore, every part of the mouse was evaluated for skin lesions, blisters, crusts or alopecia [141,149] and the percentage of the diseased area was multiplied by the following factor: each ear 0.025, each eye 0.005, snout 0.025, head and neck 0.09, each front leg 0.05, each rear leg 0.1, tail 0.1 and trunk 0.1 according to published protocols [174]. The total score equals the sum of all individual subpart scores, e.g. a score of seven indicates that in total 7 % of the skin is affected by EBA. The total disease severity during the whole period of observation was calculated as the area under the curve (AUC). The scoring in the immunization-induced model and the autoantibody-transfer-induced model is performed in the same way apart from the hind foots, which are not evaluated in the immunization-induced model due to the subcutaneous injection of the antigen/adjuvant emulsion at that place. All scoring was done in a blinded manner according to a weekly routine from week four (immunization-induced model) or every third day from day three (autoantibody-transfer-induced model). In the case of large experiments, the final evaluation of the disease score was one day before the sacrifice. The mice were anesthetized by i.p. injection of 10 µl/g body weight of 1 x anesthetics (containing 5 mg/ml Ketanest S and 1.5 mg/ml Rompun) before scoring, supplied with eye cream and placed under red light for recovery from anesthesia. In addition, the initial weight was measured to control the health condition of the mouse over the duration of the experiment.

5.5 *In vivo* IL-10 receptor blockade

The IL-10 receptor signaling was blocked with a neutralizing antibody (anti-IL-10R antibodies, clone 1B1.3) or a control antibody was used (rat IgG control). The clone 1B1 recognizes an epitope at the murine IL-10R1 ligand binding domain and inhibits binding of IL-10, thereby neutralizing its effects [187].

In the immunization-induced model, the IL-10R was blocked in the effector phase (week three) with 1 mg of antibodies. In the autoantibody-transfer-induced model, the IL-10R was blocked with 0.5 mg of antibodies one day before the first injection of anti-mCOL7c IgG (t-1) to avoid formation of antibody complexes. The antibody was diluted in PBS to obtain a final concentration of 2 mg/ml and 250 µl was injected i.p.

5.6 Mouse dissection and tissue sampling

5.6.1 Sampling of spleen, bones and lymph nodes

Mice were sacrificed by cervical dislocation and pinned backside down to a dissection board. The skin was disinfected with Spitacid to avoid decontamination. The skin was cut along the ventral midline and the spleen was taken after opening of the peritoneum. The surrounding connective tissue was removed and the spleen was stored in PBS/BSA on ice. In the immunization-induced EBA model, all draining lymph nodes (dLN, inguinal and popliteal, dexter and sinister) were taken, the surrounding connective tissue was removed and pooled dLN were stored in PBS/BSA on ice. For bone marrow isolation, both hind legs (femur and tibia) were removed from skin and muscles and taken completely without bone fracture to keep the bone marrow sterile. Remaining muscles were removed as much as possible and the bone was stored in PBS either on ice (flow cytometry) or at RT (functional assays).

5.6.2 Sampling of blood

Mice were anesthetized by i.p. injection of 10 µl/g body weight of 1 x anesthetics (containing 5 mg/ml Ketanest S and 1.5 mg/ml Rompun) and blood was taken directly from the heart using a 26 G cannula and 1 ml syringes prefilled with 20 µl 0.5 M EDTA. The blood was either transferred into an EDTA-coated tube, gently inverted and stored on ice (flow cytometry) or transferred into a serum separator tube, gently inverted and stored at RT (ELISA). Mice were immediately killed by cervical dislocation after drawing of blood. For separation of serum, tubes were centrifuged for ten min at 2,000 x g and the supernatant (serum) above the gel was transferred into a new tube and stored at -80°C.

5.6.3 Sampling of skin

Mice were sacrificed by cervical dislocation and ear tissue was taken by cutting at the lowest part of the ears. Remaining hair was removed as much as possible and ears were snap-frozen separately in safe-lock tubes in liquid nitrogen for myeloperoxidase assay.

5.7 Preparation of single cell suspensions

For flow cytometry, all preparations of single cells from tissue were carried out entirely on ice with cooled buffers and solutions. For functional assays such as neutrophil migration or ROS release, cells were kept at RT, and prewarmed buffer and media were used. For cell culture experiments, all steps were performed sterile under the laminar flow cabinet.

5.7.1 Spleen and lymph nodes

Single cell suspensions from spleen and bone marrow were obtained by grinding the organ between the rough sides of two microscopy slides in a Petri dish. The slides and dish were rinsed with PBS/BSA and filtered with a 10 ml syringe through a 70 µm cell strainer into a 50 ml Falcon. The suspension was filled up to 40-50 ml with cold PBS/BSA and counted with a CASY TT cell counter (spleen, 1:1,000) or Neubauer chamber (dLN; 1:2 with Trypan blue). Cells were centrifuged for ten min at 350 x g at 4°C and the pellet was resuspended in cold PBS/BSA or warm cell culture medium to achieve the desired cell count/ml.

5.7.2 Bone marrow

Bone marrow cells were isolated by a centrifugation step. Therefore, the bone was cut on the hip and the foot side and folded at the knee with both open sides facing downwards. The folded bone was placed into a diagonally cut 1 ml pipette tip in a 15 ml Falcon in a way that the bone marrow can be flushed out. The tube was centrifuged for five min at 1,800 x g at RT or 4°C and the bone was removed. The cell pellet was resuspended in 4 ml cold PBS/BSA (flow cytometry) or 3 ml 1 x red blood cell lysis buffer at RT (functional assays).

For flow cytometry experiments, cells from both legs were pooled through a 70 µm cell strainer and filled up to 40 ml with cold PBS/BSA. An aliquot was taken for counting of cells with CASY TT cell counter (1:250). Cells were centrifuged for ten min at 350 x g at 4°C and the cell pellet was resuspended in cold PBS/BSA or warm cell culture medium.

For functional assays such as neutrophil migration or ROS release assays, red blood cells were lysed for exactly three min at RT and the reaction was stopped with 10 ml prewarmed 1 x PBS. Cells from both legs were pooled by transfer through a 70 µm cell strainer into a 50 ml Falcon and filled up with 1 x PBS. The following procedure is analogous to the preparation for flow cytometry as mentioned above but performed at RT. For functional assays, the stock concentration of cells was six million cells/ml in PBS (migration assay) or two million cells/ml in ROS release medium (ROS release assay).

5.7.3 Blood

As described in chapter 5.6.2, blood was sampled into EDTA-coated tubes for flow cytometry and transferred into a 15 ml Falcon containing 5 ml 1 x red blood cell lysis buffer prepared in ddH_2O. The tube was gently inverted and incubated for ten min at 4°C for lysis of erythrocytes. Turbidity was observed each five min to evaluate whether lysis was completed. Cells were filled up with 10 ml cold PBS/BSA and centrifuged at 300 x g at 4°C. The supernatant was carefully removed with a pipette and the pellet resuspended in 10 ml cold PBS/BSA for another washing step. Thereafter, the supernatant should be only slightly pink. Cells were resuspended in 2 ml cold PBS/BSA and an aliquot was taken for counting in the Neubauer chamber (1:2 with Trypan blue).

5.8 Flow cytometry

Flow cytometry is widely used in the research field of immunology. With this method, it is possible to analyze the characteristics of individual cells, e.g. the cell properties (size, granularity) or surface, intracellular and intranuclear proteins. Therefore, cells can be fluorescently labeled with monoclonal antibodies targeting cell surface or intracellular/intranuclear markers specific for a certain cell type or subset. Labeled cells are then measured in a sheath fluid with a single cell at a time to detect the fluorescence signal and scattered light. Different lasers are commonly used to excite fluorochromes at a specific wavelength and the emitted light is separated with different filters, thus blocking certain wavelengths while transmitting others, and detected by photomultipliers. With flow cytometry, multiple signals from one cell can be analyzed within one measurement and cells can be identified by their forward or sideward scatter (size or granularity, respectively) or by their fluorescence signal [188].

5.8.1 Coupling of vWFA2 to fluorochrome

In order to detect autoreactive plasma cells in the immunization-induced EBA model, the antigen (vWFA2) must be coupled to a fluorochrome and plasma cells stained intracellularly for the binding of the autoantibody to the antigen [135]. The coupling of vWFA2 to Alexa Fluor 405 (A405) was performed with the Fluorochrome Coupling Kit Alexa Fluor 405 according to the manufacturer protocol. Briefly, the fluorochrome A405 (1,028 Da) was solved in DMSO for a stock concentration of 8.33 mg/ml, vWFA2 (20,000 Da) concentration was 1.8 mg/ml and the relation of protein to fluorochrome was 1:15. All reagents were rapidly thawed and all steps were performed at RT. The calculated volume

of vWFA2 (e.g. 95 µl) was transferred into a fresh reaction tube, 1 M bicarbonate buffer (1/10 of the protein volume, e.g. 9.5 µl) was added and the tube was filled up with 1 x PBS to 250 µl (for one column). The solution was mixed and 20 µl of the fluorochrome stock solution was added drop by drop. The tube was incubated for 1 h in the dark for the coupling reaction and gently inverted every 15 min. For removal of unbound fluorochromes, Fluorescent Dye Removal Columns with resin were used. Resin was homogenized, 350 µl was added to the column and centrifuged for 30 sec at 1,000 x g for removal of storage solution. 270 µl of the coupling mixture was added onto the column, briefly mixed and centrifuged at 1,000 x g for 30 sec. This fluorochrome removal step was repeated with a fresh column with resin. The concentration of the vWFA2-A405 conjugate was measured with NanoDrop (absorbance at 280 nm) and sodium azide was added to a final concentration of 0.02 % for long-term stability. The conjugate was stored at 4°C in the dark.

5.8.2 Staining of surface receptors

After preparation of single cell suspensions from spleen, bone marrow, dLN or blood (chapter 5.7), between one and five million cells were stained for surface receptors dependent on the organ. For control stainings (isotypes, FMO, single stainings, unstained), pooled cells from all mice were used with the same cell density. All steps were performed on ice and centrifugation at 4°C. Cells were washed once with cold PBS/BSA for ten min at 350 x g and the pellet was resuspended in 50 µl PBS/BSA containing 1.6 µg/ml anti-CD16/CD32 antibodies (FcγRIII/IIb) to block unspecific binding of the staining antibodies to Fcγ receptors on the surface of cells. This step was omitted when Fcγ receptors were stained on neutrophils. After ten min of incubation, 50 µl the surface antibody master mix was added and incubated for 15 min on ice in the dark. Therefore, the master mix was prepared in PBS/BSA and most of the antibodies had a final concentration of 0.5 to 2 µg/ml. The best concentration was always determined by titration prior to the experiment. The master mix was centrifuged for one min at 14,000 x g to pellet antibody complexes and only the supernatant was used for staining. Normally, all antibodies were added at the same time apart from the anti-CD3 antibody, which was added seven min after the master mix to avoid direct competition with other T cell-specific antibodies, e.g. anti-CD4 or anti-γδTCR antibodies. After incubation with antibodies, cells were washed one (dLN, blood) or two (spleen, bone marrow) times with PBS/BSA at 350 x g for ten min and resuspended in 300-400 µl cold PBS/BSA containing 0.1 mg/ml DNase I to avoid DNA aggregation. Samples were stored on ice in the dark until measurement.

5.8.3 Cell culture and restimulation

Freshly isolated lymphocytes only show low to undetectable amounts of cytokines, therefore, an *in vitro* restimulation of mature cytokine-competent T cells is necessary to improve the signal-to-noise ratio in flow cytometry [189]. As described in chapter 5.7, single cell suspensions were prepared and cells were resuspended in prewarmed cell culture medium to achieve a final cell density of 20 to 40 million cells/ml dependent on the organ. All steps were performed at RT and under sterile conditions. 500 µl of cells (10-20 million cells) was transferred into each well of a 48-well flat bottom cell culture plate and for controls the same volume was used from pooled cells from all mice. A stimulation mix was prepared and 500 µl was added to the cells to achieve a final concentration of 3.33 ng/ml PMA, 1 µg/ml ionomycin and 10 µg/ml LPS. PMA is a protein kinase C activator and ionomycin a Ca^{2+} ionophore, inducing extracellular Ca^{2+} influx, and together these reagents are potent activators of signaling cascades in lymphocytes [189]. LPS is the ligand for TLR4 and can stimulate B lymphocytes in a T cell-independent manner, e.g. to produce IL-10 [190]. Pre-experiments revealed that especially the detection of IL-10 in T lymphocytes was three-fold improved when the cells were stimulated with LPS in addition to PMA/ionomycin, which is probably due to secondary effects of LPS on cell types other than T cells. For the unstimulated control, 500 µl cell culture medium without stimuli was added to one well. The cells were incubated for 1 h at 37°C and 5 % carbon dioxide (CO_2) before Brefeldin A was added in a final concentration of 3 µg/ml. Brefeldin A is indirect inhibitor of intracellular protein transport from the endoplasmic reticulum to the Golgi, and it thereby blocks cytokine secretion [191]. It is able to improve the detection of cytokines within activated cells by flow cytometry [189]. The cells were incubated for another 4 h at 37°C and 5 % CO_2 and harvested after a total 5 h of restimulation.

5.8.4 Intracellular staining of cytokines

After 5 h restimulation of cytokine-competent T cells (chapter 5.8.3), fixation (to immobilize cytokines) and permeabilization (to obtain access to the cytokines) of cells is necessary to stain intracellular cytokines with fluorochrome-coupled monoclonal antibodies [189].

In this thesis, a two-step protocol including a surface staining (as described in chapter 5.8.2) followed by an intracellular staining after fixation and permeabilization was applied. Until cell fixation, all steps were performed on ice and centrifugation at 4°C and afterwards at RT. After surface staining, cells were washed one time with 1 x PBS without BSA (to avoid

interference with the fixation) at 350 x g for ten min and resuspended in 100 µl 1 x fixation buffer. After 20 min incubation at RT in the dark, cells were either washed with 1 x PBS and resuspended in 300 µl 1 x PBS to store the cells overnight at 4°C, or the cells were directly centrifuged at 350 x g for ten min. The cell pellet was resuspended in 100 µl of 1 x Permeabilization/Wash buffer (diluted in 1x PBS) and incubated for 20 min at RT in the dark. Due to the permeabilized cells, centrifugation with higher speed was performed for seven min at 1.700 x g and the supernatant was carefully removed by decanting. The intracellular cytokine master mix was centrifuged for one min at 14,000 x g to pellet antibody complexes and only the supernatant was used for staining. The pellet was resuspended in 100 µl master mix prepared in 1 x Permeabilization/Wash buffer and incubated for 20 min at RT in the dark. The concentration of intracellular antibodies was between 0.5 and 1 µg/ml. After incubation, cells were washed with 1x PBS at 1.700 x g for seven min and resuspended in 300 µl 1 x PBS containing 0.1 mg/ml DNase I to avoid DNA aggregation. Samples were stored in the dark until measurement.

5.8.5 Staining of antigen-specific plasma cells

Plasma cells specific for a certain antigen can be detected by using the fluorescently labeled antigen of interest. Apart from IgM, plasma cells usually lag the expression of membrane bound immunoglobulins and are filled with secretory antibodies [105], thus, an intracellular staining of non-secreted antibodies was performed. The staining was carried out as previously described [135]. Briefly, single cell suspensions were prepared from different organs as described in chapter 5.7. All steps before fixation were performed on ice and centrifugation at 4°C and afterwards at RT. For staining of antigen-specific plasma cells, ten million cells were transferred into a new reaction tube and washed with cold PBS/BSA for ten min at 350 x g. The Fcγ receptor blockade and surface marker staining was performed as described in chapter 5.8.2. After staining, cells were washed with 1 x PBS and fixation and permeabilization was performed according to the protocol of chapter 5.8.4. Intracellular staining was performed with the A405-coupled vWFA2 (chapter 5.8.1) with a final concentration of 7.5 µg/ml in 1 x Permeabilization/ Wash buffer for 20 min at RT in the dark. After a final washing step with 1 x PBS at 1,700 x g for seven min, the pellet was resuspended in 350 µl 1 x PBS containing 0.1 mg/ml DNase I to avoid DNA aggregation. Samples were stored in the dark until measurement.

5.8.6 Staining of antigen-specific T cells

Although T helper cells specific for a certain antigen are rare, they can be easily assessed by the CD40 ligand method [192,193]. CD40L (CD154) short-term expression is induced only in antigen-specific T cells after *in vitro* restimulation with the corresponding antigen, but CD154 is also rapidly removed from the cell surface after binding to APCs [194,195]. Blockade of the protein transport and secretion with Brefeldin A enables the intracellular staining of CD154 after fixation and permeabilization and therefore characterization of antigen-specific T cells.

For this method, cells were isolated as described in chapter 5.7, prepared for *in vitro* restimulation as explained in chapter 5.8.3. and ten million cells were transferred into each well of a 48-well cell culture plate. Autoantigen-specific restimulation was performed with a final concentration of 0.1 mg/ml vWFA2 for 5 h at 37°C and 5 % CO_2 and 3 µg/ml Brefeldin A was used for the last 4 h. Unstimulated cells (negative control) and a general T-cell stimulation with PMA/ionomycin/LPS (positive control) were included to evaluate the vWFA2-specific stimulation. After 5 h, cells were harvested and stained as described for intracellular cytokines in chapter 5.8.4. Intracellular staining included the anti-CD154 antibody (1 µg/ml) and the corresponding isotype control with the same fluorochrome.

5.8.7 Staining of regulatory T cells

Forkhead box protein 3 (Foxp3) was found to be a transcription factor selectively expressed in Tregs and is important for their suppressive capacity [39]. This factor was regarded as a key marker to specifically stain Tregs for flow cytometry [196]. Transcription factors such as Foxp3 are usually located in the nucleus, therefore, intranuclear staining using a special permeabilization buffer for the nuclear membrane is required.

In this thesis, staining of $Foxp3^+$ Tregs was always used in combination with intracellular staining of cytokines after 5 h restimulation *in vitro*. From the FOXP3 Fix/Perm Buffer Set, only the permeabilization buffer was used for nuclear permeabilization and combined with the fixation buffer from the cytokine staining kit. Pre-experiments revealed that the fixation buffer provided in the FOXP3 Fix/Perm Buffer Set is weaker than the fixation buffer for cytokine staining, thus, specifically declining the signal for cytokines such as IL-10 in Tregs. For detection of cytokines in Tregs and antigen-specific Tregs, cells were stimulated with 100 µg vWFA2 as described in chapter 5.8.6, stained for surface markers and fixed as indicated in chapter 5.8.4. After fixation, cells were washed in 500 µl of 1 x FOXP3 perm

buffer diluted in 1 x PBS and directly centrifuged for seven min at 1,700 x g. The supernatant was carefully removed by decanting and cells were permeabilized with 200 µl of the same buffer for 15 min at RT in the dark. After another centrifugation step as described above, 100 µl of the intracellular and intranuclear antibody master mix was added to the cells and incubated for 60 min at 4°C in the dark. Therefore, the master mix was centrifuged for one min at 14,000 x g to pellet antibody complexes and only the supernatant was used for staining. The concentration of antibodies was between 0.5 and 1 µg/ml. After incubation, cells were washed with 1 x PBS and resuspended in 250 µl 1 x PBS containing 0.1 mg/ml DNase I to avoid DNA aggregation. Samples were stored in the dark until measurement.

5.8.8 Analysis of flow cytometry data

Flow cytometry data was acquired with a LSRII (BD Biosciences) and the FACS Diva software. FCS files (version 3.0) were exported and analyzed with FlowJo software. Prior to analysis, the spillover due to the overlap of the emission spectra of two fluorochromes was corrected using the manual compensation matrix of the program. Single stained controls can be used to check for correct compensation when the negative and positive populations for one fluorochrome are aligned with the same mean fluorescence intensity. After compensation, cells were gated according to their viability (*in vitro* restimulated cells were always stained with a fixable permeabilization dye due to a higher frequency of dead cells after cell culture) and forward (FSC-A) and side scatter (SSC-A) to exclude cell debris. Cell doublets were excluded in the FSC-A vs FSC-H scatter and autofluorescence with an empty channel (e.g. in Brilliant Violet (BV)510 or corresponding channels such as fluorescein isothiocyanate (FITC) wavelengths specifically for autofluorescence of natural cellular molecules can be detected). Cell subsets were defined by gates around the stained population in the dot plot, which were set according to the isotype or FMO control. In case of IL-10-eGFP, the gate was set according to a vWFA2-immunized wildtype C57Bl/6J mouse. With isotype controls, unspecific binding of the staining antibody can be determined since the control antibody matches the host species, fluorochrome and isotype. Isotype controls used in this thesis always showed a low or undetectable signal. By contrast, FMO controls completely omit one staining antibody while keeping all the others, which allows one to define the border between positive and negative signals. However, FMO controls are sometimes not suitable due to a strong shift of the negative population towards low intensities. In this case, gates set according to these controls would not accurately reflect the border between stained and unstained populations.

5.9 Detection of reactive oxygen species (ROS) release by innate effector cells

Polymorphonuclear neutrophils (PMNs) are the most common type of leucocytes and mature neutrophils can be found in a high number in the bone marrow [145]. These cells are important for host defense and can be rapidly activated, e.g. by immune complexes or inflammatory mediators, resulting in an oxidative burst producing and releasing reactive oxygen and reactive nitrogen species [197]. The release of ROS by PMNs and other innate effector cells can be used as a measure of their ability to be stimulated and activated. The luminol-amplified luminescence technique exploits the reaction of luminol with ROS (e.g. superoxide radicals) generated by immune complex-activated innate effector cells to produce an excited aminophtalate anion that emits light when returning to ground state [197].

Bone marrow cells were isolated and red blood cell lysis was performed as described in chapter 5.7.2. All steps were carried out at RT with prewarmed medium or buffers to avoid cellular stress in sensitive neutrophils. For the ROS release assay, a special medium without phenol red was used for a proper read-out of luminescence. The assay was performed in duplicate or triplicate for each experimental condition.

5.9.1 Incubation of bone marrow cells with IL-10 *in vitro*

In order to analyze the effect of IL-10 on neutrophil functions such as ROS release, isolated bone marrow cells were preincubated with rmIL-10 in different concentrations for 45 min at 37°C and 5 % CO_2. Therefore, 500 µl of a ten million cells/ml cell suspension was transferred into a 48-well cell culture plate and stimulated with 500 µl of ROS release medium containing IL-10 with a final concentration between 1 and 25 ng/ml. Only 500 µl medium without IL-10 was used as a control. After 45 min, cells were carefully resuspended, transferred into a new tube and filled up with ROS release medium to obtain two million cells/ml. For the positive and negative control in the ROS release assay, cells from each condition were pooled.

5.9.2 ROS release assay

The ROS release assay was performed as previously described with minor modifications [198]. A special high binding 96-well plate (LUMITRAC) was coated with 50 µl of a 20 µg/ml vWFA2 solution in 1 x PBS for 1 h at 37°C with shaking. The plate was washed

three times with washing buffer (PBS/0.05 % Tween20) and incubated with 100 µl PBS/BSA for 1 h at RT to block unspecific binding sites. After another washing step with washing buffer (three times), 50 µl serum from vWFA2-immunized mice was added for 1 h at RT. The ROS release assay can be either performed to compare the quality of serum from experimental and control mice or it can be used to compare the isolated bone marrow cells from two experimental groups. In the first case, serum was either prediluted 1:10 in PBS/BSA or all sera were normalized to the same quantity according to the ELISA data (4 units of vWFA2-specific IgG). In the latter case, the serum was a pool taken from another experiment of mice with a good vWFA2 titer according to the ELISA data and prediluted 1:10 in PBS/BSA. The negative control was incubated with 50 µl PBS/BSA instead of the serum.

Luminol solution was prepared by solving 2 mg luminol in 8 µl 2 M NaOH and filling up with ddH_2O to 1 ml to reach a concentration of 2 mg/ml. The plate was washed three times with washing buffer and 100 µl of ROS release medium was added in each well. The luminol solution was added 1:20 to the cells and 200.000 cells (100 µl) were transferred into the 96-well plate. For the positive control, 1 µg of PMA was added and for the blank control, only 200 µl of ROS release medium was used.

5.9.3 Detection of luminescence

The ROS release plate was immediately measured in the Omega FLUOstar ELISA reader detecting the luminescence over 1 h at 37°C. Within 1 h, 30 to 60 measurements were made, allowing to analyze the increase of luminescence over time. The data was corrected by the averaged blank value and the average of duplicates or triplicates for each condition was calculated. For analysis, the relative luminescence units (RLU) were depicted in dependence of the time and the area under the curve was calculated with GraphPad Prism.

5.10 Neutrophil infiltration in ears

Myeloperoxidase (MPO) is a key enzyme in neutrophils found in azurophilic granules catalyzing the formation of reactive oxygen species, thus, contributing to respiratory burst and host defense [199]. In 1982, BRADLEY and colleagues demonstrated that MPO can be used as a marker for skin neutrophil content due to its direct correlation with neutrophil numbers [200]. Therefore, MPO is a good indicator for neutrophil infiltration in inflamed ears in the EBA mouse model.

5.10.1 Myeloperoxidase assay

The myeloperoxidase (MPO) assay consists of two parts: the extraction of the enzyme from ear tissue and the determination of the enzyme's activity with tetramethylbenzidine (TMB) which directly correlated with the neutrophil content in the sample.

For extraction of MPO, ears were cut in small pieces and homogenized with permanent cooling. After homogenization, 50 µl of 5 % hexadecyl-trimethylammonium bromide (HTAB) was added as a detergent and properly mixed with the tissue. To destroy the cell integrity, the cell suspension was repeatedly frozen and thawed for five min at -80°C and centrifuged for 15 min at 14,000 rpm at 4°C. The supernatant, containing the extracted enzyme, was transferred into a new tube and stored at -80°C.

To determine the enzyme activity, a MPO standard was prepared in potassium phosphate buffer containing 0.8 µg MPO to obtain a final activity of 543 mU/ml. The standard was titrated 1:1.33 in seven steps to 97 U/ml and a blank value was included. Dependent on the amount of MPO, the sample was either used undiluted or up to 1:10 prediluted in potassium phosphate buffer. 50 µl of the sample and 50 µl TMB, the substrate for MPO, were mixed in a low-binding 96-well plate and incubated for 15 min at RT in the dark. The reaction was stopped with 50 µl 20 % sulfuric acid and the absorbance was measured at 405 nm in an ELISA reader. The results were determined from duplicates, corrected by the average blank value and the activity was calculated from the standard curve by linear regression. The values were normalized to the total protein amount (chapter 5.10.2), the average from both ears was calculated and results depicted as mU/µg protein.

5.10.2 Protein determination

For normalization of the MPO values to the protein amount in the sample, the Pierce bicinchoninic acid (BCA) Protein Assay kit was used according to manufacturer protocol. Briefly, the working solution was prepared in a 50:1 ratio of Reagent A and Reagent B. The standard contained eight samples with a final BSA concentration of 25 to 2,000 µg/ml. 25 µl of the pure sample or the standard was transferred into a non-binding 96-well plate and 200 µl of the working solution was added. The plate was incubated for 30 min at 37°C, cooled down to RT and absorbance was measured at 562 nm in an ELISA reader. The results were determined from duplicates, corrected by the average blank value and the protein concentration was calculated from the standard curve by linear regression.

5.11 Neutrophil migration in Boyden chamber

PMNs are able to sense a variety of chemotactic factors such as C5a and IL-8 and migrate along a chemotactic gradient [145]. The Boyden chamber assay is a technique to analyze chemotactic migration of leukocytes originally introduced by Boyden. The chamber consists of two compartments separated by a microporous membrane. The cells are placed in the upper chamber and the chemoattractant is placed in the lower chamber. Cells which have migrated to the lower side of the membrane are then fixed, stained and counted [201].

Cells were isolated and red blood cell lysis was performed as described in chapter 5.7.2. All steps were performed at RT or 37°C with prewarmed buffers. Six million cells were taken from a six million cells/ml cell suspension in 1 x PBS, transferred into a 48-well cell culture plate and incubated for 30 min at 37°C and 5 % CO_2 for recovery of neutrophils after the isolation procedure. The chemoattractant rmC5a was diluted in PBS to a final concentration of 12.5 nM and 28.4 µl of the C5a solution or 1 x PBS as a control was transferred into the wells of the lower chamber by avoiding air bubbles. The 3 µm polycarbonate membrane was carefully placed with forceps on top and the upper chamber was fixed to assemble the whole Boyden chamber. Cells were carefully resuspended, 50 µl (300.000 cells) was transferred into each well of the upper chamber and incubated for 30 min at 37°C and 5 % CO_2. Each condition was performed in duplicate. After incubation, the membrane was removed from the chamber and rinsed at the upper side (the one facing to the cell chamber) with 1 x PBS to remove non-migrated cells. In addition, remaining non-migrated cells were removed by peeling the washed side of the membrane over a flexible scarper. The membrane was dried overnight in a 15 ml Falcon.

The staining of the membrane was performed with the Hemacolor staining kit. Briefly, the cells were fixed with Hemacolor 1 (methanol) and stained with Hemacolor 2 and 3. At the end, the membrane was washed with 1 x PBS and placed onto a microscopy slide with the migrated cells facing downwards and dried overnight. VectaMount permanent mounting medium was added and the membrane was covered with a cover slip by avoiding air bubbles. The slides were dried overnight and analyzed with a 40 x magnification in a transmitting light microscope. Purple stained PMNs that have migrated through the membrane were counted in five high-power fields for each condition and the average number of migrated cells was calculated and corrected by the PBS blank value. The neutrophils per mm^2 were calculated according to a standard scale for the microscope.

5.12 Enzyme-linked immunosorbent assay

In order to determine the anti-vWFA2 titer in serum samples of mice from the immunization-induced EBA mouse model, an enzyme-linked immunosorbent assay (ELISA) was performed. The antigen (vWFA2) was coated on the plate and serum autoantibodies were allowed to form immune complexes immobilized at the plate. A biotin-coupled secondary antibody, binding the specific subclass of the serum antibody via its Fc-part, was added. The construct was detected by the addition of streptavidin-coupled alkaline phosphatase (ALP) and the hydrolyzation of its substrate *p*-nitrophenyl phosphate to the yellow-colored water-soluble product *p*-nitrophenol [202].

5.12.1 Detection of vWFA2-specific autoantibodies

A high-binding 96-well pate was coated with 50 µl of 1 µg/ml vWFA2 diluted in 0.05 M bicarbonate buffer. The bicarbonate buffer was prepared from the 1 M stock in ddH_2O. The plate was sealed and incubated overnight at 4°C. To remove unbound antigen, the plate was washed three times with washing buffer (PBS/0.05 % Tween20) and 200 µl PBS/BSA was added for blocking of unspecific binding sites. Incubation was performed for 30 min at 37°C in a Labocult Incubator and afterwards, plates were washed again three times with washing buffer. There is no commercial standard for vWFA2 available. Therefore, a standard of pooled serum from vWFA2-immunized control mice was used for all ELISA in this thesis. Aliquots of the standard were stored at -80°C to avoid repeated freezing cycles. The standard and the sample predilution (in PBS/BSA) were dependent on the subclass and experimental time point (table 22). The best dilution for the standard was always determined by titration in pre-experiments.

Table 22: Sample and standard dilutions for detection of vWFA2-specific antibodies

Experiment	Sample dilution	Standard dilution
Subclass IgG1	1:100 (B6.s) and 1:10 (B6)	1:25
Subclass IgG2b	1:400 (B6.s) and 1:40 (B6)	1:300
Subclass IgG2c	1:400 (B6.s) and 1:40 (B6)	1:300
Subclass IgM	1:25 (B6.s) and 1:5 (B6)	1:10
IL-10R blockade	1:500	1:500
IL-10 kinetics 5 weeks	1:500	1:500
IL-10 kinetics 10 days	1:1	1:500

150 µl of the prediluted samples and the standard was placed in the top row the ELISA plate and 100 µl PBS/BSA was added in all the remaining wells. One well containing 150 µl PBS/BSA was used as a blank control. A 1:3 serial dilution was performed in each lane by repeated transfer of 50 µl sample/standard. The plate was incubated at 37°C for 1 h and washed three times with washing buffer. The secondary biotin-labeled anti-mouse antibody (table 7) was diluted 1:500 in PBS/BSA for a final concentration of 1 µg/ml. 50 µl of the antibody was added in each well and incubated at 37°C for 1 h. The streptavidin-coupled ALP was diluted 1:3,000 in PBS/BSA (333 mU) and 50 µl was added after the plate was washed six times with washing buffer and incubated for 1 h at 37°C. ALP reagent was prepared according to the manufacturer protocol with a 1:5 mixture of the yellow and clear reagent. After a final washing step (six times with washing buffer), 50 µl ALP reagent was added and the development of the optical density (OD) was measured every five min at 405 nm in an Omega FLUOstar ELISA reader until the OD value reached 3.5.

5.12.2 Evaluation of ELISA data

The ELISA data was analyzed with MARS Data Analysis Software and Microsoft Excel. All OD values were corrected by the average blank value and the 1:3 titrated standard was displayed in a logarithmic scale by setting the highest standard value as 100. A non-linear regression (sigmoidal curve) was applied on the curve and the linear range of the OD was defined. All sample OD values were interpolated according to the standard curve and corrected by the dilution factor. The average was only calculated from the values within the linear range of the standard curve. The average of all values for each ALP substrate incubation time, which yielded a good standard curve with a long linear range (e.g. 15 to 25 min), was calculated and displayed as arbitrary units (AU).

5.13 Statistical analysis

Statistical analysis was performed and data illustrated with GraphPad Prism 5.03 software. Unless otherwise indicated, data for a certain number of mice per group (n) was presented as mean ± standard error of the mean (SEM). Experiments with two groups of mice were tested for normal distribution (D'Agostino-Pearson normality test and box-and-whisker plot analysis) and compared using the Mann-Whitney test for non-parametrical data or student's unpaired t-test for parametrical data. Experiments with three or more groups were tested for normal distribution and parametric data was compared by one-way analysis of variance (ANOVA) with Bonferroni post-test. If two independent parameters from several

groups were compared, e.g. EBA disease development over time, a two-way ANOVA with a Bonferroni post-test was applied. Correlation analysis of the score and the autoantibody titer was performed by a linear regression followed by Spearman correlation for non-parametrical data. Differences were considered significant when the P-value was smaller than 0.05, with *$p \leq 0.05$, **$p \leq 0.01$ and ***$p \leq 0.001$.

6. Results

6.1 IL-10 can down-modulate skin-inflammation in the immunization-induced EBA model

In order to study the role of IL-10 under pathophysiological conditions of an autoimmune blistering skin disease, the immunization-induced EBA mouse model was used. The model is well-established in regard to autoantibody responses, complement activation and therapy approaches [118,174]. EBA can be induced either by immunization with an immunodominant part of the autoantigen mCOL7 [141] or by transfer of autoantibodies targeting distinct epitopes of mCOL7 at the dermal-epidermal junction in the skin [149]. The immunization-induced EBA model reflects the complete EBA disease development from the break of tolerance (afferent phase) until induction of skin inflammation and blistering (effector phase). By contrast, the transfer of autoantibodies just mimics the effector phase and skips the induction of autoreactive lymphocytes. Hence, these models can be used to investigate the impact of IL-10 on the whole disease development or only on the effector phase, respectively.

6.1.1 IL-10 receptor blockade in the beginning of the effector phase augments EBA skin inflammation

To investigate the role of IL-10 in the natural course of the autoimmune skin disease, the immunization-induced EBA model was used. Therefore, susceptible B6.s mice were subcutaneously immunized with the autoantigen vWFA2 (figure 5).

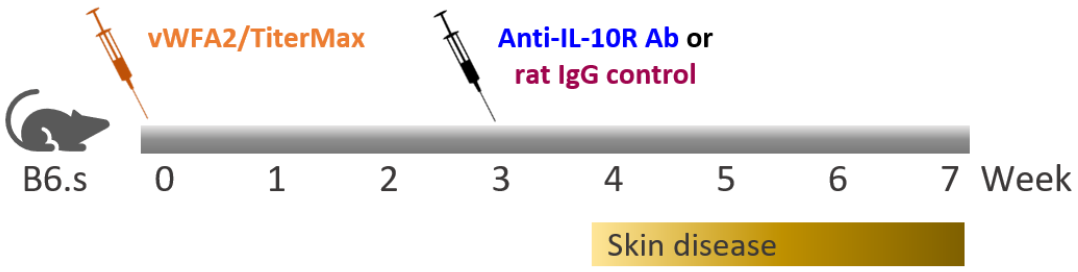

Figure 5: Experimental setup for IL-10 receptor blockade in the immunization-induced EBA model. EBA was induced in susceptible B6.s mice by immunization with vWFA2 (von Willebrand factor A-like domain 2) in TiterMax. Mice were treated with an anti-IL-10 receptor antibody (anti-IL-10R Ab) or a control antibody (rat IgG control) before the first symptoms of the skin disease developed. The disease was scored weekly from week four and final analysis took place after seven weeks.

Although symptoms of skin inflammation and blistering do not manifest earlier than four weeks after immunization [134,137], circulating and tissue-bound autoantibodies are rapidly induced within one week, already reaching a plateau after three to four weeks [137,138]. In line with this, autoreactive plasma cells and $CD4^+$ T cells are detected in dLN after three weeks before the first signs of inflammation are observed [135,137,138]. To study the role of IL-10 in the EBA effector phase, IL-10R-blocking antibodies (anti-IL-10R Abs) were intraperitoneally injected one week before manifestation of the skin disease (figure 5). The treatment was performed after the adaptive immune response had reached its peak to minimize the impact of the blockade on the plasma cell response in the afferent phase. IgG antibodies have a half-life of approximately one week [203], thus, application of 1 mg of antibodies was expected to block IL-10 signaling until the remainder of the observation period.

Blockade of the IL-10R in the beginning of the effector phase augmented EBA skin inflammation six to seven weeks after immunization compared to the control group (figure 6A). Moreover, the total disease score defined as the area under the curve showed a significant increase in the anti-IL-10R antibody treated group and was approximately twice as high compared to the control group (figure 6B). As expected, the vWFA2-specific autoantibody titer seven weeks after immunization was not modulated by IL-10R blockade (figure 6C). Thus, the blockade of the IL-10R had a considerable impact on the disease score independent of the production of circulating autoantibodies. This data indicates that IL-10 is produced during the natural course of the disease and suppresses EBA skin inflammation downstream of autoantibodies.

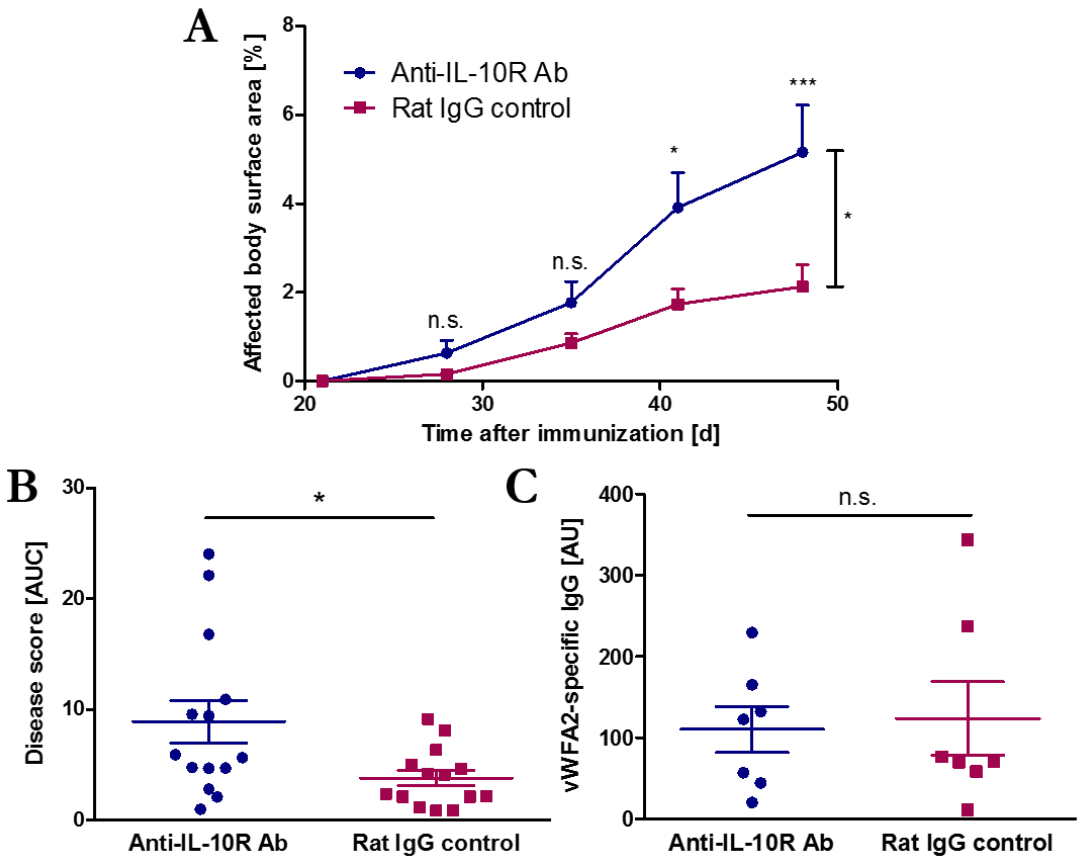

Figure 6: Mice treated with an IL-10 receptor-blocking antibody show an increased disease score but a normal autoantibody titer. EBA was induced by immunization with vWFA2 and mice were treated with an IL-10 receptor-blocking antibody (anti-IL-10R Ab) or a control antibody (rat IgG control) as described in the scheme in figure 5. **(A)** The disease manifestation was evaluated as the percentage of affected body surface area at various times after immunization, as indicated (n=14 combined from two independent experiments and each experiment reached statistical significance, two-way ANOVA with Bonferroni post-test). **(B)** The total disease score was defined as the area under the curve (AUC) (n=14 pooled from two independent experiments, Mann-Whitney test). **(C)** vWFA2-specific total IgG in the serum seven weeks after immunization was measured by ELISA (n=7, Mann-Whitney test). Data are expressed as mean ± SEM. *p ≤ 0.05; ***p ≤ 0.001. *AU, arbitrary units; n.s., not significant.*

6.1.2 IL-10 receptor blockade does not modulate plasma cell formation and the cytokine response of CD4$^+$ T cells

Blockade of the IL-10R signaling revealed that IL-10 is an important anti-inflammatory cytokine under pathophysiological conditions of EBA (chapter 6.1.1). The IL-10R is expressed by most hematopoietic cells, thus, IL-10 has a broad range of targets among innate and adaptive immune cells [46]. In order to analyze which cell types were affected by IL-10R blockade and can be responsible for the observed increased EBA disease score, first, the plasma cell compartment in spleen and dLN was analyzed by flow cytometry (figure 7A). Plasma cells can be defined by their surface expression of CD138 (syndecan-1) and transmembrane activator and CAML interactor (TACI).

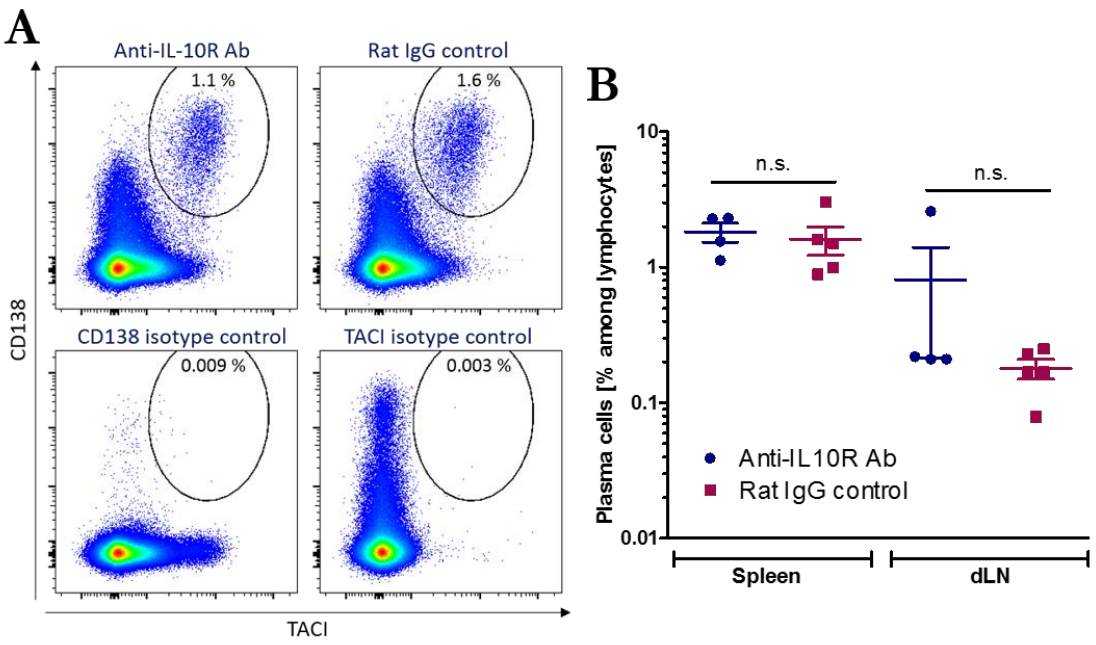

Figure 7: IL-10 receptor blockade does not reduce plasma cell frequencies in draining lymph nodes and spleen. EBA was induced by immunization with vWFA2 and mice were treated with an IL-10 receptor-blocking antibody (anti-IL-10R Ab) or a control antibody (rat IgG control) as described in the scheme in figure 5. Seven weeks after immunization, mice were sacrificed and plasma cells in spleen and draining lymph nodes (dLN) were analyzed by flow cytometry. **(A)** Representative flow cytometry data from spleen. Plasma cells were defined as $CD138^{hi}$ $TACI^{+}$ cells (upper panel) compared to the isotype controls (lower panel). **(B)** Frequency of plasma cells among lymphocytes in spleen and dLN (n=4-5, unpaired t-test). Data are expressed as mean ± SEM. *n.s., not significant.*

The treatment with anti-IL-10R antibodies did not modulate the frequency of $CD138^{hi}$ $TACI^{+}$ plasma cells in spleen and dLN seven weeks after immunization (figure 7B). Furthermore, the absolute cell number of these cells was not changed due to the treatment (supplementary figure 1A). As expected, IL-10R blockade in the beginning of the effector phase did not modulate plasma cell formation as a parameter of the afferent phase, which is in line with the observations on the autoantibody titer.

Next, the effect of IL-10R blockade on $CD4^{+}$ T cells was analyzed. $CD4^{+}$ T cells in dLN and their cytokine response have been shown to be important for the initiation and development of experimental EBA by inducing the production of autoantibodies [136,138]. In addition, the cytokines produced by B lymphocytes are able to directly modulate the cytokine profile of $CD4^{+}$ T cells [85]. To investigate whether IL-10R blockade had an effect on the cytokine response of $CD4^{+}$ T cells and $CD19^{+}$ B cells, cells from dLN were restimulated *in vitro* with PMA, ionomycin and LPS for 5 h and cytokine-producing cells were analyzed by flow cytometry (figure 8A). Seven weeks after immunization, IFNγ and IL-10 production by $CD4^{+}$ T cells and $CD19^{+}$ B cells in dLN were not affected by the blockade of IL-10R signaling (figure 8B and supplementary figure 1B). This suggests that

IL-10R blockade did not shift the inflammatory cytokine pattern of these cells, represented by the respective key cytokines IL-10 and IFNγ. Hence, changes in IFNγ production, which are suggested to be important for EBA initiation in the afferent phase [136,138], appear to not be responsible for the IL-10R blockade mediated increase in inflammation.

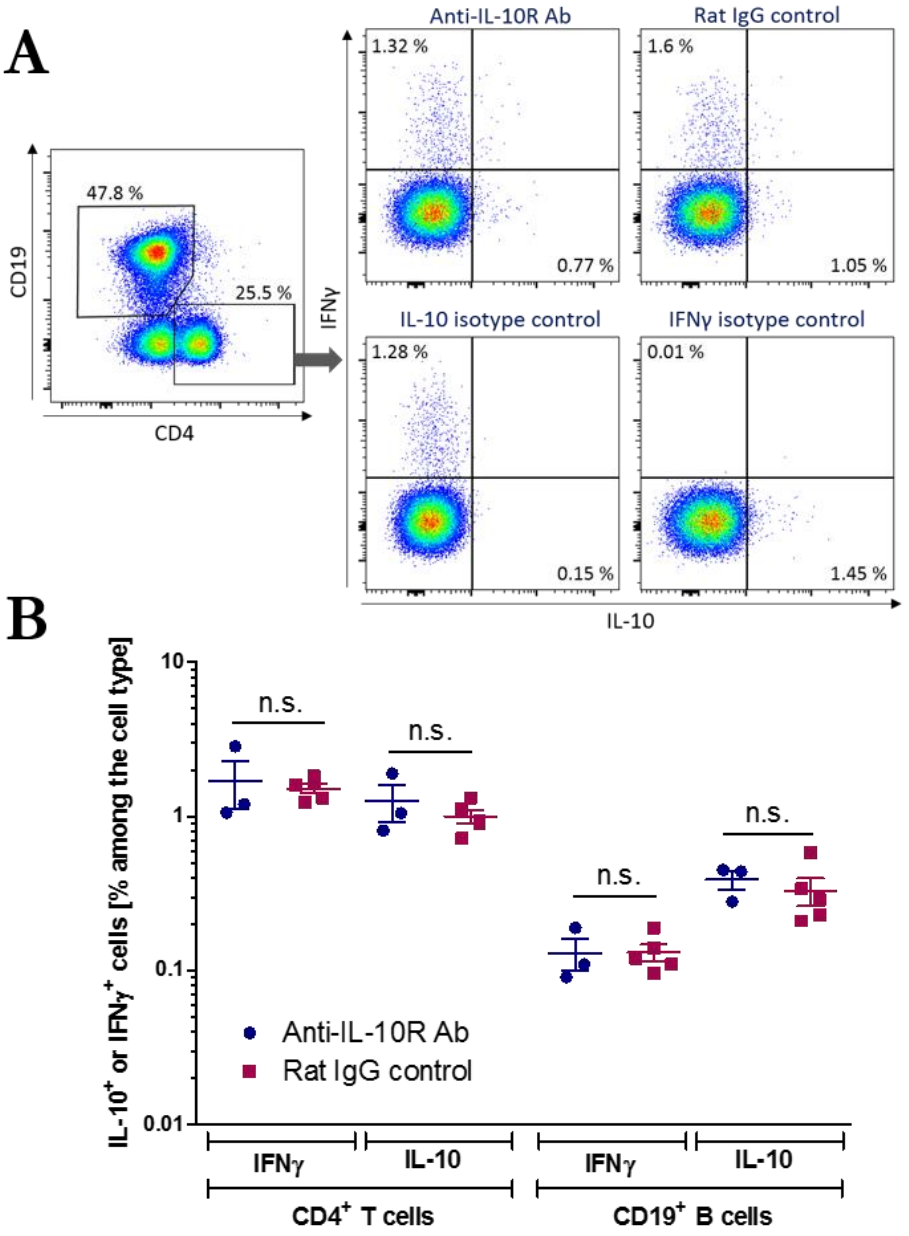

Figure 8: CD4⁺ T-cell and CD19⁺ B-cell cytokines in draining lymph nodes are not affected by IL-10 receptor blockade. EBA was induced by immunization with vWFA2 and mice were treated with an IL-10 receptor-blocking antibody (anti-IL-10R Ab) or a control antibody (rat IgG control) as described in the scheme in figure 5. Cytokine expression was analyzed seven weeks after immunization in draining lymph nodes by flow cytometry. **(A)** Representative flow cytometry data. Cells were stimulated for 5 h with PMA, ionomycin and LPS and treated for the last 4 h with Brefeldin A. CD4⁺ T cells and CD19⁺ B cells were gated and analyzed for their expression of IFNγ and IL-10 (upper panel) compared to the isotype controls (lower panel). **(B)** Frequency of IFNγ⁺ or IL-10⁺ among CD4⁺ T cells or CD19⁺ B cells (n=3-5, unpaired t-test). Data are expressed as mean ± SEM. *n.s., not significant.*

6.1.3 IL-10 receptor blockade has a moderate effect on effector cells important for EBA development

The effector phase of EBA is characterized by the recruitment of neutrophils and other effector cells into the skin, e.g. via the complement factor C5a and autoantibodies. Innate-like effector T cells such as γδ T cells and NKT cells have been described to amplify autoantibody-induced skin inflammation and blistering [161]. These cells not only directly contribute to inflammation but also increase the recruitment to and/or activation of neutrophils at the site of inflammation [161]. To investigate the impact of IL-10R blockade on effector T cells, NKT and γδ T cells (figure 9A&B) and their cytokine expression (figure 10A) were analyzed after 5 h *in vitro* restimulation with PMA, ionomycin and LPS by flow cytometry. The surface marker NK1.1, originally defined on natural killer cells, and γδ TCR can be used together with CD3 to define NKT cells and γδ T cells, respectively.

$NK1.1^+$ $CD3^+$ T cells were not affected by anti-IL-10R Ab treatment (figure 9C), but the frequency was generally very low and the staining was not as clear as in other experiments (figure 44A). The frequency of γδ TCR^+ $CD3^+$ T cells among splenic lymphocytes was slightly but significantly decreased compared to control mice (figure 9C). By contrast, the reduction of the absolute cell number of γδ T cells in spleen was only weak (supplementary figure 2A). It has been suggested that γδ T cells migrate to the inflammatory site in the skin to drive local inflammation, e.g. in psoriasis [204]. A reduction of these cells in other lymphoid organs could indicate an emigration of γδ T cells from the spleen to the skin, contributing to a stronger inflammation in the anti-IL-10R Ab treated group compared to control mice.

NKT and γδ T cells have various immunomodulatory functions mediated by their secretion of a broad range of cytokines, such as IFNγ, TNF, IL-17 or IL-10 [11,205]. Since IL-10R blockade already influenced γδ T cells, further analysis of their pro- and anti-inflammatory cytokine expression, represented by the key cytokines IFNγ and IL-10, after 5 h *in vitro* restimulation with PMA, ionomycin and LPS was performed (figure 10A). Seven weeks after immunization, neither IFNγ nor IL-10 expression by splenic NKT and γδ T cells were affected by IL-10R blockade (figure 10B and supplementary figure 2B), which does not exclude that the cytokine profile of these cells was modulated in the skin.

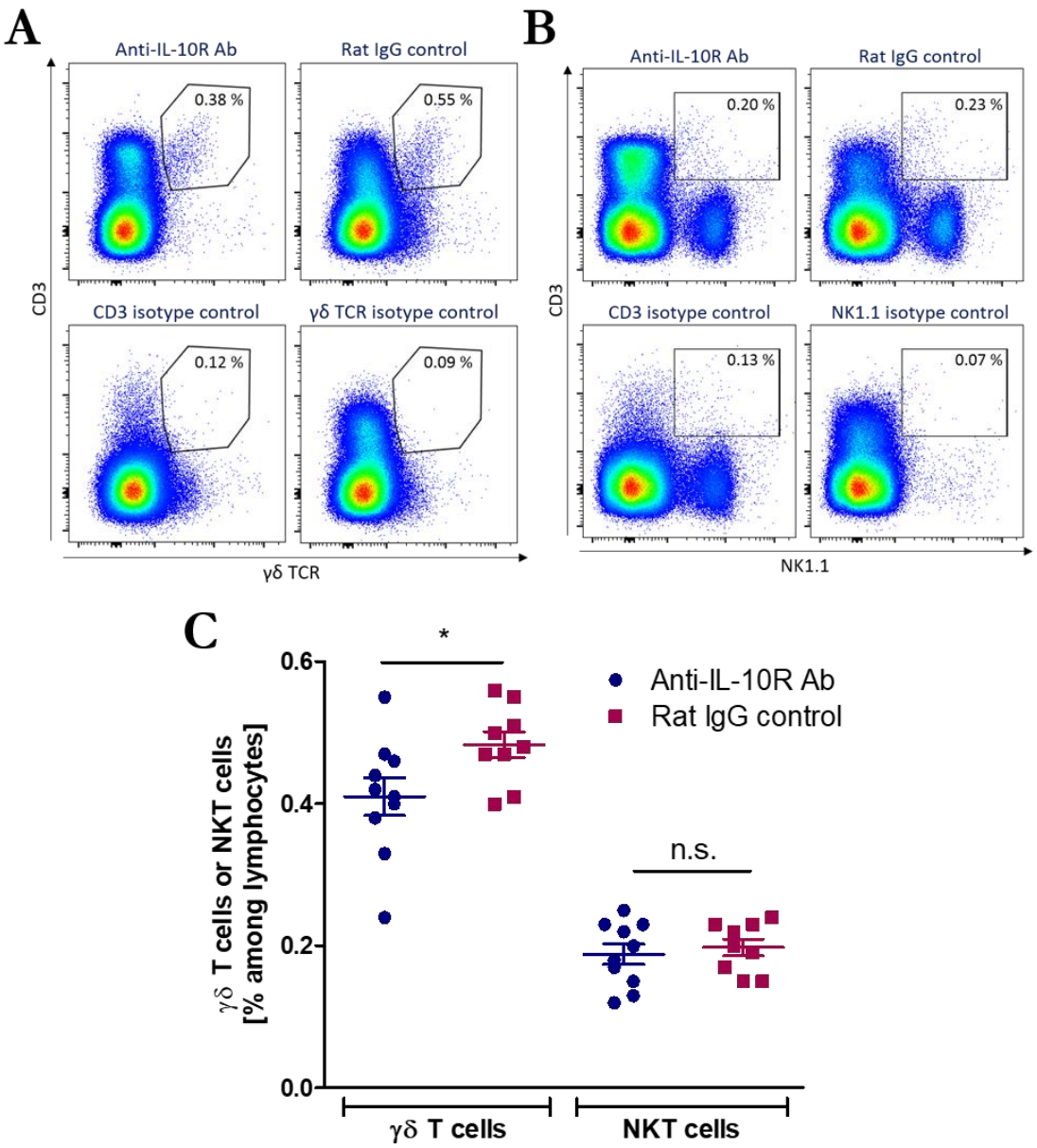

Figure 9: The frequency of splenic γδ T cells but not NKT cells is modulated by IL-10 receptor blockade. EBA was induced by immunization with vWFA2 and mice were treated with an IL-10 receptor-blocking antibody (anti-IL-10R Ab) or a control antibody (rat IgG control) as described in the scheme in figure 5. γδ T and NKT cells were analyzed seven weeks after immunization in spleen by flow cytometry. **(A)** Representative flow cytometry data. γδ T cells were defined as γδTCR$^+$ CD3$^+$ lymphocytes (upper panel) compared to the isotype controls (lower panel) and **(B)** NKT cells were defined as NK1.1$^+$ CD3$^+$ lymphocytes (upper panel) compared to the isotype controls (lower panel). **(C)** Frequency of splenic γδ T cells and NKT cells among lymphocytes (n=9-10, unpaired t-test). Data are expressed as mean ± SEM. *$p \leq 0.05$. *n.s., not significant.*

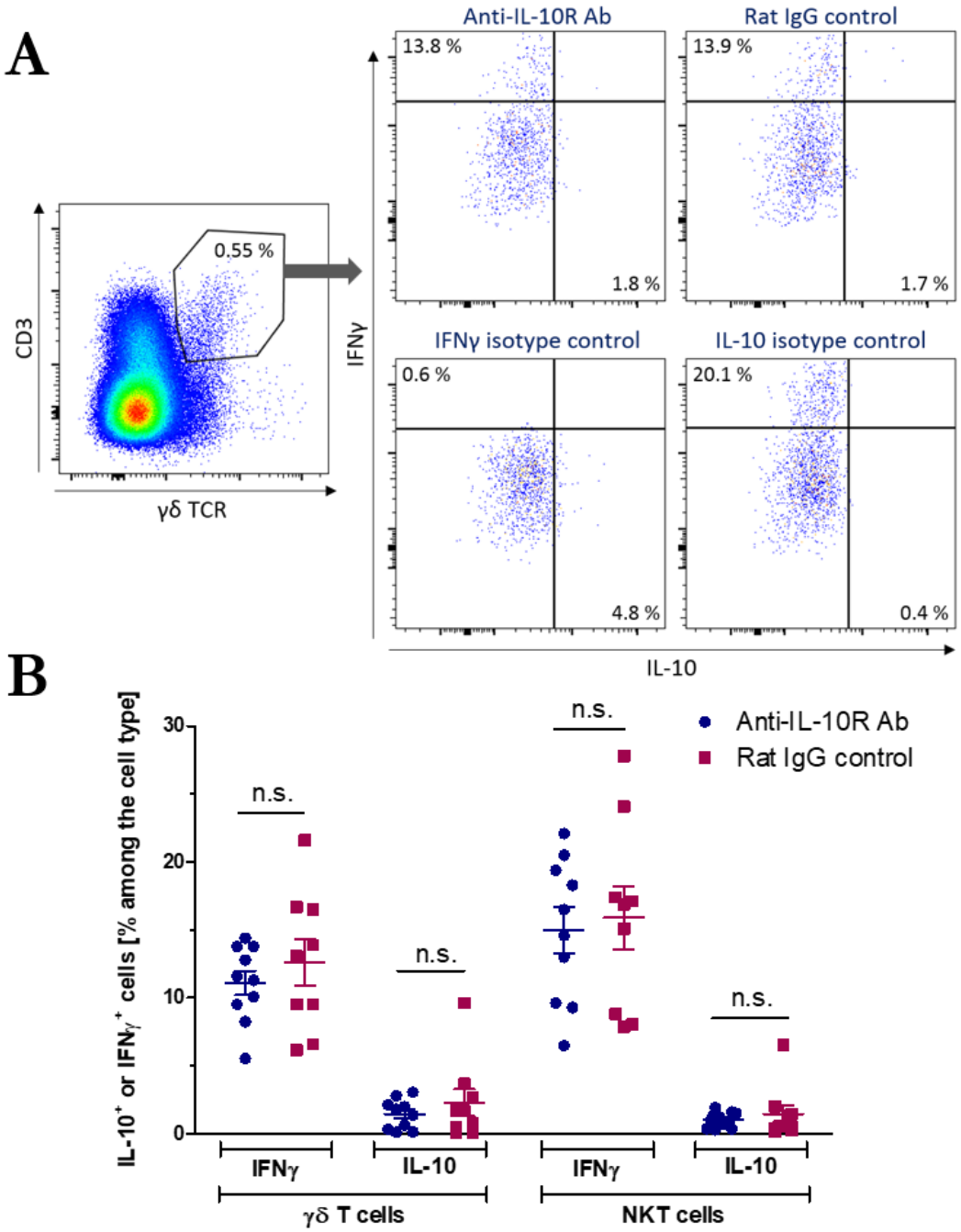

Figure 10: IL-10 and IFNγ production by NKT and γδ T effector cells in spleen is not affected by IL-10 receptor blockade. EBA was induced by immunization with vWFA2 and mice were treated with an IL-10 receptor-blocking antibody (anti-IL-10R Ab) or a control antibody (rat IgG control) as described in the scheme in figure 5. NKT and γδ T cells were analyzed seven weeks after immunization in spleen by flow cytometry as described in figure 9. **(A)** Representative flow cytometry data from spleen. Cells were stimulated for 5 h with PMA, ionomycin and LPS and treated for the last 4 h with Brefeldin A. IL-10 and IFNγ expression by γδ T cells (upper panel) was defined compared to the isotype controls (lower panel). A similar gating strategy was performed to analyze cytokine expression in NKT cells. **(B)** Frequency of IL-10$^+$ and IFNγ$^+$ cells among splenic γδ T cells and NKT cells (n=9-10, Mann-Whitney test). Data are expressed as mean ± SEM. *n.s., not significant.*

Next, the effects of IL-10R blockade on neutrophils were investigated. Neutrophils are regarded as the major innate effector cells in EBA mediating tissue damage and blister formation by their release of ROS and proteases [115]. After attraction and extravasation into the skin, neutrophils bind via their FcR to the tissue bound autoantibody Fc portion and via their C5aR to the complement factor C5a [115,127]. Important FcγRs on neutrophils are the activating FcγRIII and FcγRIV and the inhibitory FcγRIIb [206]. The expression of these receptors on different subsets of peripheral (figure 11A) and bone marrow neutrophils (supplementary figure 5A) was investigated by flow cytometry after IL-10R blockade in order to analyze, whether an elevated activation state of neutrophils was responsible for an increased disease score in the anti-IL-10R Ab treated group.

IL-10R blockade did not modulate the frequency (figure 11B) and the absolute cell number (supplementary figure 3A) of lymphocyte antigen 6 complex, locus G $(Ly6G)^+$ neutrophils in blood and bone marrow seven weeks after immunization. These neutrophils were further analyzed for their expression of different FcγRs, indicating a homogeneous expression of FcγRIII but two distinct subsets of FcγRIIb and FcγRIV (figure 11A). Neither the frequency (figure 11C) nor the absolute cell number and the mean fluorescence intensity (MFI) (supplementary figure 4A&B) of these neutrophil subsets in blood revealed any difference between the anti-IL-10R Ab treated and the control group. Moreover, neutrophils in bone marrow did not show any change in their FcγR pattern. Neither the frequency nor the MFI (supplementary figure 5B&C) of different FcγR-expressing bone marrow neutrophil subsets was affected by IL-10R blockade. Together, this indicates that the increased disease score after anti-IL-10R Ab treatment was not caused by changing of neutrophil formation, of neutrophil recirculation in the blood or by upregulation of activating or down-regulation of inhibitory FcγRs on neutrophils. Of note, this does not exclude that neutrophils in the skin are modulated by the treatment.

Neutrophil functions are not only determined by their ability to bind autoantibodies in the skin but also by their ability to extravasate from blood vessels and migrate to the site of inflammation in the skin. IL-10 has been reported to impair neutrophil adhesion and recruitment into the infected tissue [207,208]. C-C chemokine receptor type 2 (CCR2) is a key receptor that drives infiltration of activated neutrophils into the tissue during sepsis or in RA [209,210]. Moreover, IL-10 was shown to influence neutrophil tissue infiltration by the inhibition of CCR2 expression on circulating neutrophils [211]. Therefore, the expression of CCR2 on blood and bone marrow neutrophils was analyzed by flow cytometry (figure 12A). $Ly6G^+$ $CD11b^+$ neutrophils in blood and bone marrow did not

increase their expression of CCR2 after IL-10R blockade compared to the control group. Neither the frequency of CCR2$^+$ neutrophils (figure 12B) nor the absolute cell number (supplementary figure 3B) was modulated, indicating that the increased disease score after IL-10R blockade is not caused by a stronger ability of neutrophils to be chemotactically attracted to the site of inflammation via CCR2 and its ligands.

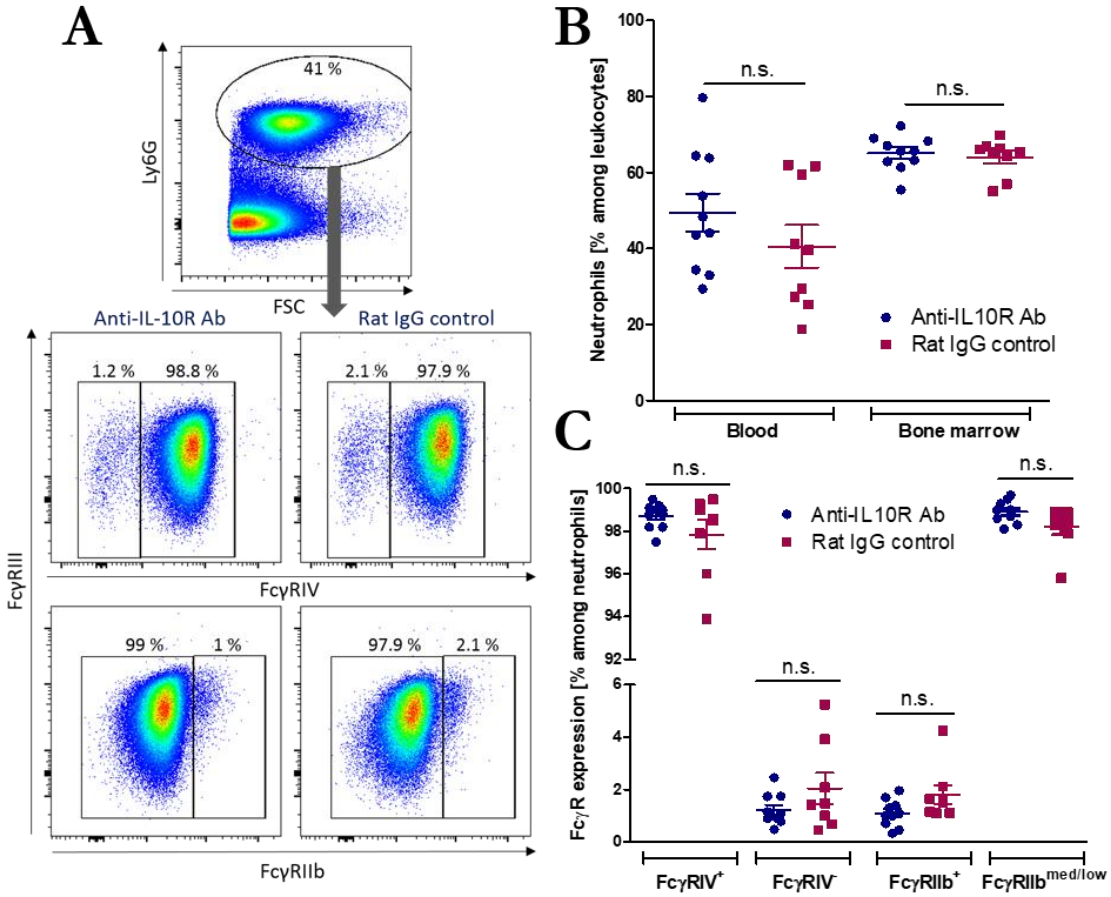

Figure 11: IL-10 receptor blockade has no influence on neutrophil frequencies and their Fcγ receptor expression in blood and bone marrow. EBA was induced by immunization with vWFA2 and mice were treated with an IL-10 receptor-blocking antibody (anti-IL-10R Ab) or a control antibody (rat IgG control) as described in the scheme in figure 5. Neutrophils were analyzed seven weeks after immunization by flow cytometry in blood and bone marrow. **(A)** Representative flow cytometry data from blood. Neutrophils were defined as Ly6G$^+$ leukocytes and further gated for their expression of Fcγ receptor III (FcγRIII, CD16), FcγRIV (CD16.2) and FcγRIIb (CD32). The gating for bone marrow-derived neutrophils is depicted in supplementary figure 5. **(B)** Frequency of Ly6G$^+$ neutrophils among leukocytes in blood and bone marrow (n=9-10, unpaired t-test). **(C)** Frequency of peripheral neutrophil subsets expressing a specific pattern of FcγRs. Neutrophils divide into two subsets characterized by their FcγRIV expression (FcγRIV$^+$ and FcγRIV$^-$) and by their FcγRIIb (FcγRIIb$^+$ and FcγRIIb$^{med/low}$) expression, respectively (n=8-10, Mann-Whitney test). Data are expressed as mean ± SEM. *n.s., not significant.*

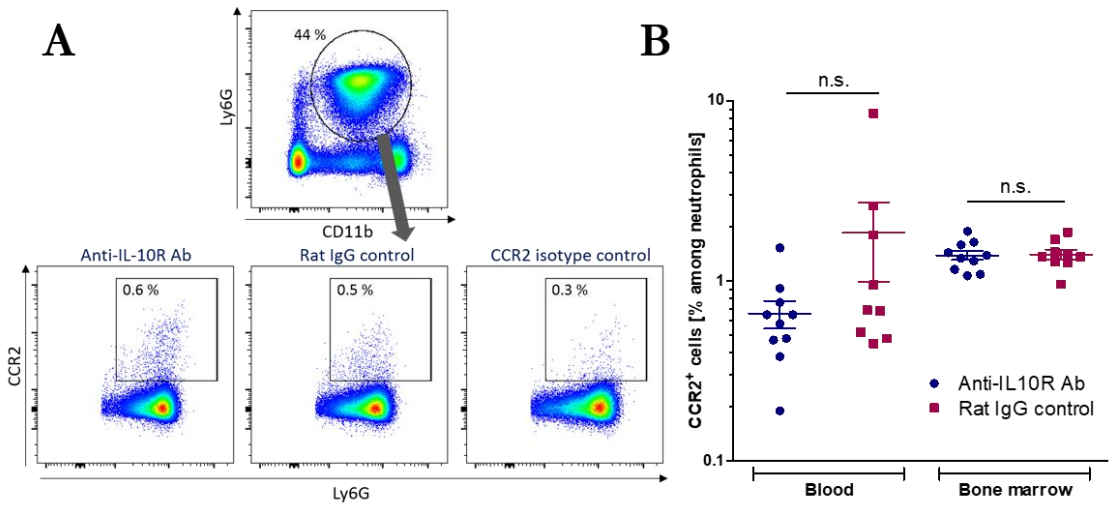

Figure 12: The expression of the chemokine receptor CCR2 on neutrophils is not affected by IL-10 receptor blockade. EBA was induced by immunization with vWFA2 and mice were treated with an IL-10 receptor-blocking antibody (anti-IL-10R Ab) or a control antibody (rat IgG control) as described in the scheme in figure 5. Neutrophils were analyzed seven weeks after immunization by flow cytometry in blood and bone marrow. **(A)** Representative flow cytometry data from blood. Neutrophils were defined as $Ly6G^+$ $CD11b^+$ leukocytes (upper panel) and further analyzed for their CCR2 expression compared to an isotype control (lower panel right). **(B)** Frequency of $CCR2^+$ neutrophils in blood and bone marrow (n=9-10, unpaired t-test). Data are expressed as mean ± SEM. *n.s., not significant.*

Although neutrophil CCR2 expression was not altered after IL-10R blockade, the general ability of neutrophils to be attracted and migrate to the place of inflammation was not investigated thus far. Therefore, neutrophil infiltration into the inflamed ears and neutrophil migration to C5a were analyzed by MPO and Boyden chamber assay, respectively (figure 13). Myeloperoxidase is a key enzyme contributing to respiratory burst in neutrophils and directly correlates with neutrophil numbers in skin [200]. Quantification of neutrophil content in the ears of mice seven weeks after immunization revealed no difference between the anti-IL-10R Ab treated group and the control group (figure 13A). Neutrophils are able to sense a variety of chemotactic factors such as the complement component C5a, which plays an important role in the pathogenesis of EBA [127]. With a Boyden chamber, chemotactic migration of neutrophils to C5a from the upper to the lower chamber through a microporous membrane was investigated. The number of bone marrow-derived neutrophils was not modulated by IL-10R blockade seven weeks after immunization (figure 13B).

This data indicates that the increased disease score due to the blockade of the IL-10R was not caused by an increased number of infiltrating neutrophils or an enhanced migratory capacity of these cells, at least not under the here applied experimental conditions and time points.

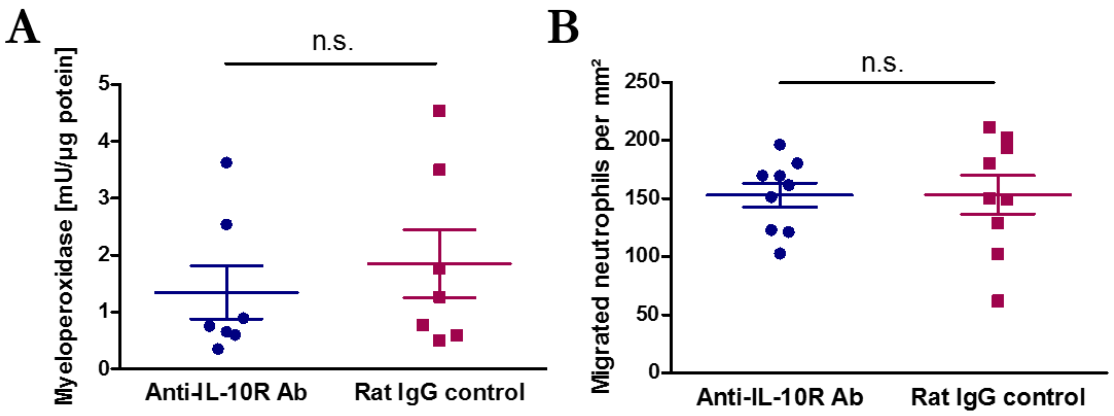

Figure 13: Neutrophil infiltration into inflamed ears and migration towards C5a are not influenced by IL-10 receptor blockade. EBA was induced by immunization with vWFA2 and mice were treated with an IL-10 receptor-blocking antibody (anti-IL-10R Ab) or a control antibody (rat IgG control) as described in the scheme in figure 5. **(A)** Neutrophils were quantified within both ears by a myeloperoxidase (MPO) assay seven weeks after immunization (n=7, Mann-Whitney test). **(B)** Bone marrow was isolated from the two treatment groups and cell migration towards the chemoattractant C5a was performed with a Boyden chamber and analyzed by microscopy of hematologically stained neutrophils (n=9, unpaired t-test). Neutrophils were counted in five high-power fields for each condition with a 40 x magnification. The values were corrected by the number of neutrophils migrated in PBS control wells without C5a. Data are expressed as mean ± SEM. *n.s., not significant.*

Neutrophils are regarded as the major effector cells in EBA due to their destructive functions at the site of inflammation such as the release of ROS and proteases [115]. Since neutrophil migration and chemotactic properties were not affected by IL-10R blockade, neutrophil functions such as ROS release might have been increased, leading to stronger inflammation and blister formation in the skin. IL-10 has already been reported to display anti-inflammatory effects on human neutrophil respiratory burst [62,212]. The immune complex-stimulated release of ROS was measured with a luminol-amplified luminescence assay using bone marrow-derived innate effector cells from both treatment groups (figure 14). Neutrophils are the most common type of leucocytes in the bone marrow with the ability to produce ROS [145,213], thus, ROS released by total bone marrow-derived innate effector cells will be mainly attributed to this cell type.

Analyzing the kinetics of ROS release over 60 min of incubation time with plate-coated immune complexes, bone marrow-derived innate effector cells from anti-IL-10R Ab treated mice appeared to release more ROS than bone marrow cells from control animals, but the overall difference between the groups was not significant (figure 14A). Moreover, the total ROS release defined as the area under the curve from anti-IL-10R Ab treated mice showed a slightly but not significantly higher value compared to control mice (figure 14B).

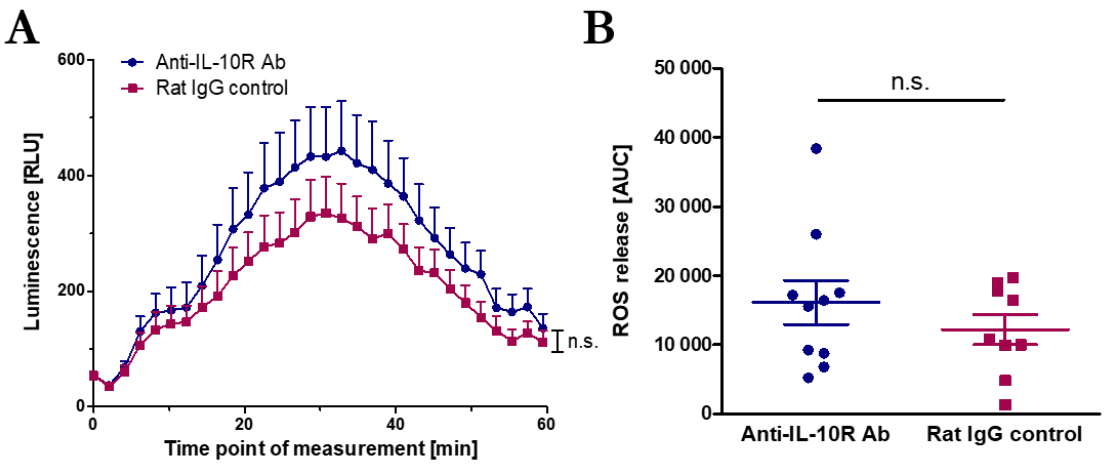

Figure 14: Oxidative burst by bone marrow-derived innate effector cells after IL-10 receptor blockade. EBA was induced by immunization with vWFA2 and mice were treated with an IL-10 receptor-blocking antibody (anti-IL-10R Ab) or a control antibody (rat IgG control) as described in the scheme in figure 5. Seven weeks after immunization, bone marrow cells were isolated and their oxidative burst was measured by the immune complex-stimulated release of reactive oxygen species (ROS) with a luminol-amplified luminescence assay. **(A)** Increase of luminescence due to release of ROS by immune complex-activated bone marrow cells over time (n=9-10, two-way ANOVA). **(B)** Total ROS release defined as the area under the curve (AUC) (n=9-10, unpaired t-test). Data are expressed as mean ± SEM. *n.s., not significant; RLU, relative luminescence units.*

Taken together, IL-10R blockade in the beginning of the effector phase had a considerable impact on the EBA skin disease score independent of the production of circulating autoantibodies. This suggests that the anti-inflammatory cytokine IL-10 has a strong effect on the natural course of the disease, already down-modulating the skin disease under pathophysiological conditions. However, data obtained from flow cytometry and functional assays at the endpoint of the experiment seven weeks after immunization revealed only a moderate effect of IL-10R blockade on different effector cell types such as γδ T cells and neutrophils, which could be responsible for the observed differences in the EBA disease score.

6.1.4 IL-10 can inhibit oxidative burst of bone marrow-derived innate effector cells in a concentration-dependent manner

In vivo IL-10R blockade only had a moderate effect on different effector cells important for EBA development. However, these effects could be measured only at the endpoint of the experimental setup. Previous studies already revealed that IL-10 has the potential to inhibit neutrophil migration to C5a *in vitro* in a concentration-dependent manner [70]. To further analyze whether IL-10 also influences other functions such as ROS release by these effector cells, a luminol-amplified luminescence assay was performed (figure 15). Prior to the assay, freshly isolated bone marrow cells from naïve C57Bl/6J mice were cultured for 45 min with

various concentration of rmIL-10. Oxidative burst was inhibited by IL-10 in a concentration-dependent manner. 25 ng/ml were sufficient to inhibit ROS release by approximately 25 % compared to the unstimulated control (0 ng/ml rmIL-10). These results suggest that IL-10 has indeed the potential to limit innate effector cell functions such as ROS release, a key step for the development of EBA inflammation and blistering.

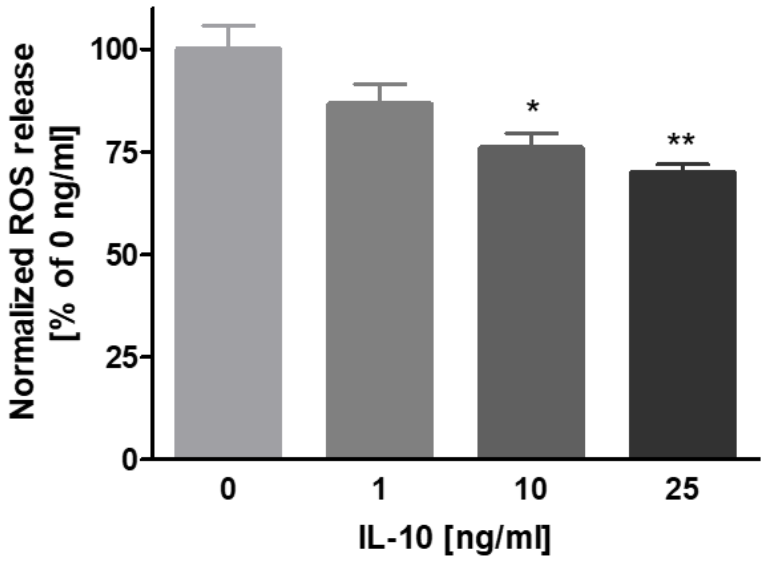

Figure 15: IL-10 concentration-dependently inhibits oxidative burst of bone marrow-derived innate effector cells. Bone marrow cells from naïve C57Bl/6J mice were isolated and their oxidative burst after incubation with different IL-10 concentrations was measured by the immune complex-stimulated release of reactive oxygen species (ROS) with a luminol-amplified luminescence assay. Inhibition was performed with different concentrations of rmIL-10 for 45 min or only medium was used as a control, as indicated. The area under the curve (AUC) was calculated from each condition and normalized to the unstimulated control (100 %) from each mouse (n=3, one-way ANOVA with Bonferroni post-test). Representative data shown from one of two experiments. Data are expressed as mean ± SEM. *$p \leq 0.05$ and **$p \leq 0.01$ compared to 0 ng/ml. One-way ANOVA overall P-value was ***$p \leq 0.001$.

6.1.5 IL-10 does not play a major role in the autoantibody-transfer-induced EBA model

The transfer of autoantibodies targeting mCOL7 in the skin is used to mimic exclusively the effector phase of EBA. This phase is characterized by the cascade induced after the binding of the autoantibodies, e.g. recruitment of neutrophils into the skin and tissue destruction. However, this model omits the break of tolerance and the induction of autoreactive lymphocytes. In contrast to the immunization-induced model, the repeated injection of autoantibodies against mCOL7 rapidly induces blister formation. First signs of inflammation can be observed after two to four days and the full-blown disease is usually seen at day five to six, depending on the amount of autoantibodies injected [118]. Of note,

the host's xenogeneic response to the autoantibodies produced in rabbits may contribute to the inflammation at late time points in this model [178]. Thus, the observation period was stopped at day twelve to avoid this xenoreactive immune response.

In order to investigate the effect of *in vivo* IL-10R blockade exclusively on the effector phase, the autoantibody-transfer-induced EBA model was used (figure 16A). The IL-10R was blocked with antibodies one day before EBA was induced by the first injection of total rabbit anti-mCOL7c IgG. Rat IgG antibodies were used as a control treatment. In contrast to the immunization-induced model, IL-10R blockade did not augment EBA skin inflammation in the autoantibody-transfer-induced model but showed only a slight trend in an increased disease score (figure 16B+C). Of note, the disease score was in general very low and as known from the literature, mice can show a high variation of the score [149,175], making small differences difficult to detect in this experiment.

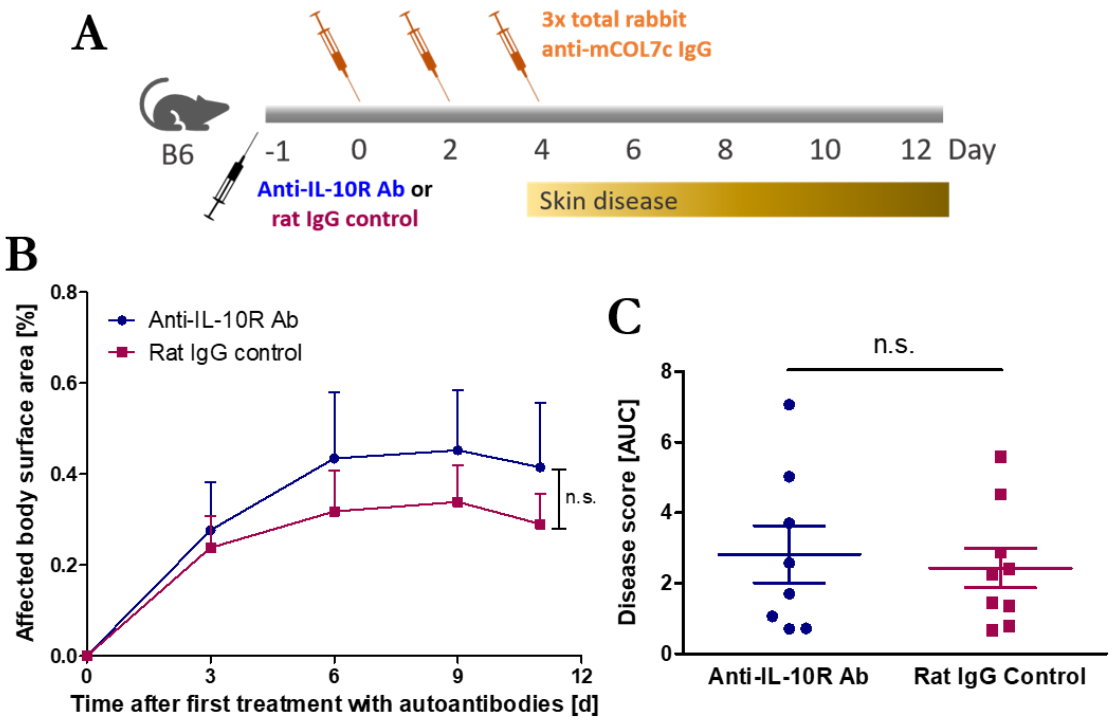

Figure 16: IL-10 receptor blockade does not modulate the disease score in the autoantibody-transfer-induced EBA model. (A) Experimental setup. C57Bl/6J mice were treated with an anti-IL-10 receptor antibody (anti-IL-10R Ab) or a control antibody (rat IgG control) one day before disease induction. EBA was induced by repeated injections of total rabbit anti-mCOL7c IgG on day zero, two and four and skin disease was monitored from day three. Final analysis was after twelve days. **(B)** The disease manifestation was evaluated as the percentage of the affected body surface area at various times after first treatment with autoantibodies, as indicated (n=8-9, two-way ANOVA). **(C)** The total disease score was defined as the area under the curve (AUC) (n=8-9, unpaired t-test). Data are expressed as mean ± SEM. *n.s., not significant.*

In line with the findings that mice treated with an IL-10R-blocking antibody only show a trend in an increased disease score, the oxidative burst of bone marrow-derived innate effector cells, measured with an luminol-amplified luminescence assay, was also only slightly but not significantly increased on day twelve (figure 17A+B). This indicates that the effect of IL-10R blockade was not strong enough to considerably modulate ROS release and, in turn, the disease score, at least not under the here applied experimental conditions.

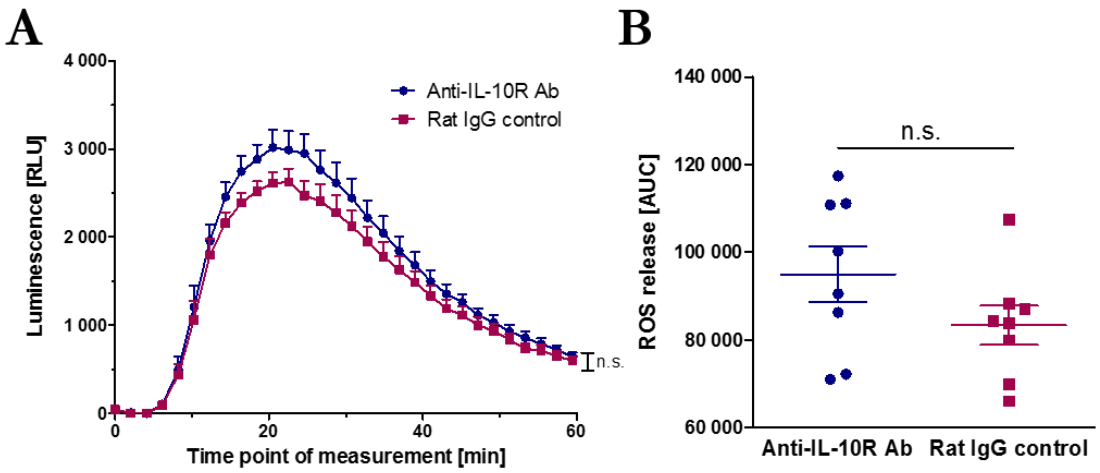

Figure 17: Oxidative burst by bone marrow-derived innate effector cells is not affected by IL-10 receptor blockade in the autoantibody-transfer-induced EBA model. Mice were treated with an IL-10 receptor-blocking antibody (anti-IL-10R Ab) or a control antibody (rat IgG control) one day before EBA was induced as described in the scheme in figure 16. On day twelve, bone marrow cells were isolated and their oxidative burst was measured by the immune complex-stimulated release of reactive oxygen species (ROS) with a luminol-amplified luminescence assay. **(A)** Increase of luminescence due to release of ROS by immune complex-activated bone marrow cells over time (n=8, two-way ANOVA). **(B)** Total ROS release defined as the area under the curve (AUC) (n=8, unpaired t-test). Data are expressed as mean ± SEM. *n.s., not significant; RLU, relative luminescence units.*

IL-17-producing T cells (Th17 cells) play a pivotal role in many autoimmune diseases [214] and IL-17R-deficient mice have been shown to be at least partially protected from autoantibody-induced EBA [164]. Not only $CD4^+$ T cells produce IL-17 but also γδ T cells are responsible for much of the IL-17 produced in different disease models in context of an early and local, innate-like immune response [215,216].

Although EBA disease score and ROS release were found to be not affected by IL-10R blockade in the autoantibody-transfer-induced model, the frequency and absolute cell number of $IL\text{-}17A^+$ $CD4^+$ T cells in in spleen were four-fold increased compared to control mice on day twelve (figure 18A&B and supplementary figure 6A). $IL\text{-}17A^+$ $CD4^+$ T cells were also increased in bone marrow (supplementary figure 6B). γδ T cells were the major producer of IL-17A and mice treated with an anti-IL-10R Ab showed approximately two-

fold more IL-17A expression by γδ T cells than control mice (figure 18B). Since the frequency of IFNγ$^+$ CD4$^+$ T cells and IFNγ$^+$ γδ T cells was not affected by IL-10R blockade, the ratio between IL-17A$^+$ and IFNγ$^+$ T cells was strongly increased in mice treated with an anti-IL-10R Ab (figure 18C).

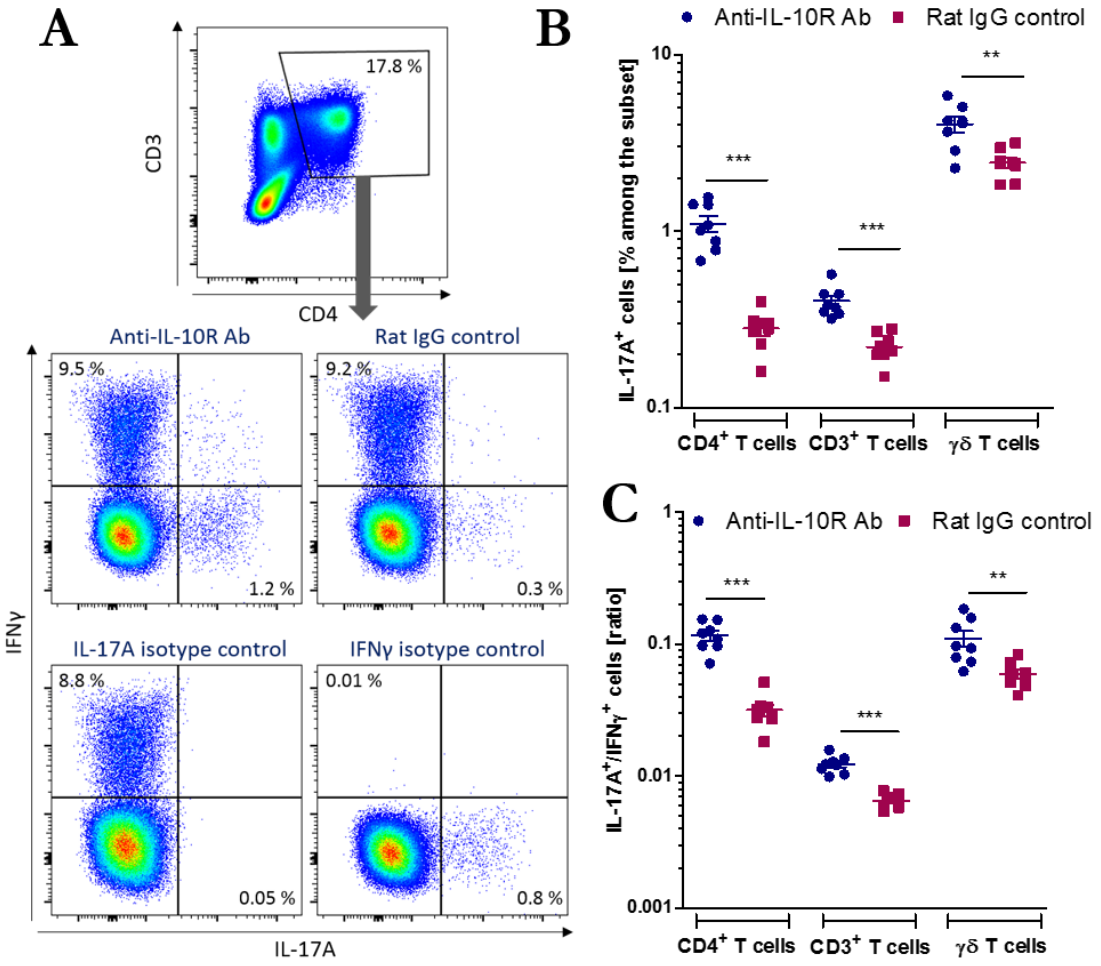

Figure 18: IL-10 receptor blockade increases IL-17A production by all splenic T-cell subsets in the autoantibody-transfer-induced EBA model. Mice were treated with an IL-10 receptor-blocking antibody (anti-IL-10R Ab) or a control antibody (rat IgG control) one day before EBA was induced as described in the scheme in figure 16. On day twelve, splenic T-cell subsets were analyzed for their IL-17A and IFNγ expression by flow cytometry. **(A)** Representative flow cytometry data from spleen for CD4$^+$ T cells. CD4$^+$ T cells were gated for their IL-17A and IFNγ expression (middle panel) compared to the isotype controls (lower panel). γδ T cells were defined as γδTCR$^+$ CD3$^+$ lymphocytes as shown in figure 10. A similar gating was performed for IFNγ and IL-17A expression by γδ T cells and CD3$^+$ T cells. **(B)** Frequency of IL-17$^+$ cells among CD4$^+$ T cells, CD3$^+$ T cells (without CD4$^+$ T cells) and γδ T cells in spleen (n=8, unpaired t-test). **(C)** Ratio of IL-17A$^+$ and IFNγ$^+$ CD4$^+$ T cells, CD3$^+$ T cells (without CD4$^+$ T cells) and γδ T cells in spleen (n=8, unpaired t-test). Data are expressed as mean ± SEM. **p ≤ 0.01; ***p≤0.001.

Taken together, IL-10R blockade before EBA induction by autoantibodies was not able to considerably increase the disease score or the release of ROS by innate effector cells, a hallmark of the EBA effector phase. By contrast, IL-10R blockade increased the production of proinflammatory IL-17A by $CD4^+$ T cells and γδ T cells, together indicating that increased IL-17A production is not sufficient to increase EBA skin inflammation in this experimental setting. In contrast to the immunization-induced EBA model, disease induction by transfer of autoantibodies excludes the adaptive immune response. Thus, the production of IL-10 might not be induced in this model, which could explain the differential effects of IL-10R blockade (chapter 6.1.1 and 6.1.5). The following chapters address the question whether IL-10 production kinetics are indeed different between the immunization-induced and the autoantibody-transfer-induced EBA model.

6.2 Plasma cell-derived IL-10 is induced in the natural course of EBA after immunization with the autoantigen

The anti-inflammatory cytokine IL-10 down-modulates the autoimmune blistering skin disease EBA under pathophysiological conditions despite the presence of circulating autoantibodies (chapter 6.1). However, the cellular source of IL-10 in this autoimmune disease remained to be investigated. IL-10 transcriptional reporter mice (Vert-x), which express eGFP under the control of the *Il10* promotor, are a useful tool to detect IL-10-expressing cells by flow cytometry. Although Vert-x mice do not reflect a direct IL-10 read-out, it has been shown that eGFP expression correlates well with IL-10 protein expression on an individual cell basis [70,183].

6.2.1 Plasma cells expand in the immunization-induced EBA model and represent a major source of IL-10

Only a low frequency of cells express IL-10 under steady state but their numbers increase after immune stimulation, e.g. during autoimmune diseases or infection [46]. Using IL-10 reporter mice, different immune cell types were analyzed for their eGFP expression by flow cytometry (figure 19). EBA was induced by subcutaneous immunization with vWFA2 and EBA susceptible B6.SJL-$H2^s$ $C3^c$/1CyJ IL-10 reporter (B6.s IL-10 reporter) mice and congenic, non-susceptible C57Bl/6J IL-10 reporter (B6 IL-10 reporter) mice were analyzed at different stages of the disease (afferent phase after ten days and effector phase after four and five weeks) or under steady state conditions (day zero).

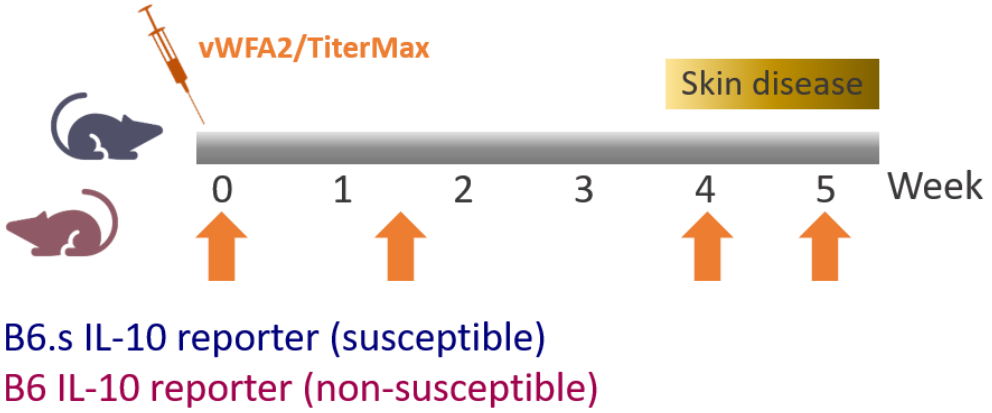

Figure 19: Experimental setup for analysis of IL-10 kinetics in the immunization-induced EBA model. EBA was induced in susceptible B6.s IL-10 reporter and non-susceptible B6 IL-10 reporter (Vert-x) mice by immunization with the autoantigen vWFA2 (von Willebrand factor A-like domain 2) in TiterMax. IL-10-eGFP expression in different cell types was analyzed in spleen, bone marrow and draining lymph nodes at various time points, as indicated (orange arrow). Identically immunized wildtype C57Bl/6J mice were used as a gating control for flow cytometry (figure 20). Susceptible B6.s IL-10 reporter mice were treated with only TiterMax and were used to define autoreactive lymphocytes by flow cytometry.

The IL-10-eGFP expression by different cell types was analyzed by flow cytometry (figure 20). Wildtype C57Bl/6J mice were treated similarly to the experimental mice and were used for definition of the positive eGFP signal in each experiment. As depicted in figure 20, plasma cells were defined as $CD138^{hi}$ $TACI^{+}$ cells and within the remaining population of non-plasma cells, B cells were identified as $CD19^{+}$ cells. In addition, IL-10-eGFP expression was analyzed in $CD4^{+}$ T cells, $CD11b^{+}$ myeloid cells and $CD11b^{+}$ $Ly6G^{+}$ neutrophils.

Although many cells are able to produce IL-10, the ability of B cells to counteract proinflammatory immune responses via IL-10 has been in the focus of research for more than a decade [85,99]. More recently, $CD138^{hi}$ plasmablasts in spleen and lymph nodes were shown to be the major producers of IL-10 in EAE and they have the ability to limit this autoimmune disease [84,92]. Furthermore, $CD138^{hi}$ plasma cells were found to exhibit anti-inflammatory activities in EBA after induction of a strong but non-physiological plasmacytosis [70].

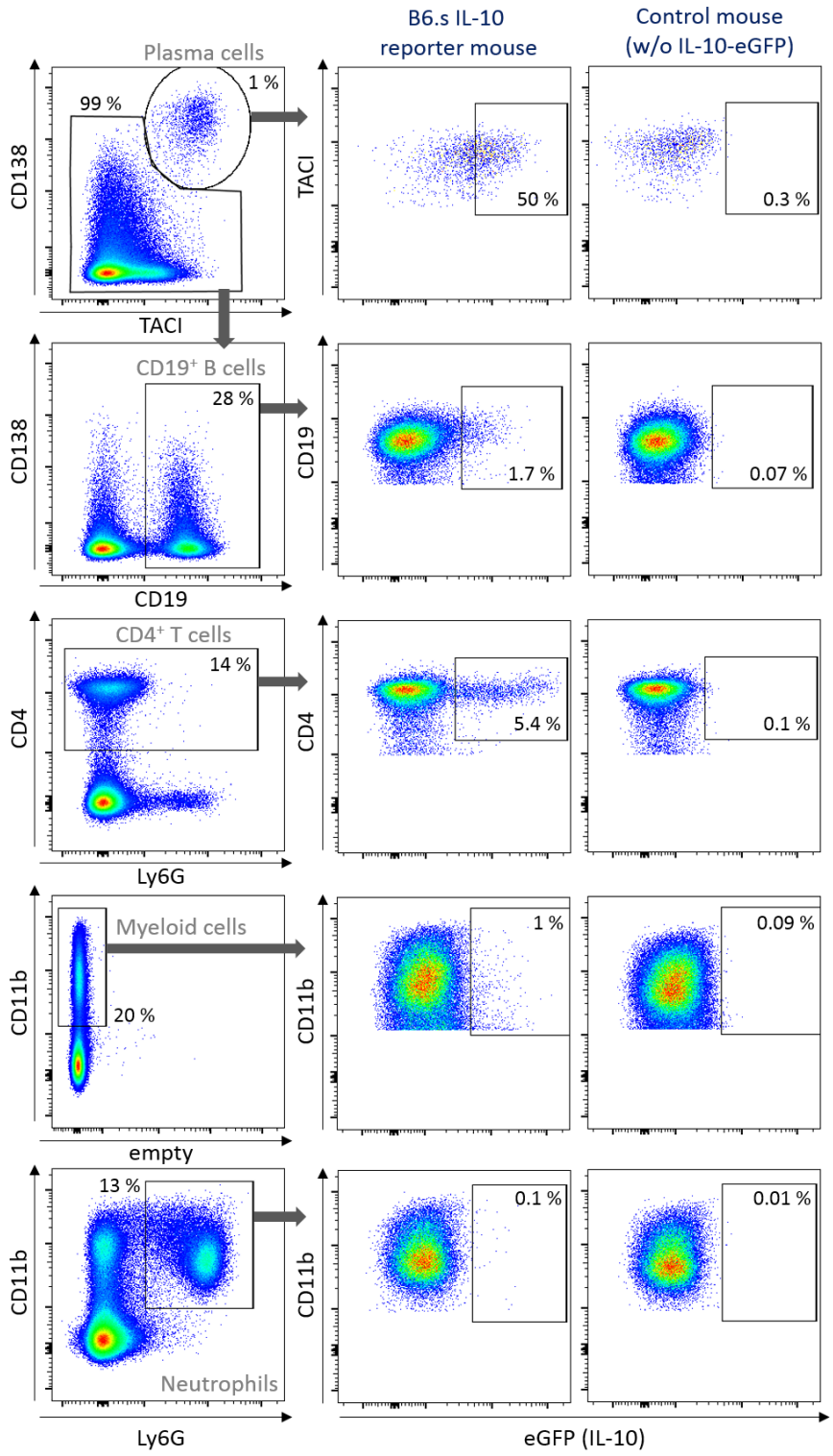

Figure 20: Gating strategy for analysis of IL-10-eGFP expression by different splenic cell types in IL-10 reporter mice. EBA was induced in susceptible B6.s IL-10 reporter mice by immunization with vWFA2 as described in the scheme in figure 19 and different lymphoid organs were analyzed by flow cytometry. The figure shows the gating strategy in spleen ten days after immunization and is representative for draining lymph nodes and bone marrow and other time points. Cells were pre-gated on single lymphocytes and plasma cells were defined as $CD138^{hi}$ $TACI^{+}$ lymphocytes (1^{st} row) and the remaining cells were gated for $CD19^{+}$ B cells (2^{nd} row). $CD4^{+}$ T cells were defined as $CD4^{+}$ lymphocytes (3^{rd} row), myeloid cells as $CD11b^{+}$ cells (4^{th} row) and neutrophils as $CD11b^{+}$ $Ly6G^{+}$ cells (5^{th} row). All cells were further gated for their IL-10-eGFP signal and the gate was defined as compared to a wildtype C57Bl/6J control mouse without eGFP expression (right panels). *w/o, without.*

In line with these findings, plasma cells were also major producers of IL-10 in the natural course of EBA in susceptible B6.s mice (figure 21). Depending on the organ, between 30 and 60 % of plasma cells expressed IL-10-eGFP five weeks after immunization, but only a low frequency of the other cell types, especially CD19$^+$ B cells (figure 21A). The absolute cell number of IL-10-eGFP$^+$ cells in different organs showed that IL-10-producing plasma cells matched or even exceeded the number of the other IL-10-expressing cells (figure 21B), although plasma cells represented only around 0.5 to 1.5 % of lymphocytes (figure 22B). The same observations were made in the acute phase of the disease ten days after immunization (supplementary figure 7A&B).

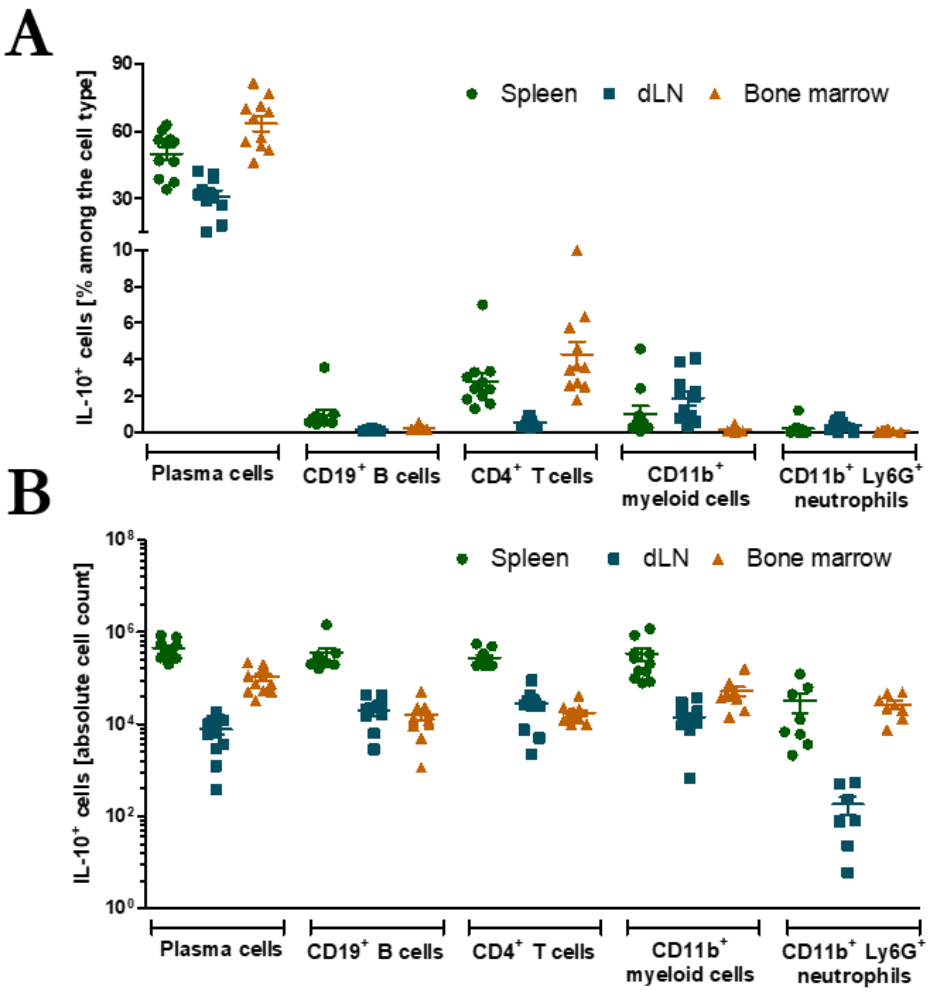

Figure 21: Plasma cells represent major producers of IL-10 in all lymphoid organs. EBA was induced in susceptible B6.s IL-10 reporter mice by immunization with vWFA2 as described in the scheme in figure 19 and different lymphoid organs were analyzed by flow cytometry after five weeks. The gating was performed as depicted in figure 20. **(A)** Frequency of IL-10-eGFP$^+$ cells and **(B)** absolute cell number of IL-10-eGFP$^+$ cells in spleen, draining lymph nodes (dLN) and bone marrow (n=8-11 pooled from two or three independent experiments). For one data point of the absolute cell number of IL-10$^+$ B cells, IL-10$^+$ myeloid cells and IL-10$^+$ neutrophils in dLN, respectively, the value was zero and is therefore not indicated in the logarithmic scale. Data are expressed as mean ± SEM and IL-10-eGFP frequencies are corrected by the value obtained from the C57Bl/6J control mouse indicating the unspecific background staining.

Further analysis of the kinetics of total plasma cells and IL-10-eGFP-expressing plasma cells revealed that these cells were strongly induced after immunization in dLN (pooled inguinal and popliteal lymph nodes) and declined again in the effector phase (figure 22A).

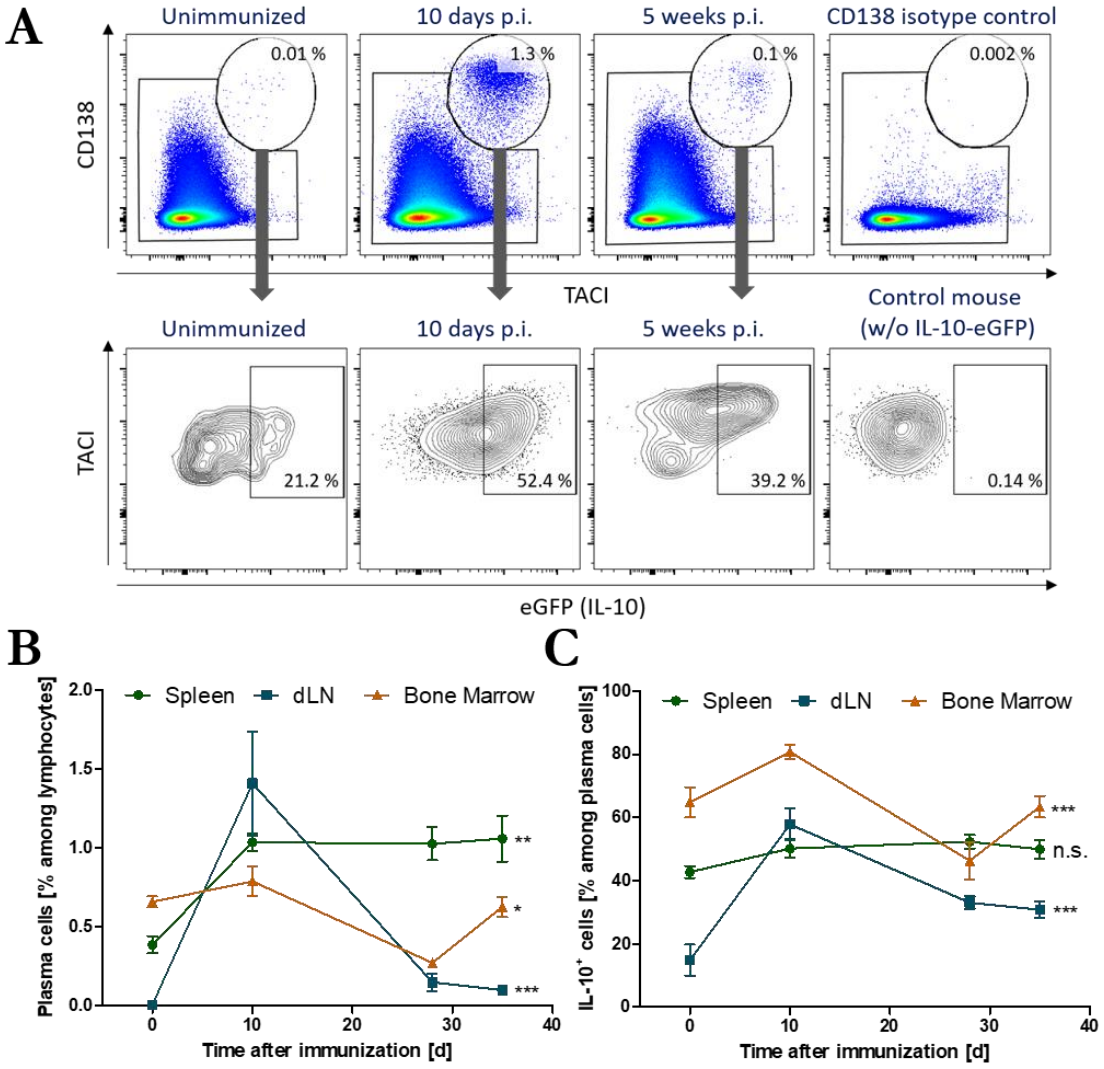

Figure 22: The frequency of plasma cells and IL-10-producing plasma cells in draining lymph nodes is increased after immunization. EBA was induced in susceptible B6.s IL-10 reporter mice by immunization with vWFA2 as described in the scheme in figure 19 and different lymphoid organs were analyzed by flow cytometry. **(A)** Representative flow cytometry data from draining lymph nodes (dLN). At different time points after immunization, $CD138^{hi}$ $TACI^{+}$ plasma cells (upper panel) were further analyzed for their IL-10-eGFP signal (lower panel) as compared to the wildtype C57Bl/6J control mouse. **(B)** Kinetics of plasma cell frequencies among lymphocytes and **(C)** IL-10-eGFP^{+} cells among plasma cells in spleen, dLN and bone marrow (n=3-11 pooled from two (zero and ten days) or three (five weeks) independent experiments, one-way ANOVA). Data are expressed as mean ± SEM and IL-10-eGFP frequencies are corrected by the value obtained from the C57Bl/6J control mouse indicating the unspecific background staining. *$p \leq 0.05$; **$p \leq 0.01$ or ***$p \leq 0.001$ indicates a significant change of the frequency over time within one organ. A significant increase of plasma cell frequencies after ten days compared to steady state was observed in dLN and spleen and of IL-10-eGFP^{+} plasma cells only in dLN. *p.i., post immunization; w/o, without.*

Plasma cells were very rare in dLN under steady state conditions and frequencies and absolute cell numbers considerably increased ten days after immunization before they decreased again until week four to five (figure 22B and supplementary figure 8A). In other lymphoid organs such as spleen and bone marrow plasma cells only slightly increased after immunization and remained relatively constant during the course of the disease. In dLN, not only the absolute cell number of plasma cells but also the one of IL-10$^+$ plasma cells considerably increased after immunization (supplementary figure 8B). The frequency of IL-10-eGFP$^+$ cells among plasma cells was four-fold higher in the acute phase ten days after immunization (figure 22C). In the effector phase, the frequency and absolute cell number declined again. By contrast, IL-10-eGFP$^+$ plasma cells remained relatively constant in spleen and bone marrow with a decreasing trend in the effector phase in the bone marrow.

Taken together, plasma cells in spleen, dLN and bone marrow represented a considerable fraction of IL-10$^+$ cells during the acute and the effector phase of EBA. Immunization with the autoantigen induced a substantial, acute plasma cell response that declined during the ensuing effector phase. Furthermore, the frequency and absolute cell number of IL-10-eGFP$^+$ plasma cells expanded after immunization, indicating that dLN-derived plasma cells are the primary induced source of anti-inflammatory IL-10 with the potential to control EBA skin disease under pathophysiological conditions. Of note, IL-10$^+$ plasma cells were also abundant in other lymphoid organs, thus they can also contribute to the total IL-10 production, e.g. in the effector phase.

6.2.2 IL-10$^+$ plasma cells are more frequent in spleen and bone marrow of susceptible mice compared to non-susceptible mice

Multiple factors are known to contribute to EBA susceptibility in mice, e.g. the MHCII haplotype, the antibody subclass or distinct APCs [134,137,141]. To test whether different quantities of IL-10-producing plasma cells also contribute to EBA susceptibility, B6.s and B6 IL-10 reporter mice were analyzed for their IL-10-eGFP expression by flow cytometry (figure 23 and figure 24).

The frequency of IL-10-eGFP expression among plasma cells was considerably increased in susceptible B6.s mice compared to non-susceptible B6 mice in spleen (figure 23A&B) and bone marrow (figure 23C). After ten days and five weeks, B6.s mice had approximately 1.5- to 2-fold more IL-10-eGFP expression in plasma cells as compared to B6 mice.

Furthermore, the absolute cell number of IL-10-eGFP$^+$ plasma cells in spleen and bone marrow was more than twice that of non-susceptible B6 mice at these time points (supplementary figure 9A&B). This indicates that IL-10-induction in plasma cells was restricted to susceptible mice in spleen and bone marrow and that IL-10$^+$ plasma cells in non-susceptible mice remained constant or even decreased over time.

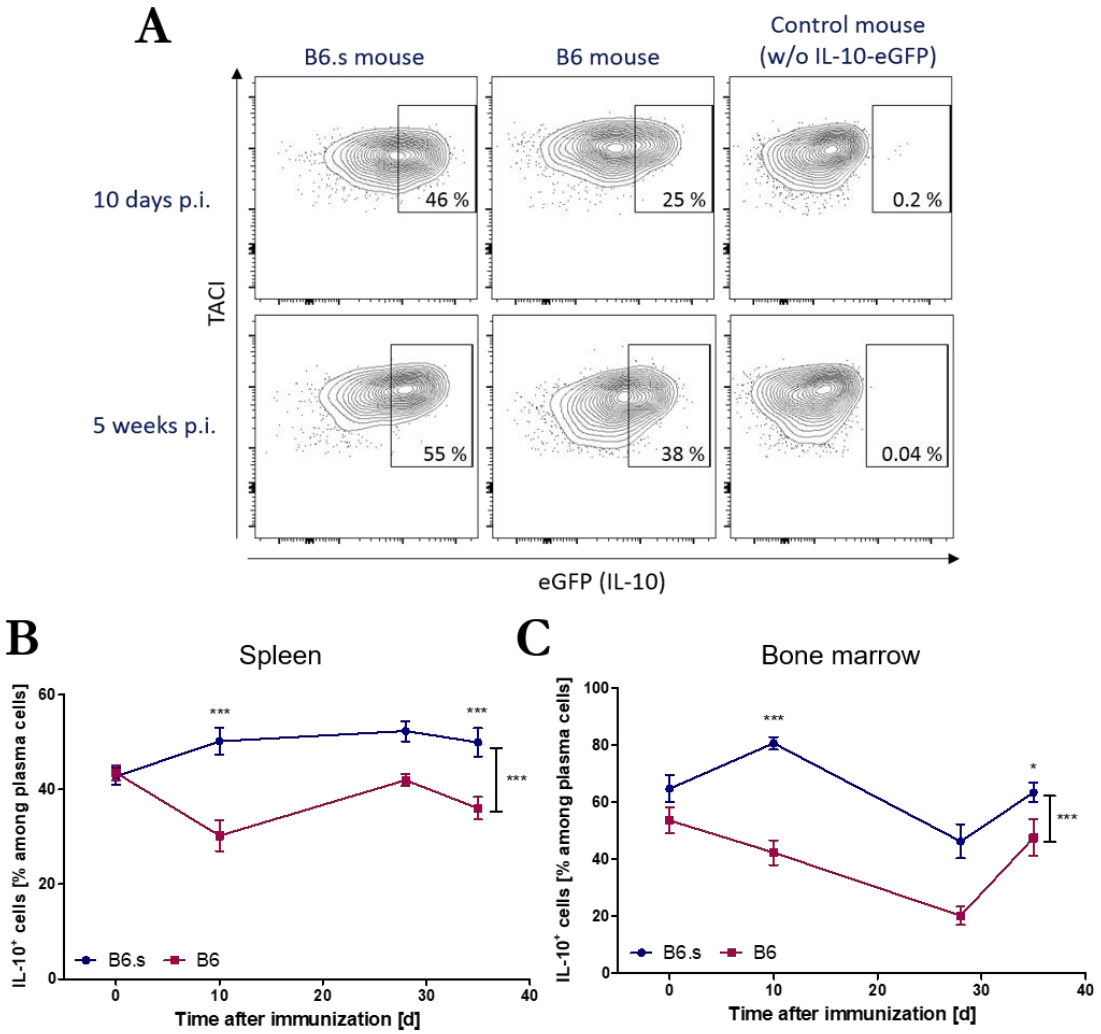

Figure 23: Plasma cell IL-10-induction in spleen and bone marrow is restricted to susceptible mice. EBA was induced in susceptible B6.s IL-10 reporter and non-susceptible B6 IL-10 reporter mice by immunization with vWFA2 as described in the scheme in figure 19 and spleen and bone marrow were analyzed by flow cytometry. **(A)** Representative flow cytometry data from spleen. Plasma cells were defined as described in figure 20 and gated for their IL-10-eGFP expression ten days (upper panel) and five weeks (lower panel) after immunization as compared to the wildtype C57Bl/6J control mouse (right plots). **(B)** Kinetics of the frequency of IL-10-eGFP$^+$ cells among plasma cells in spleen and **(C)** bone marrow (n=3-11 pooled from two (zero and ten days) or three (five weeks) independent experiments, two-way ANOVA with Bonferroni post-test). Data are expressed as mean ± SEM and IL-10-eGFP frequencies are corrected by the value obtained from the C57Bl/6J control mouse indicating the unspecific background staining. *$p \leq 0.05$; ***$p \leq 0.001$. *p.i., post immunization; w/o, without.*

While induction of EBA led to an expanded IL-10$^+$ plasma cell population in susceptible B6.s mice, IL-10 expression by other cell types was not affected. In the effector phase (figure 24A&B, supplementary figure 9C&D) as well as in the acute phase (supplementary figure 10A&B) of EBA the frequency and absolute cell number of IL-10-eGFP$^+$ plasma cells were considerably increased in susceptible B6.s mice. Only a small fraction of the other cell types analyzed in this experiment was IL-10-eGFP$^+$ and they showed no considerable difference, indicating that IL-10-induction in context of EBA in susceptible mice is restricted to plasma cells.

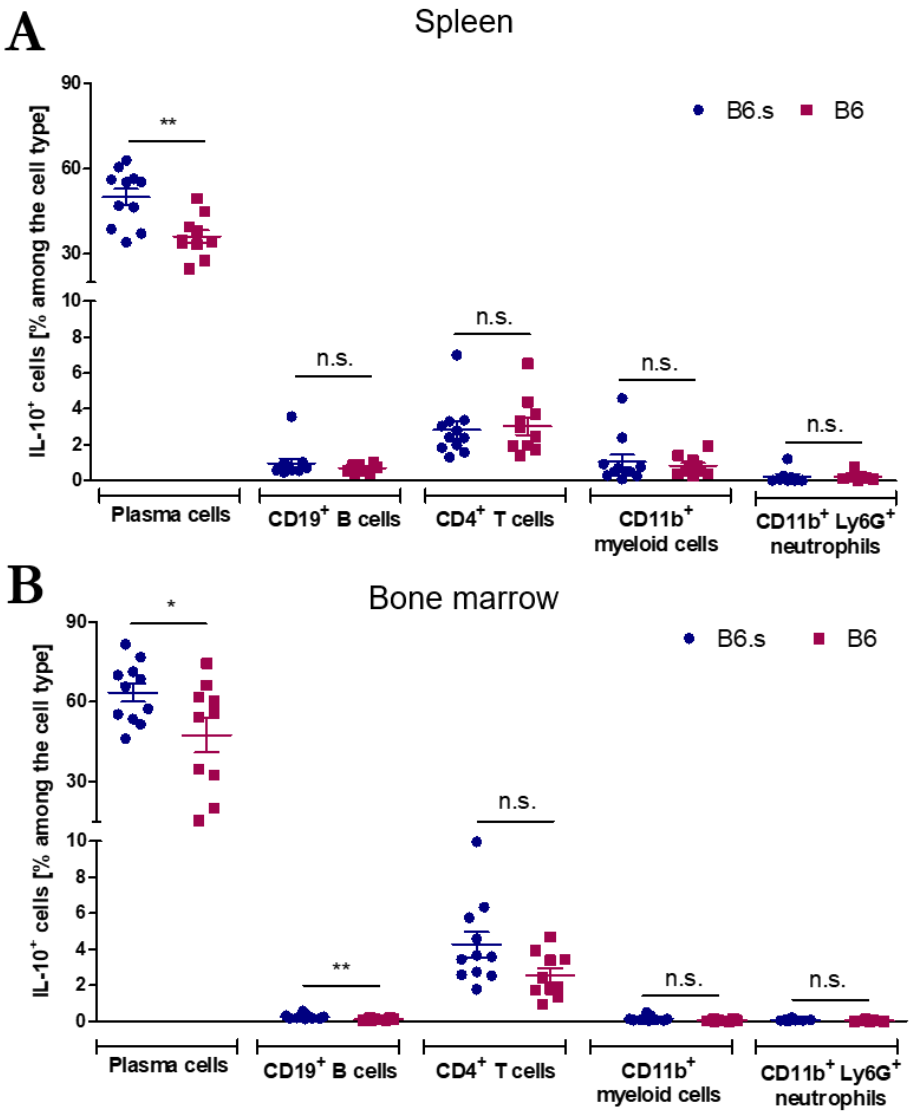

Figure 24: IL-10-induction in spleen and bone marrow of susceptible mice is plasma cell-specific. EBA was induced in susceptible B6.s IL-10 reporter and non-susceptible B6 IL-10 reporter mice by immunization with vWFA2 as described in the scheme in figure 19 and spleen and bone marrow were analyzed by flow cytometry. The gating was performed as depicted in figure 20. **(A)** Frequency of IL-10-eGFP$^+$ cells among the cell type indicated in spleen and **(B)** bone marrow five weeks after immunization (n=7-11 pooled from two or three independent experiments, unpaired t-test). Data are expressed as mean ± SEM and IL-10-eGFP frequencies are corrected by the value obtained from the C57Bl/6J control mouse indicating the unspecific background staining. *p ≤ 0.05; **p ≤ 0.01. *n.s., not significant.*

Interestingly, the IL-10$^+$ plasma cell compartment in dLN was comparable between susceptible and non-susceptible mice, and mice treated only with the adjuvant TiterMax induced plasma cell IL-10 to the same extent (figure 25A). These results indicate that the adaptive immune response to the autoantigen vWFA2 is not required to drive the generation of IL-10$^+$ plasma cells.

The frequency (figure 25B) and the absolute cell number (supplementary figure 11A) of IL-10-eGFP$^+$ plasma cells showed no difference in dLN, but IL-10-eGFP$^+$ myeloid cells were increased in susceptible mice, both in frequency and absolute cell number. As described in chapter 6.2.1, IL-10-eGFP expression by plasma cells in dLN strongly increased after immunization in the acute phase of the disease and declined thereafter. Compared to the observations in spleen and bone marrow, susceptible and non-susceptible mice did not show any differences in IL-10-eGFP$^+$ plasma cell kinetics in dLN (figure 25C and supplementary figure 11B).

Susceptible B6.s IL-10 reporter and non-susceptible B6 IL-10 reporter mice showed considerable differences in IL-10$^+$ plasma cell kinetics and their location. IL-10-producing plasma cells were comparable in dLN but more frequent in spleen and bone marrow of susceptible mice, suggesting that the induction could be mediated by regulatory feedback mechanisms in the context of the systemic, disease-induced inflammation. This effect could be an indirect consequence of the inflammatory phenotype determined by the differential genetic background of the two mouse strains. Nevertheless, non-susceptible mice were not protected from the disease due to an expanded IL-10$^+$ plasma cell subset, thus, other factors contribute to disease susceptibility (chapter 6.4).

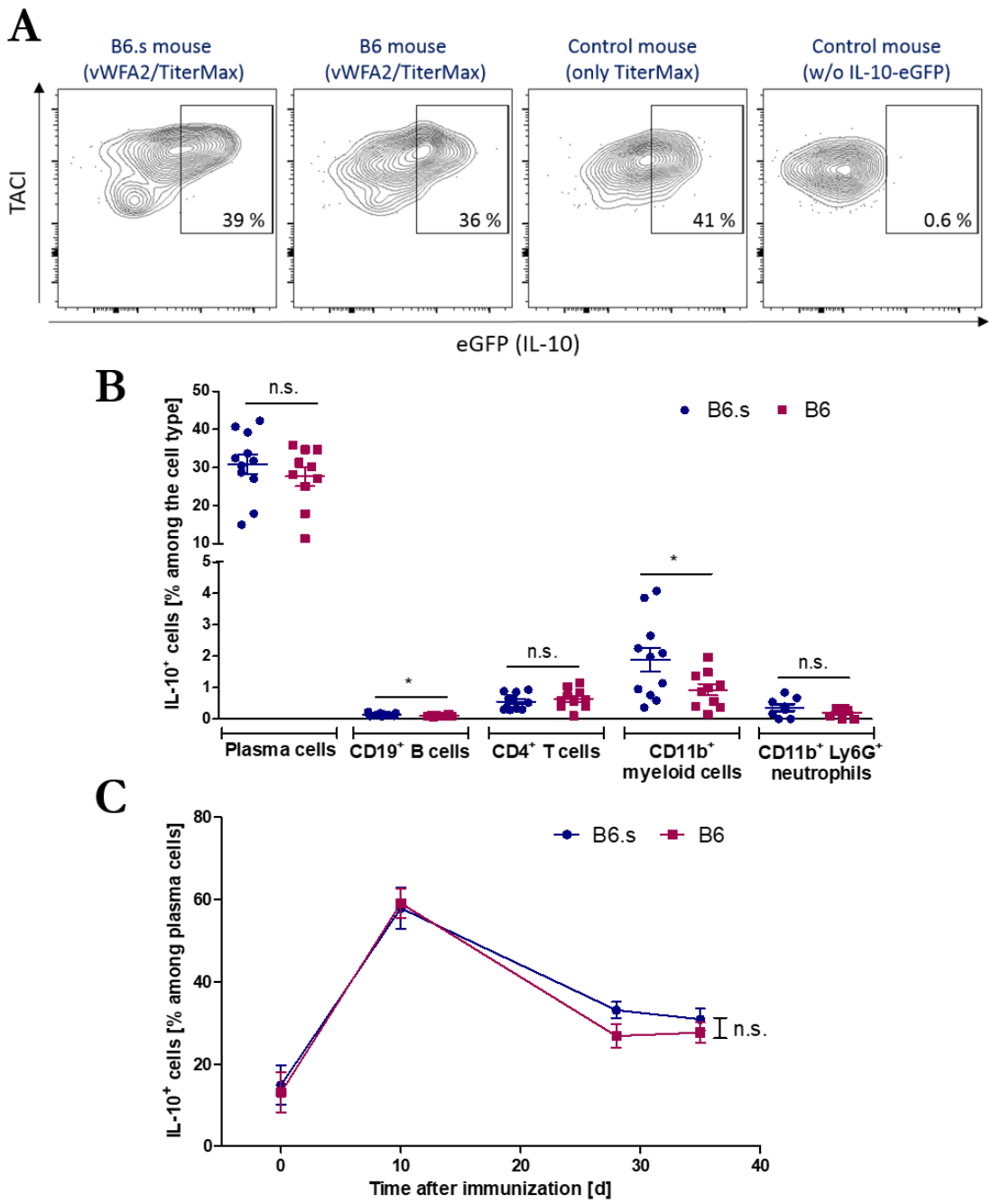

Figure 25: Susceptible and non-susceptible mice exhibit comparable frequencies of IL-10⁺ plasma cells in draining lymph nodes. EBA was induced in susceptible B6.s IL-10 reporter and non-susceptible B6 IL-10 reporter mice by immunization with vWFA2 as described in the scheme in figure 19 and draining lymph nodes were analyzed by flow cytometry. **(A)** Representative flow cytometry data. Plasma cells were defined as depicted in figure 20 and gated for their IL-10-eGFP expression five weeks after immunization as compared to the wildtype C57Bl/6J control mouse (right plot). **(B)** Frequency of IL-10-eGFP⁺ cells among the cell type indicated five weeks after immunization (n=7-11 pooled from two or three independent experiments, unpaired t-test). **(C)** Kinetics of the frequency of IL-10-eGFP⁺ cells among plasma cells (n=3-11 pooled from two (zero and ten days) or three (five weeks) independent experiments, two-way ANOVA). Data are expressed as mean ± SEM and IL-10-eGFP frequencies are corrected by the value obtained from the C57Bl/6J control mouse indicating the unspecific background staining. *p ≤ 0.05. *n.s., not significant; w/o, without.*

6.2.3 IL-10 is not induced in plasma cells in the autoantibody-transfer-induced EBA model

The autoantibody-transfer-induced EBA model reflects the effector phase of the disease characterized by binding of autoantibodies and complement in the skin and the subsequent tissue damage and blister formation. IL-10R blockade before induction of EBA by transfer of autoantibodies revealed no effect on the disease score (chapter 6.1.5.). In order to analyze whether the induction of IL-10 in the autoantibody-transfer-induced EBA model may be not sufficient for considerable effects on the disease manifestation after IL-10R blockade, B6 IL-10 reporter mice were analyzed by flow cytometry at different time points after EBA induction by autoantibodies (figure 26).

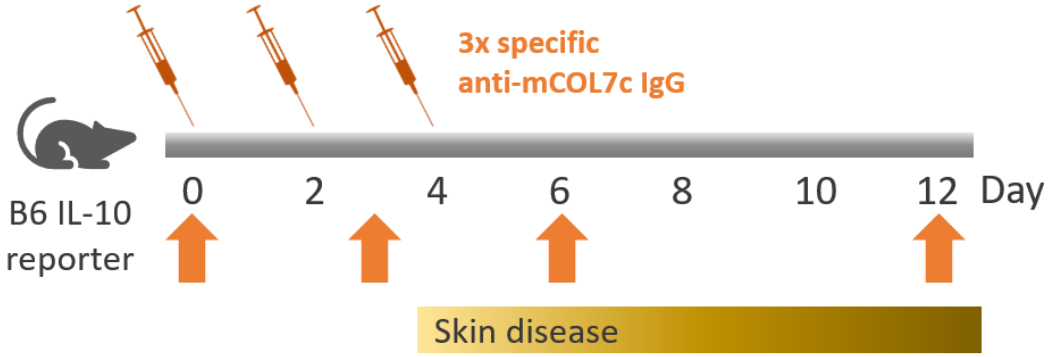

Figure 26: Experimental setup for analysis of IL-10 kinetics in the autoantibody-transfer-induced EBA model. B6 IL-10 reporter mice (Vert-x) were repeatedly treated with specific rabbit anti-mCOL7c IgG on day zero, two and four. IL-10-eGFP expression in different cell types was analyzed in spleen and bone marrow at various time points, as indicated (orange arrow). An identically treated wildtype C57Bl/6J mouse was used as a gating control for flow cytometry.

EBA was induced by repeated injections of specific rabbit anti-mCOL7c IgG and IL-10-eGFP expression was analyzed before (day three) and after disease manifestation (day six and twelve) or under steady state conditions (day zero) in different immune cells with an identical gating strategy as depicted in figure 20. A similar to the experimental mice treated wildtype C57Bl/6J mouse was used to determine positive eGFP signals (figure 27A). In line with the results from the immunization-induced model (chapter 6.2.1), plasma cells were also major producers of IL-10 in the autoantibody-transfer-induced model (figure 27B). Dependent on the organ, approximately 45 to 65 % of plasma cells were IL-10-eGFP$^+$ on day twelve, but only a minor part of the other cell types were IL-10-eGFP$^+$ with the largest fraction of 3 % found among CD4$^+$ T cells. The absolute number of IL-10-eGFP$^+$ plasma cells in spleen and bone marrow matched or even exceeded the one of the other IL-10-producing cell types (supplementary figure 12A). Furthermore, the fraction of

IL-10-expressing plasma cells did not increase over time in spleen and bone marrow (figure 27C, supplementary figure 12B). During the late phase of EBA after six to twelve days, the frequency and the absolute cell number of splenic IL-10-eGFP$^+$ plasma cells was only 10 to 15 % higher compared to naïve mice. The autoantibody-transfer-induced EBA model does not include an adaptive immune response against the vWFA2-autoantigen, which primarily takes place in dLN. Spleen and bone marrow did not show a considerable IL-10-induction after transfer of autoantibodies, suggesting that the IL-10 response was not sufficient to down-modulate the skin disease in this model.

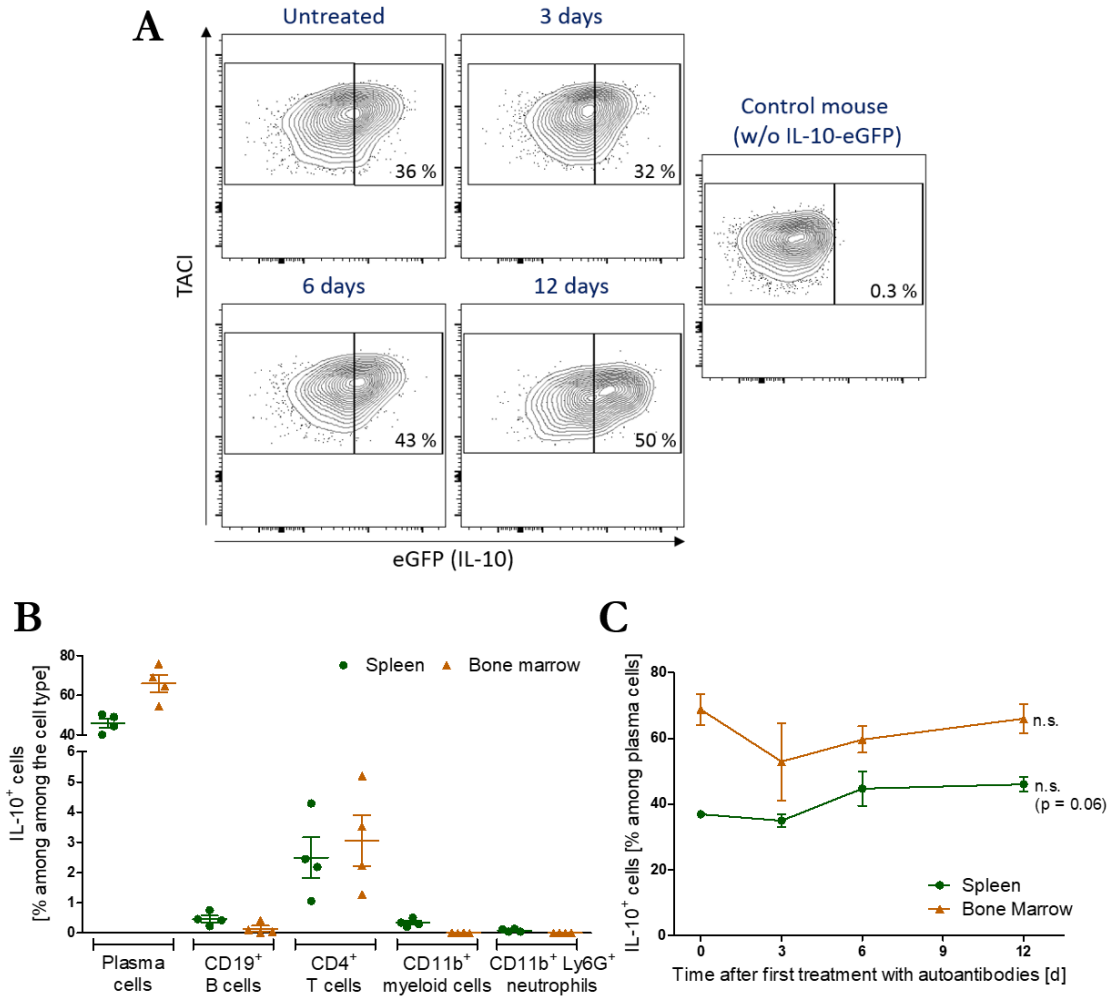

Figure 27: The frequency of IL-10-producing plasma cells does not increase in the autoantibody-transfer-induced EBA model. EBA was induced in B6 IL-10 reporter mice as described in the scheme in figure 26 and IL-10-eGFP$^+$ cells were gated as depicted in figure 20. **(A)** Representative flow cytometry data from spleen. Plasma cells were defined as CD138^{hi} TACI$^+$ cells and further gated for their IL-10-eGFP expression as compared to the wildtype C57Bl/6J control mouse (right plot). **(B)** Frequency of IL-10-eGFP$^+$ cells in spleen and bone marrow twelve days after first treatment with autoantibodies (n=4). **(C)** Kinetics of IL-10-eGFP$^+$ cells among plasma cells in spleen and bone marrow (n=3-4, one-way ANOVA). Data are expressed as mean ± SEM and IL-10-eGFP frequencies are corrected by the value obtained from the C57Bl/6J control mouse indicating the unspecific background staining. *n.s., not significant; w/o, without.*

6.2.4 Splenic LAG-3$^+$ plasma cells are found in the immunization-induced EBA model and produce IL-10

LAG-3 is an immune checkpoint inhibitor receptor known to control activation and effector functions on the surface of T lymphocytes [217]. Recently, LAG-3$^+$ plasma cells have been identified as a pre-existing subset of "natural regulatory plasma cells" which rapidly respond to bacterial infection by the production of anti-inflammatory IL-10 [71]. To test whether LAG-3$^+$ plasma cells also exist in autoimmune-diseased mice, LAG-3 expression by CD138^{hi} TACI$^+$ plasma cells was analyzed ten days after immunization with vWFA2 in B6.s mice by flow cytometry. In addition, naïve B6.s IL-10 reporter mice were analyzed for LAG-3 and IL-10-eGFP expression to compare the data to steady state conditions.

Compared to unimmunized mice, the population of splenic CD138^{hi} TACI$^+$ plasma cells increased about ten-fold (figure 28A). Approximately 23 % of splenic plasma cells expressed the surface receptor LAG-3 in unimmunized mice and this fraction slightly increased after immunization up to 30 % (figure 28B), suggesting that autoimmune inflammation can trigger the expansion of LAG-3$^+$ plasma cells. Of note, the absolute cell number of LAG-3$^+$ plasma cells was more than ten-fold increased after immunization (figure 28C). The discrepancy between the mild increase in frequencies and the substantial increase of absolute LAG-3$^+$ plasma cells was due to a general increase of plasma cells numbers in spleen ten days after immunization (figure 28A). Interestingly, LAG-3$^+$ plasma cells were absent in dLN at this time point (supplementary figure 13), indicating that LAG-3$^+$ plasma cells are tissue-specific. This finding also suggests that LAG-3$^+$ plasma cells are not formed as a result of the adaptive immune reaction to the autoantigen, which peaks ten days after immunization in dLN.

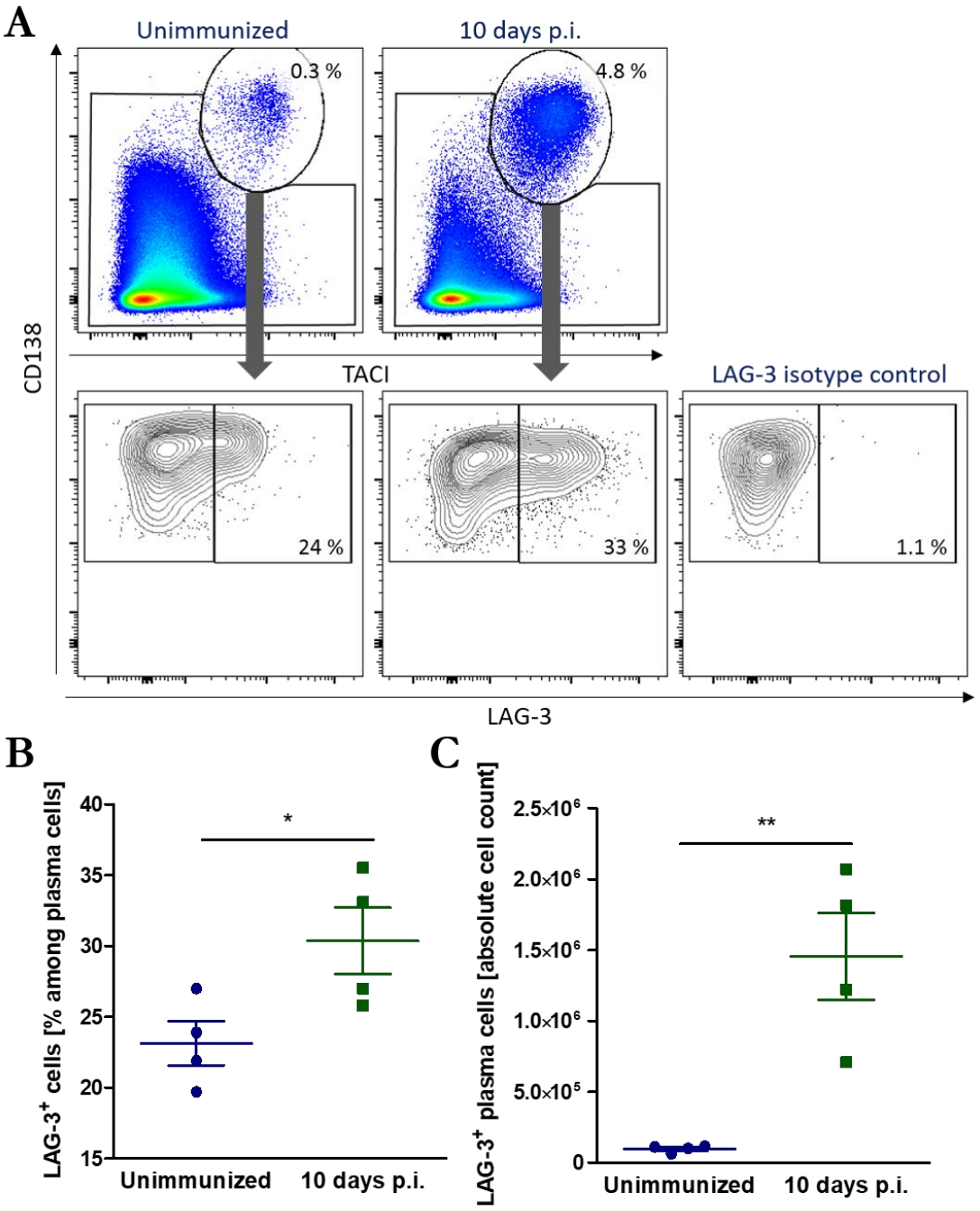

Figure 28: LAG-3-expressing plasma cells are found in the natural course EBA. Susceptible B6.s mice were either immunized with vWFA2 and analyzed after ten days, as described in the scheme in figure 19, or left untreated. **(A)** Representative flow cytometry data from spleen. Plasma cells were defined as CD138^{hi} TACI^{+} cells (upper panel) and further gated for their LAG-3 expression (lower panel) as compared to the isotype control (right plot). **(B)** Frequency of LAG-3^{+} cells among plasma cells and **(C)** absolute cell number of LAG-3^{+} plasma cells in spleen in unimmunized mice and ten days after immunization (n=4, unpaired t-test). Data are expressed as mean ± SEM. *p ≤ 0.05; **p ≤ 0.01. *p.i., post immunization.*

To further test the possibility that LAG-3$^+$ plasma cells are induced because of autoimmune inflammation in the absence of an adaptive immune response to the autoantigen, the autoantibody-transfer-induced EBA model was used to mimic the effector phase of the disease. There was a slight increase of LAG-3$^+$ plasma cell frequencies in spleen but not in bone marrow on day twelve compared to earlier time points after autoantibody injection (figure 29A&B). By contrast, the absolute cell number of LAG-3$^+$ plasma cells did not increase over time in spleen and bone marrow (supplementary figure 14).

LAG-3 expression identifies a subset of "natural regulatory plasma cells" with the ability to produce IL-10 [71]. To test whether LAG-3$^+$ plasma cells already express IL-10 under steady state conditions, naïve B6.s IL-10 reporter mice were analyzed for their LAG-3 and IL-10-eGFP expression by flow cytometry (figure 30A). LAG-3$^+$ splenic plasma cells expressed more IL-10-eGFP compared to LAG-3$^-$ plasma cells (figure 30B). However, only about 50 % of LAG-3$^+$ plasma cells co-expressed IL-10-eGFP. Of note, the absolute cell number of IL-10$^+$ LAG-3$^+$ plasma cells was much lower compared to IL-10$^+$ LAG-3$^-$ plasma cells due to the lower abundance of LAG-3$^+$ plasma cells in general (figure 30C).

Taken together, LAG-3$^+$ plasma cells were already present in spleen in naïve mice and further increased in the context of autoimmune inflammation. However, LAG-3 surface expression was not a requirement for IL-10-eGFP production in splenic plasma cells, at least not under steady state conditions.

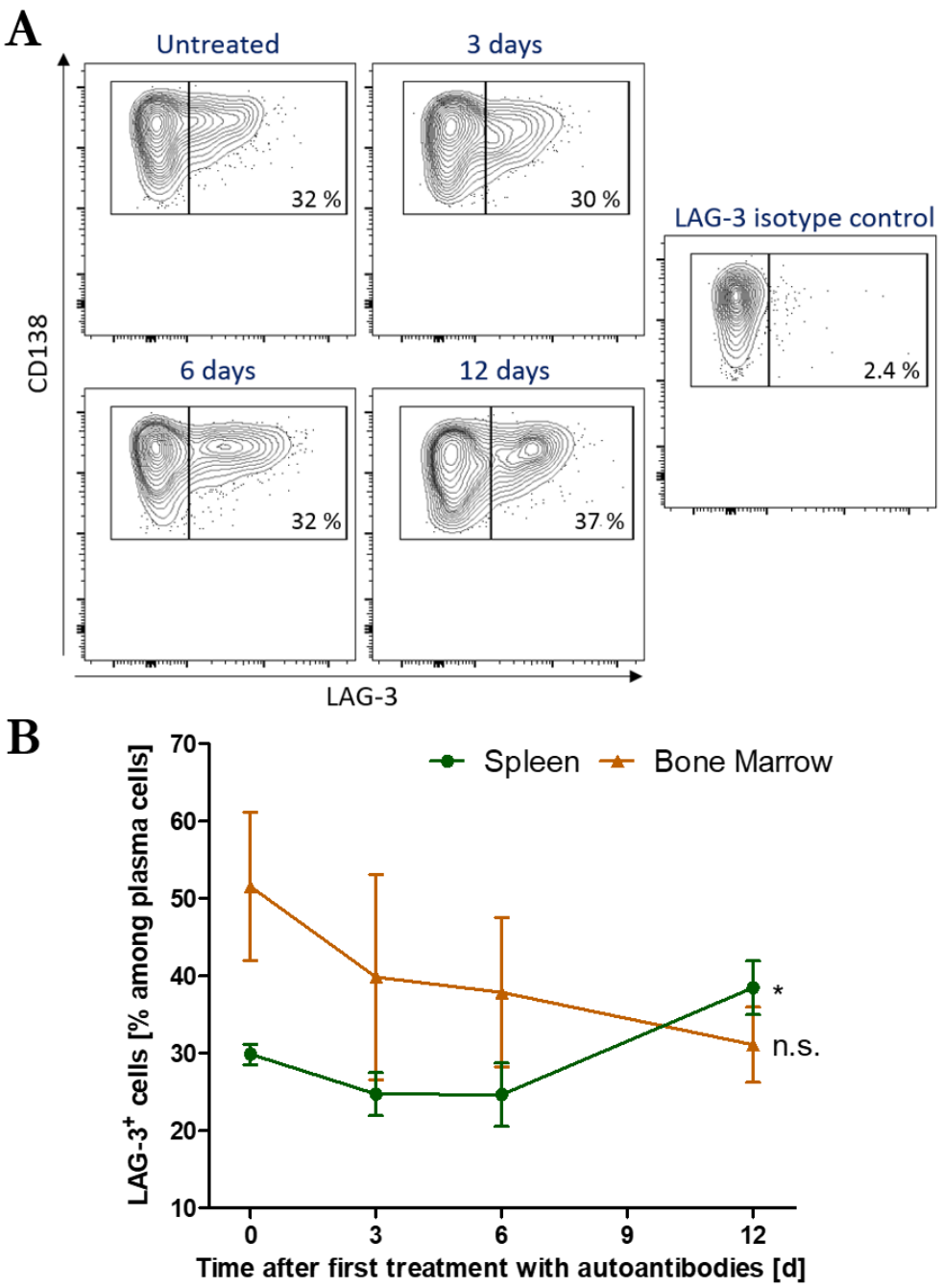

Figure 29: The frequency of splenic LAG-3$^+$ plasma cells increases after EBA induction by autoantibodies. EBA was induced in B6 IL-10 reporter mice as described in the scheme in figure 26 and spleen and bone marrow were analyzed by flow cytometry. **(A)** Representative flow cytometry data from spleen. Plasma cells were defined as CD138^{hi} TACI$^+$ cells and further gated for their LAG-3 expression as compared to the isotype control (right plot). **(B)** Frequency of LAG-3$^+$ cells among plasma cells in spleen and bone marrow at different time points after the first treatment with autoantibodies, as indicated (n=3-4, one-way ANOVA). Data are expressed as mean ± SEM. *$p \leq 0.05$ indicates a significant change of the frequency over time within one organ. A significant increase of LAG-3$^+$ plasma cells was observed at day twelve compared to day three and six in spleen. *n.s., not significant.*

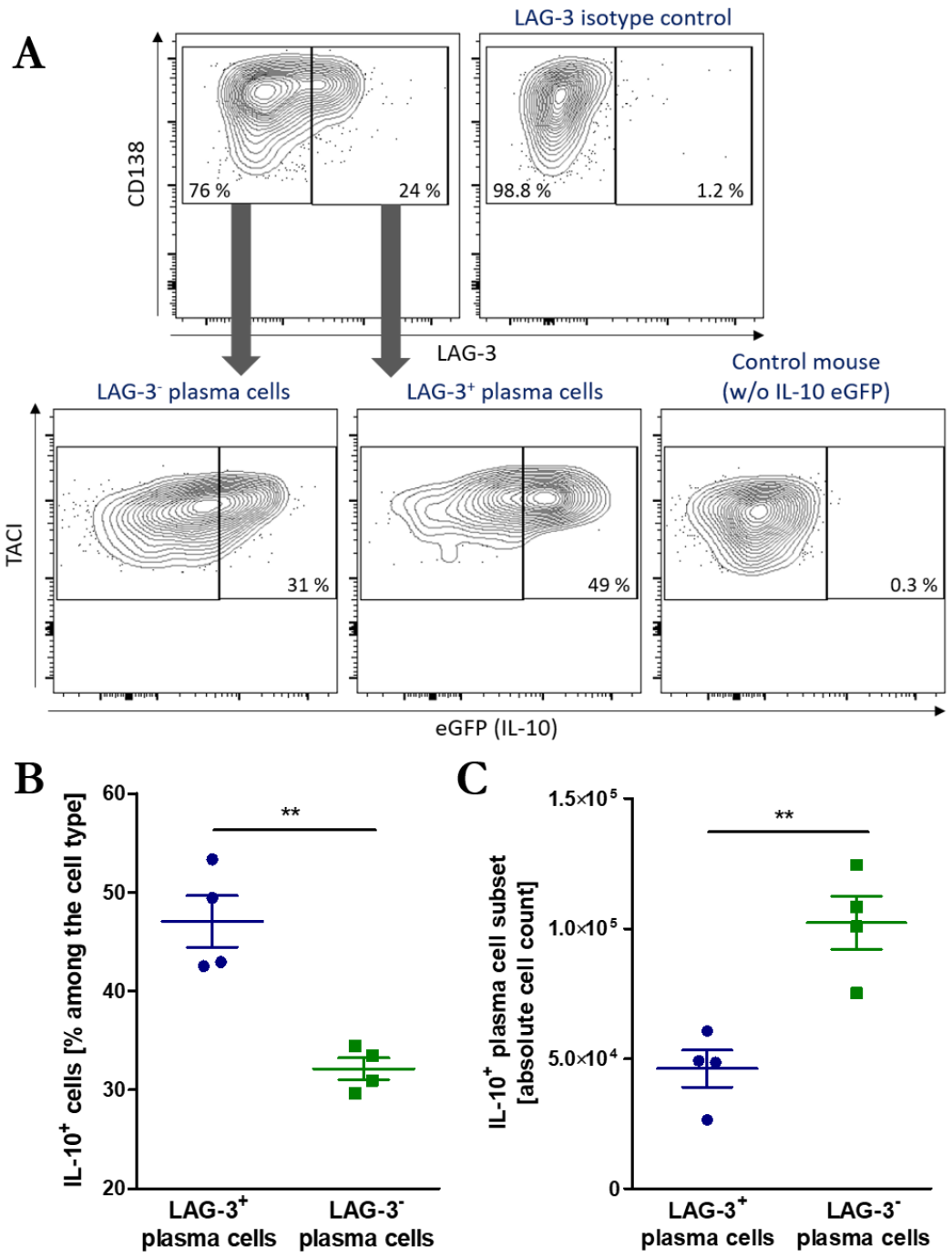

Figure 30: LAG-3⁺ and LAG-3⁻ plasma cells produce IL-10 under steady state conditions. Splenic cells from naïve susceptible B6.s IL-10 reporter mice were analyzed by flow cytometry. **(A)** Representative flow cytometry data. Plasma cells were defined as CD138^{hi} TACI^{+} cells and further gated for their LAG-3 expression compared to the isotype control (upper panel). LAG-3^{+} and LAG-3^{-} plasma cells were analyzed for their IL-10-eGFP expression as compared to the wildtype C57Bl/6J control mouse (lower panel). **(B)** Frequency of IL-10-eGFP^{+} cells among LAG-3^{+} or LAG-3^{-} plasma cells and **(C)** absolute cell number of IL-10-eGFP^{+} LAG-3^{+} or LAG-3^{-} plasma cells in spleen in unimmunized mice (n=4, unpaired t-test). Data are expressed as mean ± SEM and IL-10-eGFP frequencies are corrected by the value obtained from the C57Bl/6J control mouse indicating the unspecific background staining. **p ≤ 0.01. *w/o, without.*

6.3 IL-10 is produced by autoreactive and non-self-reactive plasma cells

$CD138^{hi}$ plasma cells and plasmablasts have been reported to counteract autoimmune inflammation via their provision of anti-inflammatory cytokines such as IL-10 and IL-35 [84,92]. Moreover, plasma cells are also major producers of IL-10 in the autoimmune disorder EBA and $IL\text{-}10^{+}$ plasma cells are induced in the natural course of the disease (chapter 6.2). However, the nature and origin of these immunosuppressive cells is still under debate. So-called "regulatory plasmablasts" are suggested to develop either from a mature B cells in dLN or from immature B cells or "Breg" precursors in spleen [106]. To test whether $IL\text{-}10^{+}$ plasma cells in EBA developed via an antigen-dependent pathway, their specificity to the autoantigen vWFA2 was measured by flow cytometry. Susceptible B6.s IL-10 reporter mice were immunized with vWFA2 and analyzed at different time points of the disease. Since plasma cells are filled up with secretory antibodies, an intracellular staining with the fluorescently labeled autoantigen was performed as previously described [135].

6.3.1 Self-reactive plasma cells are found in dLN but are rare in other lymphoid organs

Previous studies showed that mCOL7-specific plasma cells can be mainly found 14 weeks after immunization with mCOL7c-GST in dLN [135]. Similarly, immunization with vWFA2 induced a high frequency of vWFA2-specific $CD138^{hi}$ $B220^{med/low}$ plasma cells in dLN (figure 31A) but not in spleen in bone marrow. Approximately 15 % of plasma cells were self-reactive in the acute phase of EBA ten days after immunization and this frequency remained constant until the effector phase (figure 31B). By contrast, spleen and bone marrow showed frequencies only slightly above the background staining, found in mice treated only with the adjuvant, and were almost undetectable at early time points. The absolute number of $vWFA2^{+}$ plasma cells in dLN decreased from approximately 0.5 million cells at day ten to a few thousand in the effector phase at week five (figure 31C).

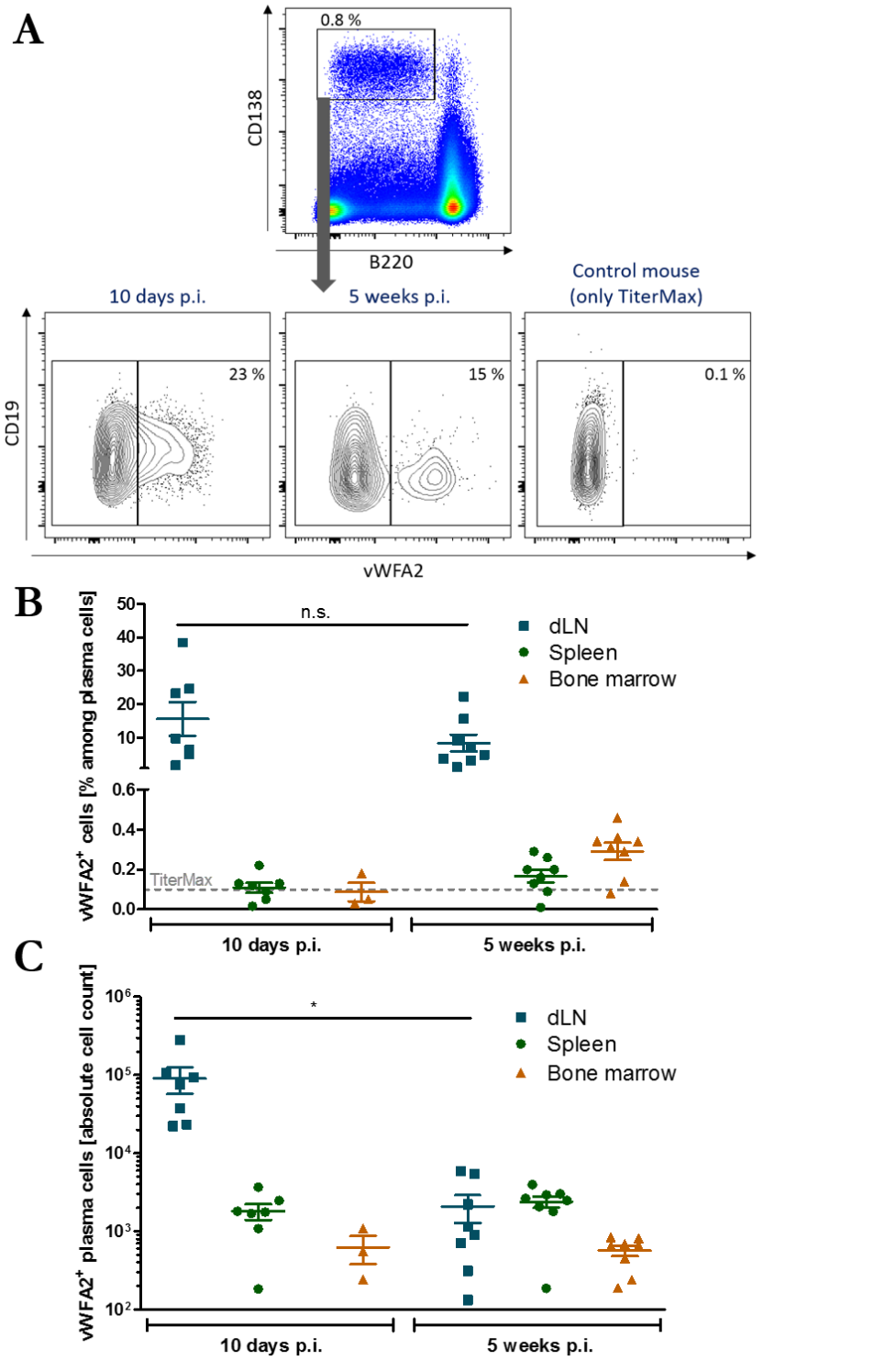

Figure 31: Autoreactive plasma cells are found in draining lymph nodes in the early and late phase of EBA. EBA was induced in susceptible B6.s IL-10 reporter mice by immunization with vWFA2 as described in the scheme in figure 19 and vWFA2-specific plasma cells were analyzed by flow cytometry. **(A)** Representative flow cytometry data from draining lymph nodes (dLN). Plasma cells were defined as $CD138^{hi}$ $B220^{med/low}$ cells (upper panel) and further gated for their binding of fluorescently labeled vWFA2 (lower panel) as compared to the control mouse treated only with TiterMax (right plot). **(B)** Frequency of $vWFA2^+$ cells among plasma cells and **(C)** absolute cell number of $vWFA2^+$ plasma cells in in dLN, spleen and bone marrow ten days and five weeks after immunization (n=3-8 pooled from two independent experiments, unpaired t-test). The dashed line shows the frequency in the TiterMax control mouse indicating the unspecific background staining (n=2/time point). Data are expressed as mean ± SEM. *p ≤ 0.05. *p.i., post immunization.*

6.3.2 Non-self-reactive plasma cells produce more IL-10 than autoreactive plasma cells

Since autoreactive plasma cells were almost exclusively found in dLN, further analysis of IL-10-eGFP expression in vWFA2-immunized B6.s IL-10 reporter mice was performed in this organ (figure 32A).

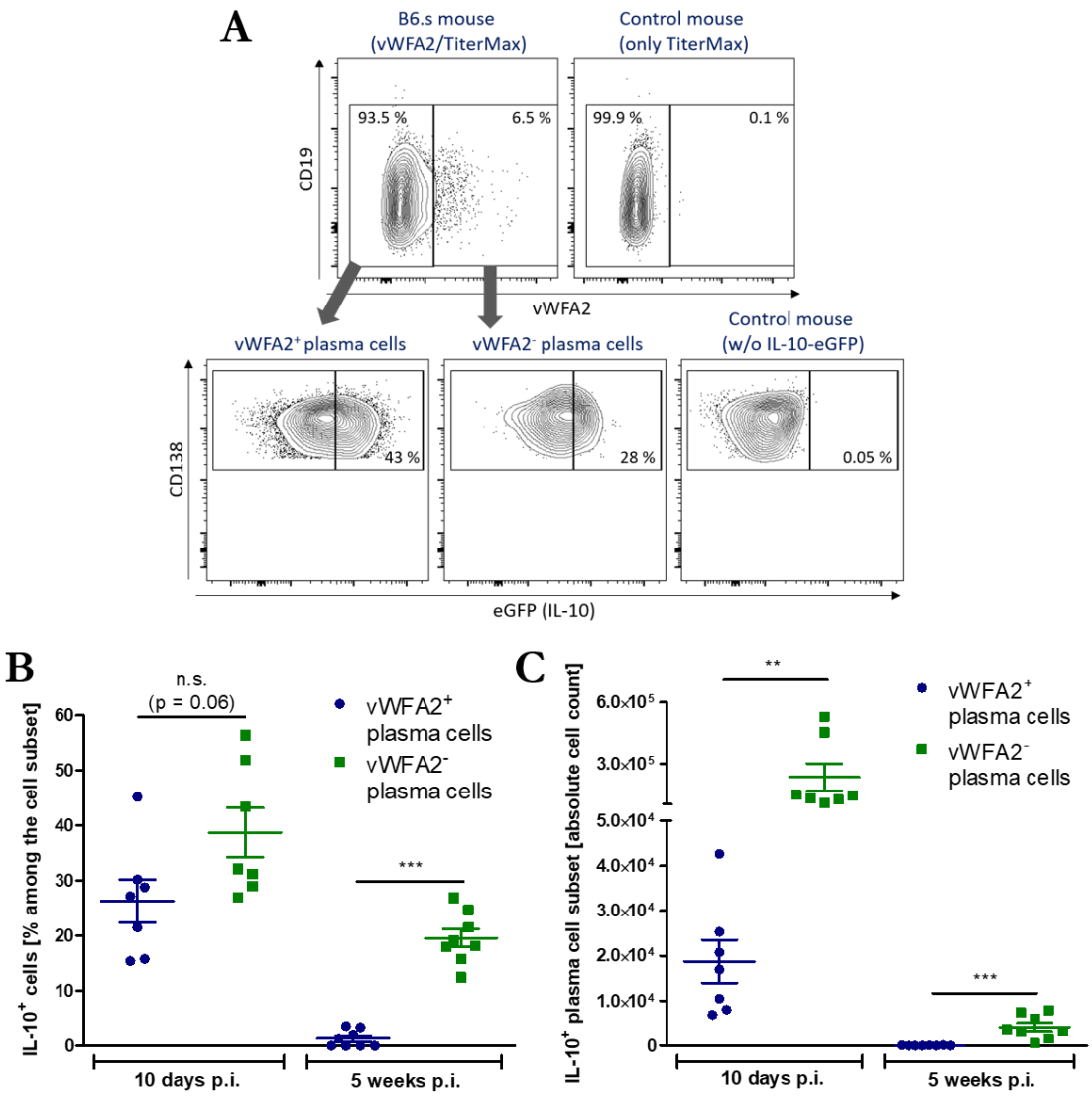

Figure 32: Non-autoantigen-specific plasma cells produce less IL-10 compared to vWFA2-specific plasma cells. EBA was induced in susceptible B6.s IL-10 reporter mice by immunization with vWFA2 as described in the scheme in figure 19 and vWFA2-specific plasma cells were analyzed by flow cytometry. **(A)** Representative flow cytometry data from draining lymph nodes ten days after immunization. Plasma cells were defined as CD138^{hi} B220$^{med/low}$ cells and further gated for their binding of fluorescently labeled vWFA2 (upper panel) as compared to the control mouse treated with only TiterMax (right plot). vWFA2^{+} and vWFA2^{-} plasma cells were analyzed for their IL-10-eGFP expression as compared to a wildtype C57Bl/6J control mouse (right plot). **(B)** Frequency of IL-10-eGFP^{+} cells among vWFA2^{+} and vWFA2^{-} plasma cells and **(C)** absolute cell number ten days and five weeks after immunization (n=7-8 pooled from two independent experiments, unpaired t-test). Data are expressed as mean ± SEM and IL-10-eGFP frequencies are corrected by the value obtained from the C57Bl/6J control mouse indicating the unspecific background staining. **p ≤ 0.01; ***p ≤ 0.001. *n.s., not significant; p.i., post immunization; w/o, without.*

Approximately 25 % of self-reactive plasma cells produced IL-10-eGFP in the acute phase of the disease and 2 % in the effector phase. By contrast, non-self-reactive plasma cells expressed 1.5- or 9-fold more IL-10-eGFP than autoreactive plasma cells after ten days or five weeks, respectively (figure 32B). The absolute cell number of IL-10$^+$ autoreactive plasma cells was considerably lower compared to IL-10$^+$ non-self-reactive plasma cells (figure 32C), due to the fact that vWFA2$^+$ plasma cells represented only 15 % of the population (figure 31B).

These data indicate that self-reactive plasma cells are found almost exclusively in dLN, and that both self-reactive and non-self-reactive plasma cells can produce IL-10. However, autoreactive plasma cells contribute relatively little to the absolute IL-10 production. This suggests that IL-10-producing plasmablasts in dLN are primarily derived independent of the specificity to the immunizing autoantigen.

6.3.3 IL-10$^+$ self-reactive and non-self-reactive plasma cells have a comparable IgM phenotype

The phenotype and origin of IL-10-producing B cells is still a matter of discussion. Based on findings in humans and mice, these cells have been found to express high levels of IgM, suggesting that IgM$^+$ "regulatory plasmablasts/plasma cells" could directly develop from immature B cells or precursor "Bregs", e.g. murine T2-MZP B cells or human CD24^{hi} CD38^{hi} B cells [85]. In addition, LAG-3$^+$ "natural regulatory plasma cells" have been reported to be a subset of IgM$^+$ plasma cells [71]. Thus, analysis of IgM expression allows further insights into the phenotype and origin of IL-10$^+$ plasma cells.

To investigate whether EBA disease-induced plasma cells co-express IgM and IL-10-eGFP, susceptible B6.s IL-10 reporter mice were immunized with vWFA2 and analyzed by flow cytometry in the acute phase of the disease (figure 33A). Autoantigen-specific and non-self-reactive plasma cells displayed a similar IgM and IL-10 phenotype (figure 33B). Between 15 to 25 % of both plasma cell subsets co-expressed IgM and IL-10-eGFP while 8 % showed an IL-10-eGFP$^+$ IgM$^-$ phenotype. Interestingly, 75 % of non-self-reactive IL-10$^+$ plasma cells were IgM$^+$ and 55 % only expressed IL-10 but not IgM, indicating that IgM$^-$ class-switched plasma cells can also produce IL-10 (figure 33C).

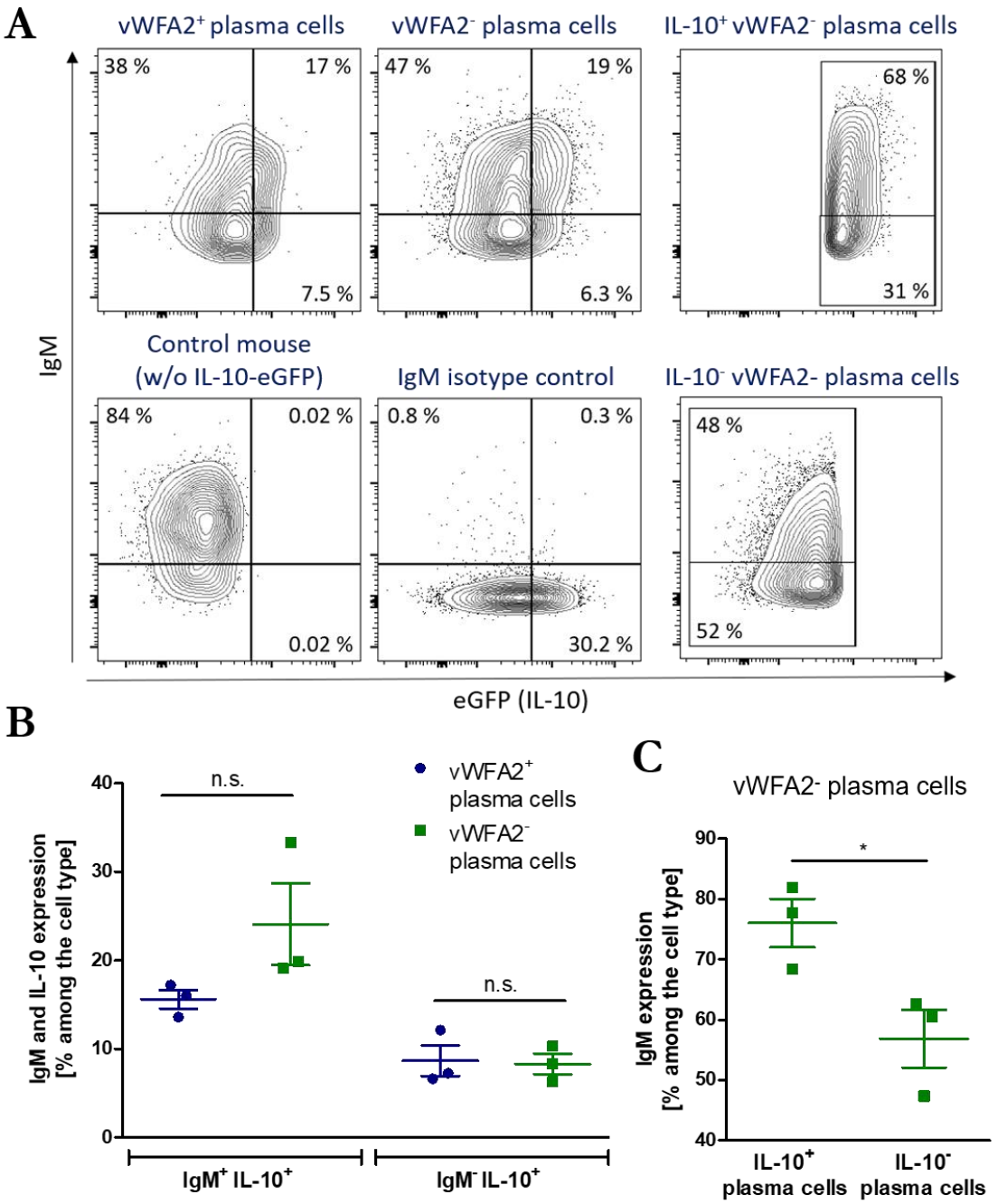

Figure 33: Autoreactive and non-self-reactive plasma cells exhibit a comparable IL-10 and IgM phenotype. EBA was induced in susceptible B6.s IL-10 reporter mice by immunization with vWFA2 as described in the scheme in figure 19 and vWFA2-specific plasma cells were analyzed by flow cytometry. **(A)** Representative flow cytometry data from draining lymph nodes ten days after immunization. The gating for vWFA2$^+$ and vWFA2$^-$ plasma cells was performed as depicted in figure 31. Self-reactive and non-self-reactive plasma cells were analyzed for their IL-10-eGFP and IgM expression (upper panel left) as compared to the wildtype C57Bl/6J control mouse and the IgM isotype control (lower panel left). IgM expression was analyzed in IL-10-eGFP$^+$ (upper panel right) and IL-10-eGPF$^-$ (lower panel right) non-self-reactive plasma cells. **(B)** Frequency of IgM$^+$ IL-10-eGFP$^+$ and IgM$^-$ IL-10-eGFP$^+$ self-reactive and non-self-reactive plasma cells and **(C)** frequency of IgM expression among IL-10$^+$ and IL-10$^-$ non-self-reactive plasma cells ten days after immunization (n=3, unpaired t-test). Data are expressed as mean ± SEM and IL-10-eGFP frequencies are corrected by the value obtained from the C57Bl/6J control mouse indicating the unspecific background staining. *p ≤ 0.05. *n.s., not significant; w/o, without.*

Analysis of IgM and IL-10-eGFP co-expression revealed that autoreactive and non-self-reactive plasma cells have a comparable phenotype. However, IgM expression was enriched in non-self-reactive IL-10$^+$ plasma cells compared to the IL-10$^-$ fraction, suggesting that this subset could be derived from IgM$^+$ precursor cells as suggested in the "regulatory plasmablast" hypothesis [106].

6.4 EBA susceptibility is associated with autoantibodies and autoreactive lymphocytes

The genetic background of the mouse strain strongly influences the susceptibility to EBA with the MHC haplotype representing the most prevalent genetic risk factor [118,134]. Susceptible mouse strains carrying the H2s haplotype (e.g. B6.s) develop signs of blistering and skin inflammation, while EBA-resistant strains (e.g. C57Bl/6 with a H2b haplotype) produce autoantibodies but do not develop symptoms of the disease [134,137]. The mechanism how different MHC haplotypes orchestrate the cellular and humoral immune response in context of an autoimmune disease has not been investigated in detail thus far. Recent studies suggest that the specificity and subclass of the autoantibody [134,141] as well as APC-mediated CD4$^+$ T-cell help [137] and Th1 polarization [138] are required for disease development.

6.4.1 The quality and quantity of autoantibodies from susceptible mice is different compared to non-susceptible mice

B6.s mice carry the H2s haplotype from the susceptible SJL/J strain on a C57Bl/6J background [181], which renders B6.s mice prone to EBA disease development after immunization with a recombinant fragment of mCOL7. By contrast, the congenic C57Bl/6J strain with an H2b haplotype (here termed B6) is protected from skin inflammation and blistering. In order to investigate the cellular and humoral effect of these MHC haplotypes on EBA, susceptible B6.s and non-susceptible B6 mice were immunized with vWFA2 as described in the scheme in figure 19 and the autoantibody titer was analyzed in the acute and the effector phase of the disease by ELISA (figure 34).

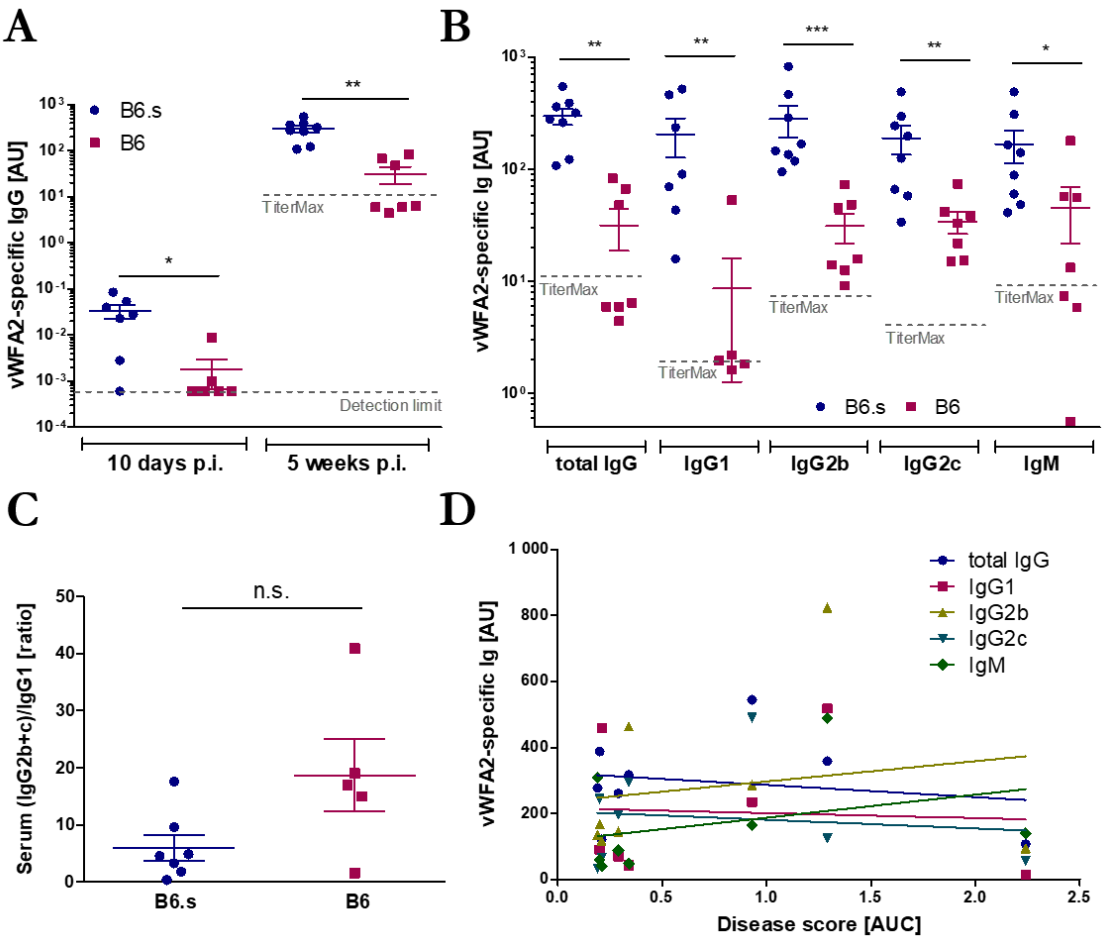

Figure 34: The autoantibody titer of susceptible mice is higher compared to non-susceptible mice but does not correlate with the disease score. EBA was induced in susceptible B6.s IL-10 reporter and non-susceptible B6 IL-10 reporter mice by immunization with vWFA2 as described in the scheme in figure 19 and the serum autoantibody titer was measured by ELISA. **(A)** vWFA2-specific total IgG in the serum ten days and five weeks after immunization (n=7-8 pooled from two independent experiments, Mann-Whitney test). One value for B6.s, five values for B6 and the value for the TiterMax control are below the detection limit of total IgG. **(B)** vWFA2-specific immunoglobulins (Ig) of different subclasses five weeks after immunization (n=7-8 pooled from two independent experiments, Mann-Whitney test). Two values for B6 mice are below the detection limit of IgG1. **(C)** Ratio of serum (IgG2b+c)/IgG1 five weeks after immunization (n=5-7 pooled from two independent experiments, Mann-Whitney test). Two B6 mice, where the values for IgG1 were below the detection limit, were excluded from the calculation. **(D)** Correlation of the score with vWFA2-specific Ig subclasses five weeks after immunization in susceptible B6.s mice (n=7-8 pooled from two independent experiments, linear regression was performed and Spearman correlation was not significant for all subclasses). The dashed lines show the value in the TiterMax control mouse indicating unspecific background signals (n=2/time point). Data are expressed as mean ± SEM. *p ≤ 0.05; **p ≤ 0.01; ***p ≤ 0.001. *AU, arbitrary units; AUC, area under the curve; n.s., not significant.*

Both strains developed IgG autoantibodies against vWFA2, which were detectable in a low quantity already ten days after immunization and further increased until week five (figure 34A). Non-susceptible B6 mice developed a delayed and approximately ten-fold lower autoantibody titer compared to susceptible B6.s mice. Of note, 70 % of B6 mice had a titer below the detection limit of the assay ten days after immunization and 60 % of B6 mice

showed a value below the TiterMax control mouse, indicating unspecific background signals, five weeks after immunization. Further analysis of vWFA2-specific immunoglobulins five weeks after immunization revealed that susceptible B6.s mice produce considerably more autoantibodies of all subclasses compared to non-susceptible B6 mice (figure 34B). B6.s mice had more than twenty-fold IgG1, ten-fold more IgG2b, six-fold more IgG2c and four-fold more IgM than B6 mice. Of note, several B6 mice showed a vWFA2-specific IgG1 and IgM titer below the TiterMax control mouse. The ratio between all serum IgG2 (IgG2b+c) and IgG1 autoantibodies five weeks after immunization was not different between the mouse strains (figure 34C), indicating no shift in the serum subclass distribution. There was no correlation between the autoantibody titer of vWFA2-specific immunoglobulin subclasses and the disease score from each individual mouse (figure 34D). Moreover, some diseased B6.s mice had a titer below the one found in individual non-diseased B6 mice and a considerable level of autoantibodies was detected in B6 mice at least at later time points of the disease. These findings suggests that the autoantibody quantity alone does not exclusively determine the EBA disease phenotype.

In addition to considerable differences in the autoantibody quantity between B6.s and B6 mice, the autoantibody quality was also different between the two mouse strains (figure 35). The immune complex-stimulated release of ROS was measured with a luminol-amplified luminescence assay using bone marrow-derived innate effector cells from naïve C57Bl/6J mice and normalized serum. The serum from vWFA2-immunized susceptible B6.s mice induced a higher release of ROS compared to non-susceptible B6 mice. The kinetics of ROS release over 120 min of incubation time with plate-coated immune complexes showed a clear but over-all not significant difference between the groups (figure 35A), but the area under the curve was significantly increased in B6.s mice (figure 35B). Of note, 40 % of B6 mice sera induced a ROS release below the TiterMax control mouse serum, indicating unspecific background signals.

The autoantibody titer of IgM and all IgG subclasses did not correlate well with the disease score in B6.s mice, indicating that the autoantibody quantity or subclass distribution is not sufficient to induce the disease. Moreover, autoantibodies from B6.s mice exhibited a greater potential to induce ROS release from innate effector cells, which is known to be a hallmark of EBA pathogenesis [115]. These data suggest that non-susceptible mice are protected from EBA due to a lower quantity of autoantibodies and reduced capacity to induce ROS.

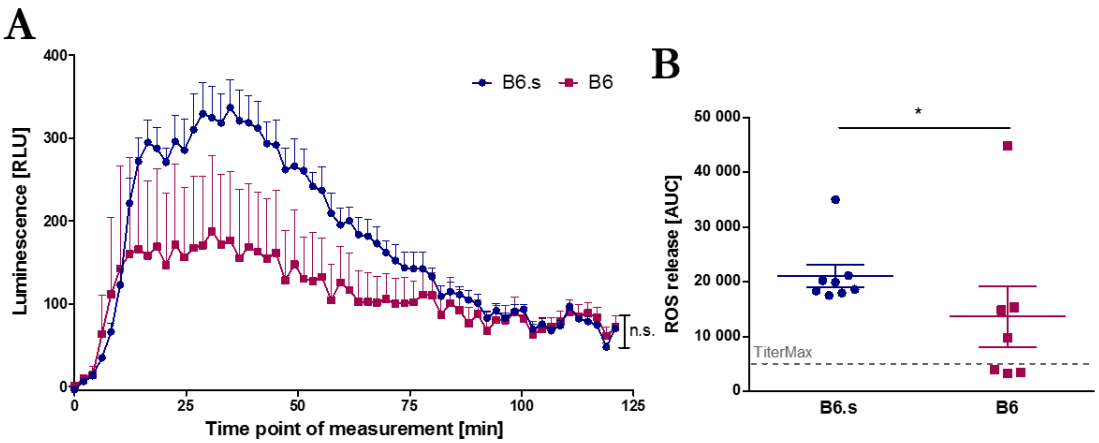

Figure 35: Autoantibodies from susceptible mice induce a higher oxidative burst by bone marrow-derived innate effector cells compared to non-susceptible mice. EBA was induced in susceptible B6.s IL-10 reporter and non-susceptible B6 IL-10 reporter mice by immunization with vWFA2 as described in the scheme in figure 19. Immune complex-stimulated release of reactive oxygen species (ROS) was measured with a luminol-amplified luminescence assay. Sera were collected five weeks after immunization and normalized to their individual total IgG autoantibody content according to the ELISA data shown in figure 34A. **(A)** Increase of luminescence due to release of ROS by immune complex-activated bone marrow cells from a naïve C57Bl/6J mouse over time (n=7-8, serum from two independent experiments, two-way ANOVA). **(B)** Total ROS release defined as the area under the curve (AUC) (n=7-8, serum from two independent experiments, Mann-Whitney test). The dashed line shows the ROS released by the serum from the TiterMax control mouse indicating unspecific background signals (n=1). Data are expressed as mean ± SEM. *p ≤ 0.05. *n.s., not significant; RLU, relative luminescence units.*

6.4.2 Disease susceptibility is associated with a high abundance of autoreactive plasma cells

Susceptible B6.s mice showed a higher autoantibody titer compared to non-susceptible B6.s mice (chapter 6.4.1). Since plasma cells represent the source of self-reactive antibodies in context of an autoimmune disease [218], vWFA2-specific CD138^{hi} B220$^{med/low}$ plasma cells were analyzed in B6.s and B6 mice by flow cytometry (figure 36A). Previous experiments revealed that autoreactive plasma cells are abundant in dLN, especially in the acute phase of the disease ten days after immunization (chapter 6.3.1). In susceptible B6.s mice, the frequency of vWFA2-specific plasma cells was more than ten-fold higher compared to non-susceptible B6 mice, which displayed frequencies below (ten days) or only slightly above (five weeks) the TiterMax control mouse, indicating unspecific background staining (figure 36B). Moreover, the absolute cell number of autoantigen-specific plasma cells in dLN was 100- or 10-fold higher in B6.s mice in the acute or in the effector phase, respectively (figure 36C).

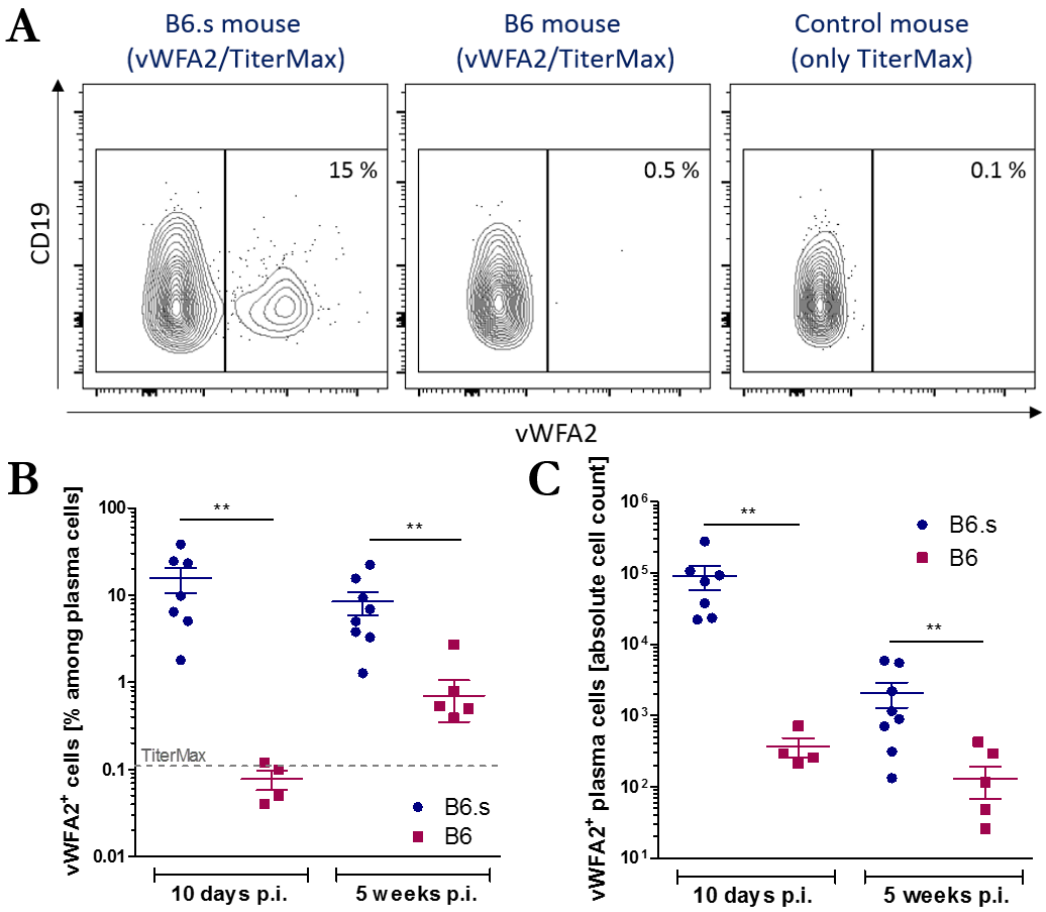

Figure 36: Susceptible mice have more autoantigen-specific plasma cells compared to non-susceptible mice. EBA was induced in susceptible B6.s IL-10 reporter and non-susceptible B6 IL-10 reporter mice by immunization with vWFA2 as described in the scheme in figure 19 and autoantigen-specific plasma cells were analyzed by flow cytometry. **(A)** Representative flow cytometry data from draining lymph nodes five weeks after immunization. Plasma cells were defined as $CD138^{hi}$ $B220^{med/low}$ cells and further gated for their binding of fluorescently labeled vWFA2 as compared to the control mouse treated only with TiterMax (right plot). **(B)** Frequency of $vWFA2^+$ cells among plasma cells and **(C)** absolute cell number of $vWFA2^+$ plasma cells ten days and five weeks after immunization (n=4-8 pooled from two independent experiments, Mann-Whitney test). The dashed line shows the frequency in the TiterMax control mouse indicating the unspecific background staining (n=2/time point). Two data points for the frequency and absolute cell number of $vWFA2^+$ plasma cells in B6 five weeks p.i. are zero and therefore not indicated in the logarithmic scale. Data are expressed as mean ± SEM. $^{**}p \leq 0.01$. *p.i., post immunization.*

Susceptible B6.s already showed a considerable fraction of vWFA2-specific plasma cells ten days after immunization, which partly remained until the effector phase. By contrast, non-susceptible B6 mice developed autoreactive plasma cells in dLN at later time points and after five weeks still had not reached the levels observed in B6.s mice. This fits to the observed kinetics of the autoantibody titer and suggests that a much lower abundance of vWFA2-specific plasma cells in B6 mice is responsible for the lower autoantibody titer found in these mice. However, autoreactive plasma cells are present and produce a considerable amount of autoantibodies in B6 mice at late time points, indicating no tight immunological tolerance in these mice.

6.4.3 Susceptible mice are characterized by a high frequency of autoreactive CD4$^+$ T cells and follicular T helper cells

The results shown above indicate that susceptible B6.s mice exhibit a higher autoantibody titer probably due to a higher abundance of autoreactive plasma cells in dLN. Tfh cells play a pivotal role for B-cell help in the GC. These cells provide soluble and membrane-bound stimuli to the activated B cell, e.g. IL-21, IL-4 and CD40L (CD154), to promote proliferation and survival of activated B cells as well as plasma cell differentiation in the GC [17]. Tfh cells can be defined by their surface expression of programmed cell death protein 1 (PD-1) and chemokine C-X-C motif receptor 5 (CXCR5). During autoimmune inflammation, autoreactive T helper cells have been found in dLN and spleen and their induction required the presence of APCs [135,137]. In order to analyze whether the higher frequency of autoreactive plasma cells was connected to a higher abundance of autoreactive T cells in dLN of B6.s mice, vWFA2-specific CD4$^+$ T cells and Tfh cells were assessed with the CD40L method [192]. CD40L short-term expression is induced only in vWFA2-specific T cells after 5 h *in vitro* restimulation with the autoantigen. By contrast, PMA/ionomycin stimulation upregulates CD40L in the majority of CD4$^+$ T cells. Of note, CD40L is rapidly removed from the cell surface after binding to APCs [195], thus, intracellular staining of this receptor was performed.

Ten days after immunization with vWFA2, autoreactive CD4$^+$ T cells were detectable in dLN (figure 37) and spleen (supplementary figure 15) of susceptible B6.s and non-susceptible B6 mice. Both mouse strains showed a clear population of CD154$^+$ CD4$^+$ T cells, which was not found in the mouse treated only with the adjuvant TiterMax (figure 37A). However, susceptible B6.s mice exhibited four- or five-fold more CD154$^+$ CD4$^+$ T cells in dLN or spleen, respectively, compared to non-susceptible B6 mice (figure 37B and supplementary figure 15A). Moreover, the absolute cell number of CD154$^+$ CD4$^+$ T cells was also increased in dLN and spleen of susceptible B6.s mice (figure 37C and supplementary figure 15B).

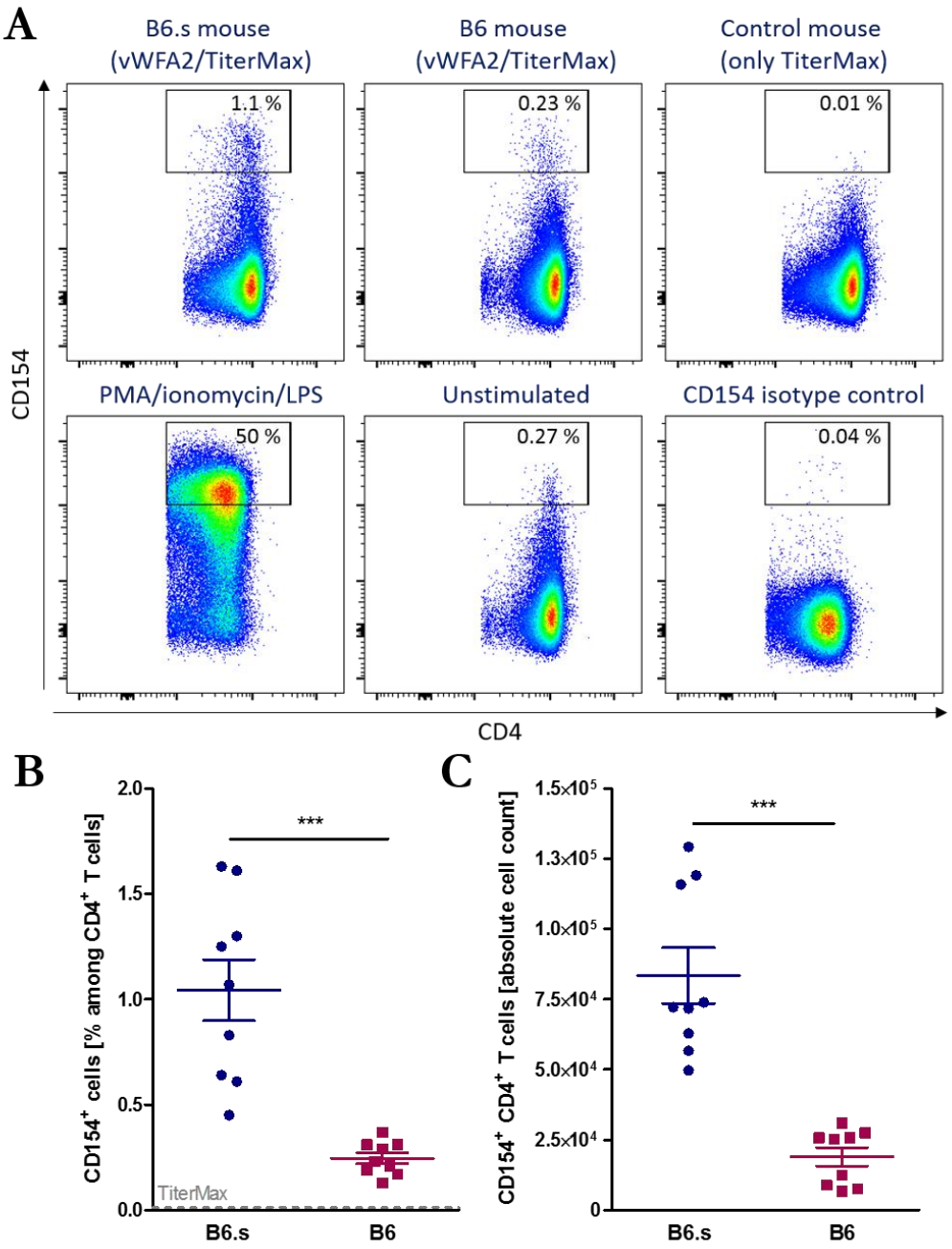

Figure 37: Susceptible B6.s mice have more autoreactive CD4⁺ T cells in draining lymph nodes compared to non-susceptible B6 mice. EBA was induced in susceptible B6.s and non-susceptible B6 mice by immunization with vWFA2 as described in the scheme in figure 19 and autoantigen-specific CD4⁺ T cells were analyzed ten days after immunization by flow cytometry using the CD40 ligand (CD40L) method. **(A)** Representative flow cytometry data. Cells from draining lymph nodes were stimulated for 5 h with 0.1 mg/ml vWFA2 and CD154 (CD40L) expressing cells, indicating autoreactive CD4⁺ T cells, were analyzed (upper panel) compared to the control mouse treated with TiterMax (right plot). As controls, cells were treated with PMA, ionomycin and LPS for 5 h or no stimulus was added (lower panel). For the last 4 h of culture, Brefeldin A was added to block protein transport. **(B)** Frequency of CD154⁺ cells among CD4⁺ T cells and **(C)** absolute cell number of CD154⁺ CD4⁺ T cells ten days after immunization (n=9, unpaired t-test). The dashed line shows the frequency in the TiterMax control mouse indicating the unspecific background staining (n=2). Data are expressed as mean ± SEM. ***$p \leq 0.001$.

To further investigate strain-dependent effects on Tfh cells and specifically autoreactive Tfh cells in dLN, PD-1$^+$ CXCR5$^+$ CD4$^+$ T cells (figure 38A) and CD154$^+$ PD-1$^+$ CXCR5$^+$ CD4$^+$ T cells (figure 38B) were analyzed by flow cytometry after 5 h *in vitro* stimulation with vWFA2.

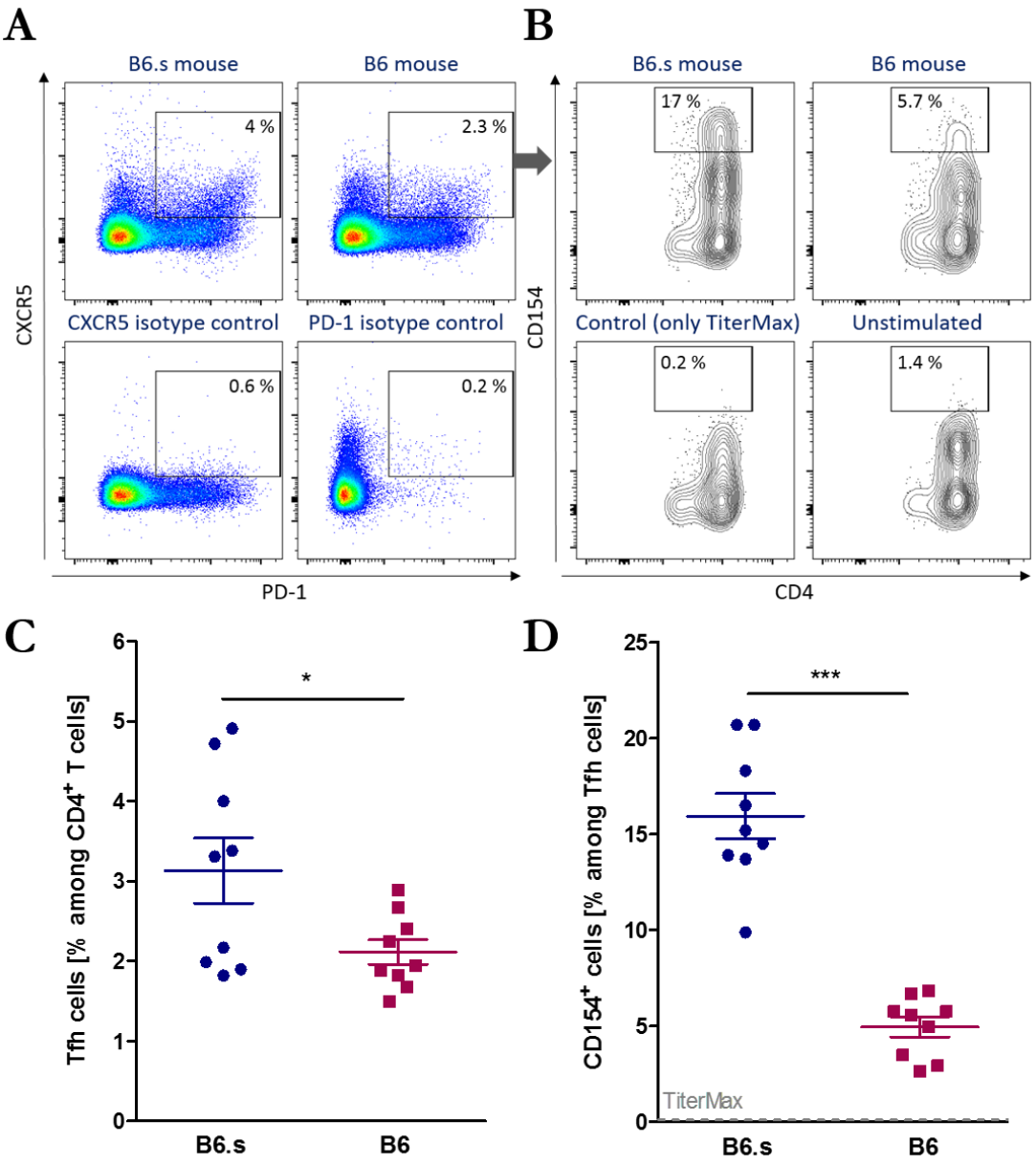

Figure 38: Susceptible mice are characterized by a higher frequency of total and autoreactive follicular T helper cells compared to non-susceptible mice. EBA was induced in susceptible B6.s and non-susceptible B6 mice by immunization with vWFA2 as described in the scheme in figure 19 and cells from draining lymph nodes were analyzed by flow cytometry ten days after immunization. **(A+B)** Representative flow cytometry data. Cells were stimulated for 5 h with 0.1 mg/ml vWFA2 and treated the last 4 h with Brefeldin A. **(A)** Follicular T helper (Tfh) cells were defined as CXCR5$^+$ PD-1$^+$ CD4$^+$ T cells (upper panel) compared to the isotype controls (lower panel). **(B)** Tfh cells were further gated for their CD154 (CD40L) expression indicating autoreactive cells (upper panel). A mouse treated only with TiterMax and unstimulated cells served as controls (lower panel). **(C)** Frequency of Tfh cells among CD4$^+$ T cells and **(D)** frequency of CD154$^+$ cells among Tfh cells ten days after immunization (n=9, unpaired t-test). The dashed line shows the frequency in the TiterMax control mouse indicating the unspecific background staining (n=2). Data are expressed as mean ± SEM. *p ≤ 0.05; ***p ≤ 0.001.

Susceptible B6.s mice were characterized by a higher frequency and absolute cell number of total Tfh cells compared to non-susceptible B6 mice (figure 38C and supplementary figure 16A). In line with previous findings, B6.s mice exhibited also a higher frequency and total number of autoreactive cells among the Tfh cell population (figure 38D and supplementary figure 16B). B6.s mice had 1.5-fold more Tfh cells and tree-fold more autoreactive Tfh cells in dLN.

These data indicate that the genetic susceptibility of B6.s mice allowed more autoreactive $CD4^+$ T cells and Tfh cells to escape tolerance mechanisms and in turn to activate more autoreactive plasma cells in dLN accompanied by a higher level of autoantibodies. Moreover, more Tfh are able to increase the extent of help for plasma cell differentiation.

6.4.4 IFNγ and IL-21 production by $CD4^+$ T cells and Tfh cells in dLN is increased in susceptible mice

Tfh cells provide help for B cells in the GC by their provision of cytokines. In order to analyze whether susceptible mice also differ in the cytokine response of Tfh and autoreactive $CD4^+$ T cells in dLN, IFNγ, IL-10 and IL-21 production were analyzed by flow cytometry (figure 39A).

Autoreactive $CD154^+$ $CD4^+$ T cells showed no difference in their cytokine expression between susceptible and non-susceptible mice (figure 39B). Of note, the frequency of $IL\text{-}10^+$ and $IL\text{-}21^+$ autoreactive $CD4^+$ T cells was very low after 5 h *in vitro* vWFA2 stimulation and the variation between mice relatively high. Tfh cells displayed a 1.8-fold increase of IFNγ and 1.6-fold increase of IL-21 expression after 5 h *in vitro* restimulation with PMA/ionomycin/LPS (figure 39C). By contrast, IL-10 was only slightly but still significantly increased in susceptible B6.s mice by 25 % compared to non-susceptible B6 mice. B6.s mice had a higher number of IFNγ-, IL-10- and IL-21-producing autoreactive $CD4^+$ T cells and Tfh cells (supplementary figure 17A&B) but this was due to the increased amount of total Tfh and autoreactive $CD4^+$ T cells in B6.s mice. The frequency of cytokine-producing autoreactive Tfh cells was too low to investigate.

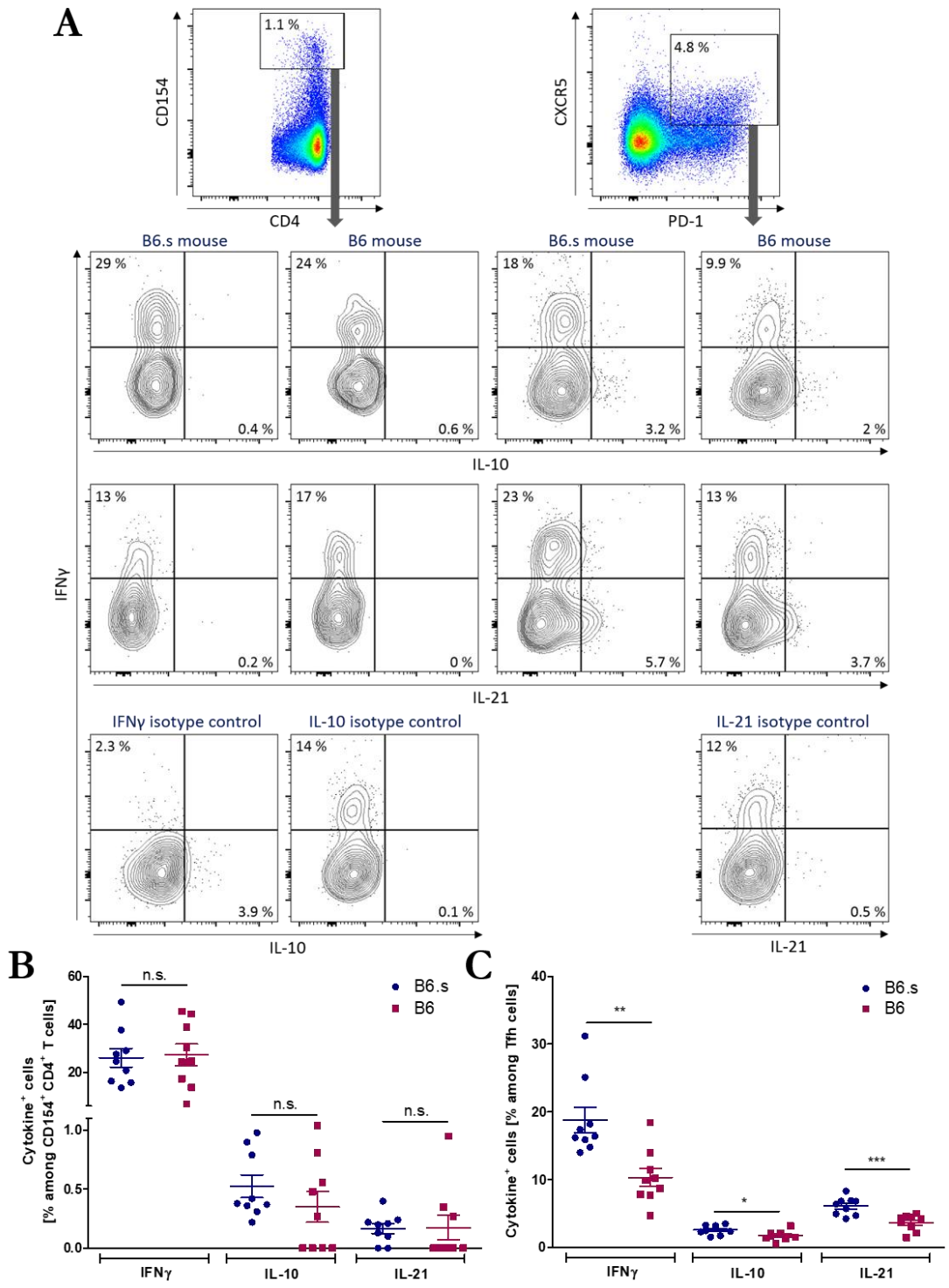

Figure 39: The cytokine production by follicular T helper cells but not by autoreactive CD4⁺ T cells is different between susceptible and non-susceptible mice. EBA was induced in susceptible B6.s and non-susceptible B6 mice by immunization with vWFA2 as described in the scheme in figure 19 and cells from draining lymph nodes were analyzed by flow cytometry ten days after immunization. **(A)** Representative flow cytometry data. Cells were either stimulated for 5 h with 0.1 mg/ml vWFA2 to analyze the cytokines from autoreactive T cells (left plots) or with PMA, ionomycin and LPS for 5 h to analyze the cytokines from follicular T helper (Tfh) cells (right plots). Autoreactive T cells were defined as $CD154^+$ $CD4^+$ T cells and Tfh cells as $CXCR5^+$ $PD\text{-}1^+$ $CD4^+$ T cells. Both subsets were gated for their expression of IFNγ, IL-10 (second row) and IL-21 (third row) compared to the isotype controls (last row). **(B)** Frequency of $IFN\gamma^+$, $IL\text{-}10^+$ or $IL\text{-}21^+$ cells among autoreactive T cells and **(C)** among Tfh cells ten days after immunization (n=9, unpaired t-test). Data are expressed as mean ± SEM. *$p \leq 0.05$; **$p \leq 0.01$; ***$p \leq 0.001$. *n.s., not significant.*

As observed for Tfh cells, susceptible mice were also characterized by a higher frequency (figure 40A&B) and absolute cell number (supplementary figure 18) of IFNγ- and IL-21-producing total CD4$^+$ T cells after 5 h *in vitro* restimulation with PMA/ionomycin/LPS. IFNγ and IL-21 expression were 1.7- and 1.5-fold increased, respectively, compared to non-susceptible B6 mice. By contrast, IL-10 production by CD4$^+$ T cells did not differ between the two mouse strains.

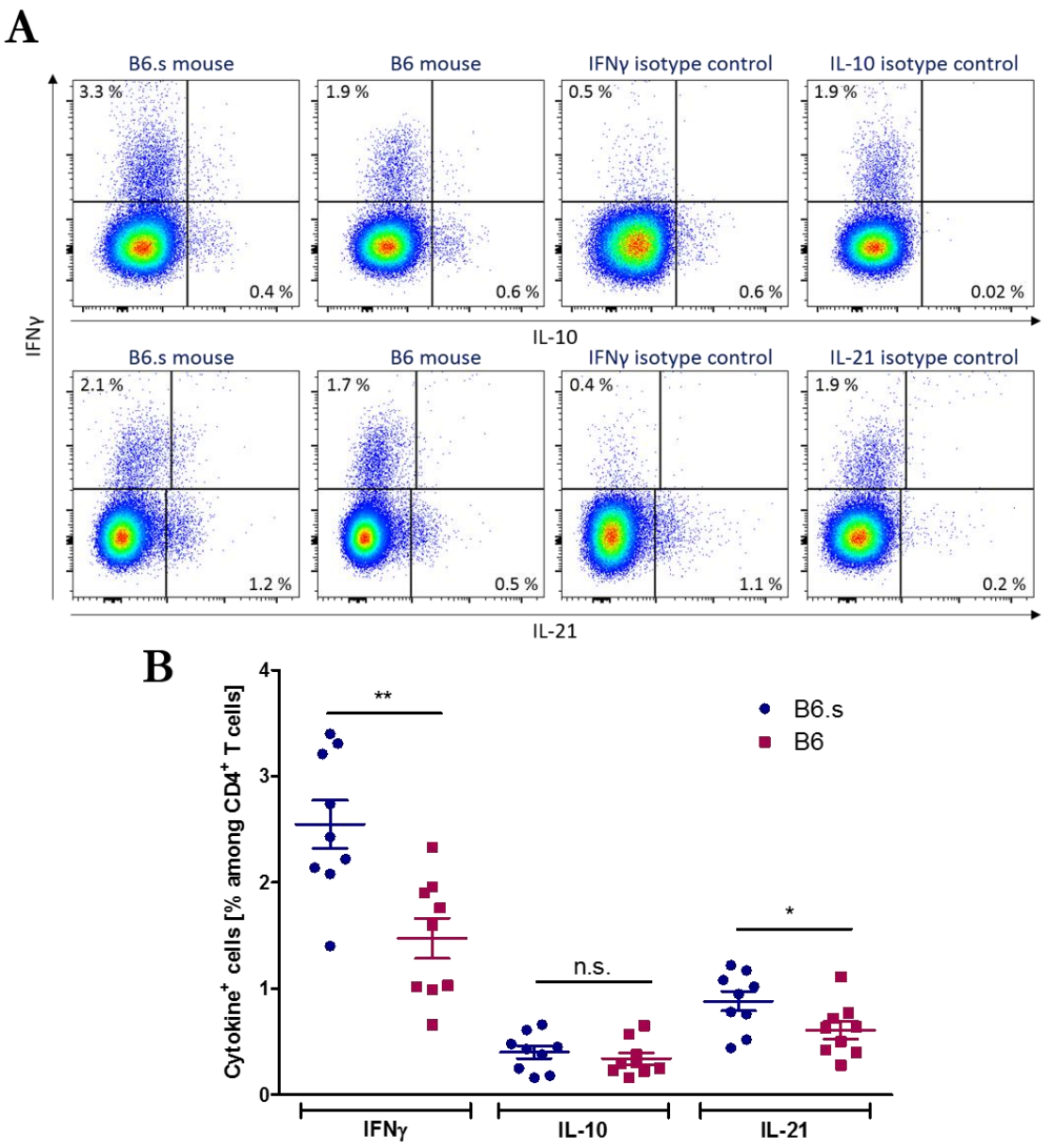

Figure 40: CD4$^+$ T cells from susceptible mice produce more IFNγ and IL-21 compared to non-susceptible mice. EBA was induced in susceptible B6.s and non-susceptible B6 mice by immunization with vWFA2 as described in the scheme in figure 19 and cells from draining lymph nodes were analyzed by flow cytometry ten days after immunization. **(A)** Representative flow cytometry data. Cells were stimulated for 5 h with PMA, ionomycin and LPS and treated for the last 4 h with Brefeldin A. CD4$^+$ T cells were gated for their expression of IFNγ, IL-10 (upper panel) and IL-21 (lower panel) compared to the isotype controls (right plots). **(B)** Frequency of IFNγ$^+$, IL-10$^+$ or IL-21$^+$ cells among CD4$^+$ T cells ten days after immunization (n=9, unpaired t-test). Data are expressed as mean ± SEM. *p ≤ 0.05; **p ≤ 0.01. *n.s., not significant.*

The results shown above indicate that the genetic susceptibility of B6.s mice allowed more autoreactive $CD4^+$ T cells and Tfh cells to escape tolerance mechanisms. Moreover, susceptible B6.s mice were characterized by an increased IL-21 production by Tfh cells and $CD4^+$ T cells, which is suggested to be the most potent cytokine for stimulation of plasma cell differentiation in the GC [17], and IFNγ expression, an important Th1 cytokine supporting EBA inflammation [138], class switch [219] and Tfh differentiation [220].

6.4.5 The formation of regulatory T cells and autoreactive regulatory T cells is not altered in susceptible mice

$Foxp3^+$ $CD4^+$ T cells (Tregs) represent an important regulatory T-cell subset with the ability to limit immune responses via their provision of anti-inflammatory cytokines such as IL-10 [221]. Furthermore, Tregs have been described to counteract EBA inflammation and blistering after transfer of autoantibodies [162]. To check whether an increased Treg population in non-susceptible mice could contribute to limited autoantibody production and to protection from EBA skin disease, Tregs and autoreactive Tregs were analyzed in dLN in the acute phase of the disease by flow cytometry (figure 41A). Susceptible B6.s and non-susceptible B6 mice expressed similar frequencies of $Foxp3^+$ cells among $CD4^+$ T cells of approximately 4 % (figure 41B).

It is still under debate whether autoreactivity is increased among Tregs or whether it is rather an exception compared to conventional T helper cells [41]. Nevertheless, they are able suppress autoimmunity as a peripheral tolerance mechanism by the detection of self-antigens [41,42]. Therefore, antigen-specific IL-10-producing Tregs could represent a specific "suppressor subset" mediating disease protection in B6 mice. In the acute phase of EBA, the frequency of $CD154^+$ autoreactive cells among Tregs was low (0.5 %) but still clearly distinguishable from the TiterMax control mouse (figure 41A). However, susceptible and non-susceptible mice did not show any difference in the frequency of autoreactive Tregs (figure 41C). Of note, the absolute cell numbers of Tregs and $CD154^+$ Tregs was slightly increased in B6.s mice (supplementary figure 19A&B) due to the fact that the total count of dLN cells was already elevated in B6.s mice. Cytokine production by Tregs after 5 h *in vitro* stimulation with vWFA2 was too low to analyze by flow cytometry but figure 40 already showed that $IL\text{-}10^+$ $CD4^+$ T cells were not different between the mouse strains.

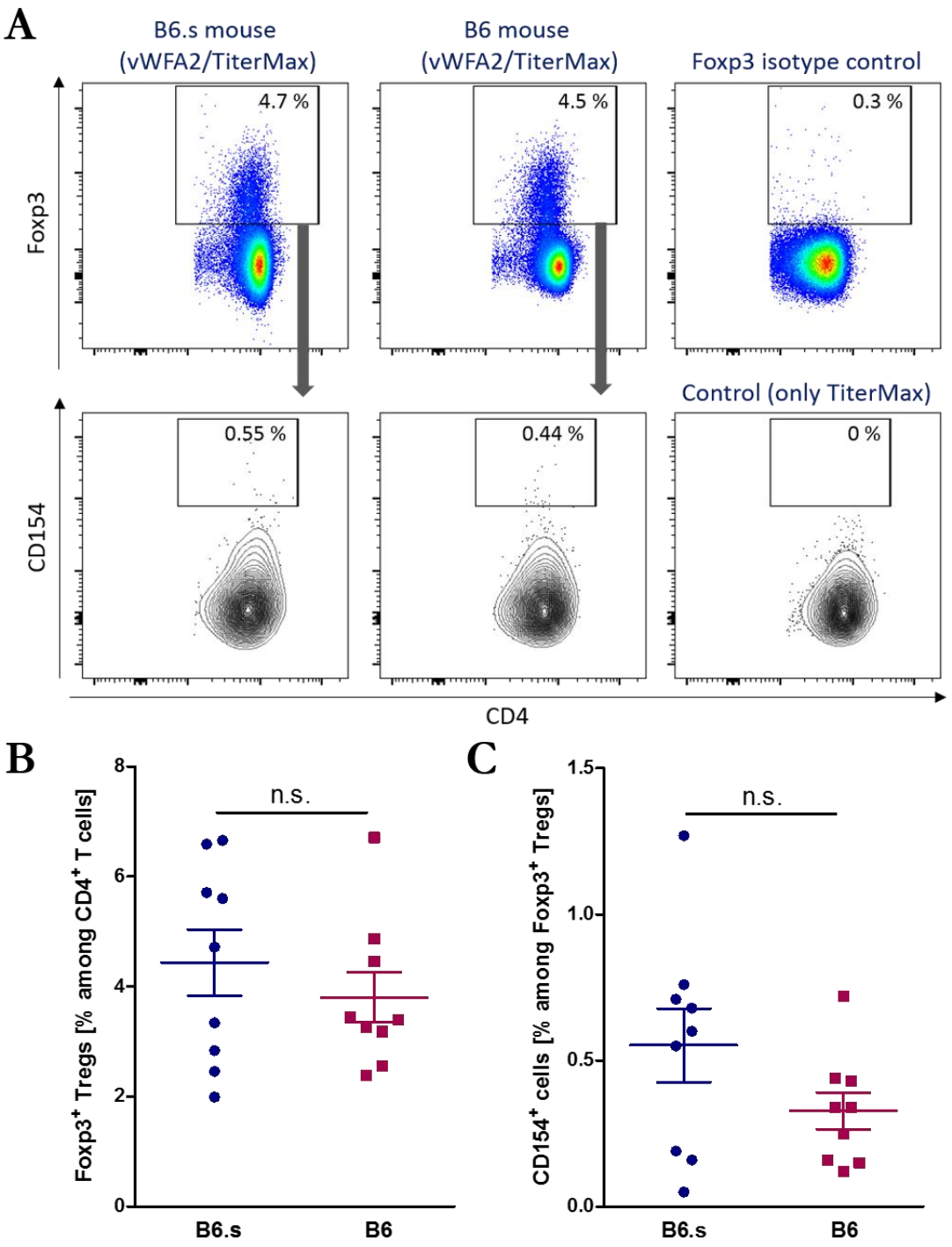

Figure 41: There is no difference in Foxp3⁺ regulatory T cells (Tregs) and autoreactive Tregs between susceptible and non-susceptible mice. EBA was induced in susceptible B6.s and non-susceptible B6 mice by immunization with vWFA2 as described in the scheme in figure 19 and cells from draining lymph nodes were analyzed by flow cytometry ten days after immunization. **(A)** Representative flow cytometry data. Cells were stimulated for 5 h with 0.1 mg/ml vWFA2 and treated the last 4 h with Brefeldin A. Tregs were defined as Foxp3⁺ CD4⁺ T cells (upper panel) compared to the isotype control (right plot). Cells were further gated for their expression of CD154 (CD40L) compared to a control mouse treated only with TiterMax (lower panel). **(B)** Frequency of Foxp3⁺ Tregs among CD4⁺ T cells and **(C)** frequency of CD154⁺ cells among Tregs ten days after immunization (n=9, unpaired t-test). The control mice treated with TiterMax had no vWFA2⁺ Tregs (n=2). Data are expressed as mean ± SEM. *n.s., not significant.*

These data indicate that T-cell tolerance to vWFA2 was broken in both mouse strains, allowing to provide help for autoreactive B cells by autoantigen-specific Tfh cells and for the formation of autoantibodies. However, the quantity of autoreactive T cells and autoreactive plasma cells was strongly increased in susceptible B6.s mice and the proinflammatory T-cell cytokine phenotype in B6.s mice could attribute to the pathogenic potential of the autoantibodies. By contrast, there was no expansion of "suppressor subsets" such as Foxp3$^+$ Tregs or IL-10$^+$ CD4$^+$ T helper cells in non-susceptible B6 mice, which could contribute to the protection of this mouse strain.

6.5 Deficiency of B lineage-derived IL-10 has no major impact in the immunization-induced EBA model

In the autoantibody-transfer-induced EBA mouse model, repeated injections of anti-mCOL7 autoantibodies rapidly induce skin inflammation and blister formation within several days [149]. The model reflects the effector phase of the disease but lacks an adaptive autoimmune reaction. As shown above, IL-10 was not induced in this model (chapter 6.2.3) compared to the immunization-induced EBA model (chapter 6.2.1). To investigate whether steady state IL-10, possibly produced by B lineage cells, is able to influence EBA skin disease induced by transfer of autoantibodies, B lineage-specific IL-10-deficient mice were used. Applying the Cre/loxP-system, CD19$^+$ B cells expressing the Cre recombinase directly delete the *loxP*-flanked *Il10* gene from the genome. CD19 is expressed from the pre-B-cell stage on in the bone marrow and lost during final differentiation to plasma cells [222]. However, Cre recombinase-mediated deletion of the *Il10* gene is irreversible, thus, all B-cell populations including plasma cells are lacking IL-10 expression.

6.5.1 B-cell IL-10-deficiency does not significantly affect EBA skin inflammation and oxidative burst by innate effector cells

In order to analyze the impact of B lineage-derived IL-10 on the effector phase of EBA, EBA was induced by transfer of autoantibodies in B-cell IL-10 KO mice (CD19cre$^+$ IL-10$^{flox/flox}$ on a C57Bl/6J background) with specific rabbit anti-mCOL7c IgG and the disease manifestation was evaluated until day twelve (figure 42A). IL-10-competent littermate mice (CD19cre$^-$ IL-10$^{flox/flox}$) were used as controls in this experiment. In the autoantibody-transfer-induced EBA model, B-cell IL-10-deficiency did not significantly increase the disease score compared to IL-10-competente littermate controls (figure 42B), though there appears to be a tendency.

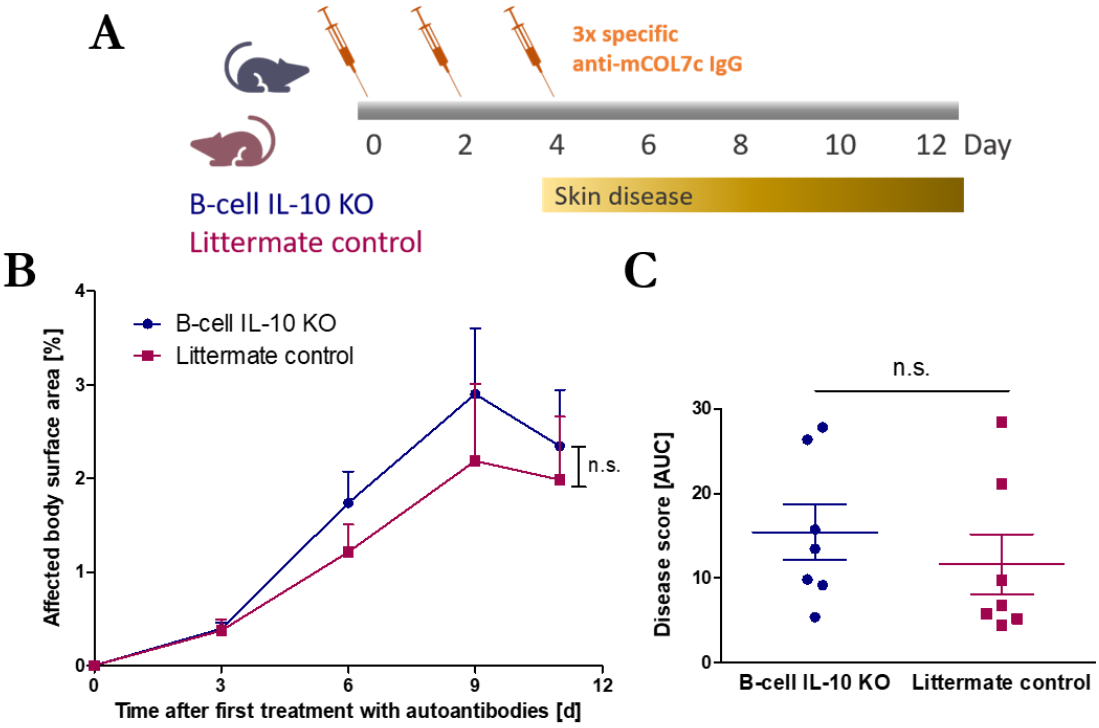

Figure 42: EBA skin disease is not considerably affected by B-cell IL-10-deficiency in the autoantibody-transfer-induced mouse model. (A) Experimental setup. B-cell IL-10 knock-out mice ($CD19cre^{+}$ $IL\text{-}10^{flox/flox}$) and IL-10-competent littermate controls ($CD19cre^{-}$ $IL\text{-}10^{flox/flox}$) were repeatedly treated with specific rabbit anti-mCOL7c IgG on day zero, two and four and skin disease was monitored from day three. Final analysis was after twelve days. **(B)** The disease manifestation was evaluated as the percentage of affected body surface area at various times after treatment, as indicated (n=7, two-way ANOVA). **(C)** The total disease score was defined as the area under the curve (AUC) (n=7, unpaired t-test). Data are expressed as mean ± SEM. *KO, knock-out; n.s., not significant.*

Moreover, the total disease score defined as the area under the curve only showed a trend but was not significantly elevated in B-cell IL-10 KO mice (figure 42C), suggesting a minor role of B lineage-derived IL-10 in this model.

Next, ROS release of bone marrow-derived innate effector cells was measured with a luminol-amplified luminescence assay (figure 43A+B). Neutrophils are the major effector cells in EBA and their release of ROS contributes to the inflammatory phenotype [115]. These cells are the most frequent cell type in bone marrow with the ability to produce ROS [145,213], thus, ROS release by total bone marrow-derived innate effector cells will be mainly attributed to neutrophils. In line with the findings that B-cell IL-10 KO mice have a tendency for an elevated disease score, these mice also showed a slight but not significant increase in ROS release compared to littermate controls on day twelve. This suggests that B lineage-derived IL-10 has no considerable impact on the disease development in the autoantibody-transfer-induced EBA model, which is mediated by the activation of neutrophils and their release of ROS.

Together with the results shown above (chapter 6.2.3), this indicates that steady state IL-10, neither from plasma cells nor from other cell types, has an effect on neutrophil function and EBA skin disease in the autoantibody-transfer-induced model.

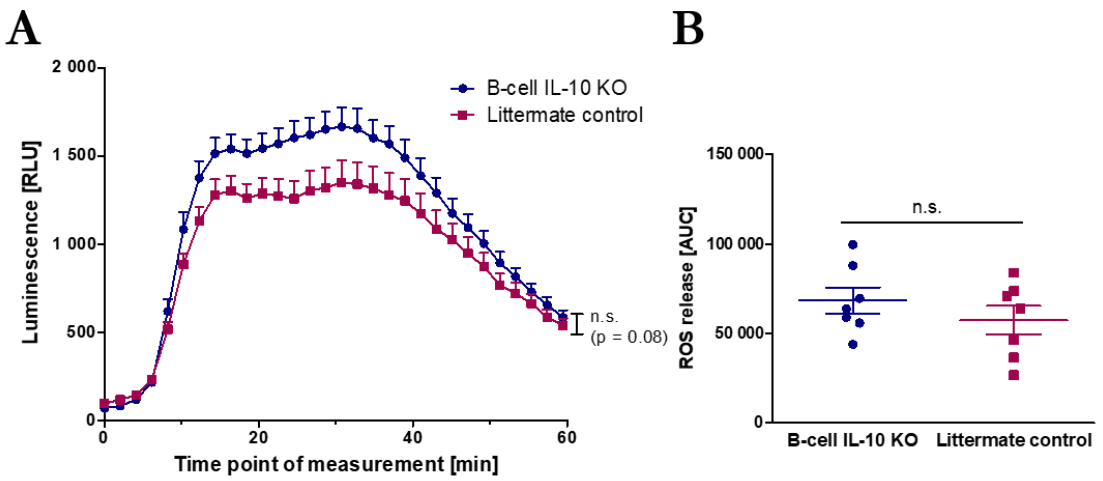

Figure 43: B-cell IL-10-deficiency has no considerable impact on oxidative burst by bone marrow-derived innate effector cells in the autoantibody-transfer-induced mouse model. EBA was induced in B-cell IL-10 knock-out mice (CD19cre^{+} IL-10$^{flox/flox}$) and IL-10-competent littermate controls (CD19cre^{-} IL-10$^{flox/flox}$) as described in the scheme in figure 42. On day twelve, bone marrow cells were isolated and their oxidative burst was measured by the immune complex-stimulated release of reactive oxygen species (ROS) with a luminol-amplified luminescence assay. **(A)** Increase of luminescence due to release of ROS by immune complex-activated bone marrow cells over time (n=7, two-way ANOVA). **(B)** Total ROS release defined as the area under the curve (AUC) (n=7, unpaired t-test). Data are expressed as mean ± SEM. *KO, knock-out; n.s., not significant; RLU, relative luminescence units.*

6.5.2 Cytokine expression by effector and CD4^{+} T cells is not affected by B-cell IL-10-deficiency

B cell-derived IL-10 is well known to modulate T-cell cytokines such as IFNγ and IL-17A [99]. Furthermore, effector T-cell subsets such as γδ and NKT cells were described to support EBA after transfer of autoantibodies [161]. Therefore, splenic CD4^{+} T cells as well as γδ (γδTCR^{+} CD3^{+}) and NKT (NK1.1^{+}CD3^{+}) effector cells were analyzed for their production of IFNγ, IL-10 and IL-17A after 5 h *in vitro* restimulation with PMS/ionomycin/LPS (figure 44A). The proinflammatory cytokine IFNγ was mainly produced by γδ and NKT cells, whereas γδ T cells were the major producer of IL-17A in line with previous findings (chapter 6.1.5) and the literature [215,216]. By contrast, CD4^{+} T cells produced much more IL-10 than the other subsets. However, B-cell IL-10 KO mice did not show any difference in the cytokine expression by all of these cell types compared to IL-10-competent littermate controls (figure 44B and supplementary figure 20).

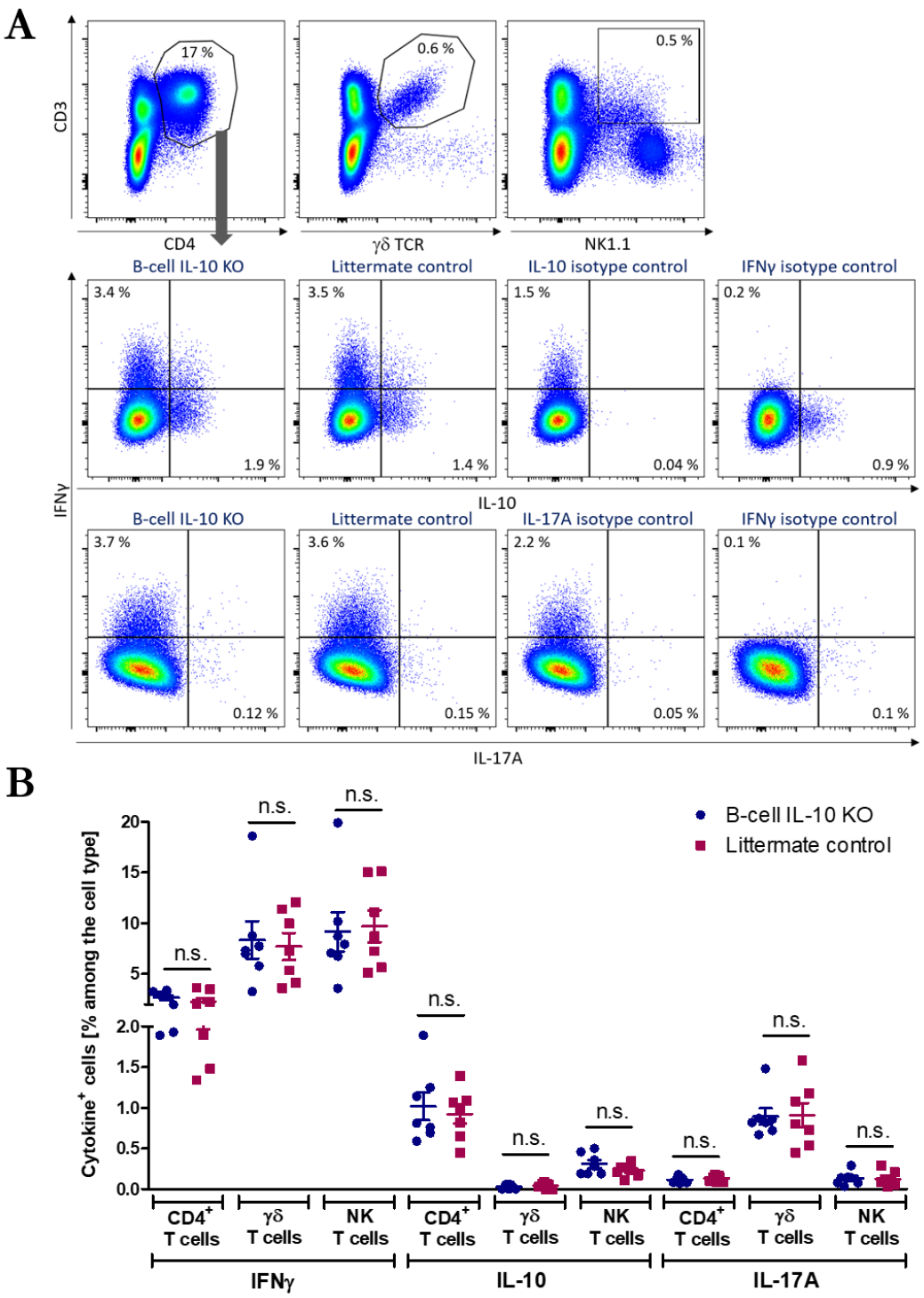

Figure 44: Cytokine expression by different splenic T cells subsets is not influenced by B-cell IL-10-deficiency in the autoantibody-transfer-induced mouse model. EBA was induced in B-cell IL-10 knock-out mice (CD19cre^{+} IL-10$^{flox/flox}$) and IL-10-littermate controls (CD19cre^{-} IL-10$^{flox/flox}$) as described in the scheme in figure 42. On day twelve, splenic T-cell subsets were analyzed for their IFNγ, IL-10 and IL-17A expression by flow cytometry. **(A)** Representative flow cytometry data from spleen. Cells were stimulated for 5 h with PMA, ionomycin and LPS and treated for the last 4 h with Brefeldin A. CD4^{+} T cells (upper panel) were gated for their IFNγ, IL-10 (middle panel) and IL-17A (lower panel) expression compared to the isotype controls. γδ T cells were defined as γδ TCR^{+} CD3^{+} lymphocytes and NKT cells as NK1.1^{+} CD3^{+} lymphocytes (upper right panel) and gated for their cytokine expression in the same way. **(B)** Frequency of IFNγ^{+}, IL-10^{+} and IL-17A^{+} cells among the T-cell subset indicated (n=7, unpaired t-test). Data are expressed as mean ± SEM. *KO, knock-out; n.s., not significant.*

The results suggest that physiological IL-10 levels and B lineage-derived IL-10 have no considerable effects in the autoantibody-transfer-induced model. Investigations of the IL-10 kinetics in this model (chapter 6.2.3) revealed that splenic IL-10^+ plasma cells were not induced after autoantibody transfer, suggesting that steady state IL-10 is not able to considerably suppress the skin inflammation in the autoantibody-transfer-induced EBA model. This is in contrast to the results obtained from the immunization-induced EBA model, indicating that IL-10-induction in plasma cells and an increased IL-10 production in the context of the disease are required to suppress EBA skin inflammation.

7. Discussion

7.1 Overview

In this thesis, the inhibitory potential of IL-10 on the natural course of the autoimmune skin disease EBA was investigated and IL-10-producing plasma cells were characterized. IL-10 was able to down-modulate skin inflammation and blistering under pathophysiological conditions despite the presence of autoantibodies, at least partially via the modulation of effector cells *in vivo*. This was shown in the immunization-induced EBA mouse model by blockade of the IL-10R in the beginning of the effector phase. Furthermore, IL-10 was able to concentration-dependently inhibit oxidative burst by innate effector cells *in vitro*, an effector mechanism that represents a hallmark of EBA pathogenesis. The data identified plasma cells as a major IL-10-producing cell type in all lymphoid organs analyzed. Importantly, IL-10-induction in context of the systemic, disease-induced inflammation in susceptible mice was plasma cell-specific and restricted to spleen and bone marrow. However, non-susceptible mice were not protected from EBA due to an increased abundance of regulatory lymphocyte subsets such as Tregs and IL-10$^+$ plasma cells, but presumably via a diminished availability of autoreactive lymphocytes with an proinflammatory cytokine profile, in line with a lower quantity and ROS-inducing capacity of circulating autoantibodies. Further characterization of IL-10-producing plasma cells revealed that IL-10 was produced by both autoreactive and non-self-reactive plasma cells. IgM and LAG-3 surface expression correlated moderately with IL-10 expression in plasma cells. There was no induction of IL-10 in plasma cells in the autoantibody-transfer-induced model, hence, no considerable effects of B-cell IL-10-deficiency and IL-10 receptor blockade on disease severity and effector cell functions were detected.

Taken together, this thesis showed that the anti-inflammatory cytokine IL-10 down-modulates EBA skin inflammation under pathophysiological conditions. Plasma cells are the only induced source of IL-10 in the natural course of the disease and the direct or indirect inhibition of effector cell functions appears to be an important mechanism how IL-10 can down-regulate EBA skin inflammation. Moreover, a suppressive role of IL-10 was associated with induction of IL-10$^+$ plasma cells in the immunization-induced EBA model but not in the autoantibody-transfer-induced model, where IL-10 production was not increased above steady state. IL-10-expressing plasma cells can be either derived via an (auto)antigen-driven pathway or from a systemic, inflammation-driven route, suggesting the existence of different IL-10$^+$ plasma cells subsets.

7.2 Impact of IL-10 on the pathogenesis of EBA and its effector cells

The anti-inflammatory cytokine IL-10 plays a pivotal role in the suppression of autoimmune inflammation and IL-10 deficiency promotes autoimmune pathology in various experimental disease models [223]. Moreover, IL-10R blockade with a neutralizing antibody has been shown to reverse IL-10-mediated inhibition of macrophage activation and neutrophil recruitment and to suppress regulatory T-cell functions [187,208,224], important mechanisms involved in autoimmune diseases. In this thesis, the blockade of the IL-10R had a considerable impact on the disease score in an immunization-induced autoimmune skin disease model, indicating that IL-10 already limits skin inflammation under pathophysiological conditions in this model. IL-10 is a pleiotropic cytokine by acting on various IL-10R-expressing cell types and by inhibiting a broad range of effector cell functions, such as proinflammatory cytokine production and T lymphocyte/myeloid cell activation [73]. However, data gained during this theses revealed only a moderate impact of IL-10 on different effector cells, which have been reported to be critically involved in the pathogenesis of EBA [152,161]. It is possible that IL-10 is inhibiting other factors or cells at distinct time points of the disease, which have not been addressed in this thesis with the here applied experimental strategies.

7.2.1 γδ T cells represent a possible target for IL-10-mediated suppression of EBA skin inflammation

The specialized γδ T-cell subset is involved in rapid innate-like immune responses to non-protein antigens [10] and has been implicated to promote EBA skin disease induced by the transfer of autoantibodies [161]. Interestingly, in this thesis, the frequency of splenic γδ T cells was decreased in mice that exhibited a more pronounced skin disease due to IL-10R blockade observed in the immunization-induced EBA model. γδ T cells represent only a small fraction of T cells in the periphery and are even more rare in lymphoid organs such as spleen or LN [225], since many of them directly migrate to skin or intestine to serve as tissue-resident γδ T cells [10]. It is suggested that during MS pathogenesis, γδ T lymphocytes migrate to lesional tissue via distinct signaling pathways involving the chemokine receptors CXCR3 and CXCR5 [225]. In psoriasis, γδ T cells are recruited to the skin, are activated and produce a broad range of effector cytokines [204]. Therefore, it is possible that due to IL-10R blockade-accelerated EBA autoimmune inflammation, more

γδ T cells emigrated from the spleen to the place of inflammation in the skin. Thus, their frequency in the peripheral lymphoid organ was reduced and they locally promoted the skin disease. The cytokine response of γδ T cells in spleen was not affected by IL-10R blockade. However, this does not exclude that the cytokine profile is modulated directly in the skin supporting inflammation and neutrophil infiltration, e.g. via an increased secretion of IFNγ and IL-17 or a decreased production of IL-10 [204,205]. This hypothesis is further supported by the observation that γδ T cells can suppress the activation and recruitment of neutrophils in the effector phase of EBA [161]. Naïve γδ T cells are an important source of IL-17 and can enhance recruitment and activation of innate immune cells and inhibit the expansion and suppressive function of Tregs [216]. In addition, IL-10 can in general suppress the expression of IL-17 by T cells and macrophages [226], suggesting an indirect regulatory link of IL-10 and neutrophil functions via IL-17$^+$ γδ T cells in the skin. This idea is supported by the induction of IL-17A-expressing CD4$^+$ T cells and γδ T cells in mice treated with an IL-10R-blocking antibody in the autoantibody-transfer-induced EBA model (chapter 7.2.2). Therefore, analysis of IL-17 expression by these cells after IL-10R blockade in the immunization-induced model would provide additional information on the regulatory mechanisms during the entire pathophysiological disease development.

7.2.2 IL-10 regulates the generation of IL-17-producing T-cell subsets

IL-17-producing T cells are crucially involved in many autoimmune diseases and IL-17R-deficient mice have been shown to be partially protected from autoantibody-induced EBA [164,214]. Moreover, IL-10 is able to suppress IL 17 secretion from macrophages and T cells [226]. IL-17A-expression in CD4$^+$ T cells and γδ T cells was strongly upregulated after IL-10R blockade in the autoantibody-transfer-induced EBA model, indicating an increased inflammatory state. However, this was not sufficient to induce a higher disease score in these mice. Interestingly, IL-10R blockade but not B-cell IL-10-deficiency considerably upregulated IL-17A expression by different T-cell subsets after transfer of autoantibodies. This suggests that B lineage-derived IL-10 is not required to limit IL-17A expression by T cells. IL-10-expressing Tregs, myeloid cells or even Th17 cells themselves may compensate for the loss of IL-10-producing B lineage cells in this model [49]. Data obtained from an EAE mouse model show that plasmablast-deficient mice exhibit exacerbated EAE development and Th17 cell expansion, and IL-10-deficient plasmablasts strongly induce Th17 cell generation *in vitro* [92]. This may suggest a direct regulatory link between B cell-/plasma cell-derived IL-10 and IL-17-expressing T cells in models where autoimmune diseases are induced by immunization. It would be interesting to see whether

this connection can be confirmed in the immunization-induced EBA model. In this context, γδ T cells [161] and IL-17A$^+$ γδ T cells [204,227] have been shown to promote activation and infiltration of neutrophils to the site of inflammation, which could represent an indirect regulatory mechanisms between plasma cell-derived IL-10 and neutrophil functions. Moreover, a Th17 immune response has been shown to affect the Fc-linked glycosylation pattern by inducing proinflammatory antibodies produced by newly generated plasma cells after a T cell-dependent B-cell response [154,228]. In addition to the stimulatory effects on neutrophils, IL-17 from T cells could also promote proinflammatory autoantibodies supporting EBA skin inflammation (chapter 7.2.4).

7.2.3 IL-10 inhibits migration and oxidative burst of neutrophils

Neutrophils are considered as the major innate effector cells mediating tissue damage and inflammation during EBA pathogenesis [119,152]. Several studies have demonstrated that IL-10 is able to suppress neutrophil recruitment [208] and adhesion [207] as well as their respiratory burst, ROS production and cytotoxic capacity [62,212,229]. Moreover, IL-10 is able to concentration-dependently inhibit C5a-mediated neutrophil migration [70] but also ROS release by innate effector cells *in vitro*, as shown in this thesis. However, effects of IL-10R blockade on neutrophil oxidative burst were only moderate and there was no impact on their migratory capacity under the here applied experimental conditions *ex vivo* and *in vivo*. In particular, neutrophil migration to C5a, their infiltration into inflamed ears, their chemokine receptor CCR2 expression as well as their FcγR expression were not affected. Different factors can be responsible for these observations.

Concerning neutrophil oxidative burst measured by the immune complex-stimulated release of ROS, no isolated neutrophils but total bone marrow cells were used. Neutrophils are the most common ROS-producing leukocyte in the bone marrow, thus, signals will be mainly produced by this cells type [145,213]. Furthermore, the isolation of sensitive neutrophils by sorting bears the risk of undesired (pre-)activation or damage. Stimulation of other bone marrow-derived phagocytes will contribute to the total ROS release. It has already been shown that monocytes/macrophages produce ROS after immune complex stimulation, thus, contributing to blister formation in EBA skin lesions [160]. Moderate effects of IL-10R blockade on total bone marrow cell-derived ROS release could indicate that IL-10 is acting differentially on the oxidative burst of phagocytes. Moreover, functional effects on bone marrow neutrophils do not necessarily reflect the impact of IL-10 on peripheral or tissue-infiltrated neutrophils.

Concerning neutrophil migratory properties, IL-10 has already been demonstrated to inhibit macrophage antigen-1 (Mac-1)-dependent adhesion and C5a-mediated infiltration *in vivo* and *in vitro* [70,207]. However, IL-10R blockade did not alter neutrophil migration to C5a, at least not under the applied experimental conditions used in this thesis. It is possible that migration to other potent chemoattractants such as IL-8 or leukotriene B4 (LTB4) is affected [152,230]. LTB4 has recently been shown to be a critical driver of EBA skin inflammation by the recruitment of neutrophils into to the lesional skin [152]. Moreover, the murine IL-8 homologue chemokine C-X-C motif ligand 1/2 (CXCL1/2) is upregulated in EBA skin and linked to neutrophil-mediated blister formation [231]. Although it has been demonstrated that IL-10 is able to down-regulate the expression of the chemokine receptor CCR2, thus, partially attenuating tissue infiltration in a model of sepsis [211], IL-10R blockade did not affect the expression on peripheral and bone marrow neutrophils in the experimental EBA model. As described above, this does not exclude that CCR2 expression in tissue-infiltrated neutrophils and/or other important chemokine receptors were modulated by IL-10R blockade. Furthermore, the surface expression of inducible chemokine receptors such as CCR2 is tightly regulated e.g. by gene expression or protein degradation [232], thus, influencing their detection by flow cytometry.

Concerning the expression of activating and inhibitory FcγRs expression, their distinct composition on neutrophils has been shown to play an important role for Fc-mediated autoantibody binding in the skin as well as their effector functions [119,233]. Activating FcγRs (e.g. type VI) promote skin inflammation while the inhibitory FcγRIIb mediates protection in experimental EBA models [119,156,234]. However, IL-10R blockade did not affect the expression of both inhibitory and activating FcγRs on peripheral and bone marrow neutrophils. This is in line with a study from CAPSONI and colleagues showing that IL-10 decreased the lysis capacity of neutrophils but not the surface expression of various FcγRs and FcγR-mediated phagocytosis [229].

Neutrophil migration, respiratory burst and their expression of FcγRs was analyzed at the endpoint of the experiment seven weeks after immunization and not directly after IL-10R blockade. Neutrophils have a short half-life of six to eight hours in the periphery and rapidly respond to pathogenic stimuli [235]. Already 24 h after infection, neutrophils have infiltrated the affected tissue in great quantities [236]. It is possible that the assays were not performed at the right time point after the inhibition of the IL-10R signaling and that pronounced effects on neutrophil functions were not detectable anymore.

In vitro studies from this thesis and previous work [70] indicated that at least 25 to 50 ng/ml of IL-10 are needed to considerably inhibit neutrophil functions, a concentration afar the values found in the blood under physiological or pathological conditions in the pg/ml range [70,237]. This raises the question where IL-10 is acting to suppress effector cell functions. Previous work from our group showed that plasma cells, as important IL-10 producer, and neutrophils can co-localize in lymphoid organs such as the spleen [70]. IL-10 can reach a much higher local concentration between the IL-10-secreting and the -sensing cell as compared to the systemic release of IL-10. It is possible that neutrophils are already affected in lymphoid organs, inhibiting their tissue infiltration and/or effector cell functions in the skin. Furthermore, innate-like B1 cells have been shown to be an important source of B cell-derived IL-10 and are able to home to the healthy and inflamed skin [238,239]. This suggests that IL-10-producing cells such as B cells could directly interact with effector cells in the skin to locally regulate inflammation.

7.2.4 IL-10 potentially affects isotype and glycosylation pattern of autoantibodies

In this thesis, IL-10R blockade in the beginning of the effector phase did not affect the autoantibody titer. However, the extent of inflammation can also be determined by other characteristics of the autoantibody. The antibody subclass and its Fc N-linked glycosylation pattern crucially determine the function and pathogenic properties [206]. Murine IgG1 is suggested to have protective anti-inflammatory effects through its preferential binding to FcγRIIb and murine IgG2 antibodies have a more proinflammatory function, e.g. via their complement-fixing abilities and their binding of activating FcγRs on myeloid cells [206,240,241]. In this context, IgG2 has been shown to fix and activate the complement system, thus, driving EBA pathogenesis [138,141]. IL-10 is a potent differentiation factor for B cells and promotes class switch to IgG1 or IgG3 [46,67] and induces IgM and IgG plasmablasts in activated human B cells [103]. Whether IL-10R blockade also affects the subclass distribution, e.g. by inducing class switch to more proinflammatory complement-fixing isotypes and thereby promoting skin inflammation, needs to be further investigated.

A distinct composition of Fc-linked sugar residues on antibodies represent another important mechanism how antibodies can modulate the immune response in a pro- or anti-inflammatory manner [26]. For instance, the Fc-linked sugar structure has been shown to modulate FcγR expression in the skin, thus, affecting EBA inflammation [155]. Th1 and Th17 immune responses shift the glycosylation pattern to a more proinflammatory,

agalactosylated pattern whereas a T cell-independent B-cell response induces suppressive sialylated IgG [154]. Moreover, galactosylated IgG1 is suggested to be anti-inflammatory through C5aR inhibition by the inhibitory FcγRIIb, which has been associated with the reduction of EBA skin inflammation and blistering [156]. Together, these results suggest that cytokines can affect the glycosylation pattern of autoantibodies produced by autoreactive B cells during early plasma cells development, e.g. via the expression of sialyltransferase [228]. However, the influence of IL-10 on this process needs to be further analyzed.

7.3 Characterization of IL-10-producing plasma cells

During the last decade, the suppressive function of IL-10-producing B cells has been investigated in detail but thus far, the phenotype and origin of these cells remains uncertain. Some studies suggest that various developmental stages from immature B cells to fully differentiated plasma cells can acquire regulatory functions in humans and mice within a certain environment and that this function is transient [98,104]. By contrast, other studies suggest the existence of a distinct "Breg" lineage with corresponding progenitor cells that suppress autoimmune inflammation [98,99]. However, no unique marker has been found to characterize "Bregs", although several surface receptors have been described to be associated with IL-10 production in B lineage cells [85], e.g. LAG-3 or TNFR2 [71,102]. Especially plasma cells/plasmablasts are a prominent source of IL-10 suppressing several experimental autoimmune diseases [70,84,92]. In this thesis, new aspects could be added to the characterization of IL-10-expressing B cells, in particular IL-10$^+$ plasma cells.

7.3.1 IL-10 is produced by inflammation-driven and autoantigen-specific plasma cells

In the "regulatory plasmablast hypothesis", MAURI and BLAIR suggest that IL-10- and IL-35-producing plasmablasts can be derived either from naïve mature B cells in lymph nodes or from immature and/or "Breg" progenitors in spleen, e.g. via TLR stimulation [106] (figure 45). The exact contribution of TLR and BCR signaling to the developmental pathways has not yet been fully elucidated [85,106]. In this thesis, it was shown that both self-reactive plasma cells, almost exclusively found in dLN, and non-self-reactive plasma cells can produce IL-10. A large fraction of non-autoreactive IL-10$^+$ plasma cells was found in other lymphoid organs such as spleen and bone marrow and this subset was strongly upregulated in susceptible mice in context of the disease. This supports the "regulatory

plasmablast" idea and suggests that IL-10$^+$ plasma cells can either develop via an (auto)antigen-dependent or -independent, inflammation-driven pathway (figure 45).

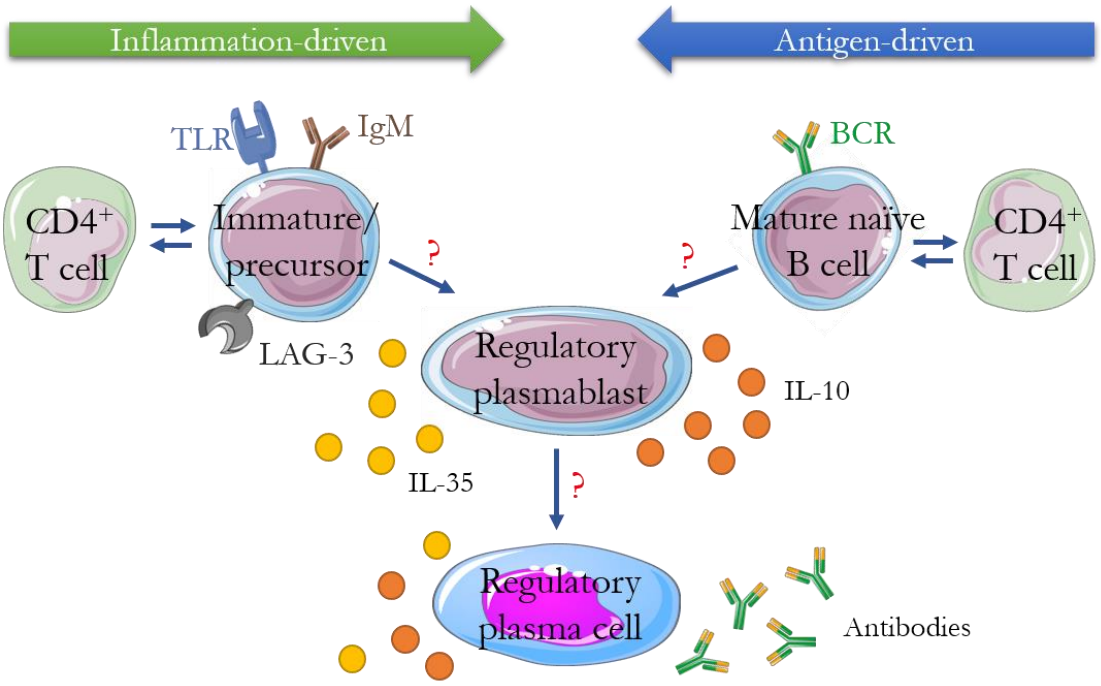

Figure 45: "Regulatory plasmablasts/plasma cells" are suggested to develop via different pathways. The "regulatory plasmablast" hypothesis suggests that IL-10-producing plasmablasts can develop from different pathways, either via immature B cells and/or "regulatory B cell" precursors or via mature naïve B cells during inflammation in lymph nodes independent of a precursor cell. Toll-like receptors (TLR) and the B-cell receptor (BCR) play important roles for the induction of IL-10$^+$ plasmablasts but their exact contribution has not been fully understood. Both pathways can give rise to regulatory plasma cells/plasmablasts producing anti-inflammatory IL-10 and IL-35 as well as antibodies. Basic concept adapted from MAURI and BLAIR [106] with modifications and additions. *IgM, immunoglobulin M; LAG-3, lymphocyte activation gene 3.*

On the one hand, autoreactive B cells were activated in dLN probably via BCR activation and co-stimulation by autoreactive T helper cells and a (small) fraction of newly generated plasma cells then produced IL-10. Moreover, BCR-crosslinking via goat anti-mouse IgD (GMD) leads to an induction of IL-10-producing plasma cells with the ability to suppress EBA via inhibition of neutrophil migration [70]. Moreover, BCR specificity to and signaling strength of self-antigens positively select IL-10$^+$ B cells and promote their development [242].

On the other hand, non-self-reactive B cells in dLN but also in other lymphoid organs such as spleen were activated independent of the autoantigen used for immunization. The systemic, disease-induced inflammation but not BCR-activation by the autoantigen itself triggered the expansion of a large fraction of IL-10-producing non-autoantigen-specific plasma cells and suggests the existence of a "suppressor subset" independent from self-

reactivity. It is likely that IL-10 secretion by these cells was increased during heavy inflammation due to regulatory feedback mechanisms limiting the immune response and restoring tissue homeostasis [81]. In fact, proinflammatory cytokines such as IL-1β or IL-6 can induce murine IL-10-producing B cells [243]. The idea of a "suppressor subset" was further supported by IL-10$^+$ plasma cell expansion in the acute and effector phase of the immunization-induced model. However, whether these inflammation-induced IL-10$^+$ plasma cells are the regulatory subset responsible for down-regulation of the EBA skin disease, e.g. via inhibition of innate effector cell functions (chapter 7.2.3) or modification of the autoantibody subclass/glycosylation pattern (chapter 7.2.4), needs to be further investigated with B cell-specific IL-10-deficient mice on a susceptible background (chapter 8).

7.3.2 IgM and LAG-3 expression characterize a "regulatory plasma cell" subset

As shown in this thesis, the concept of a "suppressor subset" is further supported by the existence of IgM- and LAG-3-expressing IL-10$^+$ plasma cells. "Natural regulatory plasma cells" are a preexisting, non-proliferative LAG-3$^+$ CD138^{hi} plasma cell subset which can rapidly upregulate and secrete IL-10 within hours after innate stimulation via TLR signaling [71]. In this report, IL-10-eGFP and LAG-3 expression in plasma cells correlates in infected mice to nearly 100 %. In this thesis, expression of LAG-3 also correlated with IL-10 expression in plasma cells, but only to a lesser extent. Approximately 50 % of LAG-3$^+$ plasma cells co-expressed IL-10-eGFP under steady state conditions compared to 35 % IL-10$^+$ cells among LAG-3$^-$ plasma cells. However, to clarify whether IL-10 expression by LAG-3$^+$ plasma cells is further increased in the acute phase of the disease, the correlation between IL-10 and LAG-3 expression has to be investigated after immunization.

Splenic LAG-3$^+$ plasma cells slightly increased after immunization in the acute phase of the autoimmune disease and at least the frequency of these cells was upregulated after transfer of autoantibodies in the late effector phase. This suggests that LAG-3$^+$ plasma cells are triggered due to the systemic, disease-induced inflammation independent from the formation of autoreactive plasma cells, which were almost inexistent in spleen after autoantigen-immunization and completely absent in the autoantibody-transfer-induced model. LAG-3$^+$ plasma cells were originally described after *Salmonella* infection, were TLR stimulation rapidly induced IL-10-production by preexisting LAG-3$^+$ plasma cells without previous cell expansion [71]. This thesis demonstrates that LAG-3$^+$ plasma cells are also

induced in an autoimmune model without stimulation of TLRs by bacterial components. Infection and autoimmune diseases involve different kind of stimuli and cellular mechanisms of immune responses. Although TLR signaling induced by pathogens does not play a major role in autoimmunity, TLR and proinflammatory cytokine signaling share several factors in the downstream signaling cascade, e.g. nuclear factor kappa-light-chain-enhancer of activated B cells (NF-κB) or myeloid differentiation primary response 88 (MyD88) [244,245]. It is possible that redundant mechanisms induce IL-10-expressing "natural regulatory" LAG-3$^+$ plasma cells also during autoimmune inflammation independent of TLR ligation. In contrast to the results observed in spleen, LAG-3$^+$ plasma cells were completely absent in draining lymph nodes in diseased and naïve mice, which is in line with the findings in subcutaneous lymph nodes by LINO and colleagues [71]. This indicates LAG-3$^+$ plasma cells are tissue-specific and not a consequence of the adaptive autoimmune reaction in dLN.

It is suggested that IgM expression is a widespread feature of human and murine IL-10$^+$ B cells, implying that "regulatory plasmablasts" could directly develop from IgM$^+$ precursor cells, e.g. transitional B cells or T2-MZP cells [98,106]. Moreover, LAG-3$^+$ plasma cells mainly produce IgM [71]. Therefore, IgM$^+$ plasma cells could serve as a rapidly inducible source of IL-10 after induction of an immune response in contrast to class-switched IL-10$^+$ plasma cells that develop later via GC reactions [106] (figure 45). In this thesis, self-reactive and autoreactive IL-10$^+$ plasma cells expressed comparable amounts of surface IgM. However, IgM production was enriched in the IL-10-producing non-self-reactive plasma cell subset compared to the IL-10$^-$ subset. This could indicate the existence of a suppressor subset derived via an autoantigen-independent pathway from IgM precursor cells. Furthermore, class-switched IgM$^-$ plasma cells have also the capacity to produce IL-10 in line with findings in the EAE mouse model [92].

7.3.3 IL-10-producing plasma cells are differentially regulated in lymphoid organs

Each lymphoid organ plays a distinct role in mediating the immune response to pathogens or during autoimmune inflammation. Lymph nodes in close proximity to the place of infection or immunization mediate the acute, local immune response. By contrast, other lymphoid organs such as the spleen mediate the systemic immune response, e.g. by the accumulation of immunosuppressive cells [4,5]. Moreover, some studies suggest that IL-10- and IL-35-expressing plasma cells and CD1d^{hi} CD5$^+$ "B10" cells act as important regulators

of autoimmune and infectious diseases in spleen [70,84,246]. By contrast, other reports indicate that the lymph node, but not the spleen, is the most important site for IL-10 expression by plasmablasts [92]. Thus, the tissue where IL-10-expressing plasma cells/plasmablasts are formed remains to be elucidated. Moreover, this discrepancy could indicate that different lymphoid organs harbor different plasma cell subsets with regulatory functions that are induced by different environmental stimuli. Alternatively, localization of IL-10-expressing plasma cells might be disease- or model-specific.

In this thesis, plasma cells represented the only inducible source of IL-10 in dLN during autoimmune inflammation. IL-10$^+$ plasma cells were equally abundant in dLN of susceptible and non-susceptible mice, both showing an immunization-dependent induction to the same extent. Interestingly, the TiterMax control treatment induced an IL-10$^+$ plasma cell response in dLN to the same extent as seen for mice immunized with the autoantigen vWFA2. This suggests that the induction of the IL-10-producing plasma cell subset in dLN is mainly driven by the strong, local inflammation, presumably due to the adjuvant used for boosting the immune response, and not directly dependent on the adaptive immune response to the autoantigen. In contrast to the observations in dLN, spleen and bone marrow only showed a slight induction of IL-10$^+$ plasma cells after immunization of susceptible mice with the autoantigen. Spleen and bone marrow harbor only a very small fraction of self-reactive plasma cells, indicating that IL-10 produced by plasma cells must be almost completely derived from non-self-reactive plasma cells in these organs and induced by the secondary, systemic inflammation as explained above (chapter 7.3.1).

Interestingly, susceptible and non-susceptible mice differed in their IL-10 expression by plasma cells in spleen and bone marrow already ten days after immunization. In the immunization-induced EBA model, skin disease does not manifest earlier that four weeks after immunization [134,137], although circulating and tissue bound autoantibodies or autoreactive T cells and plasma cells in dLN are found after seven days or three weeks, respectively [135,137,138]. In this thesis, autoreactive plasma cells and serum autoantibodies were already detectable ten days after immunization, indicating a strong immune reaction in dLN weeks before the first signs of skin inflammation can be observed. It has already been shown that mice develop intestinal inflammation and blister formation in the stomach, esophagus and colon in the EBA model, since COL7 is expressed in mucosal tissues [142]. Thus, it is possible that susceptible mice already developed first signs of mucosal inflammation after ten days, which were not visible on the skin surface. This could have led to a systemic induction of IL-10$^+$ plasma cells in lymphoid organs besides

the dLN at that time point. However, the study from ISHII and colleagues [142] was performed 14 weeks after immunization and investigations at earlier time points are lacking.

Taken together, the data gained in this thesis suggests that IL-10-producing plasma cells are differentially regulated in lymphoid organs and possibly belong to different subsets. Furthermore, the results indicate that IL-10-producing plasma cells can develop via an autoantigen-dependent pathway but also via an inflammation-driven route from a non-self-reactive plasma cell "suppressor subset", which could be characterized at least partially via the surface expression of IgM and LAG-3. Although this IL-10-producing plasma cell "suppressor subset" was upregulated in spleen and bone marrow of susceptible B6.s compared to non-susceptible B6 mice, this subset did not protect B6.s mice from developing the skin disease.

7.4 The quantity and proinflammatory potential of auto-antibodies and autoreactive lymphocytes contribute to EBA susceptibility

Genetic and environmental factors contribute to the development of autoimmune diseases [3], with MHC alleles representing key factors mediating susceptibility to many human autoimmune disorders [30,31]. Moreover, mouse strains carrying the MHC H2s haplotype are susceptible to EBA skin inflammation induced by immunization with the autoantigen vWFA2 and these mice show serum and tissue-bound autoantibodies as well as C3 deposition at the DEJ. By contrast, non-susceptible mouse strains with other haplotypes, e.g. the H2b haplotype, can develop circulating and tissue bound autoantibodies, however, they lack C3 deposits and clinical symptoms after immunization with vWFA2 [137] or mCOL7c-GST [134,138]. Nonetheless, the mechanism of how different MHC haplotypes orchestrate the cellular and humoral immune response in context of an autoimmune blistering skin disease has not been investigated in detail thus far.

7.4.1 Genetic susceptibility is associated with increased autoantibody production and pathogenic potential

In the immunization-induced EBA mouse model, vWFA2-specific antibodies were detectable in B6.s and B6 mice which is in line with other studies [137,138], but B6 mice showed a lower autoantibody titer. However, some individual non-susceptible B6 mice developed a moderate autoantibody titer comparable to some diseased susceptible B6.s

mice. In addition, the titer of all vWFA2-specific antibody subclasses did not correlate with the disease score in susceptible mice. Together, these observations suggest that the autoantibody quantity and the subclass distribution do not exclusively determine the disease phenotype and susceptibility. This is in accordance with data from mouse experiments and clinical data, demonstrating that the mere existence of COL7-specific antibodies and other PD-associated autoantibodies do not correlate with the disease manifestation or extent [70,143]. In contrast, in the autoantibody-transfer-induced EBA model, injection of pathogenic antibodies to COL7 is sufficient to induce skin inflammation and blistering after several days, which correlates with the amount of antibodies transferred [149,177]. One possibility for this discrepancy is that the adaptive immune reaction, which is missing in the autoantibody-transfer-induced model, can limit or even suppress skin pathogenesis to a certain extent under pathophysiological conditions. In addition, the pathogenic character of the autoantibody could play an additional, probably even more crucial, role in mediating EBA disease development. The pathogenic function of an antibody is determined by the subclass and the Fc-linked glycosylation pattern as explained below.

As shown in this thesis, there was no shift in the subclass distribution, indicated by a comparable ratio between IgG2 and IgG1 autoantibodies in the serum between B6.s and B6 mice. In contrast, HAMMERS and colleagues demonstrated that susceptible SJL mice exhibit more complement-fixing antibodies of the IgG2 subclass bound to the DEJ compared to non-susceptible BALB/c mice [138]. However, they did not find differences in serum autoantibody subclasses between the mouse strains as well. It is possible that differences in the subclass distribution contribute to genetic susceptibility in some mouse strains, e.g. SJL mice. However, BALB/c and SJL mice used by HAMMERS and colleagues are no congenic lines such as B6.s and B6 mice used in this thesis, thus, making a direct comparison difficult. Of note, quantitative differences of autoantibody subclasses between the susceptible B6.s and non-susceptible mouse B6 strain used in this thesis have been only shown for tissue-bound but not investigated for serum-derived autoantibodies [134,138].

The pathogenic potential of autoantibodies can be determined by their capability to induce ROS release by innate effector cells, an important process driving EBA pathogenesis [115]. Autoantibodies from susceptible B6.s mice induced a higher oxidative burst after immune complex formation as compared to non-susceptible B6 mice, even when the serum was normalized to the same IgG concentration. A different pathogenic potential can be achieved by distinct Fc-linked sugar residues on IgG autoantibodies and by binding of these antibodies to FcγRs [26,206]. Moreover, differential autoantibody glycosylation affects the

pathogenesis of autoimmune diseases [156,247]. Unpublished data indicates that the glycosylation pattern of vWFA2-specific autoantibodies is shifted towards a more proinflammatory pattern in susceptible mice compared to non-susceptible mice and that this could possibly influence effector cell functions such as ROS release (CLAUDER *et al.*, manuscript in preparation). A change in the glycosylation pattern can be generated by a distinct cytokine response (Th1, Th17) and in turn affects the respective binding of these antibodies to FcγRs on effector cells such as neutrophils [154,156,206]. Compared to non-susceptible B6 mice, susceptible B6.s mice exhibited an augmented IFNγ response from $CD4^+$ T helper and Tfh cells, as shown in this thesis. It has already been demonstrated that Th1 polarization is associated with the EBA disease development in susceptible mice [138]. Moreover, Th1 and/or Th17 immune responses can induce a proinflammatory glycosylation pattern of antibodies produced by newly differentiating plasma cells in a T cell-dependent B-cell response [154,228].

Taken together, the disease resistance in non-susceptible mice is not exclusively achieved by a tight immunological tolerance, which efficiently depletes or attenuates autoreactive lymphocytes with central or peripheral tolerance mechanisms, but instead appears to be associated with a reduced quantity and pathogenic potential (e.g. in terms of the glycosylation pattern) of the produced autoantibodies. A Th1-driven cytokine response in the dLN of susceptible mice could shift the autoantibody glycosylation towards a more proinflammatory pattern, hence, increasing the pathogenic potential of these autoantibodies through FcγR-binding to induce destructive innate effector cell functions.

7.4.2 Autoreactive lymphocytes are activated in B6.s and B6 mice but exhibit a different proinflammatory potential

Distinct MHC alleles have been shown to be associated with susceptibility to different autoimmune diseases [30,31]. Moreover, the MHC haplotype is suggested to determine whether mouse strains are susceptible or protected from autoimmune inflammation in the experimental EBA model [134,137]. The MHC molecule has no direct influence on B-cell development and activation, since these cells only internalize the antigen bound to the BCR and present peptide fragments to T cells as an APC [8]. By contrast, the MHC haplotype modulates the presentation of autoantigen peptide fragments by APCs and in turn the T-cell (cytokine) response during an immune reaction [31,248]. Furthermore, the MHC-TCR interaction is important during central tolerance development since the interaction strength shapes the thymic T-cell receptor repertoire [30,32]. Analysis of the cellular B- and

T-lymphocyte response in this thesis revealed that a considerable proportion of autoreactive lymphocytes was generated in B6.s and B6 mice after immunization with the autoantigen independent of the genetic susceptibility. Although non-susceptible B6 mice exhibited a tighter immunological tolerance with less autoreactive lymphocytes, tolerance was broken in these mice as well, leading to the formation of a considerable amount of autoantibodies and vWFA2-specific lymphocytes. An altered silencing or deletion of autoreactive T-cell clones during central tolerance development due to the H2s haplotype and the corresponding interaction strength between TCR and peptide-bound MHCII could be responsible for this observation. In the periphery, other mechanisms contribute to self-tolerance. It needs to be further investigated whether susceptible and non-susceptible mouse strains show differences in anergic or ignorant peripheral B and T cells, since the loss of these peripheral tolerance mechanisms due to sufficient co-stimulation and/or accessibility to the autoantigen is associated with different autoimmune diseases such as SLE or diabetes [34,38].

Tfh cells are crucial for survival of activated B cells as well as plasma cell differentiation in the GC and class switch by their provision of cytokines such as IL-21 or IFNγ [17]. In this thesis, IL-21 and IFNγ expression were increased in Tfh cells and in total $CD4^+$ T cells in B6.s mice compared to B6 mice. Moreover, IL-10 secretion by Tfh cells was slightly increased in susceptible B6.s mice, suggesting that IL-10, as an autocrine B-cell stimulation factor, additionally promotes plasma cell formation and antibody production [103,249]. IFNγ is important for Tfh differentiation and supports EBA skin inflammation [138,220]. Furthermore, a higher IFNγ/IL-4 ratio, suggesting Th1 polarization, was found in susceptible SJL and B6.s mice compared to non-susceptible B6 mice [138]. It has been demonstrated that the TCR-MHCII interaction strength and the autoantigen dosage influence the Th1/Th2 polarization and in turn the IgG subclass distribution through the corresponding T-cell cytokines [248,250,251]. It is suggested that IFNγ is associated with class-switch to complement-fixing antibodies whereas the Th2 cytokine IL-4 promotes non-complement-fixing IgG1, which exhibits considerable anti-inflammatory properties [219,251,252]. HAMMERS and colleagues suggest that these mechanisms shape the Th1/Th2 response and the subclass distribution in the EBA mouse model, making some mouse strains susceptible to the disease while protecting others [138]. However, in this thesis, an increased IFNγ production by different T-cell subsets did not promote class switch to more proinflammatory subclasses found in the serum of susceptible B6.s mice.

In addition to the MHC polymorphism, non-susceptible B6 mice and congenic, susceptible B6.s mice differ in their C3 allotypes, since the murine *H2* and the *C3* locus are linked [253]. B6.s mice are characterized by the $C3^c$ gene variant derived from SJL mice, which results in a fast, electrophoretic ability [253,254]. This C3 polymorphism (in humans termed C3F) leads to a hyperactive complement system associated with various human disorders such as IgA nephropathy or systemic vasculitis [255]. Since C3 activation and deposition plays a crucial role in driving EBA pathogenesis [144,146], the $C3^c$ allotype and the MHC haplotype could both contribute to the genetic susceptibility. Furthermore, other non-MHC genes could influence the disease phenotype in humans and mice, e.g. distinct quantitative trait loci [256].

7.4.3 Disease susceptibility of B6.s and B6 mice is not dependent on regulatory lymphocyte subsets

The regulatory function of distinct lymphocyte subsets has been mainly attributed to the expression of the anti-inflammatory cytokine IL-10. IL-10-producing $Foxp3^+$ and $Foxp3^-$ T cells and plasma cells have been shown to ameliorate autoimmune diseases such as EBA or MS [70,162,257]. Furthermore, Tregs contribute to peripheral tolerance mechanisms, e.g. by inhibiting Tfh cell expansion and autoantibody formation [258,259]. However, in this thesis no difference in (autoreactive) $Foxp3^+$ Tregs, IL-10-producing $CD4^+$ T cells and IL-10-expressing plasma cells in dLN has been found between susceptible and non-susceptible mice, suggesting that peripheral tolerance by Tregs was not affected by the genetic susceptibility. This observation was made in the acute phase of the disease, where susceptible B6.s mice already demonstrated clear differences in autoreactive plasma cell numbers and the autoantibody titer. Together, this suggests that the aforementioned "suppressor subsets" may not contribute to the EBA disease susceptibility by mediating peripheral tolerance and/or protection by the provision of IL-10 in non-susceptible mouse strains. The frequency of cytokine production by Tregs after autoantigen-restimulation was too low to investigate. However, cytokine production after a general stimulation with PMA/ionomycin/LPS could indicate whether their suppressive capacity was affected or dysregulated as seen in BP patients or other autoimmune diseases [43,44,260]. Of note, the IL-10 expression of total $CD4^+$ T helper cells, which include $Foxp3^+$ and $Foxp3^-$ T-cell subsets, was not dependent on the genetic susceptibility. However, this does not exclude that IL-10-independent functions of Tregs are altered, e.g. contact-dependent suppression or production of other soluble factors such as IL-35 and TGF-β [43].

Taken together, non-susceptible mice showed a tighter immunological tolerance. However, deletion or silencing of autoreactive lymphocyte was incomplete and both mouse strains exhibited a break of tolerance. It can be speculated that the interaction strength of MHC molecules of a distinct haplotype with the TCR shapes the autoreactive T-cell receptor repertoire during central T-cell tolerance development but also the T-cell cytokine response after TCR-dependent activation by APCs [30,31]. Thereby, a stronger (autoreactive) $CD4^+$ T cell and Tfh cell activation and proinflammatory cytokine response will promote autoreactive plasma cell differentiation and production of autoantibodies with increased pathogenic potential driving the disease.

7.5 Limitations of the autoantibody-transfer-induced EBA model

7.5.1 Transfer of rabbit mCOL7-specific autoantibodies only partially reflects the human disease

Disease induction by transfer of autoantibodies is a suitable model to investigate especially cells and mechanisms in the effector phase of EBA. However, this model does not reproduce the afferent phase of the disease, characterized by the break of tolerance and the activation of autoreactive B and T lymphocytes [118]. Therefore, the autoantibody-transfer-induced EBA mouse model has only a limited validity for the human pathogenesis due to its artificial induction and restricted pathogenic mechanisms involved [118,261]. In addition, long-term therapeutic studies are not feasible in the autoantibody-transfer model due to the limited disease maintenance after the last autoantibody injection [261] and the xenogeneic effects of rabbit IgG [178]. It is likely that rabbit IgG as a foreign antigen will also contribute to the immune reaction at earlier time points, especially in terms of cytokine production and secretion, which will be rapidly activated. However, a proinflammatory Th1 cell response and an upregulation of IL-10 was only found in dLN of mice treated with anti-mCOL7 IgG but not normal rabbit IgG after six days [178]. Nevertheless, the xenogeneic immune response to rabbit IgG will influence the disease development as well as cellular and humoral parameters, especially at later time points but possibly also before. Thus, EBA induction using murine anti-mCOL7 antibodies would be a more suitable approach to investigate the EBA effector phase, but thus far, no appropriate model has been established.

7.5.2 Specificity, dosage and purity of autoantibodies influence disease development

Another important difference between the autoantibody-transfer-induced and the immunization-induced EBA model was the different fragment of the COL7 molecule used for induction of the disease. EBA was induced by transfer of anti-mCOL7c autoantibodies and or by immunization with vWFA2, another domain of COL7 as explained in chapter 3.2.4. It has already been shown that autoantibodies targeting different epitopes of COL7, especially of the NC1 domain, induce EBA to a different extent [128] and that disease susceptibility in mice is dependent on distinct specificities of the produced autoantibodies [136]. By contrast, different parts of the NC1 domain are targeted by autoantibodies in EBA patients but no correlation of the antibody specificity and the clinical phenotype were detected thus far [127,179]. Therefore, the results obtained from the immunization-induced and the autoantibody-transfer-induced model cannot be directly compared, e.g. the IL-10 kinetics and the IL-10R blockade experiments. This is not only due to the different EBA induction routes (passive or active) but also due to the diverse recombinant fragments of COL7 (mCOL7c or vWFA2) as the basis for disease induction.

Of note, disease induction by transfer of total or purified rabbit anti-mCOL7c autoantibodies also affects EBA pathogenesis [120,151,160]. The analysis of IL-10 kinetics and B-cell IL-10 knockouts were performed after EBA induction with affinity-purified mCOL7c IgG, whereas the IL-10R blockade experiment was conducted with total rabbit anti-mCOL7c IgG due to the unavailability of the specific IgG at that time point. A much higher amount of autoantibodies is needed when total anti-mCOL7c IgG is injected (mg range) in contrast to specific anti-mCOL7c IgG, which is significantly more potent to induce the disease (µg range) [151,160]. In addition, in both types of EBA induction, the disease severity is dependent on the autoantibody dosage [151,176]. Thus, the results from IL-10R blockade after transfer of autoantibodies cannot be directly compared to other experiments. However, general effects of IL-10 on the disease severity should be obvious independent of the autoantibody purity and the concentration used for EBA induction.

7.5.3 IL-10$^+$ plasma cell induction is too low to considerably suppress EBA pathogenesis after transfer of autoantibodies

In this thesis, no increase was observed in IL-10-expressing plasma cells in spleen and bone marrow after EBA induction by injection of autoantibodies. Of note, since the transfer of autoantibodies does not induce an autoantigen-specific immune response and GC formation in dLN, this organ was not analyzed in this thesis in contrast to the immunization-induced model. In the latter, IL-10$^+$ plasma cells were strongly upregulated after ten days in dLN due to vWFA2-immunization. However, this cell type exhibited only a moderate to low induction in spleen and bone marrow at this time point after vWFA2-immunization. This is in line with the observations in these organs in the autoantibody-transfer-induced EBA model, which demonstrated only a trend in an increase of 10 to 15 % over twelve days. This suggests that due to the lack of tolerance break and the activation of autoreactive lymphocytes mainly in dLN, the overall induction of IL-10-producing plasma cells is too low to considerably suppress the disease after transfer of autoantibodies. This model does not appear to be suitable for the analysis of IL-10 under pathophysiological conditions *in vivo*, which is further supported by the minor effects of IL-10R blockade and B-cell IL-10-deficiency on the disease severity and effector cell functions observed in this model. It is possible that the lack of IL-10$^+$ plasma cell induction in dLN in the autoantibody-transfer-induced model is responsible for this observation. Nevertheless, plasma cells are a dominant source of IL-10 in spleen and bone marrow in both model systems. However, the IL-10 production by these cells was not sufficient to down-modulate autoantibody-induced EBA skin inflammation.

7.6 IL-10 and IL-10-producing plasma cells as treatment options for autoimmune (skin) diseases?

Although intense research during the last decade offered new possibilities of therapeutic approaches, current treatment strategies of many autoimmune diseases still fail to achieve long-lasting remission [262]. In autoimmune blistering skin diseases, therapy relies on corticosteroids and systemic immunosuppression, often does not lead to clinical improvement and harbors serious side effects [115]. Thus, new therapeutic approaches are needed to specifically inhibit effector cells or to maintain suppressor cell subsets.

7.6.1 Administration of IL-10 as a novel therapeutic approach

Although therapeutic injection of IL-10 demonstrated beneficial effects in various autoimmune diseases models, clinical trials using recombinant IL-10 were less successful and showed contradictory results [48]. Systemic administration of recombinant IL-10 has been shown to be safe in humans [80] and in single studies to improve disease symptoms in inflammatory bowel disease [81,82]. However, many other studies failed to ameliorate clinical symptoms and, of note, anti-IL-10 treatment has even been shown to be beneficial in SLE patients [48,83], suggesting that IL-10 could be also pathogenic. Interestingly, the administration route of IL-10 appears to influence the clinical outcome. Local application of IL-10 suppressed inflammation and showed efficacy in psoriasis patients when directly injected under the psoriatic plaque [84], which was further supported by subsequent phase I and II clinical trials [85]. It is suggested that local administration of IL-10 to the target organ is more effective than systemic treatment, thus, autoimmune bullous skin diseases and inflammatory cutaneous disorders represent attractive targets for an IL-10-based therapy [48,86]. Therefore, EBA and related, more common diseases such as BP could benefit from a local treatment with IL-10 or related IL-10R agonists when directly injected into or applied on the blistering skin. With regard to EBA pathogenesis, IL-10 could directly and locally inhibit neutrophil functions such as oxidative burst and/or further migration to the site of inflammation, as suggested in this thesis and by previous work from our group [70]. However, one simple application of IL-10 is probably not enough, since the exact timing, duration, concentration and stability of the IL-10 analogue as well as the effective delivery strategy crucially determine the therapeutic outcome [48].

7.6.2 Induction of IL-10-producing B lineage cells as an autoimmune disease therapy

Apart from the application of IL-10 itself, an expansion or induction of IL-10-expressing B cells/plasma cells could be of therapeutic benefit for various autoimmune diseases. In numerous studies, IL-10-producing B cells and plasma cells played a pivotal role in suppressing experimental autoimmune inflammation such as EAE, SLE and RA [99]. Subsequently, while research focuses on the role and function of "regulatory B lineage cells" in human autoimmune disorders, studies have revealed no clear correlation of this B-cell subset with the disease severity [81]. Moreover, no unique phenotype is described for human IL-10-producing B cells, and IL-10-expression has been attributed to various stages of B-cell development, including plasma cells/plasmablasts [100]. This suggests that

any B cell can acquire regulatory functions while sensing distinct environmental stimuli. Such stimuli to induce IL-10 expression in B cells and plasma cells can be proinflammatory cytokines (e.g. IL-21, IL-1β, IFN), TLR ligands (e.g. CpG, LPS) as well as CD40 and/or BCR signaling [100]. However, the expansion of IL-10$^+$ B lineage cells *in vivo* via these kinds of stimuli bears the risk of undesirable pathogenic side effects due to the activation of additional effector cells or autoreactive lymphocytes. As demonstrated in this thesis, IL-10$^+$ plasma cells moderately expressed surface IgM and LAG-3 and were mainly non-self-reactive, which suggests the existence of a "suppressor subset". However, they were expanded due to the systemic, disease-induced inflammation, presumably via regulatory feedback mechanisms upregulating IL-10 to curtail the systemic inflammatory response. Therefore, induction of IL-10$^+$ B lineage cells from human PBMCs *ex vivo* and re-transfer into the patient appears to be a more suitable therapeutic approach compared to a direct *in vivo* stimulation. However, an IL-10$^+$ B cell-based therapy is still challenging due to the unsolved questions of the "Breg" phenotype, stability/plasticity, site of action and its adequate transfer route [100].

8. Outlook

The results obtained in this thesis demonstrate that the anti-inflammatory cytokine IL-10 down-modulates EBA skin inflammation under pathophysiological conditions and that plasma cells are the primary induced source of IL-10 in the context of the disease. However, the direct regulatory link between plasma cell-derived IL-10 and the development of the disease has to be further investigated using B cell-specific IL-10-deficient mice on a susceptible background in the immunization-induced EBA model. IL-10-producing plasma cells/plasmablasts have already been demonstrated to suppress autoimmune diseases, e.g. via the inhibition of DCs and neutrophils [70,92]. In line with previous observations from our group [70], this thesis further supports the idea that plasma cells are a considerable "regulatory subset" with the ability to suppress autoimmune inflammation. However, a direct or indirect mechanistic link between plasma cell-derived IL-10 and effector cell functions/migration (e.g. of neutrophils/γδ T cells) or autoantibodies (e.g. of the subclass/glycosylation pattern) remains to be investigated. This could be achieved *in vivo* by using B cell-specific IL-10- or neutrophil-specific IL-10R-deficient mice on a susceptible background but also *in vitro* in plasma cell cultures. Thus far, no plasma cell-specific IL-10-deficient mouse line has been described, but mice with impaired plasma cell-differentiation develop exacerbated EAE [92], thus, this transgenic mouse line could be investigated in the EBA model. It would be interesting to see whether a combination of the immunization-induced model, inducing IL-10$^+$ plasma cells in the acute phase, and later the autoantibody-transfer-induced model, would suppress further disease development. IL-10R-blocking antibodies or B cell-specific IL-10-deficient mice could be used to determine whether the effects are mediated by IL-10 or B lineage-derived IL-10. Furthermore, a microscopic or RNA-sequencing-based analysis of the cell composition found in inflamed skin would provide additional information regarding whether IL-10-producing cells and effector cells are locally present and where they make contact to orchestrate the immunosuppressive effects of IL-10.

In this thesis, the origin and phenotype of IL-10-producing plasma cells have been further characterized, demonstrating that both the autoantigen and the systemic inflammation drive the generation of IL-10$^+$ plasma cells. However, this was differently regulated in lymphoid organs. Further analysis and characterization of these cells during the course of the disease would provide comprehensive insights into the potential of "regulatory plasma cells" to suppress autoimmune diseases. *In vitro* and *in vivo* studies testing reagents for induction of IL-10$^+$ plasma cells, e.g. CpG, IL-6 or type I IFN, or direct application of IL-10, could help to develop new therapeutic approaches to treat human autoimmune diseases.

9. References

1. Theofilopoulos AN, Kono DH, Baccala R: **The multiple pathways to autoimmunity**. *Nature Immunology* 2017, **18**:716.

2. Rao DS: **Chapter 19 - Overview and Compartmentalization of the Immune System**. In *Hematology (Seventh Edition)*. Edited by Hoffman R, Benz EJ, Silberstein LE, Heslop HE, Weitz JI, Anastasi J, Salama ME, Abutalib SA: Elsevier; 2018:199-209.e191.

3. Rosenblum MD, Remedios KA, Abbas AK: **Mechanisms of human autoimmunity**. *The Journal of clinical investigation* 2015, **125**:2228-2233.

4. Zhao L, Liu L, Guo B, Zhu B: **Regulation of adaptive immune responses by guiding cell movements in the spleen**. *Frontiers in microbiology* 2015, **6**:645-645.

5. Bronte V, Pittet MJ: **The spleen in local and systemic regulation of immunity**. *Immunity* 2013, **39**:806-818.

6. Dempsey PW, Vaidya SA, Cheng G: **The art of war: Innate and adaptive immune responses**. *Cell Mol Life Sci* 2003, **60**:2604-2621.

7. Yatim KM, Lakkis FG: **A Brief Journey through the Immune System**. *Clinical Journal of the American Society of Nephrology* 2015, **10**:1274-1281.

8. Chaplin DD: **Overview of the immune response**. *The Journal of allergy and clinical immunology* 2010, **125**:S3-S23.

9. Ghodke Y, Joshi K, Chopra A, Patwardhan B: **HLA and disease**. *Eur J Epidemiol* 2005, **20**:475-488.

10. Vantourout P, Hayday A: **Six-of-the-best: unique contributions of gammadelta T cells to immunology**. *Nat Rev Immunol* 2013, **13**:88-100.

11. Godfrey DI, Kronenberg M: **Going both ways: immune regulation via CD1d-dependent NKT cells**. *J Clin Invest* 2004, **114**:1379-1388.

12. Kidd P: **Th1/Th2 balance: the hypothesis, its limitations, and implications for health and disease**. *Altern Med Rev* 2003, **8**:223-246.

13. Sallusto F, Lanzavecchia A: **Heterogeneity of CD4+ memory T cells: functional modules for tailored immunity**. *Eur J Immunol* 2009, **39**:2076-2082.

14. Crotty S: **Follicular helper CD4 T cells (TFH)**. *Annu Rev Immunol* 2011, **29**:621-663.

15. Liu X, Nurieva RI, Dong C: **Transcriptional regulation of follicular T-helper (Tfh) cells**. *Immunol Rev* 2013, **252**:139-145.

16. Wan Z, Lin Y, Zhao Y, Qi H: **TFH cells in bystander and cognate interactions with B cells**. *Immunol Rev* 2019, **288**:28-36.

17. Crotty S: **A brief history of T cell help to B cells**. *Nature reviews. Immunology* 2015, **15**:185-189.

18. Nutt SL, Hodgkin PD, Tarlinton DM, Corcoran LM: **The generation of antibody-secreting plasma cells**. *Nat Rev Immunol* 2015, **15**:160-171.

19. Chu VT, Berek C: **The establishment of the plasma cell survival niche in the bone marrow**. *Immunol Rev* 2013, **251**:177-188.

20. Schroeder HW, Jr., Cavacini L: **Structure and function of immunoglobulins**. *The Journal of allergy and clinical immunology* 2010, **125**:S41-S52.

21. Nera KP, Kylaniemi MK, Lassila O: **Regulation of B Cell to Plasma Cell Transition within the Follicular B Cell Response**. *Scand J Immunol* 2015, **82**:225-234.

22. Mesin L, Ersching J, Victora GD: **Germinal Center B Cell Dynamics**. *Immunity* 2016, **45**:471-482.

23. Stavnezer J, Guikema JEJ, Schrader CE: **Mechanism and regulation of class switch recombination**. *Annual review of immunology* 2008, **26**:261-292.

24. Forthal DN: **Functions of Antibodies**. *Microbiology spectrum* 2014, **2**:1-17.

25. Nimmerjahn F, Ravetch JV: **Divergent immunoglobulin g subclass activity through selective Fc receptor binding**. *Science* 2005, **310**:1510-1512.

26. Collin M, Ehlers M: **The carbohydrate switch between pathogenic and immunosuppressive antigen-specific antibodies**. *Exp Dermatol* 2013, **22**:511-514.

27. Kurosaki T, Kometani K, Ise W: **Memory B cells**. *Nat Rev Immunol* 2015, **15**:149-159.

28. Wang L, Wang FS, Gershwin ME: **Human autoimmune diseases: a comprehensive update**. *J Intern Med* 2015, **278**:369-395.

29. Cho JH, Feldman M: **Heterogeneity of autoimmune diseases: pathophysiologic insights from genetics and implications for new therapies**. *Nat Med* 2015, **21**:730-738.

30. Tsai S, Santamaria P: **MHC Class II Polymorphisms, Autoreactive T-Cells, and Autoimmunity**. *Front Immunol* 2013, **4**:321.

31. Sollid LM, Pos W, Wucherpfennig KW: **Molecular mechanisms for contribution of MHC molecules to autoimmune diseases**. *Curr Opin Immunol* 2014, **31**:24-30.

32. Nurieva RI, Liu X, Dong C: **Molecular mechanisms of T-cell tolerance**. *Immunol Rev* 2011, **241**:133-144.

33. Luning Prak ET, Monestier M, Eisenberg RA: **B cell receptor editing in tolerance and autoimmunity**. *Ann N Y Acad Sci* 2011, **1217**:96-121.

34. Cambier JC, Gauld SB, Merrell KT, Vilen BJ: **B-cell anergy: from transgenic models to naturally occurring anergic B cells?** *Nat Rev Immunol* 2007, **7**:633-643.

35. Lohr J, Knoechel B, Nagabhushanam V, Abbas AK: **T-cell tolerance and autoimmunity to systemic and tissue-restricted self-antigens**. *Immunol Rev* 2005, **204**:116-127.

36. Quach TD, Manjarrez-Orduno N, Adlowitz DG, Silver L, et al.: **Anergic responses characterize a large fraction of human autoreactive naive B cells expressing low levels of surface IgM**. *J Immunol* 2011, **186**:4640-4648.

37. Parish IA, Heath WR: **Too dangerous to ignore: self-tolerance and the control of ignorant autoreactive T cells**. *Immunol Cell Biol* 2008, **86**:146-152.

38. Manjarrez-Orduno N, Quach TD, Sanz I: **B cells and immunological tolerance**. *J Invest Dermatol* 2009, **129**:278-288.

39. Li Z, Li D, Tsun A, Li B: **FOXP3+ regulatory T cells and their functional regulation**. *Cell Mol Immunol* 2015, **12**:558-565.

40. Xing Y, Hogquist KA: **T-cell tolerance: central and peripheral**. *Cold Spring Harb Perspect Biol* 2012, **4**.

41. Corthay A: **How do regulatory T cells work?** *Scandinavian journal of immunology* 2009, **70**:326-336.

42. Sakaguchi S: **Naturally arising Foxp3-expressing CD25+CD4+ regulatory T cells in immunological tolerance to self and non-self**. *Nat Immunol* 2005, **6**:345-352.

43. Buckner JH: **Mechanisms of impaired regulation by CD4(+)CD25(+)FOXP3(+) regulatory T cells in human autoimmune diseases**. *Nat Rev Immunol* 2010, **10**:849-859.

44. Sakaguchi S, Ono M, Setoguchi R, Yagi H, et al.: **Foxp3+ CD25+ CD4+ natural regulatory T cells in dominant self-tolerance and autoimmune disease**. *Immunol Rev* 2006, **212**:8-27.

45. Fiorentino DF, Bond MW, Mosmann TR: **Two types of mouse T helper cell. IV. Th2 clones secrete a factor that inhibits cytokine production by Th1 clones**. *J Exp Med* 1989, **170**:2081-2095.

46. Moore KW, de Waal Malefyt R, Coffman RL, O'Garra A: **Interleukin-10 and the interleukin-10 receptor**. *Annu Rev Immunol* 2001, **19**:683-765.

47. Saxena A, Khosraviani S, Noel S, Mohan D, et al.: **Interleukin-10 paradox: A potent immunoregulatory cytokine that has been difficult to harness for immunotherapy**. *Cytokine* 2015, **74**:27-34.

48. Saraiva M, O'Garra A: **The regulation of IL-10 production by immune cells**. *Nat Rev Immunol* 2010, **10**:170-181.

49. Ng THS, Britton G, Hill E, Verhagen J, et al.: **Regulation of Adaptive Immunity; The Role of Interleukin-10**. *Frontiers in Immunology* 2013, **4**.

50. Fillatreau S, Gray D, Anderton SM: **Not always the bad guys: B cells as regulators of autoimmune pathology**. *Nat Rev Immunol* 2008, **8**:391-397.

51. Hofmann K, Clauder AK, Manz RA: **Targeting B Cells and Plasma Cells in Autoimmune Diseases**. *Front Immunol* 2018, **9**:835.

52. Windsor WT, Syto R, Tsarbopoulos A, Zhang R, et al.: **Disulfide bond assignments and secondary structure analysis of human and murine interleukin 10**. *Biochemistry* 1993, **32**:8807-8815.

53. Liu Y, Wei SH, Ho AS, de Waal Malefyt R, et al.: **Expression cloning and characterization of a human IL-10 receptor**. *J Immunol* 1994, **152**:1821-1829.

54. Kotenko SV, Krause CD, Izotova LS, Pollack BP, et al.: **Identification and functional characterization of a second chain of the interleukin-10 receptor complex**. *The EMBO journal* 1997, **16**:5894-5903.

55. Shouval DS, Ouahed J, Biswas A, Goettel JA, et al.: **Interleukin 10 receptor signaling: master regulator of intestinal mucosal homeostasis in mice and humans**. *Adv Immunol* 2014, **122**:177-210.

56. Finbloom DS, Winestock KD: **IL-10 induces the tyrosine phosphorylation of tyk2 and Jak1 and the differential assembly of STAT1 alpha and STAT3 complexes in human T cells and monocytes**. *J Immunol* 1995, **155**:1079-1090.

57. Wehinger J, Gouilleux F, Groner B, Finke J, et al.: **IL-10 induces DNA binding activity of three STAT proteins (Stat1, Stat3, and Stat5) and their distinct combinatorial assembly in the promoters of selected genes**. *FEBS Lett* 1996, **394**:365-370.

58. Berlato C, Cassatella MA, Kinjyo I, Gatto L, et al.: **Involvement of suppressor of cytokine signaling-3 as a mediator of the inhibitory effects of IL-10 on lipopolysaccharide-induced macrophage activation**. *J Immunol* 2002, **168**:6404-6411.

59. Verma R, Balakrishnan L, Sharma K, Khan AA, et al.: **A network map of Interleukin-10 signaling pathway**. *Journal of cell communication and signaling* 2016, **10**:61-67.

60. Huhn RD, Radwanski E, Gallo J, Affrime MB, et al.: **Pharmacodynamics of subcutaneous recombinant human interleukin-10 in healthy volunteers**. *Clin Pharmacol Ther* 1997, **62**:171-180.

61. Cunha FQ, Moncada S, Liew FY: **Interleukin-10 (IL-10) inhibits the induction of nitric oxide synthase by interferon-gamma in murine macrophages**. *Biochem Biophys Res Commun* 1992, **182**:1155-1159.

62. Dang PM, Elbim C, Marie JC, Chiandotto M, et al.: **Anti-inflammatory effect of interleukin-10 on human neutrophil respiratory burst involves inhibition of GM-CSF-induced p47PHOX phosphorylation through a decrease in ERK1/2 activity**. *Faseb j* 2006, **20**:1504-1506.

63. Koppelman B, Neefjes JJ, de Vries JE, de Waal Malefyt R: **Interleukin-10 down-regulates MHC class II alphabeta peptide complexes at the plasma membrane of monocytes by affecting arrival and recycling**. *Immunity* 1997, **7**:861-871.

64. Groux H, Bigler M, de Vries JE, Roncarolo MG: **Interleukin-10 induces a long-term antigen-specific anergic state in human CD4+ T cells**. *J Exp Med* 1996, **184**:19-29.

65. Groux H, O'Garra A, Bigler M, Rouleau M, et al.: **A CD4+ T-cell subset inhibits antigen-specific T-cell responses and prevents colitis**. *Nature* 1997, **389**:737-742.

66. Rousset F, Garcia E, Defrance T, Péronne C, et al.: **Interleukin 10 is a potent growth and differentiation factor for activated human B lymphocytes**. *Proceedings of the National Academy of Sciences of the United States of America* 1992, **89**:1890-1893.

67. Malisan F, Briere F, Bridon JM, Harindranath N, et al.: **Interleukin-10 induces immunoglobulin G isotype switch recombination in human CD40-activated naive B lymphocytes**. *J Exp Med* 1996, **183**:937-947.

68. Llorente L, Zou W, Levy Y, Richaud-Patin Y, et al.: **Role of interleukin 10 in the B lymphocyte hyperactivity and autoantibody production of human systemic lupus erythematosus**. *J Exp Med* 1995, **181**:839-844.

69. Beebe AM, Cua DJ, de Waal Malefyt R: **The role of interleukin-10 in autoimmune disease: systemic lupus erythematosus (SLE) and multiple sclerosis (MS)**. *Cytokine Growth Factor Rev* 2002, **13**:403-412.

70. Kulkarni U, Karsten CM, Kohler T, Hammerschmidt S, et al.: **IL-10 mediates plasmacytosis-associated immunodeficiency by inhibiting complement-mediated neutrophil migration**. *J Allergy Clin Immunol* 2016, **137**:1487-1497.e1486.

71. Lino AC, Dang VD, Lampropoulou V, Welle A, et al.: **LAG-3 Inhibitory Receptor Expression Identifies Immunosuppressive Natural Regulatory Plasma Cells**. *Immunity* 2018, **49**:120-133.e129.

72. Couper KN, Blount DG, Riley EM: **IL-10: the master regulator of immunity to infection**. *J Immunol* 2008, **180**:5771-5777.

73. Groux H, Cottrez F: **The complex role of interleukin-10 in autoimmunity**. *J Autoimmun* 2003, **20**:281-285.

74. Finnegan A, Kaplan CD, Cao Y, Eibel H, et al.: **Collagen-induced arthritis is exacerbated in IL-10-deficient mice**. *Arthritis research & therapy* 2003, **5**:R18-R24.

75. Bettelli E, Das MP, Howard ED, Weiner HL, et al.: **IL-10 is critical in the regulation of autoimmune encephalomyelitis as demonstrated by studies of IL-10- and IL-4-deficient and transgenic mice**. *J Immunol* 1998, **161**:3299-3306.

76. Yin Z, Bahtiyar G, Zhang N, Liu L, et al.: **IL-10 regulates murine lupus**. *J Immunol* 2002, **169**:2148-2155.

77. Toto P, Feliciani C, Amerio P, Suzuki H, et al.: **Immune modulation in pemphigus vulgaris: role of CD28 and IL-10**. *J Immunol* 2000, **164**:522-529.

78. Kuhn R, Lohler J, Rennick D, Rajewsky K, et al.: **Interleukin-10-deficient mice develop chronic enterocolitis**. *Cell* 1993, **75**:263-274.

79. Persson S, Mikulowska A, Narula S, O'Garra A, et al.: **Interleukin-10 suppresses the development of collagen type II-induced arthritis and ameliorates sustained arthritis in rats**. *Scand J Immunol* 1996, **44**:607-614.

80. Gibson AWE, J.C.; Wu, J. et al.: *The Role of IL-10 in Autoimmune Pathology*: Austin (TX): Landes Bioscience; 2000-2013.

81. Miyagaki T, Fujimoto M, Sato S: **Regulatory B cells in human inflammatory and autoimmune diseases: from mouse models to clinical research**. *Int Immunol* 2015, **27**:495-504.

82. Mizoguchi A, Bhan AK: **A case for regulatory B cells**. *J Immunol* 2006, **176**:705-710.

83. Barr TA, Shen P, Brown S, Lampropoulou V, et al.: **B cell depletion therapy ameliorates autoimmune disease through ablation of IL-6-producing B cells**. *J Exp Med* 2012, **209**:1001-1010.

84. Shen P, Roch T, Lampropoulou V, O'Connor RA, et al.: **IL-35-producing B cells are critical regulators of immunity during autoimmune and infectious diseases**. *Nature* 2014, **507**:366-370.

85. Mauri C, Bosma A: **Immune regulatory function of B cells**. *Annu Rev Immunol* 2012, **30**:221-241.

86. Carter NA, Rosser EC, Mauri C: **Interleukin-10 produced by B cells is crucial for the suppression of Th17/Th1 responses, induction of T regulatory type 1 cells and reduction of collagen-induced arthritis**. *Arthritis Res Ther* 2012, **14**:R32.

87. Wolf SD, Dittel BN, Hardardottir F, Janeway CA, Jr.: **Experimental autoimmune encephalomyelitis induction in genetically B cell-deficient mice**. *J Exp Med* 1996, **184**:2271-2278.

88. Fillatreau S, Sweenie CH, McGeachy MJ, Gray D, et al.: **B cells regulate autoimmunity by provision of IL-10**. *Nat Immunol* 2002, **3**:944-950.

89. Mauri C, Gray D, Mushtaq N, Londei M: **Prevention of arthritis by interleukin 10-producing B cells**. *J Exp Med* 2003, **197**:489-501.

90. Watanabe R, Ishiura N, Nakashima H, Kuwano Y, et al.: **Regulatory B cells (B10 cells) have a suppressive role in murine lupus: CD19 and B10 cell deficiency exacerbates systemic autoimmunity**. *J Immunol* 2010, **184**:4801-4809.

91. Mizoguchi A, Mizoguchi E, Takedatsu H, Blumberg RS, et al.: **Chronic intestinal inflammatory condition generates IL-10-producing regulatory B cell subset characterized by CD1d upregulation**. *Immunity* 2002, **16**:219-230.

92. Matsumoto M, Baba A, Yokota T, Nishikawa H, et al.: **Interleukin-10-Producing Plasmablasts Exert Regulatory Function in Autoimmune Inflammation**. *Immunity* 2014, **41**:1040-1051.

93. Duddy ME, Alter A, Bar-Or A: **Distinct profiles of human B cell effector cytokines: a role in immune regulation?** *J Immunol* 2004, **172**:3422-3427.

94. Duddy M, Niino M, Adatia F, Hebert S, et al.: **Distinct effector cytokine profiles of memory and naive human B cell subsets and implication in multiple sclerosis**. *J Immunol* 2007, **178**:6092-6099.

95. Iwata Y, Matsushita T, Horikawa M, Dilillo DJ, et al.: **Characterization of a rare IL-10-competent B-cell subset in humans that parallels mouse regulatory B10 cells**. *Blood* 2011, **117**:530-541.

96. Barnes BJ: **Editorial: Are regulatory B10 cells a viable target for autoimmune diseases?** *Journal of Leukocyte Biology* 2013, **94**:548-550.

97. Liu Z, Dang E, Li B, Qiao H, et al.: **Dysfunction of CD19(+)CD24(hi)CD27(+) B regulatory cells in patients with bullous pemphigoid**. *Sci Rep* 2018, **8**:703.

98. Mauri C, Menon M: **The expanding family of regulatory B cells**. *Int Immunol* 2015, **27**:479-486.

99. Kalampokis I, Yoshizaki A, Tedder TF: **IL-10-producing regulatory B cells (B10 cells) in autoimmune disease**. *Arthritis Res Ther* 2013, **15 Suppl 1**:S1.

100. Mauri C, Menon M: **Human regulatory B cells in health and disease: therapeutic potential**. *J Clin Invest* 2017, **127**:772-779.

101. Xiao S, Brooks CR, Sobel RA, Kuchroo VK: **Tim-1 is essential for induction and maintenance of IL-10 in regulatory B cells and their regulation of tissue inflammation**. *J Immunol* 2015, **194**:1602-1608.

102. Ticha O, Moos L, Wajant H, Bekeredjian-Ding I: **Expression of Tumor Necrosis Factor Receptor 2 Characterizes TLR9-Driven Formation of Interleukin-10-Producing B Cells**. *Frontiers in immunology* 2018, **8**:1951-1951.

103. Heine G, Drozdenko G, Grun JR, Chang HD, et al.: **Autocrine IL-10 promotes human B-cell differentiation into IgM- or IgG-secreting plasmablasts**. *Eur J Immunol* 2014, **44**:1615-1621.

104. Maseda D, Smith SH, DiLillo DJ, Bryant JM, et al.: **Regulatory B10 cells differentiate into antibody-secreting cells after transient IL-10 production in vivo**. *J Immunol* 2012, **188**:1036-1048.

105. Blanc P, Moro-Sibilot L, Barthly L, Jagot F, et al.: **Mature IgM-expressing plasma cells sense antigen and develop competence for cytokine production upon antigenic challenge**. *Nat Commun* 2016, **7**:13600.

106. Mauri C, Blair PA: **The incognito journey of a regulatory B cell**. *Immunity* 2014, **41**:878-880.

107. Pasparakis M, Haase I, Nestle FO: **Mechanisms regulating skin immunity and inflammation**. *Nat Rev Immunol* 2014, **14**:289-301.

108. Schmidt E, Zillikens D: **The diagnosis and treatment of autoimmune blistering skin diseases**. *Deutsches Arzteblatt international* 2011, **108**:399-III.

109. Stanley JR: **Pemphigus and pemphigoid as paradigms of organ-specific, autoantibody-mediated diseases**. *The Journal of clinical investigation* 1989, **83**:1443-1448.

110. Schmidt E, Zillikens D: **Pemphigoid diseases**. *Lancet* 2013, **381**:320-332.

111. Hofmann SC, Juratli HA, Eming R: **Bullous autoimmune dermatoses**. *J Dtsch Dermatol Ges* 2018, **16**:1339-1358.

112. Kasperkiewicz M, Zillikens D, Schmidt E: **Pemphigoid diseases: pathogenesis, diagnosis, and treatment**. *Autoimmunity* 2012, **45**:55-70.

113. Vorobyev A, Ludwig RJ, Schmidt E: **Clinical features and diagnosis of epidermolysis bullosa acquisita**. *Expert Rev Clin Immunol* 2017, **13**:157-169.

114. Jonkman MF: *Epidermolysis Bullosa Acquisita*, vol 1. Edited by Jonkman MF: Springer International Publishing AG Switzerland; 2016.

115. Ludwig RJ: **Clinical presentation, pathogenesis, diagnosis, and treatment of epidermolysis bullosa acquisita**. *ISRN Dermatol* 2013, **2013**:812029.

116. Hubner F, Recke A, Zillikens D, Linder R, et al.: **Prevalence and Age Distribution of Pemphigus and Pemphigoid Diseases in Germany**. *J Invest Dermatol* 2016, **136**:2495-2498.

117. Bertram F, Brocker EB, Zillikens D, Schmidt E: **Prospective analysis of the incidence of autoimmune bullous disorders in Lower Franconia, Germany**. *J Dtsch Dermatol Ges* 2009, **7**:434-440.

118. Sitaru C: **Experimental models of epidermolysis bullosa acquisita**. *Exp Dermatol* 2007, **16**:520-531.

119. Koga H, Prost-Squarcioni C, Iwata H, Jonkman MF, et al.: **Epidermolysis Bullosa Acquisita: The 2019 Update**. *Frontiers in medicine* 2019, **5**:362-362.

120. Gammon WR, Briggaman RA, Wheeler CE: **Epidermolysis bullosa acquisita presenting as an inflammatory bullous disease**. *Journal of the American Academy of Dermatology* 1982, **7**:382-387.

121. Prost-Squarcioni C, Caux F, Schmidt E, Jonkman MF, et al.: **International Bullous Diseases Group: consensus on diagnostic criteria for epidermolysis bullosa acquisita**. *British Journal of Dermatology* 2018, **179**:30-41.

122. Gupta R, Woodley DT, Chen M: **Epidermolysis bullosa acquisita**. *Clin Dermatol* 2012, **30**:60-69.

123. Yaoita H, Briggaman RA, Lawley TJ, Provost TT, et al.: **Epidermolysis bullosa acquisita: ultrastructural and immunological studies**. *J Invest Dermatol* 1981, **76**:288-292.

124. Woodley DT, Briggaman RA, O'Keefe EJ, Inman AO, et al.: **Identification of the skin basement-membrane autoantigen in epidermolysis bullosa acquisita**. *N Engl J Med* 1984, **310**:1007-1013.

125. Lapiere JC, Woodley DT, Parente MG, Iwasaki T, et al.: **Epitope mapping of type VII collagen. Identification of discrete peptide sequences recognized by sera from patients with acquired epidermolysis bullosa**. *J Clin Invest* 1993, **92**:1831-1839.

126. Csorba K, Chiriac MT, Florea F, Ghinia MG, et al.: **Blister-inducing antibodies target multiple epitopes on collagen VII in mice**. *J Cell Mol Med* 2014, **18**:1727-1739.

127. Kim JH, Kim SC: **Epidermolysis bullosa acquisita**. *J Eur Acad Dermatol Venereol* 2013, **27**:1204-1213.

128. Chen M, Keene DR, Costa FK, Tahk SH, et al.: **The Carboxyl Terminus of Type VII Collagen Mediates Antiparallel Dimer Formation and Constitutes a New Antigenic Epitope for Epidermolysis Bullosa Acquisita Autoantibodies**. *Journal of Biological Chemistry* 2001, **276**:21649-21655.

129. Remington J, Chen M, Burnett J, Woodley DT: **Autoimmunity to type VII collagen: epidermolysis bullosa acquisita**. *Curr Dir Autoimmun* 2008, **10**:195-205.

130. Kasperkiewicz M, Sadik CD, Bieber K, Ibrahim SM, et al.: **Epidermolysis Bullosa Acquisita: From Pathophysiology to Novel Therapeutic Options**. *J Invest Dermatol* 2016, **136**:24-33.

131. Muller R, Dahler C, Mobs C, Wenzel E, et al.: **T and B cells target identical regions of the non-collagenous domain 1 of type VII collagen in epidermolysis bullosa acquisita**. *Clin Immunol* 2010, **135**:99-107.

132. Gammon WR, Heise ER, Burke WA, Fine JD, et al.: **Increased frequency of HLA-DR2 in patients with autoantibodies to epidermolysis bullosa acquisita antigen: evidence that the expression of autoimmunity to type VII collagen is HLA class II allele associated**. *J Invest Dermatol* 1988, **91**:228-232.

133. Zumelzu C, Le Roux-Villet C, Loiseau P, Busson M, et al.: **Black patients of African descent and HLA-DRB1*15:03 frequency overrepresented in epidermolysis bullosa acquisita**. *J Invest Dermatol* 2011, **131**:2386-2393.

134. Ludwig RJ, Recke A, Bieber K, Muller S, et al.: **Generation of antibodies of distinct subclasses and specificity is linked to H2s in an active mouse model of epidermolysis bullosa acquisita**. *J Invest Dermatol* 2011, **131**:167-176.

135. Tiburzy B, Szyska M, Iwata H, Chrobok N, et al.: **Persistent autoantibody-production by intermediates between short-and long-lived plasma cells in inflamed lymph nodes of experimental epidermolysis bullosa acquisita**. *PLoS One* 2013, **8**:e83631.

136. Sitaru AG, Sesarman A, Mihai S, Chiriac MT, et al.: **T cells are required for the production of blister-inducing autoantibodies in experimental epidermolysis bullosa acquisita**. *J Immunol* 2010, **184**:1596-1603.

137. Iwata H, Bieber K, Tiburzy B, Chrobok N, et al.: **B cells, dendritic cells, and macrophages are required to induce an autoreactive CD4 helper T cell response in experimental epidermolysis bullosa acquisita**. *J Immunol* 2013, **191**:2978-2988.

138. Hammers CM, Bieber K, Kalies K, Banczyk D, et al.: **Complement-fixing anti-type VII collagen antibodies are induced in Th1-polarized lymph nodes of epidermolysis bullosa acquisita-susceptible mice**. *J Immunol* 2011, **187**:5043-5050.

139. Kim JH, Kim YH, Kim SC: **Epidermolysis bullosa acquisita: a retrospective clinical analysis of 30 cases**. *Acta Derm Venereol* 2011, **91**:307-312.

140. Cho HJ, Lee IJ, Kim SC: **Complement-fixing abilities and IgG subclasses of autoantibodies in epidermolysis bullosa acquisita**. *Yonsei Med J* 1998, **39**:339-344.

141. Sitaru C, Chiriac MT, Mihai S, Buning J, et al.: **Induction of complement-fixing autoantibodies against type VII collagen results in subepidermal blistering in mice**. *J Immunol* 2006, **177**:3461-3468.

142. Ishii N, Recke A, Mihai S, Hirose M, et al.: **Autoantibody-induced intestinal inflammation and weight loss in experimental epidermolysis bullosa acquisita**. *J Pathol* 2011, **224**:234-244.

143. Prüßmann W, Prüßmann J, Koga H, Recke A, et al.: **Prevalence of pemphigus and pemphigoid autoantibodies in the general population**. *Orphanet journal of rare diseases* 2015, **10**:63-63.

144. Mooney E, Falk RJ, Gammon WR: **Studies on complement deposits in epidermolysis bullosa acquisita and bullous pemphigoid**. *Arch Dermatol* 1992, **128**:58-60.

145. Furze RC, Rankin SM: **Neutrophil mobilization and clearance in the bone marrow**. *Immunology* 2008, **125**:281-288.

146. Witte M, Zillikens D, Schmidt E: **Diagnosis of Autoimmune Blistering Diseases**. *Front Med (Lausanne)* 2018, **5**:296.

147. Mihai S, Chiriac MT, Takahashi K, Thurman JM, et al.: **The alternative pathway of complement activation is critical for blister induction in experimental epidermolysis bullosa acquisita**. *J Immunol* 2007, **178**:6514-6521.

148. Mihai S, Hirose M, Wang Y, Thurman JM, et al.: **Specific Inhibition of Complement Activation Significantly Ameliorates Autoimmune Blistering Disease in Mice**. *Front Immunol* 2018, **9**:535.

149. Sitaru C, Mihai S, Otto C, Chiriac MT, et al.: **Induction of dermal-epidermal separation in mice by passive transfer of antibodies specific to type VII collagen**. *J Clin Invest* 2005, **115**:870-878.

150. Ludwig RJ, Vanhoorelbeke K, Leypoldt F, Kaya Z, et al.: **Mechanisms of Autoantibody-Induced Pathology**. *Front Immunol* 2017, **8**:603.

151. Chen MD, HH.; Nadelmann, C.; Woodley, DT.: *Epidermolysis Bullosa Acquisita*, vol 2. Edited by Hertl M: Springer-Verlag Wien New York; 2005.

152. Sezin T, Krajewski M, Wutkowski A, Mousavi S, et al.: **The Leukotriene B4 and its Receptor BLT1 Act as Critical Drivers of Neutrophil Recruitment in Murine Bullous Pemphigoid-Like Epidermolysis Bullosa Acquisita**. *J Invest Dermatol* 2017, **137**:1104-1113.

153. Karsten CM, Kohl J: **The immunoglobulin, IgG Fc receptor and complement triangle in autoimmune diseases**. *Immunobiology* 2012, **217**:1067-1079.

154. Hess C, Winkler A, Lorenz AK, Holecska V, et al.: **T cell-independent B cell activation induces immunosuppressive sialylated IgG antibodies**. *J Clin Invest* 2013, **123**:3788-3796.

155. Hirose M, Vafia K, Kalies K, Groth S, et al.: **Enzymatic autoantibody glycan hydrolysis alleviates autoimmunity against type VII collagen**. *J Autoimmun* 2012, **39**:304-314.

156. Karsten CM, Pandey MK, Figge J, Kilchenstein R, et al.: **Anti-inflammatory activity of IgG1 mediated by Fc galactosylation and association of FcgammaRIIB and dectin-1**. *Nat Med* 2012, **18**:1401-1406.

157. Kovacs M, Nemeth T, Jakus Z, Sitaru C, et al.: **The Src family kinases Hck, Fgr, and Lyn are critical for the generation of the in vivo inflammatory environment without a direct role in leukocyte recruitment**. *J Exp Med* 2014, **211**:1993-2011.

158. Chiriac MT, Roesler J, Sindrilaru A, Scharffetter-Kochanek K, et al.: **NADPH oxidase is required for neutrophil-dependent autoantibody-induced tissue damage**. *J Pathol* 2007, **212**:56-65.

159. Shimanovich I, Mihai S, Oostingh GJ, Ilenchuk TT, et al.: **Granulocyte-derived elastase and gelatinase B are required for dermal-epidermal separation induced by autoantibodies from patients with epidermolysis bullosa acquisita and bullous pemphigoid**. *J Pathol* 2004, **204**:519-527.

160. Hirose M, Kasprick A, Beltsiou F, Dieckhoff Schulze K, et al.: **Reduced skin blistering in experimental epidermolysis bullosa acquisita after anti-TNF treatment**. *Mol Med* 2017, **22**:918-926.

161. Bieber K, Witte M, Sun S, Hundt JE, et al.: **T cells mediate autoantibody-induced cutaneous inflammation and blistering in epidermolysis bullosa acquisita**. *Sci Rep* 2016, **6**:38357.

162. Bieber K, Sun S, Witte M, Kasprick A, et al.: **Regulatory T Cells Suppress Inflammation and Blistering in Pemphigoid Diseases**. *Front Immunol* 2017, **8**:1628.

163. Haeberle S, Wei X, Bieber K, Goletz S, et al.: **Regulatory T-cell deficiency leads to pathogenic bullous pemphigoid antigen 230 autoantibody and autoimmune bullous disease**. *J Allergy Clin Immunol* 2018, **142**:1831-1842.e1837.

164. Wannick M, Yu X, Iwakura Y, Ludwig R, et al.: **The role of IL-17A in the pathogenesis of Epidermolysis bullosa acquisita**. *Inflammatory Skin Disease Summit - The Translational Revolution* 2014, **23**:9-9.

165. Yamagami J: **The International Bullous Diseases Group consensus on diagnostic criteria for epidermolysis bullosa acquisita: a useful tool for dermatologists**. *Br J Dermatol* 2018, **179**:7.

166. Ishii N, Hashimoto T, Zillikens D, Ludwig RJ: **High-dose intravenous immunoglobulin (IVIG) therapy in autoimmune skin blistering diseases**. *Clin Rev Allergy Immunol* 2010, **38**:186-195.

167. Hughes AP, Callen JP: **Epidermolysis bullosa acquisita responsive to dapsone therapy**. *J Cutan Med Surg* 2001, **5**:397-399.

168. Piette EW, Werth VP: **Dapsone in the management of autoimmune bullous diseases**. *Dermatologic clinics* 2011, **29**:561-564.

169. Cavailhes A, Balme B, Gilbert D, Skowron F: **[Successful use of combined corticosteroids and rituximab in the treatment of recalcitrant epidermolysis bullosa acquisita]**. *Ann Dermatol Venereol* 2009, **136**:795-799.

170. Schmidt E, Hunzelmann N, Zillikens D, Brocker EB, et al.: **Rituximab in refractory autoimmune bullous diseases**. *Clin Exp Dermatol* 2006, **31**:503-508.

171. Witte M, Koga H, Hashimoto T, Ludwig RJ, et al.: **Discovering potential drug-targets for personalized treatment of autoimmune disorders - what we learn from epidermolysis bullosa acquisita**. *Expert Opin Ther Targets* 2016, **20**:985-998.

172. Kasperkiewicz M, Muller R, Manz R, Magens M, et al.: **Heat-shock protein 90 inhibition in autoimmunity to type VII collagen: evidence that nonmalignant plasma cells are not therapeutic targets**. *Blood* 2011, **117**:6135-6142.

173. Samavedam UK, Iwata H, Muller S, Schulze FS, et al.: **GM-CSF modulates autoantibody production and skin blistering in experimental epidermolysis bullosa acquisita**. *J Immunol* 2014, **192**:559-571.

174. Bieber K, Koga H, Nishie W: **In vitro and in vivo models to investigate the pathomechanisms and novel treatments for pemphigoid diseases**. *Exp Dermatol* 2017, **26**:1163-1170.

175. Woodley DT, Chang C, Saadat P, Ram R, et al.: **Evidence that anti-type VII collagen antibodies are pathogenic and responsible for the clinical, histological, and immunological features of epidermolysis bullosa acquisita**. *J Invest Dermatol* 2005, **124**:958-964.

176. Woodley DT, Ram R, Doostan A, Bandyopadhyay P, et al.: **Induction of epidermolysis bullosa acquisita in mice by passive transfer of autoantibodies from patients**. *J Invest Dermatol* 2006, **126**:1323-1330.

177. Iwata H, Witte M, Samavedam UK, Gupta Y, et al.: **Radiosensitive Hematopoietic Cells Determine the Extent of Skin Inflammation in Experimental Epidermolysis Bullosa Acquisita**. *J Immunol* 2015, **195**:1945-1954.

178. Niebuhr M, Kasperkiewicz M, Maass S, Hauenschild E, et al.: **Evidence for a contributory role of a xenogeneic immune response in experimental epidermolysis bullosa acquisita**. *Exp Dermatol* 2017, **26**:1207-1213.

179. Gammon WR, Abernethy ML, Padilla KM, Prisayanh PS, et al.: **Noncollagenous (NC1) domain of collagen VII resembles multidomain adhesion proteins involved in tissue-specific organization of extracellular matrix**. *J Invest Dermatol* 1992, **99**:691-696.

180. Vorobyev A, Ujiie H, Recke A, Buijsrogge JJA, et al.: **Autoantibodies to Multiple Epitopes on the Non-Collagenous-1 Domain of Type VII Collagen Induce Blisters**. *J Invest Dermatol* 2015, **135**:1565-1573.

181. www.jax.org/de: **JAX mice search**. accessed May 2019. The Jackson Laboratory

182. Bouabe H: **Cytokine reporter mice: the special case of IL-10**. *Scand J Immunol* 2012, **75**:553-567.

183. Madan R, Demircik F, Surianarayanan S, Allen JL, et al.: **Nonredundant roles for B cell-derived IL-10 in immune counter-regulation**. *J Immunol* 2009, **183**:2312-2320.

184. Leineweber S, Schonig S, Seeger K: **Insight into interactions of the von-Willebrand-factor-A-like domain 2 with the FNIII-like domain 9 of collagen VII by NMR and SPR**. *FEBS Lett* 2011, **585**:1748-1752.

185. Bennett B, Check IJ, Olsen MR, Hunter RL: **A comparison of commercially available adjuvants for use in research**. *J Immunol Methods* 1992, **153**:31-40.

186. www.titermax.com: **TiterMax - Quality Immunological Adjuvants**. accessed May 2019. TiterMax USA, Inc.

187. O'Farrell AM, Liu Y, Moore KW, Mui AL: **IL-10 inhibits macrophage activation and proliferation by distinct signaling mechanisms: evidence for Stat3-dependent and -independent pathways**. *Embo j* 1998, **17**:1006-1018.

188. Adan A, Alizada G, Kiraz Y, Baran Y, et al.: **Flow cytometry: basic principles and applications**. *Crit Rev Biotechnol* 2017, **37**:163-176.

189. Yin Y, Mitson-Salazar A, Prussin C: **Detection of Intracellular Cytokines by Flow Cytometry**. *Curr Protoc Immunol* 2015, **110**:6.24.21-18.

190. Matsushita T, Tedder TF: **Identifying regulatory B cells (B10 cells) that produce IL-10 in mice**. *Methods Mol Biol* 2011, **677**:99-111.

191. O'Neil-Andersen NJ, Lawrence DA: **Differential modulation of surface and intracellular protein expression by T cells after stimulation in the presence of monensin or brefeldin A**. *Clin Diagn Lab Immunol* 2002, **9**:243-250.

192. Frentsch M, Arbach O, Kirchhoff D, Moewes B, et al.: **Direct access to CD4+ T cells specific for defined antigens according to CD154 expression**. *Nat Med* 2005, **11**:1118-1124.

193. Meier S, Stark R, Frentsch M, Thiel A: **The influence of different stimulation conditions on the assessment of antigen-induced CD154 expression on CD4+ T cells**. *Cytometry A* 2008, **73**:1035-1042.

194. Kirchhoff D, Frentsch M, Leclerk P, Bumann D, et al.: **Identification and isolation of murine antigen-reactive T cells according to CD154 expression**. *Eur J Immunol* 2007, **37**:2370-2377.

195. Yellin MJ, Sippel K, Inghirami G, Covey LR, et al.: **CD40 molecules induce down-modulation and endocytosis of T cell surface T cell-B cell activating**

molecule/CD40-L. Potential role in regulating helper effector function. *J Immunol* 1994, **152**:598-608.

196. Rodriguez-Perea AL, Arcia ED, Rueda CM, Velilla PA: **Phenotypical characterization of regulatory T cells in humans and rodents**. *Clin Exp Immunol* 2016, **185**:281-291.

197. Freitas M, Lima JL, Fernandes E: **Optical probes for detection and quantification of neutrophils' oxidative burst. A review**. *Anal Chim Acta* 2009, **649**:8-23.

198. Recke A, Trog LM, Pas HH, Vorobyev A, et al.: **Recombinant human IgA1 and IgA2 autoantibodies to type VII collagen induce subepidermal blistering ex vivo**. *J Immunol* 2014, **193**:1600-1608.

199. Aratani Y: **Myeloperoxidase: Its role for host defense, inflammation, and neutrophil function**. *Arch Biochem Biophys* 2018, **640**:47-52.

200. Bradley PP, Christensen RD, Rothstein G: **Cellular and extracellular myeloperoxidase in pyogenic inflammation**. *Blood* 1982, **60**:618-622.

201. Chen HC: **Boyden chamber assay**. *Methods Mol Biol* 2005, **294**:15-22.

202. Dean RL: **Kinetic studies with alkaline phosphatase in the presence and absence of inhibitors and divalent cations**. *Biochemistry and Molecular Biology Education* 2006, **30**:401-407.

203. Vieira P, Rajewsky K: **The half-lives of serum immunoglobulins in adult mice**. *Eur J Immunol* 1988, **18**:313-316.

204. Becher B, Pantelyushin S: **Hiding under the skin: Interleukin-17-producing gammadelta T cells go under the skin?** *Nat Med* 2012, **18**:1748-1750.

205. Peters C, Kabelitz D, Wesch D: **Regulatory functions of gammadelta T cells**. *Cell Mol Life Sci* 2018, **75**:2125-2135.

206. Nimmerjahn F, Ravetch JV: **Fcgamma receptors as regulators of immune responses**. *Nat Rev Immunol* 2008, **8**:34-47.

207. Menezes GB, Lee WY, Zhou H, Waterhouse CC, et al.: **Selective down-regulation of neutrophil Mac-1 in endotoxemic hepatic microcirculation via IL-10**. *J Immunol* 2009, **183**:7557-7568.

208. Andrade EB, Alves J, Madureira P, Oliveira L, et al.: **TLR2-induced IL-10 production impairs neutrophil recruitment to infected tissues during neonatal bacterial sepsis**. *J Immunol* 2013, **191**:4759-4768.

209. Souto FO, Alves-Filho JC, Turato WM, Auxiliadora-Martins M, et al.: **Essential role of CCR2 in neutrophil tissue infiltration and multiple organ dysfunction in sepsis**. *Am J Respir Crit Care Med* 2011, **183**:234-242.

210. Talbot J, Bianchini FJ, Nascimento DC, Oliveira RD, et al.: **CCR2 Expression in Neutrophils Plays a Critical Role in Their Migration Into the Joints in Rheumatoid Arthritis**. *Arthritis Rheumatol* 2015, **67**:1751-1759.

211. Wang Y, Wang F, Yang D, Tang X, et al.: **Berberine in combination with yohimbine attenuates sepsis-induced neutrophil tissue infiltration and multiorgan dysfunction partly via IL-10-mediated inhibition of CCR2 expression in neutrophils**. *Int Immunopharmacol* 2016, **35**:217-225.

212. Chaves MM, Costa DC, de Oliveira BF, Rocha MI, et al.: **Role PKA and p38 MAPK on ROS production in neutrophil age-related: Lack of IL-10 effect in older subjects**. *Mech Ageing Dev* 2009, **130**:588-591.

213. Winterbourn CC, Kettle AJ, Hampton MB: **Reactive Oxygen Species and Neutrophil Function**. *Annu Rev Biochem* 2016, **85**:765-792.

214. Tabarkiewicz J, Pogoda K, Karczmarczyk A, Pozarowski P, et al.: **The Role of IL-17 and Th17 Lymphocytes in Autoimmune Diseases**. *Archivum immunologiae et therapiae experimentalis* 2015, **63**:435-449.

215. O'Brien RL, Roark CL, Born WK: **IL-17-producing gammadelta T cells**. *European journal of immunology* 2009, **39**:662-666.

216. Patil RS, Bhat SA, Dar AA, Chiplunkar SV: **The Jekyll and Hyde story of IL17-Producing γδT Cells**. *Frontiers in immunology* 2015, **6**:37-37.

217. Anderson AC, Joller N, Kuchroo VK: **Lag-3, Tim-3, and TIGIT: Co-inhibitory Receptors with Specialized Functions in Immune Regulation**. *Immunity* 2016, **44**:989-1004.

218. Tiburzy B, Kulkarni U, Hauser AE, Abram M, et al.: **Plasma cells in immunopathology: concepts and therapeutic strategies**. *Semin Immunopathol* 2014, **36**:277-288.

219. Scott-Taylor TH, Axinia S-C, Amin S, Pettengell R: **Immunoglobulin G; structure and functional implications of different subclass modifications in initiation and resolution of allergy**. *Immunity, Inflammation and Disease* 2018, **6**:13-33.

220. Jogdand GM, Mohanty S, Devadas S: **Regulators of Tfh Cell Differentiation**. *Frontiers in immunology* 2016, **7**:520-520.

221. Zhao H, Liao X, Kang Y: **Tregs: Where We Are and What Comes Next?** *Frontiers in immunology* 2017, **8**:1578-1578.

222. Wang K, Wei G, Liu D: **CD19: a biomarker for B cell development, lymphoma diagnosis and therapy**. *Experimental hematology & oncology* 2012, **1**:36-36.

223. Tian G, Li JL, Wang DG, Zhou D: **Targeting IL-10 in auto-immune diseases**. *Cell Biochem Biophys* 2014, **70**:37-49.

224. Asseman C, Mauze S, Leach MW, Coffman RL, et al.: **An essential role for interleukin 10 in the function of regulatory T cells that inhibit intestinal inflammation**. *J Exp Med* 1999, **190**:995-1004.

225. Poggi A, Zancolli M, Catellani S, Borsellino G, et al.: **Migratory pathways of gammadelta T cells and response to CXCR3 and CXCR4 ligands: adhesion molecules involved and implications for multiple sclerosis pathogenesis**. *Ann N Y Acad Sci* 2007, **1107**:68-78.

226. Gu Y, Yang J, Ouyang X, Liu W, et al.: **Interleukin 10 suppresses Th17 cytokines secreted by macrophages and T cells**. *European journal of immunology* 2008, **38**:1807-1813.

227. Shibata K, Yamada H, Hara H, Kishihara K, et al.: **Resident Vdelta1+ gammadelta T cells control early infiltration of neutrophils after Escherichia coli infection via IL-17 production**. *J Immunol* 2007, **178**:4466-4472.

228. Pfeifle R, Rothe T, Ipseiz N, Scherer HU, et al.: **Regulation of autoantibody activity by the IL-23-TH17 axis determines the onset of autoimmune disease**. *Nat Immunol* 2017, **18**:104-113.

229. Capsoni F, Minonzio F, Ongari AM, Carbonelli V, et al.: **Interleukin-10 down-regulates oxidative metabolism and antibody-dependent cellular cytotoxicity of human neutrophils**. *Scand J Immunol* 1997, **45**:269-275.

230. Hammond ME, Lapointe GR, Feucht PH, Hilt S, et al.: **IL-8 induces neutrophil chemotaxis predominantly via type I IL-8 receptors**. *J Immunol* 1995, **155**:1428-1433.

231. Hirose M BL, Zimmer D, Götz J, Westermann J, Allegretti M, Moriconi A, Recke A, Zillikens D, Kalies K and Ludwig RJ: **The Allosteric CXCR1/2 Inhibitor DF2156A Improves Experimental Epidermolysis Bullosa Acquisita**. *J Genet Syndr Gene Ther* 2013, **S3:005**.

232. Bennett LD, Fox JM, Signoret N: **Mechanisms regulating chemokine receptor activity**. *Immunology* 2011, **134**:246-256.

233. Rosales CU-Q, E.: **Neutrophil Activation by Antibody Receptors**. *Neutrophils, Maitham Khajah, IntechOpen* 2018.

234. Kasperkiewicz M, Nimmerjahn F, Wende S, Hirose M, et al.: **Genetic identification and functional validation of FcgammaRIV as key molecule in autoantibody-induced tissue injury**. *J Pathol* 2012, **228**:8-19.

235. Summers C, Rankin SM, Condliffe AM, Singh N, et al.: **Neutrophil kinetics in health and disease**. *Trends Immunol* 2010, **31**:318-324.

236. Kim MH, Liu W, Borjesson DL, Curry FR, et al.: **Dynamics of neutrophil infiltration during cutaneous wound healing and infection using fluorescence imaging**. *J Invest Dermatol* 2008, **128**:1812-1820.

237. Nemunaitis J, Fong T, Shabe P, Martineau D, et al.: **Comparison of serum interleukin-10 (IL-10) levels between normal volunteers and patients with advanced melanoma**. *Cancer Invest* 2001, **19**:239-247.

238. Geherin SA, Gomez D, Glabman RA, Ruthel G, et al.: **IL-10+ Innate-like B Cells Are Part of the Skin Immune System and Require alpha4beta1 Integrin To Migrate between the Peritoneum and Inflamed Skin**. *J Immunol* 2016, **196**:2514-2525.

239. O'Garra A, Chang R, Go N, Hastings R, et al.: **Ly-1 B (B-1) cells are the main source of B cell-derived interleukin 10**. *Eur J Immunol* 1992, **22**:711-717.

240. Nimmerjahn F, Bruhns P, Horiuchi K, Ravetch JV: **FcgammaRIV: a novel FcR with distinct IgG subclass specificity**. *Immunity* 2005, **23**:41-51.

241. Lilienthal G-M, Rahmöller J, Petry J, Bartsch YC, et al.: **Potential of Murine IgG1 and Human IgG4 to Inhibit the Classical Complement and Fcγ Receptor Activation Pathways**. *Frontiers in immunology* 2018, **9**:958-958.

242. Zhang J, Wan M, Ren J, Gao J, et al.: **Positive selection of B10 cells is determined by BCR specificity and signaling strength**. *Cell Immunol* 2016, **304-305**:27-34.

243. Rosser EC, Oleinika K, Tonon S, Doyle R, et al.: **Regulatory B cells are induced by gut microbiota-driven interleukin-1beta and interleukin-6 production**. *Nat Med* 2014, **20**:1334-1339.

244. Cohen P: **The TLR and IL-1 signalling network at a glance**. *Journal of cell science* 2014, **127**:2383-2390.

245. Liu T, Zhang L, Joo D, Sun S-C: **NF-κB signaling in inflammation**. *Signal Transduction And Targeted Therapy* 2017, **2**:17023.

246. Yanaba K, Bouaziz JD, Haas KM, Poe JC, et al.: **A regulatory B cell subset with a unique CD1dhiCD5+ phenotype controls T cell-dependent inflammatory responses**. *Immunity* 2008, **28**:639-650.

247. Seeling M, Bruckner C, Nimmerjahn F: **Differential antibody glycosylation in autoimmunity: sweet biomarker or modulator of disease activity?** *Nat Rev Rheumatol* 2017, **13**:621-630.

248. Murray JS: **How the MHC selects Th1/Th2 immunity**. *Immunol Today* 1998, **19**:157-163.

249. Guthmiller JJ, Graham AC, Zander RA, Pope RL, et al.: **Cutting Edge: IL-10 Is Essential for the Generation of Germinal Center B Cell Responses and Anti-Plasmodium Humoral Immunity**. *J Immunol* 2017, **198**:617-622.

250. Murray JS, Pfeiffer C, Madri J, Bottomly K: **Major histocompatibility complex (MHC) control of CD4 T cell subset activation. II. A single peptide induces either humoral or cell-mediated responses in mice of distinct MHC genotype**. *Eur J Immunol* 1992, **22**:559-565.

251. Toellner KM, Luther SA, Sze DM, Choy RK, et al.: **T helper 1 (Th1) and Th2 characteristics start to develop during T cell priming and are associated with an immediate ability to induce immunoglobulin class switching**. *The Journal of experimental medicine* 1998, **187**:1193-1204.

252. Snapper CM, Paul WE: **Interferon-gamma and B cell stimulatory factor-1 reciprocally regulate Ig isotype production**. *Science* 1987, **236**:944-947.

253. Da Silva FP, Hoecker GF, Day NK, Vienne K, et al.: **Murine Complement Component 3: Genetic Variation and Linkage to H-2**. *Proceedings of the National Academy of Sciences of the United States of America* 1978, **75**:963-965.

254. Natsuume-Sakai S, Amano S, Hayakawa J-I, Takahashi M: **Preparation of an Alloantiserum to Murine C3 and Demonstration of Multiple Alleles**. *The Journal of Immunology* 1978, **121**:2025-2029.

255. Delanghe JR, Speeckaert R, Speeckaert MM: **Complement C3 and its polymorphism: biological and clinical consequences**. *Pathology* 2014, **46**:1-10.

256. Ludwig RJ, Muller S, Marques A, Recke A, et al.: **Identification of quantitative trait loci in experimental epidermolysis bullosa acquisita**. *J Invest Dermatol* 2012, **132**:1409-1415.

257. Pot C, Apetoh L, Kuchroo VK: **Type 1 regulatory T cells (Tr1) in autoimmunity**. *Semin Immunol* 2011, **23**:202-208.

258. Wing JB, Ise W, Kurosaki T, Sakaguchi S: **Regulatory T cells control antigen-specific expansion of Tfh cell number and humoral immune responses via the coreceptor CTLA-4**. *Immunity* 2014, **41**:1013-1025.

259. Fujio K, Okamura T, Sumitomo S, Yamamoto K: **Regulatory T cell-mediated control of autoantibody-induced inflammation**. *Frontiers in immunology* 2012, **3**:28-28.

260. Muramatsu K, Ujiie H, Kobayashi I, Nishie W, et al.: **Regulatory T-cell dysfunction induces autoantibodies to bullous pemphigoid antigens in mice and human subjects**. *J Allergy Clin Immunol* 2018, **142**:1818-1830.e1816.

261. Bieber K, Sun S, Ishii N, Kasperkiewicz M, et al.: **Animal models for autoimmune bullous dermatoses**. *Exp Dermatol* 2010, **19**:2-11.

262. Chandrashekara S: **The treatment strategies of autoimmune disease may need a different approach from conventional protocol: a review**. *Indian journal of pharmacology* 2012, **44**:665-671.

10. Supplementary

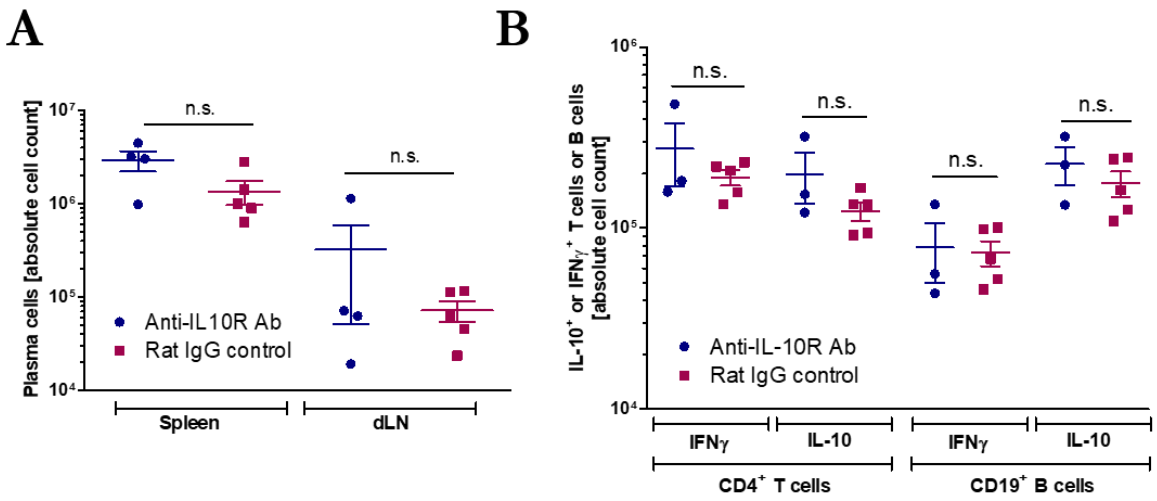

Supplementary figure 1: IL-10 receptor blockade does not affect the total amount of plasma cells as well as CD4⁺ T-cell and CD19⁺ B-cell cytokines. EBA was induced by immunization with vWFA2 and mice were treated with an IL-10 receptor-blocking antibody (anti-IL-10R Ab) or a control antibody (rat IgG control) as described in the scheme in figure 5. Seven weeks after immunization, mice were sacrificed and plasma cells and CD4⁺ T-cell and CD19⁺ B-cell cytokines analyzed by flow cytometry. **(A)** Absolute cell number of plasma cells in spleen and draining lymph nodes (n=4-5, unpaired t-test). The gating was performed as depicted in figure 7. (**B)** Absolute cell number of IFNγ⁺ or IL-10⁺ CD4⁺ T cells or CD19⁺ B cells in draining lymph nodes (n=3-5, unpaired t-test). The gating was performed as depicted in figure 8. Data are expressed as mean ± SEM. *n.s., not significant.*

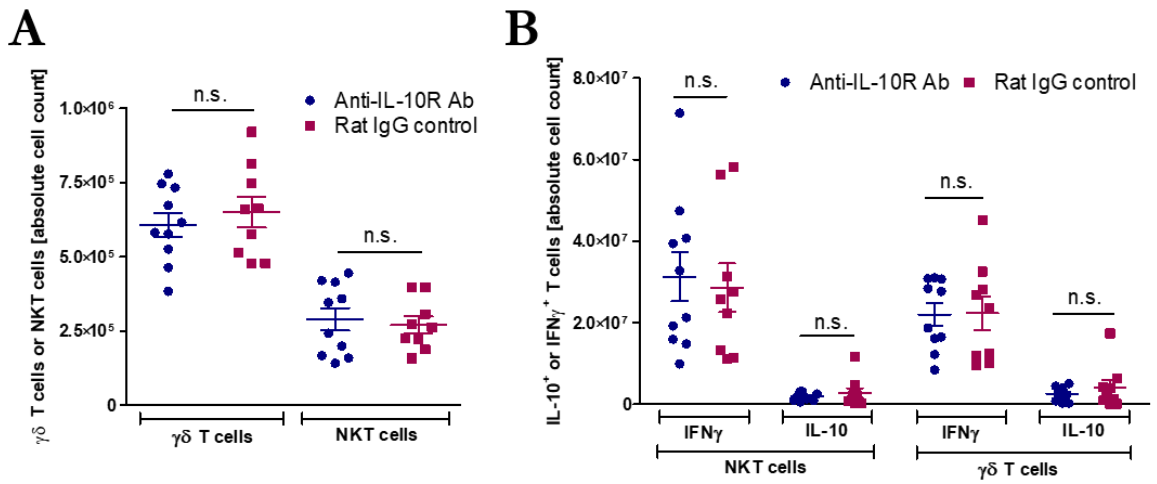

Supplementary figure 2: The total cell number of γδ T cells and NKT cells as well as the IFNγ and IL-10 production by these cells is not affected by IL-10 receptor blockade. EBA was induced by immunization with vWFA2 and mice were treated with an IL-10 receptor-blocking antibody (anti-IL-10R Ab) or a control antibody (rat IgG control) as described in the scheme in figure 5. Seven weeks after immunization, mice were sacrificed and γδ T cells and NKT cells and their cytokine expression was analyzed by flow cytometry. **(A)** Absolute cell number of γδ T cells and NKT cells in spleen (n=9-10, unpaired t-test). The gating was performed as depicted in figure 9. **(B)** Absolute cell number of IFNγ⁺ or IL-10⁺ γδ T cells and NKT cells in spleen (n=9-10, Mann-Whitney test). The gating was performed as depicted in figure 10. Data are expressed as mean ± SEM. *n.s., not significant.*

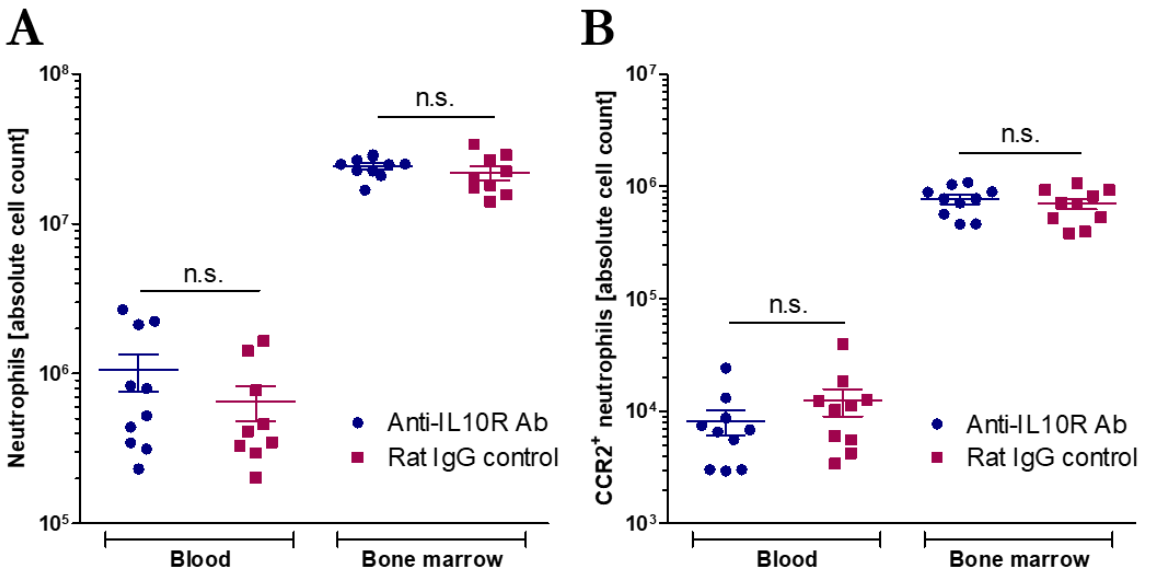

Supplementary figure 3: The absolute cell number of neutrophils and CCR2⁺ neutrophils in blood and bone marrow is not modulated by IL-10 receptor blockade. EBA was induced by immunization with vWFA2 and mice were treated with an IL-10 receptor-blocking antibody (anti-IL-10R Ab) or a control antibody (rat IgG control) as described in the scheme in figure 5. Seven weeks after immunization, mice were sacrificed and neutrophils and their CCR2 expression were analyzed by flow cytometry. **(A)** Absolute cell number of neutrophils in blood and bone marrow (n=9-10, unpaired t-test). The gating was performed as depicted in figure 11. **(B)** Absolute cell number of CCR2⁺ neutrophils in blood and bone marrow (n=9-10, unpaired t-test). The gating was performed as depicted in figure 12. Data are expressed as mean ± SEM. *n.s., not significant.*

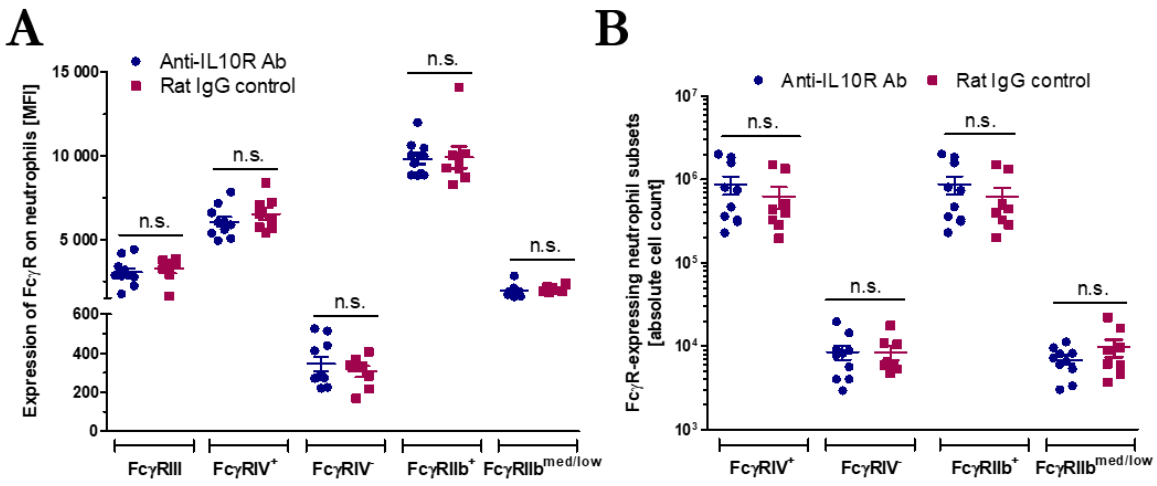

Supplementary figure 4: Inhibitory and activating Fcγ receptor expression on different peripheral neutrophil subsets is not affected by IL-10 receptor blockade. EBA was induced by immunization with vWFA2 and mice were treated with an IL-10 receptor-blocking antibody (anti-IL-10R Ab) or a control antibody (rat IgG control) as described in the scheme in figure 5. Seven weeks after immunization, mice were sacrificed and Fcγ receptor III (FcγRIII, CD16), FcγRIV (CD16.2) and FcγRIIb (CD32) expression on peripheral neutrophils was analyzed by flow cytometry. The gating was performed as depicted in figure 11. **(A)** Mean fluorescence intensity (MFI) signals of activating or inhibiting Fcγ receptors on peripheral neutrophils (n=8-10, unpaired t-test). **(B)** Absolute cell number of neutrophils expressing a specific pattern of Fcγ receptors as depicted in figure 11 (n=8-10, unpaired t-test). Data are expressed as mean ± SEM. *n.s., not significant.*

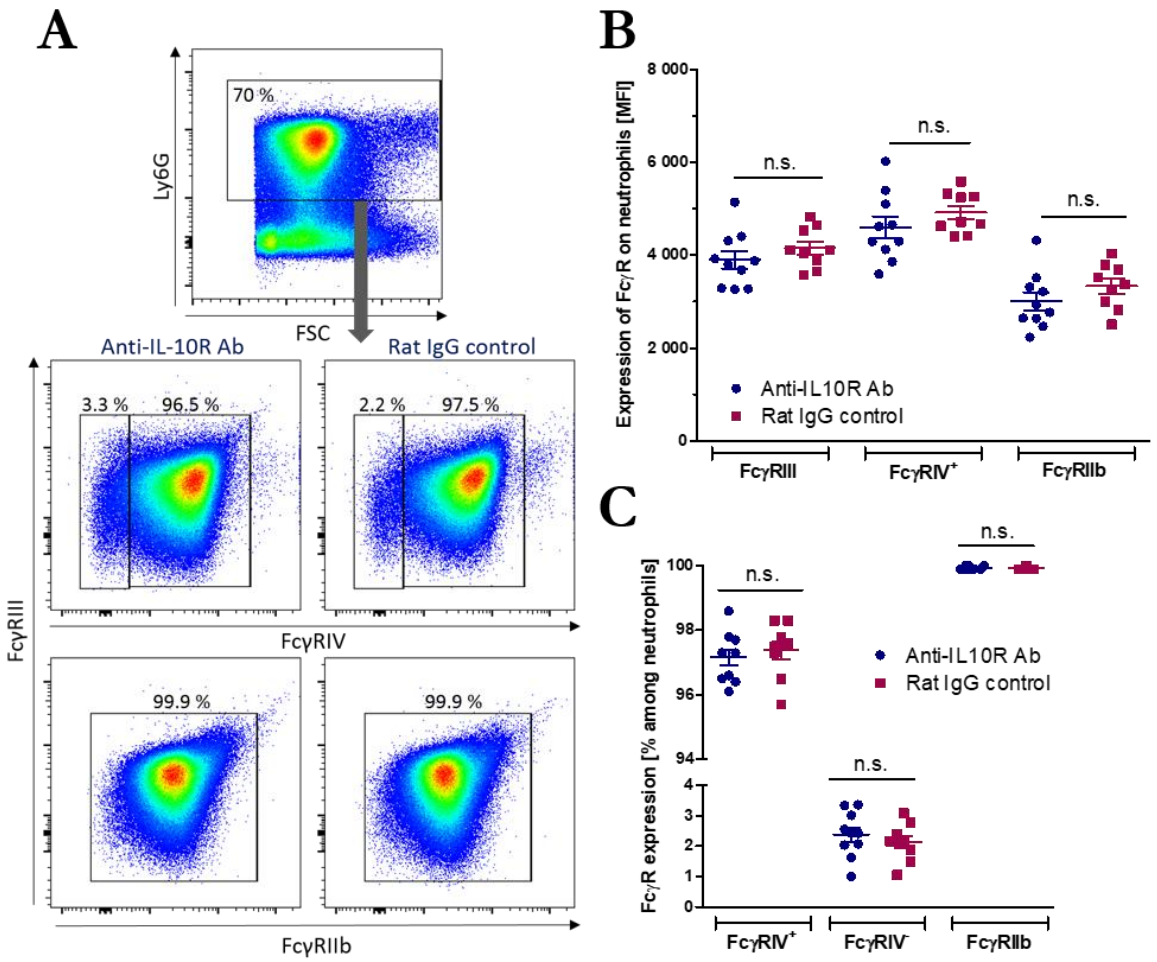

Supplementary figure 5: IL-10 receptor blockade has no influence on the Fcγ receptor expression of different neutrophil subsets in bone marrow. EBA was induced by immunization with vWFA2 and mice were treated with an IL-10 receptor-blocking antibody (anti-IL-10R Ab) or a control antibody (rat IgG control) as described in the scheme in figure 5. Seven weeks after immunization, mice were sacrificed and Fcγ receptor III (FcγRIII, CD16), FcγRIV (CD16.2) and FcγRIIb (CD32) expression on bone marrow neutrophils was analyzed by flow cytometry. **(A)** Representative flow cytometry data from bone marrow. Neutrophils were defined as $Ly6G^+$ leukocytes and further gated for their expression of Fcγ receptors. **(B)** Mean fluorescence intensity (MFI) signals of activating or inhibiting Fcγ receptors on bone marrow neutrophils (n=9-10, unpaired t-test). **(C)** Frequency of peripheral neutrophils expressing a specific pattern of Fcγ receptors. Neutrophils divide into two subsets characterized by their FcγRIV expression ($FcγRIV^+$ and $FcγRIV^-$) and one subset of FcγRIIb and FcγRIII (n=9-10, unpaired t-test). Data are expressed as mean ± SEM. *n.s., not significant.*

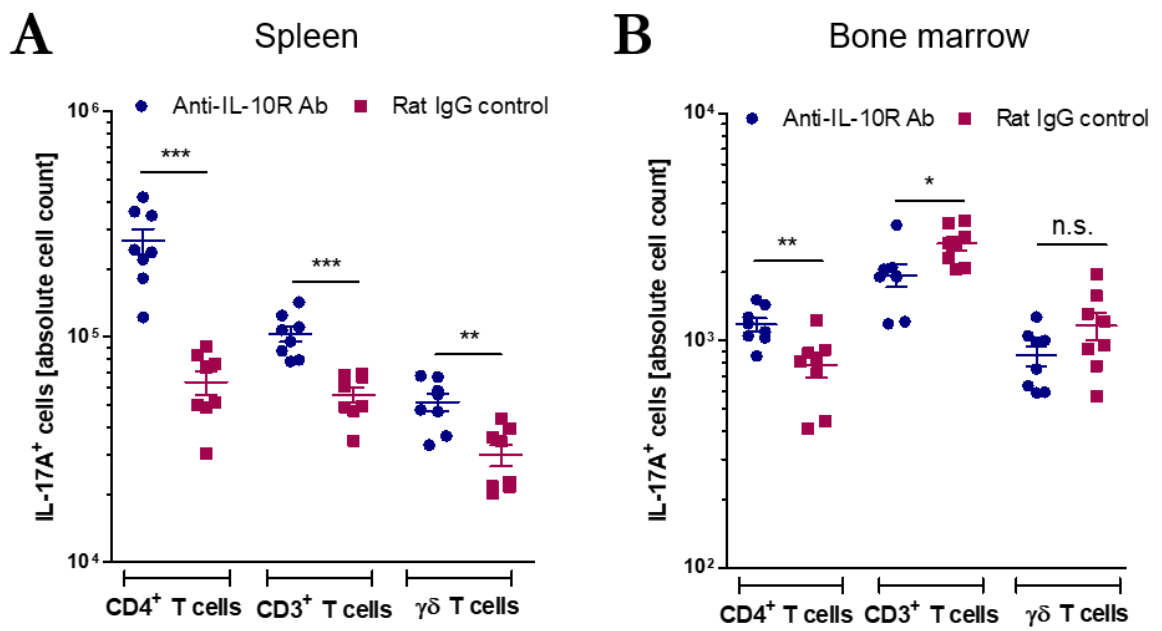

Supplementary figure 6: IL-10 receptor blockade increases the absolute cell number of IL-17⁺ T-cell subsets in the autoantibody-transfer-induced EBA model. Mice were treated with an IL-10 receptor-blocking antibody (anti-IL-10R Ab) or a control antibody (rat IgG control) one day before EBA was induced by autoantibodies as described in the scheme in figure 16. On day twelve, splenic and bone marrow T-cell subsets were analyzed for their IL-17A expression by flow cytometry. The gating was performed as depicted in figure 18. **(A)** Frequency of IL-17⁺ cells among CD4⁺ T cells, CD3⁺ T cells (without CD4⁺ T cells) and γδ T cells in spleen and **(B)** bone marrow (n=8, unpaired t-test). Data are expressed as mean ± SEM. *p ≤ 0.05; **p ≤ 0.01; ***p≤0.001. *n.s., not significant.*

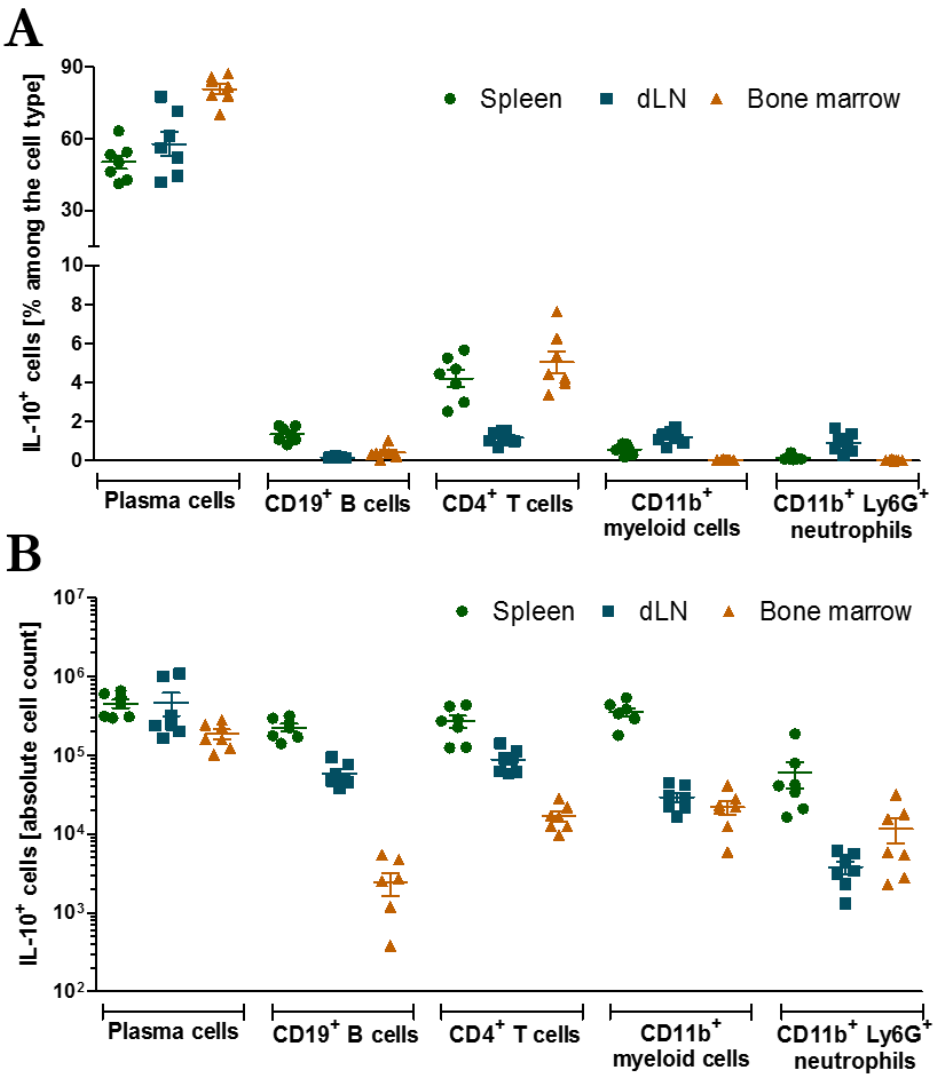

Supplementary figure 7: Plasma cells are major producers of IL-10 in the acute phase of the disease. EBA was induced in susceptible B6.s IL-10 reporter mice by immunization with vWFA2 as described in the scheme in figure 19 and different lymphoid organs were analyzed by flow cytometry after ten days. The gating was performed as depicted in figure 20. **(A)** Frequency of IL-10-eGFP$^+$ cells and **(B)** absolute cell number of IL-10-eGFP$^+$ cells in spleen, draining lymph nodes (dLN) and bone marrow (n=7 pooled from two independent experiments). For one data point of the absolute cell number of IL-10$^+$ CD19$^+$ B cells in bone marrow the value was zero and is therefore not indicated in the logarithmic scale. Data are expressed as mean ± SEM and IL-10-eGFP frequencies are corrected by the value obtained from the C57Bl/6J control mouse indicating the unspecific background staining.

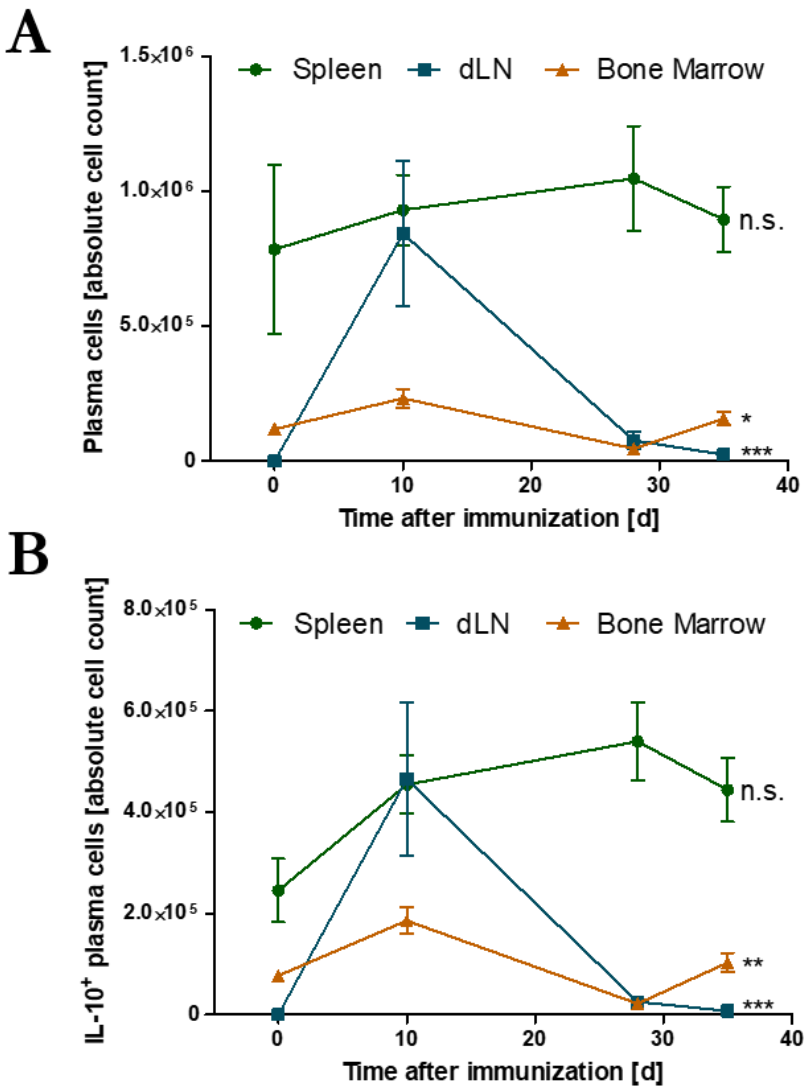

Supplementary figure 8: Immunization increases the absolute number of plasma cells and IL-10$^+$ plasma cells in draining lymph nodes. EBA was induced in susceptible B6.s IL-10 reporter mice by immunization with vWFA2 as described in the scheme in figure 19 and different lymphoid organs were analyzed by flow cytometry. The gating was performed as depicted in figure 22. **(A)** Kinetics of plasma cell numbers and **(B)** IL-10-eGFP$^+$ plasma cell numbers in spleen, draining lymph nodes (dLN) and bone marrow (n=3-11 pooled from two (zero and ten days) or three (five weeks) independent experiments, one-way ANOVA). Data are expressed as mean ± SEM and IL-10-eGFP values are corrected by the value obtained from the C57Bl/6J control mouse indicating the unspecific background staining. *$p \leq 0.05$, **$p \leq 0.01$ or ***$p \leq 0.001$ indicates a significant change of the frequency over time within one organ. A significant increase of plasma cell and IL-10-eGFP$^+$ plasma cell numbers after ten days compared to steady state was only observed in dLN. *n.s., not significant.*

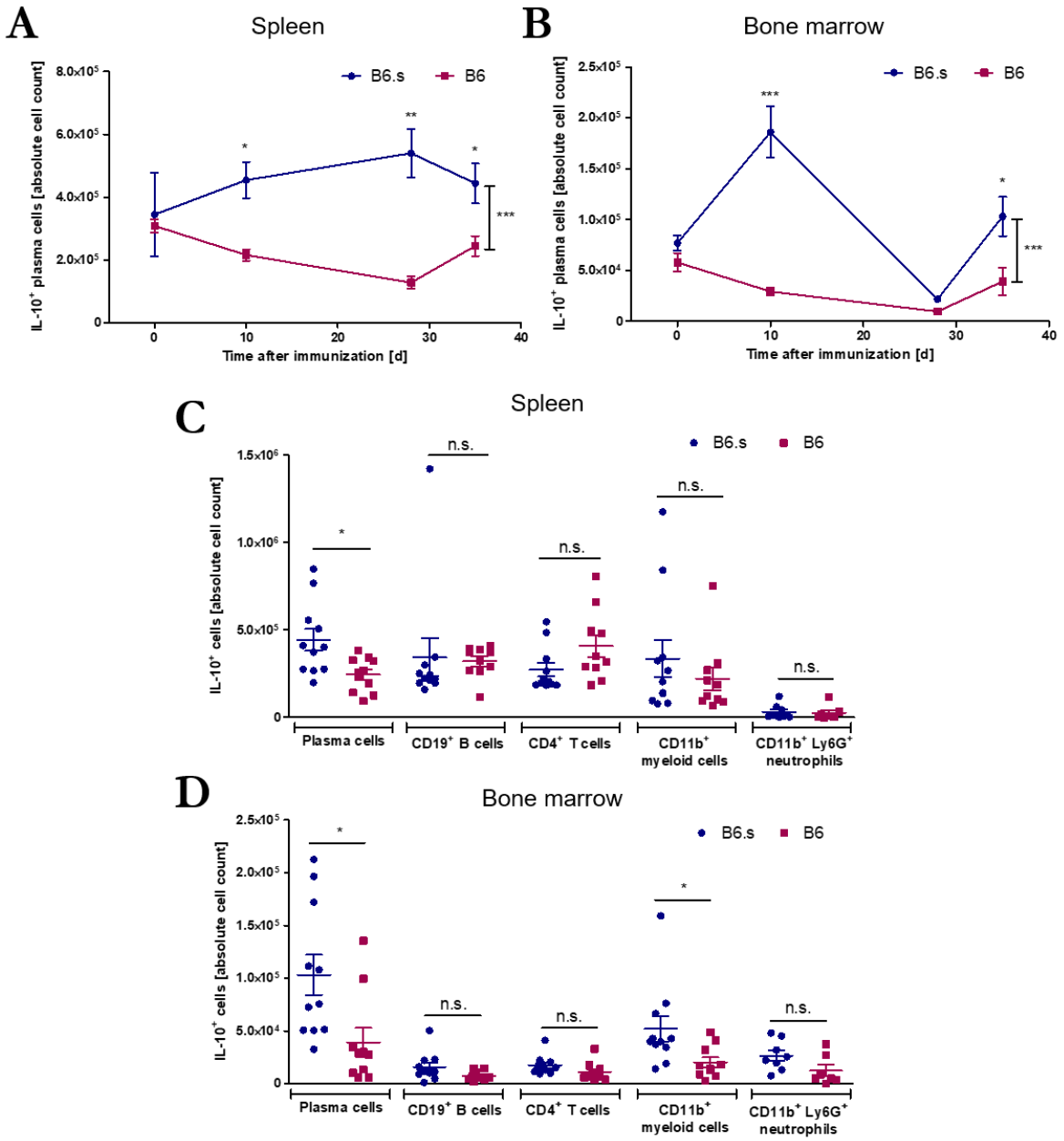

Supplementary figure 9: The absolute number of IL-10⁺ plasma cells in spleen and bone marrow is increased in susceptible mice. EBA was induced in susceptible B6.s IL-10 reporter and non-susceptible B6 IL-10 reporter mice by immunization with vWFA2 as described in the scheme in figure 19 and spleen and bone marrow were analyzed by flow cytometry. The gating was performed as depicted in figure 20 and figure 23. **(A)** Kinetics of the frequency of IL-10-eGFP⁺ plasma cells in spleen and **(B)** bone marrow (n=3-11 pooled from two (zero and ten days) or three (five weeks) independent experiments, two-way ANOVA with Bonferroni post-test). **(C)** Absolute cell number of IL-10-eGFP⁺ cells in spleen and **(D)** bone marrow five weeks after immunization (n=7-11 pooled from two or three independent experiments, unpaired t-test). Data are expressed as mean ± SEM and IL-10-eGFP values are corrected by the value obtained from the C57Bl/6J control mouse indicating the unspecific background staining. *p ≤ 0.05; **p ≤ 0.01; ***p ≤ 0.001. *n.s., not significant.*

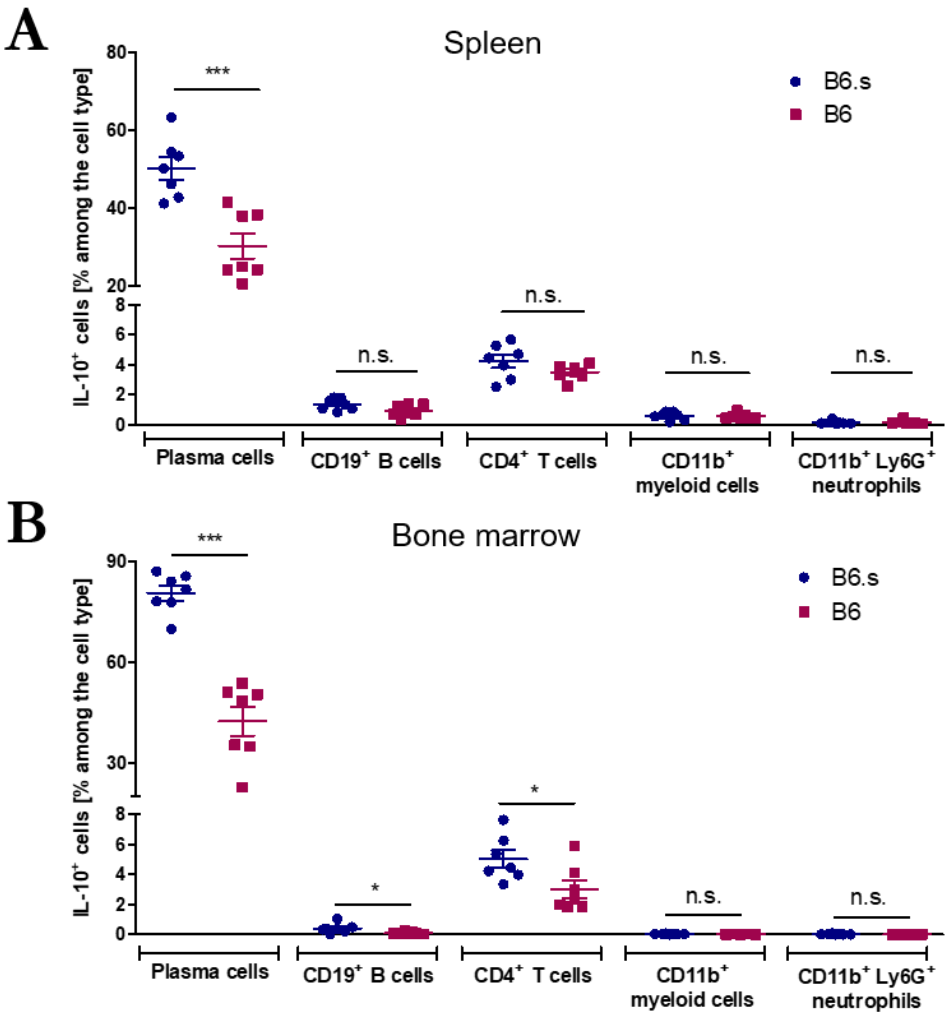

Supplementary figure 10: IL-10-induction ten days after immunization in spleen and bone marrow is plasma cell-specific. EBA was induced in susceptible B6.s IL-10 reporter and non-susceptible B6 IL-10 reporter mice by immunization with vWFA2 as described in the scheme in figure 19 and spleen and bone marrow were analyzed by flow cytometry ten days after immunization. The gating was performed as depicted in figure 20. (**A)** Frequency of IL-10-eGFP$^+$ cells among the cell type indicated in spleen and **(B)** bone marrow (n=7 pooled from two independent experiments, unpaired t-test). Data are expressed as mean ± SEM and IL-10-eGFP frequencies are corrected by the value obtained from the C57Bl/6J control mouse indicating the unspecific background staining. *$p \leq 0.05$; ***$p \leq 0.001$. *n.s., not significant.*

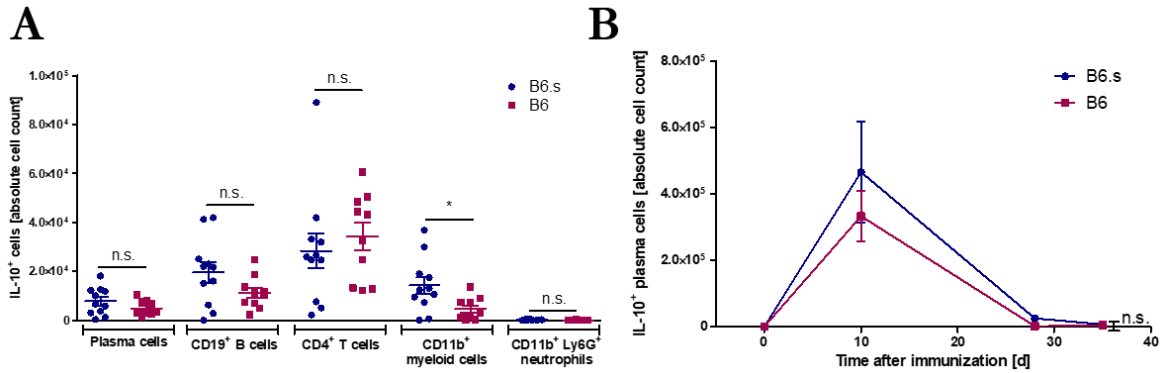

Supplementary figure 11: The absolute number of IL-10 plasma cells in draining lymph nodes is comparable between susceptible and non-susceptible mice. EBA was induced in susceptible B6.s IL-10 reporter and non-susceptible B6 IL-10 reporter mice by immunization with vWFA2 as described in the scheme in figure 19 and draining lymph nodes were analyzed by flow cytometry. The gating was performed as depicted in figure 25. **(A)** Absolute cell number of IL-10-eGFP$^+$ cells in draining lymph nodes five weeks after immunization (n=7-11 pooled from two or three independent experiments, unpaired t-test). **(B)** Kinetics of the absolute cell number of IL-10-eGFP$^+$ plasma cells (n=3-11 pooled from two (zero and ten days) or three (five weeks) independent experiments, two-way ANOVA). Data are expressed as mean ± SEM and IL-10-eGFP frequencies are corrected by the value obtained from the C57Bl/6J control mouse indicating the unspecific background staining. *p ≤ 0.05. *n.s., not significant.*

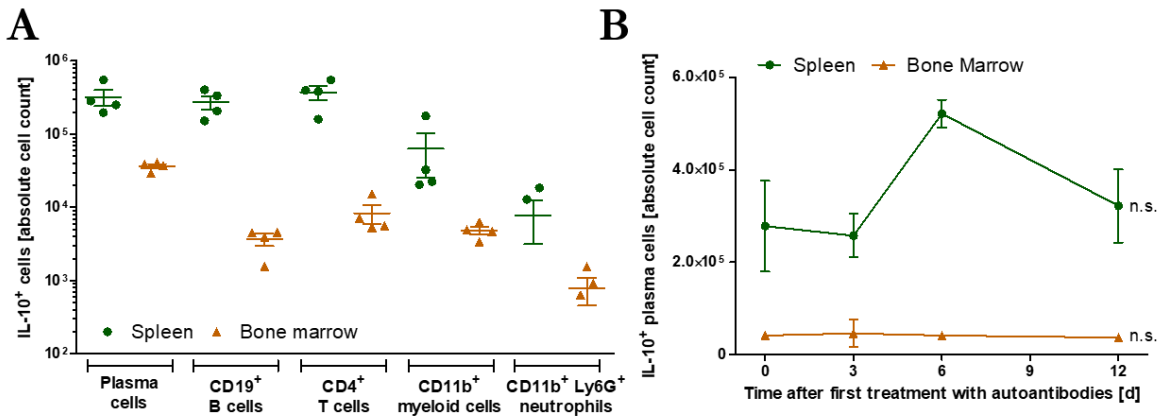

Supplementary figure 12: Plasma cells are major producers of IL-10 but the numbers of IL-10$^+$ plasma cells do not increase over time in the autoantibody-transfer-induced EBA model. EBA was induced in B6 IL-10 reporter mice as shown in the scheme in figure 26 and IL-10$^+$ cells were gated as depicted in figure 20 and figure 27. **(A)** Absolute cell number of IL-10-eGFP$^+$ cells in spleen and bone marrow twelve days after first treatment with autoantibodies (n=4). Three data points for IL-10$^+$ cells among neutrophils are zero and therefore not indicated in the logarithmic scale. **(C)** Kinetics of IL-10-eGFP$^+$ plasma cells in spleen and bone marrow (n=3-4, one-way ANOVA with Bonferroni post-test). Data are expressed as mean ± SEM and IL-10-eGFP values are corrected by the value obtained from the C57Bl/6J control mouse indicating the unspecific background staining. *n.s., not significant.*

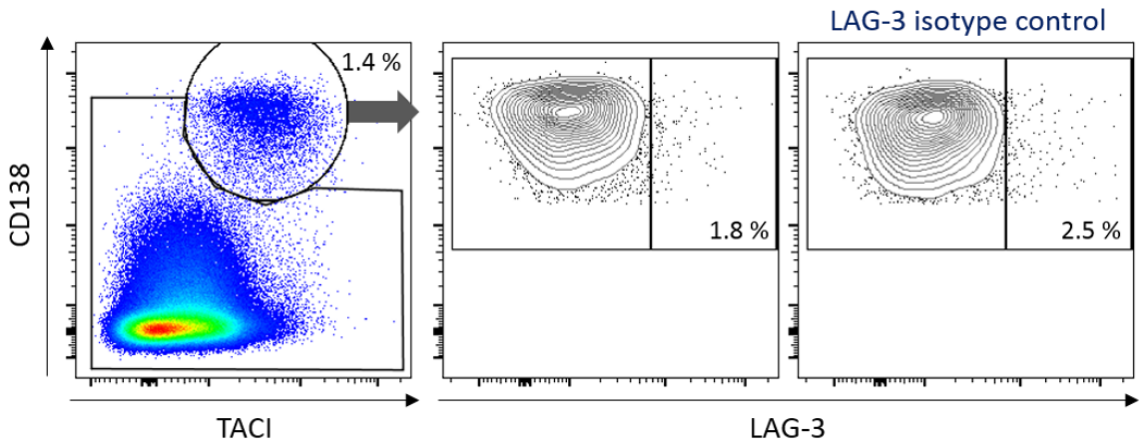

Supplementary figure 13: LAG-3$^+$ plasma cells are absent in draining lymph nodes ten days after immunization. Susceptible B6.s mice were immunized with vWFA2 and analyzed after ten days as described in the scheme in figure 19. The figure shows representative flow cytometry data from draining lymph nodes. Plasma cells were defined as CD138^{hi} TACI$^+$ cells (left plot) and further gated for their LAG-3 expression as compared to the isotype control (right plot). The plot is representative for four mice.

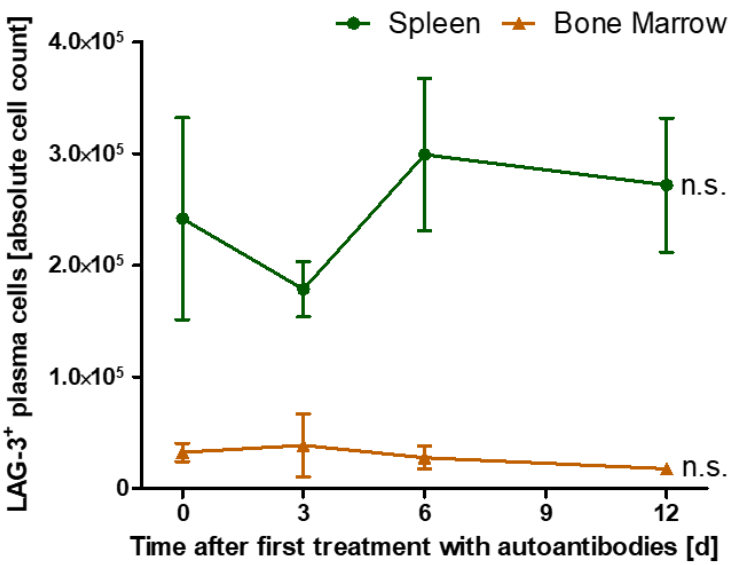

Supplementary figure 14: The absolute number of LAG-3$^+$ plasma cells in spleen and bone marrow does not increase after EBA induction by autoantibodies. EBA was induced in B6 IL-10 reporter mice as described in the scheme in figure 26 and LAG-3$^+$ plasma cells were gated as depicted in figure 29. The figure shows the kinetics of LAG-3$^+$ plasma cells in spleen and bone marrow over the duration of the disease (n=3-4, one-way ANOVA). Data are expressed as mean ± SEM. *n.s., not significant.*

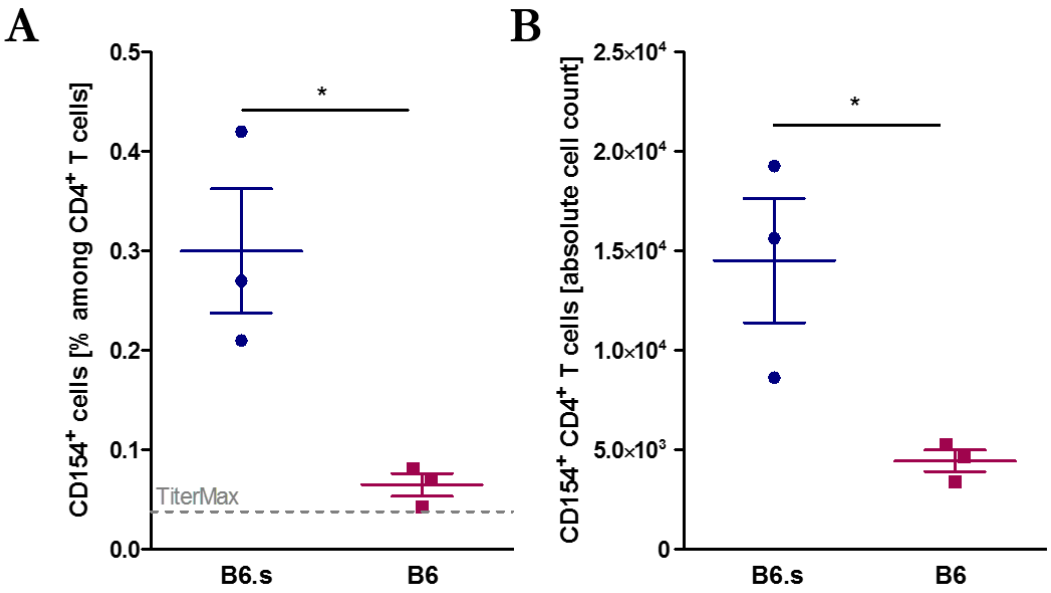

Supplementary figure 15: Susceptible mice have more autoreactive CD4⁺ T cells in spleen compared to non-susceptible mice. EBA was induced in susceptible B6.s and non-susceptible B6 mice by immunization with vWFA2 and autoantigen-specific CD4⁺ T cells were analyzed ten days after immunization by flow cytometry using the CD40 ligand (CD40L) method. Cells were stimulated and gated as depicted in figure 37. **(A)** Frequency of CD154⁺ cells among CD4⁺ T cells and **(B)** absolute cell number of CD154⁺ CD4⁺ T cells in spleen ten days after immunization (n=3, unpaired t-test). The dashed line shows the frequency in the TiterMax control mouse indicating the unspecific background staining. Data are expressed as mean ± SEM. *p ≤ 0.05.

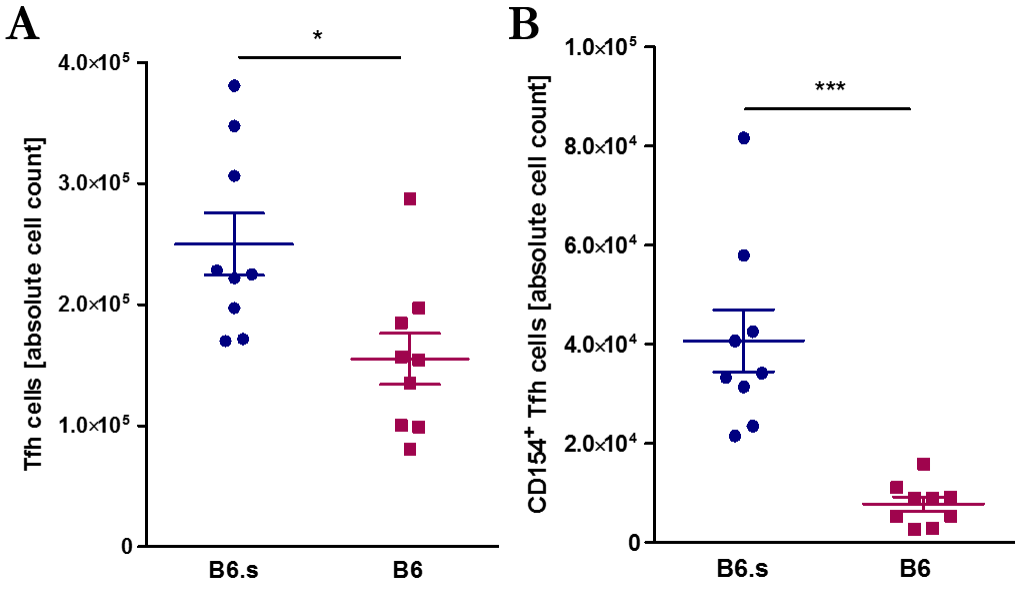

Supplementary figure 16: Susceptible mice have more follicular T helper cells (Tfh) and autoreactive Tfh cells compared to non-susceptible mice. EBA was induced in susceptible B6.s and non-susceptible B6 mice by immunization with vWFA2 and cells from draining lymph nodes were analyzed by flow cytometry. The stimulation of cells and the gating was performed as depicted in figure 38. **(A)** Absolute cell number of Tfh and **(B)** of CD154⁺ Tfh cells ten days after immunization (n=9, unpaired t-test). Data are expressed as mean ± SEM. *p ≤ 0.05; ***p ≤ 0.001.

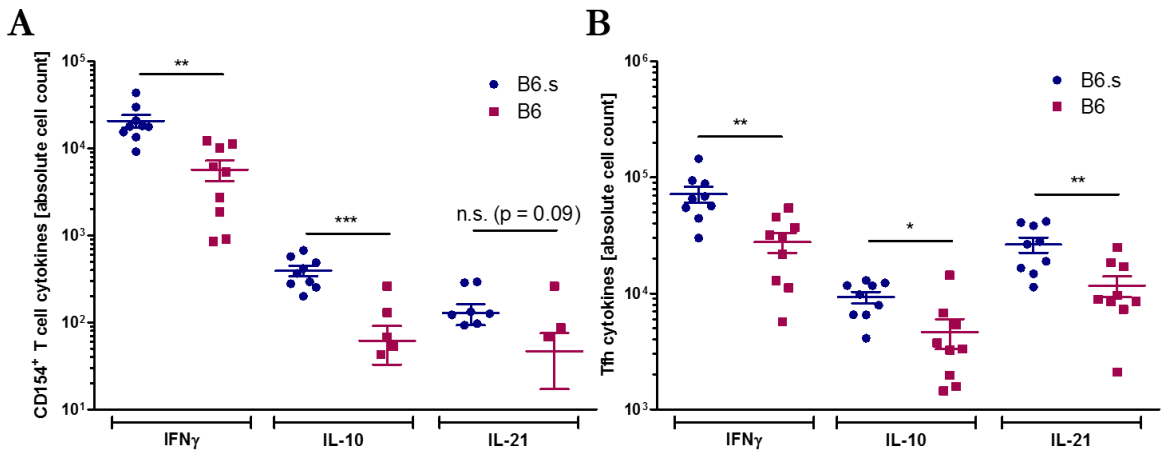

Supplementary figure 17: The number of cytokine-producing autoreactive T cells and follicular T helper cells is different between susceptible and non-susceptible mice. EBA was induced in susceptible B6.s and non-susceptible B6 mice by immunization with vWFA2 and cells from draining lymph nodes were analyzed by flow cytometry ten days after immunization. Cells were stimulated and gated as depicted in figure 39. **(A)** Absolute cell number of IFNγ$^+$, IL-10$^+$ or IL-21$^+$ CD154$^+$ autoreactive CD4$^+$ T cells and **(B)** of IFNγ$^+$, IL-10$^+$ or IL-21$^+$ Tfh cells ten days after immunization (n=9, unpaired t-test). Four data points for IL-10$^+$ and six data points for IL-21$^+$ autoreactive T cells in B6 mice are zero and therefore not indicated in the logarithmic scale. Data are expressed as mean ± SEM. *p ≤ 0.05; **p ≤ 0.01; ***p ≤ 0.001. *n.s., not significant.*

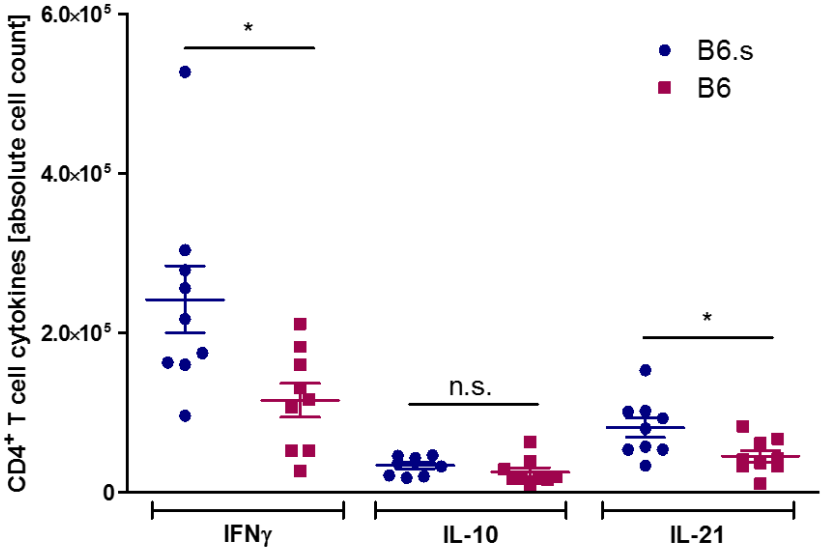

Supplementary figure 18: The absolute cell number of IFNγ- and IL-21-producing CD4$^+$ T cells is increased in susceptible mice compared to non-susceptible mice. EBA was induced in susceptible B6.s and non-susceptible B6 mice by immunization with vWFA2 and cells from draining lymph nodes were analyzed by flow cytometry ten days after immunization. Cells were stimulated and gating was performed as depicted in figure 40. The figure shows the absolute cell number of IFNγ$^+$, IL-10$^+$ or IL-21$^+$ CD4$^+$ T cells ten days after immunization (n=9, unpaired t-test). Data are expressed as mean ± SEM. *p ≤ 0.05. *n.s., not significant.*

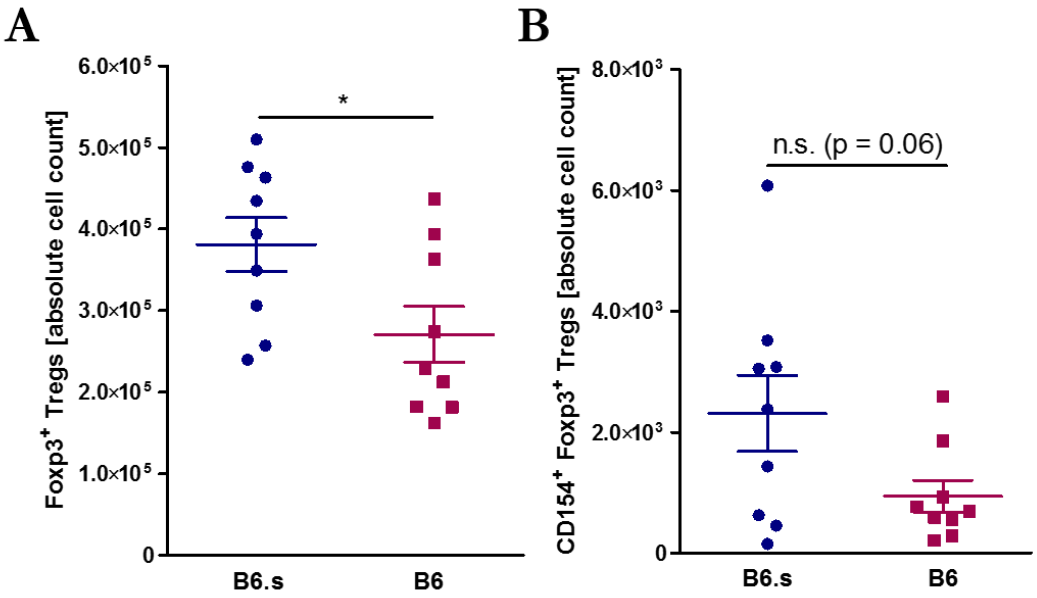

Supplementary figure 19: The absolute cell number of Foxp3⁺ regulatory T cells (Tregs) and autoreactive Tregs is increased in susceptible mice compared to non-susceptible mice. EBA was induced in susceptible B6.s and non-susceptible B6 mice by immunization with vWFA2 and cells from draining lymph nodes were analyzed by flow cytometry ten days after immunization. Cell were stimulated and Tregs and their CD154 expression were gated as depicted in figure 41. **(A)** Absolute cell number of Foxp3⁺ Tregs and **(B)** of CD154⁺ Tregs ten days after immunization (n=9, unpaired t-test). Data are expressed as mean ± SEM. *p ≤ 0.05. *n.s., not significant.*

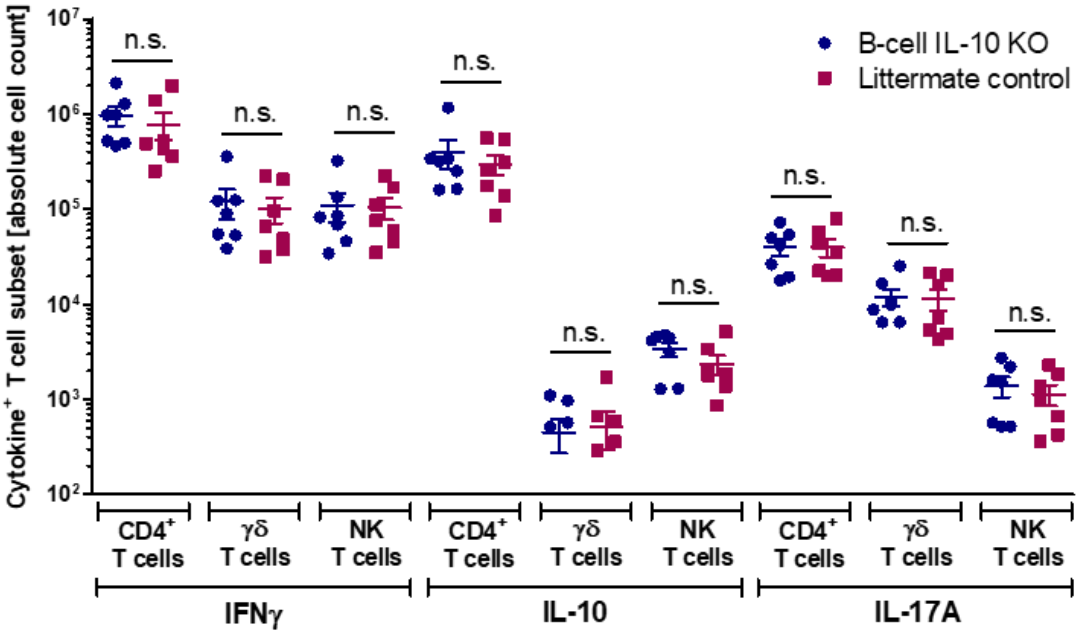

Supplementary figure 20: The absolute cell numbers of different T-cell subsets expressing IFNγ, IL-10 and IL-17A are not influenced by B-cell IL-10-deficiency in the autoantibody-transfer-induced EBA model. EBA was induced in B-cell IL-10 knock-out mice (CD19cre⁺ IL-10$^{flox/flox}$) and IL-10-competent littermate controls (CD19cre⁻ IL-10$^{flox/flox}$) as described in the scheme in figure 42. On day twelve, splenic T-cell subsets were analyzed for their IFNγ, IL-10 and IL-17A expression by flow cytometry as depicted in figure 44. The figure shows the absolute cell number of IFNγ⁺, IL-10⁺ and IL-17A⁺ T cells of the subset indicated (n=7, unpaired t-test). Five data points for IL-10⁺ γδ T cells are zero and therefore not indicated in the logarithmic scale. Data are expressed as mean ± SEM. *KO, knock-out; n.s., not significant.*

List of Tables

List of Figures

Abbreviations

A405 / A647	Alexa Fluor 405 / Alexa Fluor 647
aa	Amino acid
Ab	Antibody
ADCC	Antibody-dependent cellular cytotoxicity
ALP	Alkaline phosphatase
ANOVA	Analysis of variance
APC	Antigen-presenting cell
APC	Allophycocyanin
B220	Marker for many murine B cells
B6	C57Bl/6J wildtype mice, EBA non-susceptible mouse strain
B6.s	B6.SJL-H2^{s} C3^{c}/1CyJ, EBA-susceptible mouse strain
BCA	Bicinchoninic acid
BCR	B-cell receptor
bp	Base pairs
BP	Bullous pemphigoid
Breg	Regulatory B cell
BSA	Bovine serum albumin
BV650 / BV711	Brilliant Violet 650 / Brilliant Violet 711
C3 / C5a	Complement factor 3 / complement factor 5a
C57Bl/6	Laboratory mouse inbred strain
CCR2	C-C chemokine receptor type 2
CD	Cluster of differentiation
CO_2	Carbon dioxide
COL7	Collagen type VII
cre	Cre recombinase
CSIF	Cytokine synthesis inhibitory factor
CXCL	Chemokine C-X-C motif ligand
CXCR	Chemokine C-X-C motif receptor
Cy7 / Cy5	Cyanine 7 / Cyanine 5
DC	Dendritic cell
DEJ	Dermal-epidermal junction
dLN	Draining lymph nodes
DMSO	Dimethyl sulfoxide
DNA	Deoxyribonucleic acid
dNTP	Deoxynucleoside triphosphate
DPBS	Dulbecco's phosphate-buffered saline
e.g.	*Exempli gratia* (for example)
EAE	Experimental autoimmune encephalomyelitis
EBA	Epidermolysis bullosa acquisita
EDTA	Ethylene diamine tetra-acetic acid
eF450 / eF780	eFluor 450 / eFluor 780
eGFP	Enhanced green fluorescent protein
ELISA	Enzyme-linked immunosorbent assay
et al.	*Et alii* (and others)
$F(ab)_2$	Fragment of antigen-binding of the antibody
Fc	Fragment crystallizable region of the antibody
FCS	Fetal calf serum

FcγR	Fc-gamma receptor
FITC	Fluorescein isothiocyanate
flox	Gene flanked by two *loxP* sites
FMO	Fluorescence minus one
Foxp3	Forkhead box protein 3
FSC-A / FSC-H	Forward scatter-area / Forward scatter-height
GM-CSF	Granulocyte-macrophage colony-stimulating factor
GMD	Goat anti mouse immunoglobulin D
GST	Glutathione S-transferase
H2b	Non-susceptible haplotype in mice
H2s	EBA-susceptible haplotype in mice
HCl	Hydrochloric acid
HLA	Human leucocyte antigen
HSP90	Heat-shock protein 90
HTAB	Hexadecyl-trimethylammonium bromide
i.p.	Intraperitoneal
IFN	Interferon
Ig	Immunoglobulin
IL	Interleukin
ILC	Innate lymphoid cell
IVC	Individual ventilated cage
IVIG	Intravenous immunoglobulin
JAK1	Janus kinase 1
K_2HPO_4	Dipotassium phosphate
KCl	Potassium chloride
KH_2PO_4	Potassium dihydrogen phosphate
KO	Knock-out
L	Ligand
LAG-3	Lymphocyte-activation gene 3
LPS	Lipopolysaccharide
LTB4	Leukotriene B4
Ly6G	Lymphocyte antigen 6 complex, locus G
Mac-1	Macrophage antigen-1
mCOL7c	Recombinant murine type VII collagen fragment c
MFI	Mean fluorescence intensity
MHC	Major histocompatibility complex
MMP	Matrix metalloproteinase
MMP	Mucous membrane pemphigoid
MPO	Myeloperoxidase
MS	Multiple sclerosis
MyD88	Myeloid differentiation primary response 88
n	Number of mice in each group
Na_2CO_3	Sodium carbonate
Na_2HPO_4 x 2 H_2O	Sodium phosphate dibasic
NaCl	Sodium chloride
$NaHCO_3$	Sodium bicarbonate
NaOH	Sodium hydroxide
NC1 / NC16A	Non-collagenous domain 1 / non-collagenous domain 16A
NF-κB	Nuclear factor kappa-light-chain-enhancer of activated B cells
NK1.1	Marker for murine natural killer cells and natural killer T cells

NKT cell	Natural killer T cell
p	P-value
p.i.	Post immunization
PAMP	Pathogen-associated molecular pattern
PBS	Phosphate-buffered saline
PCR	Polymerase chain reaction
PD	Pemphigoid diseases
PD-1	Programmed cell death protein 1
PE	Phycoerythrin
PMA	Phorbol 12-myristate 13-acetate
PMN	Polymorphonuclear neutrophil
PRR	Pattern recognition receptor
R	Receptor
RA	Rheumatoid arthritis
rm	Recombinant mouse
ROS	Reactive oxygen species
RPMI	Rosewell Park Memorial Institute Medium
RT	Room temperature
s.c.	Subcutaneous
SDS	Sodium dodecyl sulfate
SEM	Standard error of the mean
SJL	Swiss Jim Lambert, laboratory mouse inbred strain
SLE	Systemic lupus erythematosus
SOCS3	Suppressor of cytokine signaling 3
SPF	specific pathogen-free
SSC-A	Sideward scatter-area
STAT	Signal transducer and activator of transcription
T2-MZP	Transitional type 2-marginal zone precursor
TACI	Transmembrane activator and CAML interactor
TAE	Tris-acetic acid-EDTA buffer
TCR	T-cell receptor
TE	Tris-EDTA buffer
Tfh cell	Follicular T helper cell
TGF	Transforming growth factor
Th cell	T helper cell
TIM-1	T-cell Ig and mucin domain-containing protein 1
TLR	Toll-like receptor
TLS	Tail lysis solution
TMB	Tetramethylbenzidine
TNF	Tumor necrosis factor
TNFR2	Tumor necrosis factor receptor 2
Treg	Regulatory T cell
Tris	Tris(hydroxymethyl)aminomethane
TYK2	Tyrosine kinase 2
UV	Ultraviolet light
Vert-x	B6.(Cg)-Il10$^{tm1.1Karp}$, IL-10 reporter mice
vWFA2	Von Willebrand factor A–like domain 2
w/o	without

Units and constants used in this thesis:

%	Percentage
°C	Degree Celsius
AU	Arbitrary unit
AUC	Area under the curve
d	Day
Da	Dalton
g	Gravitational acceleration (g = 9.81 m/s^2)
g	Gram
G	Gauge
h	Hour
l	Liter
m	Meter
M	Molar (mol/l)
min	Minute
pH	*Potentia hydrogenii*
RLU	Relative luminescence unit
rpm	Round per minute
sec	Second
U	Unit
V	Volt

Prefixes based on the International System of Units (SI):

k	10^3	kilo
m	10^{-3}	milli
µ	10^{-6}	micro
n	10^{-9}	nano

Letters assumed from the Greek alphabet:

α	alpha
β	beta
γ	gamma
δ	delta
ϰ	kappa